Many-Body Quantum Mechanics

Fabian Hassler

2025

Prof. Dr. Fabian Hassler
Institute for Quanteninformation
RWTH Aachen

The notes are largely based on the lecture notes by G. Blatter (ETH Zurich 2006). I would like to sincerely thank Gianni Blatter for providing the script. Further thanks go to Lukas Grunwald, who contributed especially in Chapter 4 and in the appendix.

Please report typos and other errors to F. Hassler. The translation has been done with the help of GPT-4o mini. In case of ambiguities, it might be helpful to consult the German version.

Contents

Literature

G. Baym
Lectures on Quantum Mechanics
(Benjamin, Menlo Park, California, 1969)
good, compact, modern

J.J. Sakurai
Modern Quantum Mechanics
(Addison Wesley, Reading, 1994) &
good, modern

W. Nolting
Theoretical Physics
5. Quantum Mechanics, 1 & 2, with exercises and solutions, (Zimmermann-Neufang, Ulmen, 1992)
introduction, clear, modern structure

A. Messiah
Quantum Mechanics I & II
(North-Holland, Amsterdam, 1976)
comprehensive

L.D. Landau and E.M. Lifshitz
Quantum Mechanics (Nonrelativistic theory)
Vol. 3 of the Course of Theoretical Physics, (Pergamon, Oxford, 1977)
classic, everything included

F. Schwabl
Quantum Mechanics
(Springer, Berlin, 1990)
newer book, an alternative selection of topics

Chapter 1

Scattering Theory

In this chapter, we will address 3D scattering problems. Specifically, we will examine the scattering of particles by time-independent and radially symmetric scattering potentials. The results can be generalized mutatis mutandis to non-radially symmetric potentials. However, the formulas will become much more complicated due to the lack of symmetry without yielding conceptually new results. This is different when the potential becomes time-dependent or when the involved particles have internal degrees of freedom, as then the possibility of inelastic scattering or complete absorption exists. These possibilities will not be addressed here.

We investigate the unbounded motion of a particle in a scattering potential $V(\boldsymbol{r})$ that is centered at the origin and is short-range, i.e., with the property that $r\,V(\boldsymbol{r}) \to 0$ as $r \to \infty$. The important example of the long-range Coulomb potential with $V(\boldsymbol{r}) \propto 1/r$ will be considered later in the exercises. In general, it is possible for $V(\boldsymbol{r})$ to have attractive regions. Then bound states with $E < 0$ can occur. Here, we consider scattering states with $E > 0$, and since $V(r \to \infty) \to 0$, these states are asymptotically free.

1.1 Wave Packets

The incoming particle is described by a wave packet. It will be important in the following that the extent of the wave packet ξ is larger than the range of the potential a. Of course, the extent ξ should be smaller than the distance between the source/detector and the scattering center so that the different stages of the scattering problem are temporally separated. Furthermore, we want to assume that the width in momentum space is sufficiently small so that we can neglect the broadening of the wave packet due to dispersion.

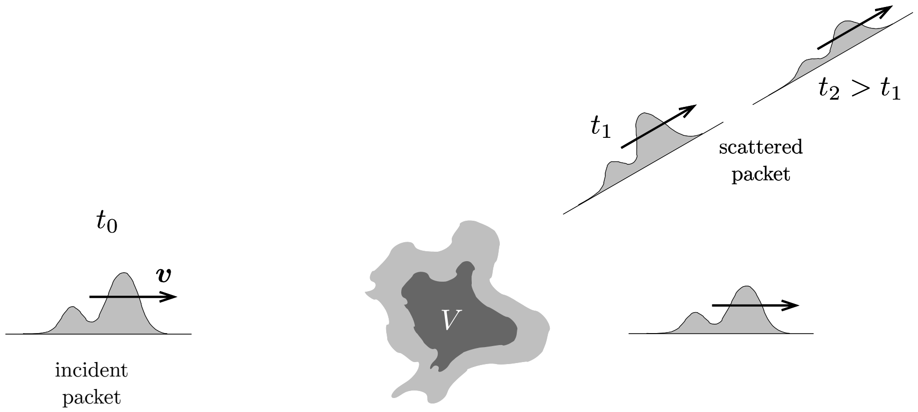

Figure 1.1: Scattering of a wave packet: The incoming packet is scattered in the direction $\Omega_{\boldsymbol{r}} \equiv \hat{\boldsymbol{r}}$ with a probability $\propto |f_{\boldsymbol{k}}(\Omega_{\boldsymbol{r}})|^2$. Note that the amplitude of the scattered part of the wave function decays as r^{-1}, see (1.23).

We consider an incoming wave packet

$$\Psi(\boldsymbol{r};t_0) = \psi_0(\boldsymbol{r}) = \int \frac{d^3q}{(2\pi)^3}\, a_{\boldsymbol{q}}\, e^{i\boldsymbol{q}\cdot\boldsymbol{r}} \tag{1.1}$$

which is centered far to the left of the scatterer at time $t = t_0$, see Figure 1.1. The amplitude $a_{\boldsymbol{q}}$ is concentrated around $\boldsymbol{k}$, so that the packet approaches the scatterer with velocity $\boldsymbol{v} = \hbar\boldsymbol{k}/m$.[1] The time evolution of the wave function $\Psi(\boldsymbol{r};t)$ determines the signal measured at the detector at a later time $t > t_0$. Our task is thus to determine $\Psi(\boldsymbol{r}; t > t_0)$, especially after it has passed through the scattering center.

Let $\Psi_{\boldsymbol{k}}$ be the exact scattering states, i.e., solutions of the eigenvalue equation

$$H\Psi_{\boldsymbol{k}}(\boldsymbol{r}) = E_k\Psi_{\boldsymbol{k}}(\boldsymbol{r}), \tag{1.2}$$

with $H = p^2/2m + V(\boldsymbol{r})$ and the definition $E_k \equiv \hbar^2k^2/2m \geq 0$[2]. The scattering states $\Psi_{\boldsymbol{k}}$ are complete in the space of extended wave functions, and we can write the time evolution of Ψ as

$$\Psi(\boldsymbol{r};t) = \int \frac{d^3q}{(2\pi)^3}\, A_{\boldsymbol{q}}\Psi_{\boldsymbol{q}}(\boldsymbol{r})e^{-iE_q(t-t_0)/\hbar}. \tag{1.3}$$

We will determine the expansion coefficients $A_{\boldsymbol{q}}$ later in Chapter 1.3 and show that $A_{\boldsymbol{q}} = a_{\boldsymbol{q}}$. In the expansion (1.3), only scattering states contribute, as we are only interested in the asymptotic expression for $r \to \infty$, and bound states decay exponentially in this region.

---

[1] Specifically, one could choose the amplitude $a_{\boldsymbol{q}} = (\xi^2/2\pi)^{3/2} e^{-iq_z z_0 - (\boldsymbol{q}-k\hat{\boldsymbol{z}})^2/2\xi^2}$ with $z_0 \gg a$.

[2] We denote v for the norm $|\boldsymbol{v}| = \sqrt{\boldsymbol{v}^2}$ of the vector $\boldsymbol{v}$.

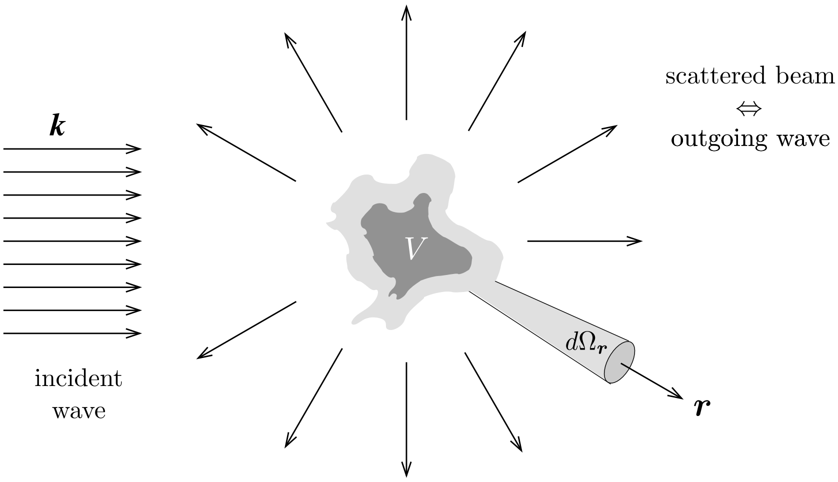

Figure 1.2: Scattering Geometry: The incoming wave $\exp(i\boldsymbol{k}\cdot\boldsymbol{r})$ is scattered by the potential $V(\boldsymbol{r})$. The scattered wave asymptotically has the form of a spherical wave modulated in solid angle $\Omega_{\boldsymbol{r}}$, $f_{\boldsymbol{k}}(\Omega_{\boldsymbol{r}})\exp(ikr)/r$.

1.2 Lippmann-Schwinger Equation

Next, we want to find at least a formal solution of the time-independent Schrödinger equation (1.2) for the scattering states. The boundary conditions are given by the scattering geometry, see Figure 1.2. Accordingly, the wave function $\Psi_{\boldsymbol{k}}$ should behave asymptotically for large distances r as

$$\Psi_{\boldsymbol{k}}(\boldsymbol{r}) \sim e^{i\boldsymbol{k}\cdot\boldsymbol{r}} + f_{\boldsymbol{k}}(\Omega_{\boldsymbol{r}})\frac{e^{ik_{\mathrm{s}}r}}{r} \tag{1.4}$$

The second term proportional to $\psi_{\mathrm{s}} = e^{ik_{\mathrm{s}}r}/r$ is an outgoing spherical wave, as can be read from the expression for the current density

$$\boldsymbol{j}_{\mathrm{s}} = \frac{\hbar}{m}\,\mathrm{Im}(\psi_{\mathrm{s}}^{*}\partial_r\psi_{\mathrm{s}})\hat{\boldsymbol{r}} = \frac{\hbar k_{\mathrm{s}}}{mr^2}\hat{\boldsymbol{r}} = j_{\mathrm{s},r}\hat{\boldsymbol{r}} \tag{1.5}$$

For elastic scattering processes, $k_{\mathrm{s}} = k$. The scattering amplitude $f_{\boldsymbol{k}}(\Omega_{\boldsymbol{r}})$ depends on the wave number $\boldsymbol{k}$ (or the energy E_k and the direction of incidence $\hat{\boldsymbol{k}}$) and the scattering angle $\Omega_{\boldsymbol{r}}$. Note that $\boldsymbol{k}$ is not a conserved quantity, and the wave function $\Psi_{\boldsymbol{k}}$ contains momentum components $\boldsymbol{k}'$ with $\boldsymbol{k}' \neq \boldsymbol{k}$.

In a first step, we solve the eigenvalue problem (1.2) with the boundary condition (1.4),

$$\underbrace{\left[\frac{\hbar^2}{2m}\nabla^2 + E_k\right]}_{\text{free Propagation}}\Psi_{\boldsymbol{k}}(\boldsymbol{r}) = \underbrace{V(\boldsymbol{r})\Psi_{\boldsymbol{k}}(\boldsymbol{r})}_{\text{Source}}, \tag{1.6}$$

where we have made a sensible grouping of the terms that is adapted to the scattering geometry. The equation (1.6) is not an eigenvalue problem in the usual sense (where

E_k is unknown), but for each energy E_k, solutions can be found. The equation (1.6) is an inhomogeneous partial differential equation, where the source $V(\boldsymbol{r})\Psi_{\boldsymbol{k}}(\boldsymbol{r})$ depends on the solution $\Psi_{\boldsymbol{k}}(\boldsymbol{r})$. Such driven differential equations are usually solved using Green's functions. We solve the free propagation problem for a point source $\delta^{(3)}(\boldsymbol{r})$,

$$(E - H_0)\, G(\boldsymbol{r}; E) = \delta^{(3)}(\boldsymbol{r}) \qquad \text{and boundary conditions for } G, \tag{1.7}$$

where we have introduced the free Hamiltonian operator $H_0 = p^2/2m$. If we know the solution to (1.7), we can write the solution to (1.6) as

$$\Psi_{\boldsymbol{k}}(\boldsymbol{r}) = \underbrace{e^{i\boldsymbol{k}\cdot\boldsymbol{r}}}_{\text{Solution of the hom. Eq.}} + \underbrace{\int d^3r'\, G(\boldsymbol{r} - \boldsymbol{r}'; E_k) V(\boldsymbol{r}')\Psi_{\boldsymbol{k}}(\boldsymbol{r}').}_{\substack{\text{Solution of the inhomogeneous equation} \\ \text{generated by the 'source' (=scattering potential).}}} \tag{1.8}$$

Here, the solution of the homogeneous equation is just the incoming wave, and the solution of the inhomogeneous equation is the scattered wave. To prove that the integral equation (1.8) is equivalent to the problem (1.6) plus boundary conditions, we apply the operator $(E_k - H_0)$ to (1.8) with the result

$$\begin{aligned}
(E_k - H_0)\Psi_{\boldsymbol{k}} &= \int d^3r'\, [(E_k - H_0)G(\boldsymbol{r} - \boldsymbol{r}'; E_k)] V(\boldsymbol{r}')\Psi'_{\boldsymbol{k}}(\boldsymbol{r}') \\
&= \int d^3r'\, [\delta^{(3)}(\boldsymbol{r} - \boldsymbol{r}')] V(\boldsymbol{r}')\Psi_{\boldsymbol{k}}(\boldsymbol{r}') \\
&= V(\boldsymbol{r})\Psi_{\boldsymbol{k}}(\boldsymbol{r}).
\end{aligned} \tag{1.9}$$

The plane wave in (1.8) gives the first term of the asymptotic behavior (1.4). The second term in (1.8) must therefore correspond to the term $\propto \exp(ikr)/r$, $r \to \infty$ in (1.4). To show this, however, we need the asymptotic behavior of the Green's function $G(\boldsymbol{r}; E)$. We determine the Green's function $G(\boldsymbol{r}; E)$ by the Fourier transformation of (1.7),

$$\int d^3r\, e^{-i\boldsymbol{q}\cdot\boldsymbol{r}}(E - H_0)G(\boldsymbol{r}; E) = \int d^3r\, \delta^{(3)}(\boldsymbol{r}) e^{-i\boldsymbol{q}\cdot\boldsymbol{r}}, \tag{1.10}$$

$$\left(E - \frac{\hbar^2 q^2}{2m}\right) G(\boldsymbol{q}; E) = 1,$$

$$G(\boldsymbol{q}; E) = \frac{1}{E - \hbar^2 q^2/2m} = \frac{1}{E - E_q}. \tag{1.11}$$

By inverse transformation, we obtain

$$\begin{aligned}
G(\boldsymbol{r}; E) &= \int \frac{d^3q}{(2\pi)^3} \frac{e^{i\boldsymbol{q}\cdot\boldsymbol{r}}}{E - E_q} = -\frac{2m}{\hbar^2} \int_0^\infty \frac{q^2 dq}{4\pi^2} \int_{-1}^{1} dz \frac{e^{iqzr}}{q^2 - 2mE/\hbar^2} \\
&= -\frac{2m}{4\pi^2\hbar^2} \int_0^\infty dq\, q^2 \frac{2\sin qr}{qr} \frac{1}{q^2 - 2mE/\hbar^2} \\
&= -\frac{m}{2\pi^2\hbar^2 ir} \int_{-\infty}^{\infty} dq\, \frac{q e^{iqr}}{q^2 - 2mE/\hbar^2}.
\end{aligned} \tag{1.12}$$

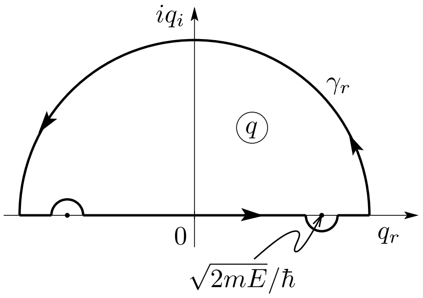

Figure 1.3: Integration path in the complex q-plane. By enclosing the pole at $q = +\sqrt{2mE}/\hbar$, we ensure the asymptotic behavior of an outgoing wave $\propto \exp[i(qr - Et/\hbar)]$. The pole at $q = -\sqrt{2mE}/\hbar$ generates an incoming wave $\propto \exp[-i(qr + Et/\hbar)]$. The choice of contour in the complex q-plane thus sets the boundary condition.

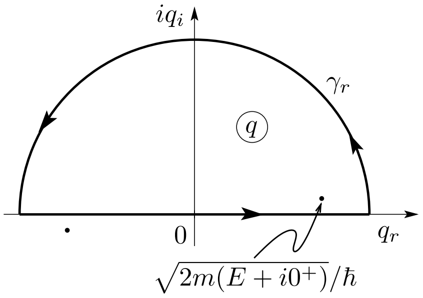

Figure 1.4: By shifting the energy into the complex plane, $E \mapsto E + i0^+$, the poles shift into the complex q-plane, $q = \pm\sqrt{2mE}/\hbar \mapsto \pm\sqrt{2m(E+i0^+)}/\hbar$. The integration along $\mathbb{R}$ then automatically takes into account the correct pole in the upper half-plane.

The last integral can be solved using the residue theorem. It is important to obtain an outgoing wave as a boundary condition. The integrand of (1.12) has poles at $q = \pm\sqrt{2mE}/\hbar$. Since $r > 0$, we must close the integration path in the upper half-plane with $q_i > 0$, as $i(q_r + iq_i)r = iq_r r - q_i r$ appears in the exponent. To obtain an outgoing wave for $r \to \infty$, we must include the pole at $+\sqrt{2mE}/\hbar$. Therefore, we choose the integration path γ_r according to Figure 1.3 and obtain the result

$$G(\boldsymbol{r}; E) = -\frac{m}{2\pi\hbar^2}\frac{e^{i\sqrt{2mE}r/\hbar}}{r}. \tag{1.13}$$

Alternatively to the path γ_r, we can integrate along the real axis and assign a small imaginary part to the energy, $E \mapsto E + i0^+$. The denominator $q^2 - 2m(E + i0^+)/\hbar^2$ then has poles at $\pm\sqrt{2m(E+i0^+)}/\hbar$, see Figure 1.4, and the integration over $q \in \mathbb{R}$ automatically picks up only the pole at $+\sqrt{2mE}/\hbar$. The Green's function $G(\boldsymbol{r}; E + i0^+)$ is called the retarded Green's function due to the property that it produces an outgoing wave. The alternative choice $G^a(\boldsymbol{r}, E) = G(\boldsymbol{r}; E - i0^+) = -(m/2\pi\hbar^2)\exp[-i\sqrt{2mE}r/\hbar]/r$ generates an incoming wave (advanced Green's function). The choice $E = E + i0^+$ thus sets the boundary conditions. With (1.13), we have found a formal solution of (1.6),

$$\Psi_{\boldsymbol{k}}(\boldsymbol{r}) = e^{i\boldsymbol{k}\cdot\boldsymbol{r}} + \int d^3r'\, G(\boldsymbol{r} - \boldsymbol{r}'; E_k)V(\boldsymbol{r}')\Psi_{\boldsymbol{k}}(\boldsymbol{r}'), \tag{1.14}$$

$$\text{with} \quad G(\boldsymbol{r}; E_k) \;=\; -\frac{m}{2\pi\hbar^2}\frac{e^{ikr}}{r}.$$

Of course, we have not really solved (1.6); we have merely rewritten the differential equation considering the boundary conditions into an integral equation.

Equation (1.14) is the Lippmann-Schwinger equation; it is physically transparent, automatically takes into account the boundary conditions, and is well-suited for implementing approximations. Furthermore, it has the nice property that the orthogonality and completeness relations[3] of $e^{i\boldsymbol{k}\cdot\boldsymbol{r}}$ are transferred to $\Psi_{\boldsymbol{k}}(\boldsymbol{r})$, i.e., in particular, the wave functions for different $\boldsymbol{k}$ are orthogonal and it holds that $\int d^3r\, \Psi_{\boldsymbol{k}'}(\boldsymbol{r})\Psi_{\boldsymbol{k}}(\boldsymbol{r}) = (2\pi)^3\delta^{(3)}(\boldsymbol{k}-\boldsymbol{k}')$.

Next, we look at the far region $r \to \infty$ in (1.14) to verify the asymptotic behavior (1.4) and to find an expression for $f_{\boldsymbol{k}}(\Omega_{\boldsymbol{r}})$ [of course depending on $V(\boldsymbol{r})$]. For $r \to \infty$, $k|\boldsymbol{r}-\boldsymbol{r}'| = kr\sqrt{(\hat{\boldsymbol{r}}-\boldsymbol{r}'/r)^2} = kr[1 - 2\hat{\boldsymbol{r}}\cdot\boldsymbol{r}'/r + (r'/r)^2]^{1/2} \approx kr - k\hat{\boldsymbol{r}}\cdot\boldsymbol{r}'$. Thus, we can rewrite (1.14) as

$$\Psi_{\boldsymbol{k}}(\boldsymbol{r}) \sim e^{i\boldsymbol{k}\cdot\boldsymbol{r}} + \left[-\frac{m}{2\pi\hbar^2}\int d^3r'\, e^{-ik\hat{\boldsymbol{r}}\cdot\boldsymbol{r}'}V(\boldsymbol{r}')\Psi_{\boldsymbol{k}}(\boldsymbol{r}')\right]\frac{e^{ikr}}{r}, \tag{1.15}$$

and by comparing with (1.4), we obtain the scattering amplitude in the form

$$f_{\boldsymbol{k}}(\Omega_{\boldsymbol{r}}) = -\frac{m}{2\pi\hbar^2}\int d^3r'\, e^{-ik\hat{\boldsymbol{r}}\cdot\boldsymbol{r}'}V(\boldsymbol{r}')\Psi_{\boldsymbol{k}}(\boldsymbol{r}'). \tag{1.16}$$

The scattering amplitude has the unit of length and depends only on the direction $\hat{\boldsymbol{r}}$, i.e., $\Omega_{\boldsymbol{r}}$, but not on the distance from the scattering center.

1.3 Differential Cross Section

Next, we want to establish the connection between the formal solution, in particular the scattering amplitude $f_{\boldsymbol{k}}(\Omega_{\boldsymbol{r}})$, and the differential cross section $d\sigma/d\Omega_{\boldsymbol{r}}$ (a measurable quantity). To do this, we recall the discussion of the scattering of a wave packet in Chapter 1.1. For the concrete determination of the time evolution of the wave packet in (1.3), we still need the connection between $a_{\boldsymbol{k}}$ (the initial condition) and $A_{\boldsymbol{k}}$ (the scattering solution). However, this is no longer difficult after the detailed discussion of the Lippmann-Schwinger equation.

At time t_0 (before scattering), (1.1) and (1.3) must match. To obtain a condition on $A_{\boldsymbol{k}}$, we rewrite (1.1) using (1.14) as

$$\Psi(\boldsymbol{r};t_0) = \psi_0(\boldsymbol{r}) = \int\frac{d^3q}{(2\pi)^3}a_{\boldsymbol{q}}\left[\Psi_{\boldsymbol{q}}(\boldsymbol{r}) + \frac{m}{2\pi\hbar^2}\int d^3r'\,\frac{e^{iq|\boldsymbol{r}-\boldsymbol{r}'|}}{|\boldsymbol{r}-\boldsymbol{r}'|}V(\boldsymbol{r}')\Psi_{\boldsymbol{q}}(\boldsymbol{r}')\right]. \tag{1.17}$$

---

[3] The wave functions $\Psi_{\boldsymbol{k}}(\boldsymbol{r})$ are only asymptotic, i.e., complete for $r \to \infty$. To obtain a completeness relation $\delta^{(3)}(\boldsymbol{r}-\boldsymbol{r}') = \int d^3k/(2\pi)^3\Psi^*_{\boldsymbol{k}}(\boldsymbol{r})\Psi_{\boldsymbol{k}}(\boldsymbol{r}') + \sum_n \Psi^*_n(\boldsymbol{r})\Psi_n(\boldsymbol{r}')$ for the entire $\mathbb{R}^3$, one must also consider possible bound states $\Psi_n(\boldsymbol{r})$.

We will use this relationship evaluated near the source $\boldsymbol{r}_Q = -r_Q\hat{\boldsymbol{k}}$, $r_Q \gg \xi$, to determine $A_{\boldsymbol{k}}$. In the second term, we have the following expression to calculate,

$$\int \frac{d^3q}{(2\pi)^3}\, a_{\boldsymbol{q}} e^{iq|\boldsymbol{r}-\boldsymbol{r}'|}\Psi_{\boldsymbol{q}}(\boldsymbol{r}'). \tag{1.18}$$

We assume that $\Psi_{\boldsymbol{q}}$ is smooth over the support of $a_{\boldsymbol{q}}$, i.e., for $|\boldsymbol{q}-\boldsymbol{k}| \lesssim \xi^{-1}$ with ξ being the extent of the wave packet, so it has no resonances (see also later). Thus, $\Psi_{\boldsymbol{q}} \approx \Psi_{\boldsymbol{k}}$, and we can factor the scattering state out of the integral in (1.18). If we also use the approximation $q = \boldsymbol{q}\cdot\hat{\boldsymbol{q}} \approx \boldsymbol{q}\cdot\hat{\boldsymbol{k}}$, we obtain

$$\begin{aligned}\int \frac{d^3q}{(2\pi)^3} a_{\boldsymbol{q}} e^{iq|\boldsymbol{r}-\boldsymbol{r}'|}\Psi_{\boldsymbol{q}}(\boldsymbol{r}') &\approx \Psi_{\boldsymbol{k}}(\boldsymbol{r}')\int \frac{d^3q}{(2\pi)^3}\, a_{\boldsymbol{q}} e^{i\boldsymbol{q}\cdot(\hat{\boldsymbol{k}}|\boldsymbol{r}-\boldsymbol{r}'|)} \\ &\overset{(1.1)}{=} \Psi_{\boldsymbol{k}}(\boldsymbol{r}')\psi_0(\hat{\boldsymbol{k}}|\boldsymbol{r}-\boldsymbol{r}'|).\end{aligned} \tag{1.19}$$

Here, $\psi_0(\hat{\boldsymbol{k}}|\boldsymbol{r}-\boldsymbol{r}'|)$ is the amplitude (of the incoming wave packet) at the initial time at the location $\hat{\boldsymbol{k}}|\boldsymbol{r}-\boldsymbol{r}'|$. In the expression (1.17), only positions with $|\boldsymbol{r}'| \lesssim a$ are needed. Since the particle is at the source $\boldsymbol{r}_Q$ (far from the scatterer) at the initial time t_0, we have $\psi_0(\hat{\boldsymbol{k}}|\boldsymbol{r}-\boldsymbol{r}'|) \approx \psi_0(\hat{\boldsymbol{k}}\,r_Q) = \psi_0(-\boldsymbol{r}_Q) \approx 0$, and the second term in (1.17) vanishes. The remainder takes the form

$$\Psi(\boldsymbol{r};t_0) = \psi_0(\boldsymbol{r}) = \int \frac{d^3q}{(2\pi)^3}\, a_{\boldsymbol{q}}\Psi_{\boldsymbol{q}}(\boldsymbol{r}), \tag{1.20}$$

from which a coefficient comparison with (1.3) gives $A_{\boldsymbol{q}} = a_{\boldsymbol{q}}$.

An evaluation of $\Psi(\boldsymbol{r};t)$ for large t yields the probability distribution at the detection time. According to (1.3), for $r \to \infty$

$$\begin{aligned}\Psi(\boldsymbol{r};t) &= \int \frac{d^3q}{(2\pi)^3}\, a_{\boldsymbol{q}}\Psi_{\boldsymbol{q}}(\boldsymbol{r})e^{-iE_q(t-t_0)/\hbar} \\ &\overset{(1.15)}{\sim} \Psi_0(\boldsymbol{r};t) + \int \frac{d^3q}{(2\pi)^3}\, a_{\boldsymbol{q}}\frac{e^{iqr}}{r} f_{\boldsymbol{q}}(\Omega_{\boldsymbol{r}})e^{-iE_q(t-t_0)/\hbar};\end{aligned} \tag{1.21}$$

here, (we use $E_q \approx -\hbar^2k^2/2m + \boldsymbol{v}\cdot\boldsymbol{q}$)

$$\Psi_0(\boldsymbol{r};t) = \overbrace{\int \frac{d^3q}{(2\pi)^3}\, a_{\boldsymbol{q}}\, e^{i\boldsymbol{q}\cdot\boldsymbol{r}}}^{=\psi_0(\boldsymbol{r})\text{ according to (1.1)}}\quad e^{-iE_q(t-t_0)/\hbar} \approx e^{i\hbar k^2(t-t_0)/2m}\,\psi_0(\boldsymbol{r}-\boldsymbol{v}(t-t_0)) \tag{1.22}$$

(up to an unimportant phase factor) describes the evolution of the incoming packet without scatterer and dispersion. With $f_{\boldsymbol{q}}$ smooth for $\boldsymbol{q} \approx \boldsymbol{k}$ (which allows us to factor $f_{\boldsymbol{q}} \approx f_{\boldsymbol{k}}$ out of the integral) and $q \approx \boldsymbol{q}\cdot\hat{\boldsymbol{k}}$ (as before), we obtain

$$\Psi(\boldsymbol{r};t) \overset{t\text{ large}}{\longrightarrow} \underbrace{\Psi_0(\boldsymbol{r};t)}_{\text{unscattered wave packet}} + \underbrace{\frac{f_{\boldsymbol{k}}(\Omega_{\boldsymbol{r}})}{r}\Psi_0(\hat{\boldsymbol{k}}\,r;t)}_{\text{scattered packet}}. \tag{1.23}$$

The scattering process is sketched in Figure 1.1. According to (1.23), it involves the superposition of the unscattered wave packet and a packet scattered in the direction $\Omega_{\boldsymbol{r}}$. The latter involves the amplitude $\Psi_0(\hat{\boldsymbol{k}}\, r;t)$ of a packet propagating forward, which must be evaluated at the correct time and distance. This packet is then multiplied by the angle-dependent scattering amplitude $f_{\boldsymbol{k}}(\Omega_{\boldsymbol{r}})/r$. Note that the above formula (1.23) is not applicable in two cases:

- if $V(r)$ is long-range, e.g., $V(r) = r^{-1}$,
- if the incoming energy E_k is resonant.

The scattering amplitude $f_{\boldsymbol{k}}(\Omega_{\boldsymbol{r}})$ contains the necessary information to calculate the differential cross section

$$\frac{d\sigma}{d\Omega_{\boldsymbol{r}}} = \frac{dN(\Omega_{\boldsymbol{r}})}{N_{\text{in}}\, d\Omega_{\boldsymbol{r}}} = \frac{\text{Number of particles scattered in } d\Omega}{\text{incoming particles per cm}^2 \times d\Omega_{\boldsymbol{r}}} \tag{1.24}$$

This has the unit of area with $[d\sigma/d\Omega_{\boldsymbol{r}}] = \text{cm}^2, \text{barn};\ 1\,\text{barn} = 10^{-24}\,\text{cm}^2$.

The density of incoming particles N_{in} and the number of particles scattered into the solid angle $d\Omega$ $dN(\Omega_{\boldsymbol{r}})$ are given by

$$N_{\text{in}} = \int_{-\infty}^{\infty} dt\, j_{\text{in}}(\boldsymbol{r}_Q;t), \qquad dN(\Omega_{\boldsymbol{r}}) = \int_{-\infty}^{\infty} dt\, j_{\text{s},r}(\boldsymbol{r};t)\, \underbrace{r^2\, d\Omega_{\boldsymbol{r}}}_{\text{Area of the detector}}.$$

Substituting the expressions for the incoming and scattered current densities,[4]

$$\boldsymbol{j}_{\text{in}}(\boldsymbol{r};t) = \frac{\hbar}{m}\,\text{Im}\,(\Psi_0^* \boldsymbol{\nabla}\Psi_0) = \frac{\hbar \boldsymbol{k}}{m}|\Psi_0(\boldsymbol{r};t)|^2, \tag{1.25}$$

$$\begin{aligned} j_{\text{s},r}(\boldsymbol{r};t) &= \frac{\hbar}{m}\,\text{Im}\left[\frac{f^*}{r}\Psi_0^*(\hat{\boldsymbol{k}}r;t)\partial_r \frac{f}{r}\Psi_0(\hat{\boldsymbol{k}}r;t)\right] \\ &\approx \frac{\hbar k}{m}\frac{|f_{\boldsymbol{k}}(\Omega_{\boldsymbol{r}})|^2}{r^2}|\Psi_0(\hat{\boldsymbol{k}}r;t)|^2, \end{aligned} \tag{1.26}$$

yield the differential cross section in the form

$$\frac{d\sigma}{d\Omega_{\boldsymbol{r}}} = \frac{|f_{\boldsymbol{k}}(\Omega_{\boldsymbol{r}})|^2 \int dt |\Psi_0(\hat{\boldsymbol{k}}r;t)|^2}{\int dt\, |\Psi_0(\boldsymbol{r}_Q;t)|^2} = |f_{\boldsymbol{k}}(\Omega_{\boldsymbol{r}})|^2, \tag{1.27}$$

with $\int dt\, |\Psi_0(\hat{\boldsymbol{k}}r;t)|^2 = \int dt\, |\Psi_0(\boldsymbol{r}_Q;t)|^2 = \int dt\, |\psi_0(\boldsymbol{v}t)|^2$ according to (1.22). Finally, we also define the total cross section as

$$\sigma = \int d\Omega_{\boldsymbol{r}}\, |f_{\boldsymbol{k}}(\Omega_{\boldsymbol{r}})|^2\,. \tag{1.28}$$

---

[4] We use $\partial_r \Psi_0(\hat{\boldsymbol{k}}r;t) = \int \frac{d^3q}{(2\pi)^3}\, i\boldsymbol{q}\cdot\hat{\boldsymbol{k}}\, a_{\boldsymbol{q}}\, e^{i\boldsymbol{q}\cdot\hat{\boldsymbol{k}}r} e^{-iE_q(t-t_0)/\hbar} \approx ik\Psi_0(\hat{\boldsymbol{k}}r;t)$.

1.4 Partial Wave Expansion

For rotationally symmetric scattering potentials $V(r)$, the Hamiltonian operator $H = p^2/2m + V(r)$ commutes with the angular momentum operators $\boldsymbol{L}$. Consequently, the angular problem can be separated, and we can decompose the scattering problem according to the irreducible representations of the rotation group. This partial wave decomposition reduces the problem to solving the subproblems in the various angular momentum sectors[5] : We decompose the total Hilbert space $L^2(\mathbb{R}^3)$ according to $L^2(\mathbb{R}^3) = L^2(\mathbb{R}^+) \otimes [\oplus_l \mathcal{H}_l]$ and solve the partial problems in $L^2(\mathbb{R}^+) \otimes \mathcal{H}_l$, where the angular problem is trivial (i.e., already diagonalized). We fully exploit the rotational symmetry by choosing a coordinate system with the z-axis parallel to the incoming beam, $\hat{\boldsymbol{z}} \parallel \boldsymbol{k}$. The entire problem is then rotationally symmetric with respect to rotations around the z-axis. Only quantum numbers with $m = 0$ appear, as the incoming particle cannot have angular momentum along the direction of motion. The spherical harmonics $Y_{lm}(\theta, \varphi)$ reduce in this case to the Legendre polynomials $Y_{l0}(\theta, \varphi) \propto P_l(\cos\theta)$ with the normalization

$$\int_{-1}^{1} dz\, P_l(z) P_{l'}(z) = \frac{2}{2l+1} \delta_{ll'}, \tag{1.29}$$

so that $P_l(1) = 1$. Furthermore, we must expand the incoming wave in eigenfunctions of the angular momentum operator,

$$\begin{aligned} e^{ikr\cos\theta} &= \sum_{l=0}^{\infty} i^l (2l+1) P_l(\cos\theta) j_l(kr) \\ &= \frac{1}{2} \sum_{l=0}^{\infty} i^l (2l+1) P_l(\cos\theta) [h_l^{(1)}(kr) + h_l^{(2)}(kr)], \end{aligned} \tag{1.30}$$

where we have introduced the spherical Bessel functions j_l and Hankel functions $h_l^{(1,2)}$. A small excursion about spherical Bessel functions and a proof of (1.30) can be found in Appendix A.

We can also develop the sought stationary solution $\Psi_{\boldsymbol{k}}(\boldsymbol{r})$ in partial waves,

$$\Psi_{\boldsymbol{k}}(\boldsymbol{r}) = \sum_{l=0}^{\infty} i^l (2l+1) \underbrace{P_l(\cos\theta)}_{\propto Y_{l0}} R_l(r), \tag{1.31}$$

where the factor $i^l(2l+1)$ is a convention that is explained by comparison with (1.30). If we substitute the ansatz (1.31) into the stationary Schrödinger equation $H\Psi_{\boldsymbol{k}} = E_k \Psi_{\boldsymbol{k}}$, we obtain the radial problem

$$\left[-\frac{p_r^2}{2m} - \frac{\hbar^2 l(l+1)}{2mr^2} + \frac{\hbar^2 k^2}{2m} \right] R_l(r) = V(r) R_l(r); \tag{1.32}$$

---

[5] The $2l+1$ dimensional Hilbert space $\mathcal{H}_l = \{Y_{lm}\}_{m=-l}^{m=l}$ is spanned by the spherical functions for l.

with $p_r^2/\hbar^2 = -r^{-1}\partial_r^2 r$, this leads to the differential equation

$$\left[\partial_r^2 - \frac{l(l+1)}{r^2} + k^2\right] r\, R_l(r) = \frac{2m}{\hbar^2} r V(r) R_l(r), \tag{1.33}$$

where $\Psi_{\boldsymbol{k}}$ must satisfy the boundary condition (1.4). For $r \to \infty$, $rV(r) \to 0$ and the right-hand side of the equation becomes negligibly small, so that (1.33) reduces to a Bessel equation, see Appendix A. In the far field ($r \to \infty$), $R_l(r)$ must therefore have the asymptotic form

$$R_l(r) \sim \alpha_l \left[h_l^{(2)}(kr) + S_l\, h_l^{(1)}(kr)\right], \tag{1.34}$$

with

$$h_l^{(1,2)}(\rho) \sim \frac{1}{\rho} \exp[\pm i(\rho - (l+1)\pi/2)], \qquad \rho = kr, \tag{1.35}$$

the two fundamental solutions for $V \equiv 0$, the incoming and outgoing spherical waves in the form of Hankel functions.

Next, we need to determine the coefficients α_l and S_l, which are functions of k or E_k; for $V \equiv 0$, it is obvious that

$$R_l(r) \;=\; j_l(kr) = \frac{1}{2}\left[h_l^{(2)}(kr) + h_l^{(1)}(kr)\right], \tag{1.36}$$

and thus $\alpha_l = 1/2$ and $S_l = 1$. For $V \not\equiv 0$, the incoming wave $h_l^{(2)}$ does not change, but the outgoing component $h_l^{(1)}$ does, which is why the latter acquires a nontrivial weight $S_l \neq 1$. It is easy to see that for elastic scattering, the conservation of particle number requires that $|S_l(E_k)| = 1$. This follows because, in the stationary solution, the total radial current density [here we use that $\int dz\, P_l^2(z) = 2/(2l+1)$]

$$\begin{aligned} j_{s,r}(r) &= \frac{\hbar}{m}\,\mathrm{Im}\,(R_l^*\,\partial_r R_l) \\ &\downarrow \quad 2R_l \sim \left[e^{-i(kr-\phi_l)}/kr + S_l\, e^{i(kr-\phi_l)}/kr\right], \quad \phi_l = (l+1)\pi/2 \\ &\sim \frac{\hbar}{4mkr^2}\left[|S_l|^2 - 1\right] \end{aligned} \tag{1.37}$$

must vanish so that the same number of particles fall in as flow out per unit time. We can then express the complex amplitude S_l

$$S_l(E_k) = e^{2i\delta_l(E_k)} \tag{1.38}$$

in terms of the real scattering phase $\delta_l(E_k)$.[6]

---

[6] In general scattering theory, $S_l(E_k)$ is an eigenvalue of the S-matrix. The S-matrix is then unitary due to particle number conservation. Here, we could reduce the problem to a one-dimensional subspace due to the spherical symmetry of the scattering problem and the assumption that we only have elastic scattering.

The scattering phases δ_l completely describe the scattering problem by determining the scattering amplitude $f_{\boldsymbol{k}}(\Omega_{\boldsymbol{r}})$. To establish this connection, we bring the solution (1.31) in the asymptotic region where the expression

$$\Psi_{\boldsymbol{k}}(\boldsymbol{r}) \sim \frac{1}{2}\sum_l i^l(2l+1)P_l(\cos\theta)\left[h_l^{(2)}(kr)+e^{2i\delta_l}h_l^{(1)}(kr)\right] \tag{1.39}$$

is valid, into the form using (1.30)

$$\Psi_{\boldsymbol{k}}(\boldsymbol{r}) \sim e^{i\boldsymbol{k}\cdot\boldsymbol{r}} + \underbrace{\frac{1}{2}\sum_l i^l(2l+1)P_l(\cos\theta)\left[e^{2i\delta_l}-1\right]h_l^{(1)}(kr)}_{\sim f_{\boldsymbol{k}}(\theta)e^{ikr}/r}\,. \tag{1.40}$$

Comparing with (1.4) $[h_l^{(1)} \sim (-i)^{l+1}e^{ikr}/kr]$ yields the scattering amplitude

$$\begin{aligned} f_{\boldsymbol{k}}(\theta) &= \frac{1}{2ik}\sum_l (2l+1)P_l(\cos\theta)\left[e^{2i\delta_l}-1\right] \\ &= \frac{1}{k}\sum_l (2l+1)P_l(\cos\theta)e^{i\delta_l}\sin\delta_l. \end{aligned} \tag{1.41}$$

The expression

$$\frac{\exp(2i\delta_l)-1}{2ik} = \frac{\exp(i\delta_l)\sin(\delta_l)}{k} = f_l \tag{1.42}$$

is called the partial wave amplitude. The total cross section σ is obtained by an angular integration,

$$\begin{aligned} \sigma &= \int d\Omega_{\boldsymbol{r}}\,|f_{\boldsymbol{k}}(\Omega_{\boldsymbol{r}})|^2 \\ &= \frac{4\pi}{k^2}\sum_l (2l+1)\sin^2\delta_l = 4\pi\sum_l (2l+1)|f_l|^2. \end{aligned} \tag{1.43}$$

The quantities

$$\sigma_l = \frac{4\pi}{k^2}(2l+1)\sin^2\delta_l \;=\; 4\pi(2l+1)|f_l|^2 \tag{1.44}$$

are called partial cross sections. Obviously, $\sigma_l \leq 4\pi(2l+1)/k^2$. Note that in the total cross section, the various contributions from the angular momentum sectors simply add up, and there is no interference between the different partial waves. However, it is not the case that all quantities simply result from the addition of the expressions of the partial waves; for example, one obtains interference terms for $d\sigma/d\Omega_{\boldsymbol{r}}$ from the various sectors.

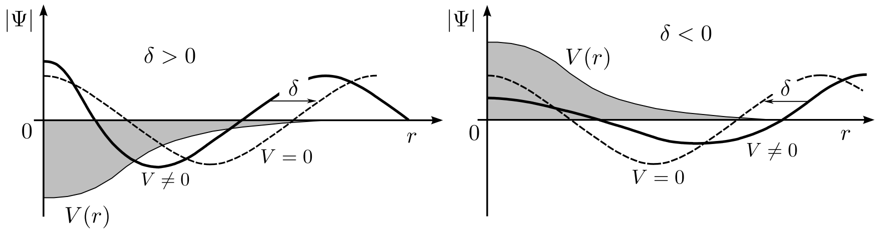

Figure 1.5: Phase shifts $\delta_l(E_k)$: An attractive potential (left) increases the kinetic energy and the wave function oscillates faster, leading to a positive phase shift. Conversely, a repulsive potential (right) slows down the oscillation of the wave function and produces a negative $\delta_l(E_k)$.

The phase shift $\exp(2i\delta_l)$ can be interpreted physically in a simple way. The wave function $R_l(r)$ has the asymptotic form

$$\begin{aligned} R_l(r) &\sim \frac{1}{2}\left[h_l^{(2)}(kr) + e^{2i\delta_l} h_l^{(1)}(kr)\right] \sim \frac{e^{i\delta_l}}{2}\left[\frac{(-i)^l e^{i(kr+\delta_l)}}{kr} + \frac{(+i)^l e^{-i(kr+\delta_l)}}{kr}\right] \\ &\overset{kr\gg\delta_l}{\sim} \frac{e^{i\delta_l}}{2}\left[\frac{(-i)^l e^{i(kr+\delta_l)}}{kr+\delta_l} + \frac{(+i)^l e^{-i(kr+\delta_l)}}{kr+\delta_l}\right] \sim e^{i\delta_l} j_l(kr+\delta_l). \end{aligned} \tag{1.45}$$

Now, comparing the case

$$V \equiv 0: \qquad R_l(r) = j_l(kr) \tag{1.46}$$

with

$$V \not\equiv 0: \qquad R_l(r) \sim e^{i\delta_l} j_l(kr+\delta_l), \tag{1.47}$$

we see that a positive phase shift $\delta_l > 0$ pulls the wave function ‘into the potential,’ while a negative phase shift $\delta_l < 0$ pushes the wave out, see Figure 1.5.

1.5 Optical Theorem

Let us consider the imaginary part of the forward scattering amplitude $f_{\boldsymbol{k}}(\theta = 0)$ in (1.41),

$$\begin{aligned} \operatorname{Im} f_{\boldsymbol{k}}(\theta=0) &= \frac{1}{k}\sum_l (2l+1) P_l(\cos\theta)\sin^2\delta_l\Big|_{\theta=0} \\ &= \frac{1}{k}\sum_l (2l+1)\sin^2\delta_l \;=\; \frac{k}{4\pi}\underbrace{\frac{4\pi}{k^2}\sum (2l+1)\sin^2\delta_l}_{\sigma}\,. \end{aligned} \tag{1.48}$$

Thus, we directly obtain the optical theorem

$$\sigma = \frac{4\pi}{k}\,\mathrm{Im}\, f_{\boldsymbol k}(\theta = 0). \tag{1.49}$$

The physical reason for the optical theorem can be found in the conservation of particle number. The scattered particle current $\propto \sigma$ must be taken from the incoming current and thus is missing in the forward amplitude ($\propto f_{\boldsymbol k}(\theta = 0)$). It is the interference of the scattered wave with the incoming wave that reduces the unscattered wave and thus creates a shadow of the scatterer in the forward direction. The particles missing in the shadow are precisely those that have been scattered. The relation (1.49) is generally valid as long as the particle number is conserved, which is the case when no trapping or transformation of the particles occurs.

To show the optical theorem for a general potential (which is not necessarily radially symmetric), we consider the radial current density $j_r = (\hbar/m)\,\mathrm{Im}(\Psi^*\partial_r\Psi)$ of a wave packet after the scattering process in the form (1.23). The radial current density

$$j_r(\boldsymbol r; t) = j_{\mathrm{in},r}(\boldsymbol r; t) + j_{\mathrm{s},r}(\boldsymbol r; t) + j_{r,\mathrm{int}}(\boldsymbol r; t) \tag{1.50}$$

is composed of the incoming current density, $j_{\mathrm{in},r}(\boldsymbol r; t) = \boldsymbol j_{\mathrm{in}}(\boldsymbol r; t)\cdot\hat{\boldsymbol r} = (\hbar\boldsymbol k\cdot\hat{\boldsymbol r}/m)|\Psi_0(\boldsymbol r; t)|^2$ (1.25), the scattered current density $j_{\mathrm{s},r}$ (1.26), and the interference current density between the scattered and the transmitted wave function[7]

$$j_{\mathrm{int},r}(\boldsymbol r; t) = \frac{\hbar k}{mr}\,\mathrm{Im}\left[i f_{\boldsymbol k}(\Omega_{\boldsymbol r})\Psi_0^*(\boldsymbol r; t)\Psi_0(\hat{\boldsymbol k}r; t)(1 + \hat{\boldsymbol k}\cdot\hat{\boldsymbol r})\right]. \tag{1.51}$$

Next, we use the fact that $\Psi_0(\hat{\boldsymbol k}r; t)$ only does not vanish at times when the particle has already arrived at the scattering center. In this case, $\Psi_0(\boldsymbol r; t)$ (and thus the interference current) is only non-zero in the forward direction. Thus, we can use the relations $\hat{\boldsymbol k}\cdot\hat{\boldsymbol r} = 1$ and $f_{\boldsymbol k}(\Omega_{\boldsymbol r}) = f_{\boldsymbol k}(\theta = 0)$ in the expression for $j_{\mathrm{int},r}$.

Essentially, the interference term produces the shadow of the scatterer by making the current in the forward direction smaller than the incoming current density $j_{\mathrm{in},r}$ and thus lowering the current in the forward direction by the scattered current. For the total particle number to be conserved, the total number of scattered particles must correspond exactly to the particles that are taken from the incoming particle beam. Or in other words: The integral of (1.51) over all solid angles and times must be exactly minus the integral of (1.26) over all solid angles and times. Now we have

$$\int d\Omega_{\boldsymbol r}\, j_{\mathrm{int},r}(\boldsymbol r; t) = \frac{2\hbar k}{r}\,\mathrm{Im}\left[i f_{\boldsymbol k}(\theta = 0)\Psi_0(\hat{\boldsymbol k}r; t)\int d\Omega_{\boldsymbol r}\,\Psi_0^*(\boldsymbol r; t)\right]. \tag{1.52}$$

For the angular integration of the wave packet Ψ_0, (1.22), we need [$q \approx \boldsymbol q\cdot\hat{\boldsymbol k}$ see (1.19)]

$$\int d\Omega_{\boldsymbol r}\, e^{i\boldsymbol q\cdot\boldsymbol r} = 2\pi\int_{-1}^{1} d(\cos\theta)\, e^{iqr\cos\theta} \overset{\boldsymbol q\approx\boldsymbol k}{\approx} \frac{2\pi\left(e^{i\boldsymbol q\cdot\hat{\boldsymbol k}r} - e^{-i\boldsymbol q\cdot\hat{\boldsymbol k}r}\right)}{ikr}.$$

---

[7] We use $\partial_r\Psi_0(\hat{\boldsymbol k}r; t) \approx ik\Psi_0(\hat{\boldsymbol k}r; t)$, $\partial_r\Psi_0(\boldsymbol r; t) \approx (i\boldsymbol k\cdot\hat{\boldsymbol r})\Psi_0(\boldsymbol r; t)$, see Chapter 1.3.

Thus, we obtain

$$\int d\Omega_{\boldsymbol{r}}\, \Psi_0(\boldsymbol{r};t) = \frac{2\pi}{ikr}[\Psi_0(\hat{\boldsymbol{k}}r;t) - \Psi_0(-\hat{\boldsymbol{k}}r;t)],$$

and (1.52) becomes

$$\int d\Omega_{\boldsymbol{r}}\, j_{\mathrm{int},r}(\boldsymbol{r};t) = -\frac{4\pi\hbar}{mr^2}\,\mathrm{Im}\, f_{\boldsymbol{k}}(\theta=0)|\Psi_0(\hat{\boldsymbol{k}}r;t)|^2, \tag{1.53}$$

since $\Psi_0(\hat{\boldsymbol{k}}r;t)\Psi_0(-\hat{\boldsymbol{k}}r;t) = 0$ in the far field. If we now compare (1.53) with the integral of (1.26) over all angles, we find the optical theorem $\sigma = (4\pi/k)\,\mathrm{Im}\, f_{\boldsymbol{k}}(\theta=0)$. Note that this proof is independent of any possible radial symmetry of the scattering problem.

1.6 Born Approximation

Except in special cases, one can only determine the scattering amplitude or the phase shifts numerically by solving (1.14) or (1.33). For weak potentials (what exactly a 'weak' potential is will be defined more precisely later), one can attempt to solve the Lippmann-Schwinger equation (1.14) iteratively,

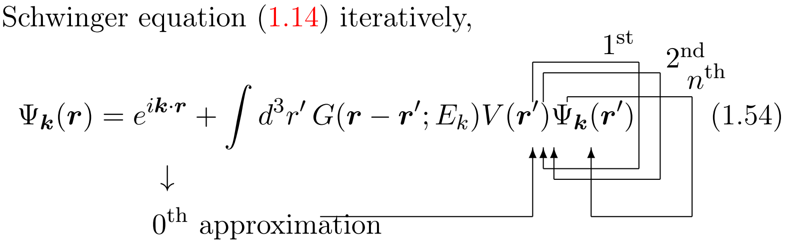

$$\Psi_{\boldsymbol{k}}(\boldsymbol{r}) = \underset{\substack{\downarrow\\ 0^{\text{th}}\text{ approximation}}}{e^{i\boldsymbol{k}\cdot\boldsymbol{r}}} + \int d^3r'\, G(\boldsymbol{r}-\boldsymbol{r}';E_k)V(\boldsymbol{r}')\Psi_{\boldsymbol{k}}(\boldsymbol{r}') \tag{1.54}$$

$$\begin{aligned}
\delta\Psi_{\boldsymbol{k}}^{(0)}(\boldsymbol{r}) &= e^{i\boldsymbol{k}\cdot\boldsymbol{r}},\\
\delta\Psi_{\boldsymbol{k}}^{(1)}(\boldsymbol{r}) &= \int d^3r'\, G(\boldsymbol{r}-\boldsymbol{r}';E_k)V(\boldsymbol{r}')\,\overbrace{e^{i\boldsymbol{k}\cdot\boldsymbol{r}'}}^{\delta\Psi_{\boldsymbol{k}}^{(0)}(\boldsymbol{r}')},\\
&\;\;\vdots\\
\delta\Psi_{\boldsymbol{k}}^{(n)}(\boldsymbol{r}) &= \int d^3r'\, G(\boldsymbol{r}-\boldsymbol{r}';E_k)V(\boldsymbol{r}')\delta\Psi_{\boldsymbol{k}}^{(n-1)}(\boldsymbol{r}'),\\
\rightarrow \Psi_{\boldsymbol{k}}^{(N)}(\boldsymbol{r}) &= \sum_{n=0}^{N}\delta\Psi_{\boldsymbol{k}}^{(n)}(\boldsymbol{r}).
\end{aligned} \tag{1.55}$$

For $N<\infty$, (1.55) is the N^{th} Born approximation, the limit $N\rightarrow\infty$ gives the Born series.

In the following, we will only use the first Born approximation,

$$\Psi_{\boldsymbol{k}}^{(1)}(\boldsymbol{r}) = e^{i\boldsymbol{k}\cdot\boldsymbol{r}} + \int d^3r'\, G(\boldsymbol{r}-\boldsymbol{r}'; E_k) V(\boldsymbol{r}')\, e^{i\boldsymbol{k}\cdot\boldsymbol{r}'}, \tag{1.56}$$

For the scattering amplitude $f_{\boldsymbol{k}}^{(1)}(\Omega_{\boldsymbol{r}})$, we find from (1.16)

$$f_{\boldsymbol{k}}^{(1)}(\Omega_{\boldsymbol{r}}) = -\frac{m}{2\pi\hbar^2}\int d^3r'\, V(\boldsymbol{r}')\, e^{i(\boldsymbol{k}-\boldsymbol{k}')\cdot\boldsymbol{r}'} \tag{1.57}$$

with $\boldsymbol{k}' = \boldsymbol{k}_s = k\hat{\boldsymbol{r}}$; i.e., $f_{\boldsymbol{k}}^{(1)}(\Omega_{\boldsymbol{r}})$ is proportional to the Fourier transform $V_{\boldsymbol{k}'-\boldsymbol{k}}$ of the scattering potential.

Next, we would like to obtain an explicit expression for the scattering phases δ_l of a spherically symmetric potential. For this, we use the fact that the scattering amplitude in this case depends only on $q = |\boldsymbol{k}-\boldsymbol{k}'| = 2k|\sin(\theta/2)|$, see Figure 1.6. The angular integration in (1.57) can therefore be performed directly and we obtain (Ω' is the angle between $\boldsymbol{r}'$ and $\boldsymbol{q}$)

$$\begin{aligned} f_{\boldsymbol{k}}^{(1)}(\theta) &= -\frac{m}{2\pi\hbar^2}\int_0^{2\pi} dr'\, r'^2\, V(r') \overbrace{\int d\Omega'\, e^{iqr'\cos\theta'}}^{2\pi(e^{iqr'}-e^{-iqr'})/iqr'} \\ &= -\frac{2m}{\hbar^2}\int_0^{\infty} dr'\, r'^2\, V(r')\frac{\sin(qr')}{qr'} \end{aligned} \tag{1.58}$$

Now, using the addition theorem of Legendre polynomials[8]

$$\frac{\sin\left[2x\sin(\theta/2)\right]}{2x\sin(\theta/2)} = \sum_{l=0}^{\infty}(2l+1)P_l(\cos\theta)j_l^2(x) \tag{1.59}$$

with $x = kr'$ and (1.41), we obtain the expression for the scattering phase shift

$$\delta_l^{(1)}(E_k) \approx e^{i\delta_l}\sin(\delta_l) = -\frac{2mk}{\hbar^2}\int_0^{\infty} dr\, r^2\, V(r)\, j_l^2(kr). \tag{1.60}$$

in the Born approximation.

The validity of the approximation must be checked on a case-by-case basis. It is certainly necessary that $|\delta\Psi^{(1)}(r)| \ll |\delta\Psi^{(0)}(\boldsymbol{r})| = 1$; thus

$$\left|\frac{m}{2\pi\hbar^2}\int d^3r' V(\boldsymbol{r}')\frac{e^{ik|\boldsymbol{r}-\boldsymbol{r}'|}}{|\boldsymbol{r}-\boldsymbol{r}'|}e^{i\boldsymbol{k}\cdot\boldsymbol{r}'}\right| \ll 1. \tag{1.61}$$

For large particle energies and weak scattering potentials, such that $V_0\, ka \ll E_k$, (where $V_0 \geq 0$ denotes the strength and a the extent of $V(r)$), the Born approximation

---

[8] See Abramowitz and Stegun 10.1.45.

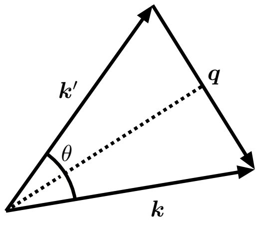

Figure 1.6: Sketch of the scattering angle θ, where $\boldsymbol{q} = \boldsymbol{k} - \boldsymbol{k}'$. Since the triangle is isosceles, the height line (dashed line) bisects the triangle and it holds that $q = 2k|\sin(\theta/2)|$.

is permissible. To show this, we examine $r = 0$ (where $\delta\Psi^{(1)}(r)$ is largest). The correction to the wave function $|\delta\Psi^{(1)}(r = 0)|$ can be written as

$$\left|\frac{m}{2\pi\hbar^2}\int d^3r'\frac{V(r')}{r'}\,e^{ikr'(1+\cos\theta')}\right| = \left|\frac{m}{\hbar^2 k}\int_0^\infty dr'\,V(r')\left(e^{2ikr'}-1\right)\right|.$$

For $ka \gg 1$ and V sufficiently smooth, the factor $\propto \exp(2ikr')$ averages out and we obtain with $V(r) \approx V_0$ (for $r < a$)

$$\left|\frac{m}{\hbar^2 k}\int_0^\infty dr\,V(r)\right| \ll 1 \Rightarrow V_0 ka \ll E_k. \tag{1.62}$$

For small energies with $ka \ll 1$, the above condition is not satisfied. However, in this limit, one can use $\exp(2ikr') - 1 \sim 2ikr'$, so that we obtain the condition

$$\left|\frac{m}{\hbar^2}\int_0^\infty dr\,r\,V(r)\right| \ll 1 \Rightarrow V_0 a^2 \ll \frac{\hbar^2}{m} \tag{1.63}$$

i.e., $V_0 \ll E_B = \hbar^2/ma^2$, which corresponds to a flat potential (a corresponding attractive flat potential has no bound states). The Born approximation is therefore applicable if either

$$V_0 ka \ll E_k \quad \text{or} \quad V_0 \ll E_B \tag{1.64}$$

is satisfied.

1.7 Eikonal Approximation

The eikonal approximation of scattering corresponds to geometric optics as an approximation for light propagation. It is valid as long as $V(r)$ changes little on the order of a wavelength $\lambda\!\!\!^{-} = k^{-1}$. Thus, $\lambda\!\!\!^{-}$ is our 'small' parameter. Note that we do not have to assume that V itself is weak as long as $E_k \gg V_0$, and therefore the range of applicability of the eikonal approximation is different from that of the Born approximation. As already discussed in the WKB approximation, one can replace the exact wave function $\Psi_{\boldsymbol{k}}(\boldsymbol{r})$ by the semiclassical wave function

$$\Psi_{\boldsymbol{k}}(\boldsymbol{r}) \sim e^{i\mathcal{S}(\boldsymbol{r})/\hbar} \tag{1.65}$$

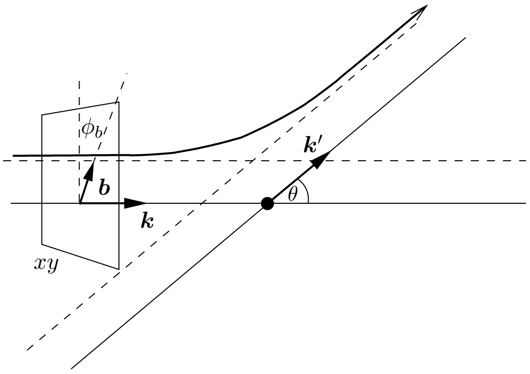

Figure 1.7: Scattering path with the impact parameter $\boldsymbol{b}$ in the xy-plane. The particle approaches (quasi-)classically the scattering center in the direction $\boldsymbol{k} \perp \boldsymbol{b}$. It is deflected by the center in the direction $\boldsymbol{k}'$ with the scattering angle $\theta \ll 1$.

If one also assumes that $\hbar|\nabla^2\mathcal{S}| \ll |\nabla\mathcal{S}|^2$, which formally corresponds to the limit $\hbar \to 0$, then the Schrödinger equation becomes the Hamilton-Jacobi equation

$$\frac{(\boldsymbol{\nabla}\mathcal{S})^2}{2m} + V(\boldsymbol{r}) = E_k \tag{1.66}$$

for the action $\mathcal{S}(\boldsymbol{r})$. The solution of the equation (1.66) consists of the solution of the classical scattering problem and is generally not explicitly determinable. Therefore, we make the additional assumption that we are only interested in small scattering angles and replace the classical trajectory with a straight line with $S(\boldsymbol{r}) = S(z)$. This reduces the partial differential equation (1.66) to an ordinary differential equation. For a particle incident with impact parameter $\boldsymbol{b} \perp \hat{\boldsymbol{z}}$ along the z-axis, see Figure 1.7, we obtain

$$\frac{\mathcal{S}}{\hbar} = \int_{-\infty}^{z} dz' \left[k^2 - \frac{2m}{\hbar^2} V\left(\sqrt{b^2 + z'^2}\right)\right]^{1/2} ; \tag{1.67}$$

the additive constant was determined by the property $\mathcal{S}/\hbar = kz$ for $V \equiv 0$ so that the scattering solution $\Psi_{\boldsymbol{k}}$ without potential reduces to a plane wave. For $E_k \gg V_0$, we can expand the square root and obtain

$$\frac{\mathcal{S}}{\hbar} \approx kz - \frac{m}{\hbar^2 k} \int_{-\infty}^{z} dz' \, V\left(\sqrt{b^2 + z'^2}\right), \tag{1.68}$$

which leads to

$$\Psi_{\boldsymbol{k}}(\boldsymbol{r}) = \Psi_{\boldsymbol{k}}(\boldsymbol{b} + z\hat{\boldsymbol{z}}) \approx e^{ikz} \exp\left[-\frac{im}{\hbar^2 k} \int_{-\infty}^{z} dz' \, V\left(\sqrt{b^2 + z'^2}\right)\right]. \tag{1.69}$$

Note that the expression (1.68) does not have the correct asymptotic form $e^{ikz} + f_{\boldsymbol{k}}(\Omega_{\boldsymbol{r}})e^{ikr}/r$ since it is only valid for the forward direction (with $\theta \approx 0$). Nevertheless, we can use (1.16) to determine the scattering amplitude

$$\begin{aligned} f_{\boldsymbol{k}}(\Omega_{\boldsymbol{r}}) \approx -\frac{m}{2\pi\hbar^2} \int d^3r'\, e^{i(\boldsymbol{k}-\boldsymbol{k}')\cdot\boldsymbol{r}'} V\left(r'\right) \\ \times \exp\left[-\frac{im}{\hbar^2 k}\int_{-\infty}^{z'} dz''\, V\left(\sqrt{b^2+z''^2}\right)\right] \end{aligned} \tag{1.70}$$

The reason is that the potential restricts the integration to the region $|\boldsymbol{r}'| \le a$, in which the relation (1.69) is valid. Note that the expression without the last factor corresponds exactly to the Born approximation.

As a final step, we perform the integration over $d^3r' = d^2b\,dz'$ in $d^2b = b\,db\,d\phi_b$. For this, we use the approximation [we use $\boldsymbol{k} \perp \boldsymbol{b}$ and $(\boldsymbol{k}-\boldsymbol{k}')\cdot\hat{\boldsymbol{z}} = O(\theta^2)$]

$$(\boldsymbol{k}-\boldsymbol{k}')\cdot\boldsymbol{r}' \approx -\boldsymbol{k}'\cdot\boldsymbol{b} \approx -kb\theta\cos\phi_b \tag{1.71}$$

for small angles and obtain

$$\begin{aligned} f_{\boldsymbol{k}}^{\text{eik}}(\Omega_{\boldsymbol{r}}) &= -\frac{m}{2\pi\hbar^2}\int_0^\infty db\, b \overbrace{\int_0^{2\pi} d\phi_b e^{-ikb\theta\cos\phi_b}}^{2\pi J_0(kb\theta)} \\ &\qquad\times \int_{-\infty}^{\infty} dz\, \underbrace{V\exp\left[-\frac{im}{\hbar^2 k}\int_{-\infty}^{z} dz'\, V\right]}_{\frac{i\hbar^2 k}{m}\frac{d}{dz}\exp\left[-\frac{im}{\hbar^2 k}\int_{-\infty}^{z} dz'\, V\right]} \\ &= -ik\int_0^\infty db\, bJ_0(kb\theta)\left[e^{2i\Delta(b)}-1\right] \end{aligned} \tag{1.72}$$

with the scattering phase

$$\Delta(b) = -\frac{m}{2k\hbar^2}\int_{-\infty}^{\infty} dz\, V\left(\sqrt{b^2+z^2}\right) \simeq \frac{V_0 ka}{E_k}. \tag{1.73}$$

In the derivation of the eikonal approximation, we have assumed that

$$V_0 \ll E_k = E_B\,(ka)^2 \quad \text{and} \quad ka \gg 1 \tag{1.74}$$

holds; i.e., the eikonal approximation is also applicable for $V_0 ka \gtrsim E_k$, where one cannot use the Born approximation. In this sense, the eikonal approximation is complementary to the Born approximation. In the limit $V_0 ka \ll E_k$, we can use $\exp[2i\Delta(b)] - 1 \approx 2i\Delta(b)$ so that we obtain with (1.71)

$$\begin{aligned} f_{\boldsymbol{k}}^{\text{eik}}(\theta) &= -\frac{m}{\hbar^2}\int_{-\infty}^{\infty} dz \int_0^\infty db\, b\, J_0(kb\theta) V\left(\sqrt{b^2+z^2}\right) \\ &= -\frac{m}{2\pi\hbar^2}\int d^3r'\, V(r') e^{i(\boldsymbol{k}-\boldsymbol{k})'\cdot\boldsymbol{r}'} \end{aligned} \tag{1.75}$$

obtained, in agreement with (1.57).

We now want to show that the eikonal approximation, in contrast to the Born approximation, satisfies the optical theorem (1.49). Thus, the eikonal approximation leads to self-consistent results that satisfy the conservation of particle number. To do this, we calculate the total scattering cross-section

$$\begin{aligned}\sigma &= 2\pi\int_0^\infty d(\cos\theta)|f_{\boldsymbol{k}}(\Omega_{\boldsymbol{r}})|^2\\ &= 2\pi k^2\int_0^\infty db\, b\left[e^{2i\Delta(b)}-1\right]\int_0^\infty db'\, b'\left[e^{-2i\Delta(b')}-1\right]\\ &\qquad\times\underbrace{\int_0^\pi d\theta\,\sin\theta\, J_0(kb\theta)J_0(kb'\theta)\,.}_{=I}\end{aligned}\tag{1.76}$$

Due to the finite range of the potential, it holds that $\Delta(b \gtrsim a)\approx 0$, so that only the region $b \lesssim a$ contributes significantly to the integral in (1.76). In the angular integral I, we therefore substitute $x = ka\theta$ and obtain[9]

$$\begin{aligned}I &= \frac{1}{ka}\int_0^{ka\pi} dx\,\underbrace{\sin(x/ka)}_{\approx x/ka}\,J_0(bx/a)J_0(b'x/a)\\ &\approx \frac{1}{(ka)^2}\int_0^\infty dx\, x J_0(bx/a)J_0(b'x/a) = \frac{1}{k^2 b}\delta(b-b'),\end{aligned}\tag{1.77}$$

where we have used that the Bessel functions cut off the integral at $x \simeq b/a \lesssim 1$, so that we can set the upper integration limit to infinity and can expand the sine. Substituting (1.77) into (1.76) yields the optical theorem

$$\sigma = 2\pi\int_0^\infty db\, b\left|e^{2i\Delta(b)}-1\right|^2 = 8\pi\int_0^\infty db\, b\sin^2\Delta(b) = \frac{4\pi}{k}\,\mathrm{Im}\, f_{\boldsymbol{k}}(\theta=0)$$

as the final result. Note that the optical theorem allows for a simple calculation of the total scattering cross-section by determining $\mathrm{Im}\, f_{\boldsymbol{k}}(\theta = 0)$.

---

[9] Here we use the orthogonality relation

$$\int_0^\infty dx\, x J_0(kx)J_0(k'x) = \frac{1}{k}\delta(k'-k)$$

of the Bessel functions, which can be derived from the well-known relation $\delta^{(2)}(\boldsymbol{r}-\boldsymbol{r}') = \int d^2k/(2\pi)^2 \times e^{i\boldsymbol{k}\cdot(\boldsymbol{r}-\boldsymbol{r}')}$ by integrating over the angle ϕ as follows

$$\begin{aligned}\frac{2\pi}{r}\delta(r-r') &= \int_0^{2\pi} d\phi\,\delta^{(2)}(\boldsymbol{r}-\boldsymbol{r}') = \int_0^\infty dk\, k\int_0^{2\pi}\frac{d\varphi}{2\pi}\overbrace{\int_0^{2\pi} d\phi\, e^{ikr\cos(\phi-\varphi)}}^{2\pi J_0(kr)}\,e^{-ikr'\cos(\phi'-\varphi)}\\ &= 2\pi\int_0^\infty dk\, k J_0(kr)J_0(kr').\end{aligned}$$

There is a nice connection between the eikonal approximation and the partial wave expansion for $l \gg 1$. In this case, one can consider l as a continuous variable. Equating the quantum mechanical angular momentum $\hbar l$ with the semiclassical angular momentum $bp = \hbar bk$ gives $l = bk$. The following relations

$$\sum_l \mapsto k \int db, \qquad P_l(\cos\theta) \overset{\theta \lll 1}{\approx} J_0(l\theta) = J_0(kb\theta), \qquad \delta_l \mapsto \Delta(b = l/k), \tag{1.78}$$

allow us to directly 'derive' the equation (1.72) from (1.41).

1.8 Analytical Properties of the Scattering Matrix

We consider a short-range potential that vanishes outside of $r = a$ (with more effort, one can show that the results remain valid as long as $r^2 V(r) \to 0$ for $r \to \infty$). The radial solution for $r > a$ is then given by

$$R_l(r) = \frac{1}{2}\left[h_l^{(2)}(kr) + S_l\, h_l^{(1)}(kr)\right], \tag{1.79}$$

while R_l for $r < a$ must be found by integrating (1.33). The scattering phase S_l is to be arranged such that both R_l and $\partial_r R_l$ are continuous at $r = a$. Since the wave function is uniquely determined only up to a (normalization) factor, we only need to require the continuity of the logarithmic derivative, $\partial_r \log R_l = (\partial_r R_l)/R_l$. Thus, we obtain the boundary condition

$$\alpha_l = \frac{1}{R_l}\frac{\partial R_l}{\partial r}\bigg|_{a^-} = \frac{\partial_r h_l^{(2)} + S_l\, \partial_r h_l^{(1)}}{h_l^{(2)} + S_l\, h_l^{(1)}}\bigg|_{a^+} = \frac{2\partial_r j_l + (S_l - 1)\partial_r h_l^{(1)}}{2j_l + (S_l - 1)h_l^{(1)}}\bigg|_{a^+}.$$

Solving for the scattering phase yields the result

$$S_l - 1 = \frac{2(\partial_r - \alpha_l)j_l}{(\alpha_l - \partial_r)h_l^{(1)}}\bigg|_{a^+} \tag{1.80}$$

$$\Big\downarrow \text{ with } S_l - 1 = \frac{2i}{\cot\delta_l - i}$$

$$\cot\delta_l = \frac{(\partial_r - \alpha_l)n_l}{(\partial_r - \alpha_l)j_l}\bigg|_{a^+}, \tag{1.81}$$

thus we have determined δ_l from α_l. The partial scattering cross-section as a function of $\cot\delta_l$ is given by

$$\sigma_l = \frac{4\pi}{k^2}(2l+1)\sin^2\delta_l = \frac{4\pi}{k^2}\frac{2l+1}{1+\cot^2\delta_l}. \tag{1.82}$$

The analysis of the expressions for $S_l(\cot\delta_l)$ and $\sigma_l(\cot\delta_l)$ shows that the following statements hold: For[10]

$$\begin{aligned} &\cot\delta_l = i \quad \text{has } S_l \text{ a pole and } \sigma_l \text{ is } \infty, \\ &\cot\delta_l = 0 \quad \text{is } S_l = -1 \text{ and } \sigma_l = 4\pi(2l+1)/k^2 \text{ is maximal.} \end{aligned} \tag{1.83}$$

As in one dimension (see exercises), the poles of S_l correspond to bound states. To understand this, we examine S_l for a bound state with $E = -E_B < 0$. The radial wave function has in this case the asymptotic form $R_l(r) \sim h_l^{(1)}(i\kappa r) \propto e^{-\kappa r}$ with the binding energy $E_B = \hbar^2\kappa^2/2m$. The term $\propto h_l^{(2)}$ is not allowed, as it corresponds to an exponentially growing wave function, which is not normalizable. The continuity condition is therefore given by

$$\alpha_l = \partial_r h_l^{(1)}/h_l^{(1)}\Big|_{a^+} = \partial_r \log h_l^{(1)}\Big|_{a^+}. \tag{1.84}$$

Substituting this relation into the general relation (1.81) yields the expected result

$$\cot\delta_l = \frac{h_l^{(1)}\partial_r n_l - n_l\,\partial_r h_l^{(1)}}{h_l^{(1)}\partial_r j_l - j_l\,\partial_r h_l^{(1)}} \overset{h_l^{(1)}=j_l+in_l}{=} i. \tag{1.85}$$

Similarly, we want to show that the zeros of $\cot\delta_l$ correspond to the scattering resonances. To do this, we expand $\cos\delta_l$ around the resonance with $E = E_r > 0$,

$$\begin{aligned} \cot\delta_l(E) &\approx \overbrace{\cot\delta_l(E_r)}^{=0} - \frac{1}{\sin^2\delta_l}\frac{d\delta_l}{dE}\Big|_{E_r}(E-E_r) \\ &= -\frac{d\delta_l}{dE}\Big|_{E_r}(E-E_r) && (1.86) \\ &\downarrow \text{with } \Gamma_r = \tfrac{2}{\delta_l'(E_r)} \\ &= -\frac{2}{\Gamma_r}(E-E_r). && (1.87) \end{aligned}$$

By substituting into (1.82), we see that the partial scattering cross-section σ_l exhibits a resonance around E_r with width Γ_r,

$$\sigma_l = \frac{4\pi}{k^2}(2l+1)\frac{(\Gamma_r/2)^2}{(E-E_r)^2+(\Gamma_r/2)^2}, \tag{1.88}$$

cf. Figure 1.8. Analogously, we find that the scattering amplitude $S_l(E)$ has a pole

---

[10] Note, that $\cot\delta_l = i$ is not possible for $\delta_l(E)$ with $E \in \mathbb{R}^+$. We consider here the analytical continuation of δ_l to the entire complex plane. On the real axis, we have $\sigma_l \leq 4\pi(2l+1)/k^2$ and the maximum is reached for $\cot\delta_l = 0$.

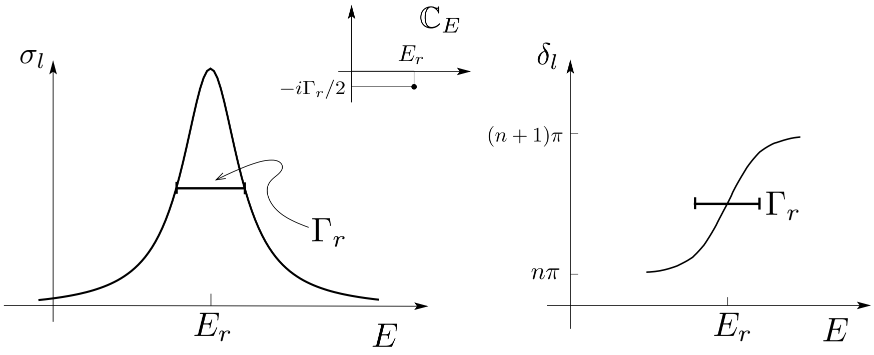

Figure 1.8: Resonance of width Γ_r: On the left the scattering cross-section $\sigma_l(E)$ and on the right the scattering phase $\delta_l(E)$; in the middle, the position of the pole in the complex E-plane is sketched.

in the second Riemann surface of the complex E-plane with

$$S_l - 1 = \frac{-i\Gamma_r}{E - (E_r - i\Gamma_r/2)}. \tag{1.89}$$

Across a resonance, the scattering phase $\delta_l(E)$ increases by π, the narrower the resonance, the steeper the increase. The value $\delta_l(E=0)$ is proportional to the number of bound states ν_l in the angular momentum sector l. It holds that $\delta_l(0) = \nu_l \pi$, with an additional phase shift $+\pi/2$ occurring in the sector $l = 0$ if a 'virtual' state[11] exists at $E = 0$. This is the statement of Levinson's theorem.

In the following, we will examine the low-energy $ka \ll 1$ behavior for a scatterer of extent a in more detail.

1.9 Low-energy Scattering, $ka \ll 1$

Low-energy scattering is a very relevant topic nowadays, as it represents the main scattering process of cold atoms in quantum atom optics. We use the expansions[12] $j_l \sim x^l/(2l+1)!!$ and $n_l \sim (2l-1)!!/x^{l+1}$ in (1.81) and obtain for $ka \ll 1$

$$\cot \delta_l \approx \frac{(2l+1)!!\,(2l-1)!!}{(ka)^{2l+1}} \frac{l+1+a\,\alpha_l(E)}{l - a\,\alpha_l(E)}. \tag{1.90}$$

For $ka \to 0$, $\cot \delta_l \to \infty$, since $\alpha_l(E) \approx \alpha_l(0)$, with the result

$$\delta_l \approx \sin \delta_l \approx \tan \delta_l \sim (ak)^{2l+1}; \tag{1.91}$$

---

[11] In the $l = 0$ sector, a bound state at $E < 0$ becomes a virtual state (instead of a resonance) when the binding energy vanishes, i.e., as $E_B \to 0$.

[12] The double factorial $(2l-1)!!$ of an odd number $2l-1$ is defined by $(2l-1)!! = (2l)!/(2^l l!) = 1 \cdot 3 \cdot 5 \cdots (2l-1)$.

i.e., the scattering phases δ_l and the partial scattering cross-sections σ_l become rapidly smaller in the low-energy region with increasing angular momentum. The s-wave sector is therefore dominant, and we focus on this case. It is instructive to express the scattering phase δ_0 in terms of the scattering length a_s,

$$k\cot\delta_0 \overset{\alpha_0(E)\approx\alpha_0(0)}{\approx} -\frac{1+a\alpha_0(0)}{a^2\alpha_0(0)} = -\frac{1}{a_s}; \tag{1.92}$$

thus, the scattering length a_s becomes the only relevant parameter in the problem. For the important case that $a\alpha_0 \gg 1$, we have $a_s \approx a$.[13] The total scattering cross-section σ is

$$\sigma \approx \sigma_0 = \frac{4\pi}{k^2}\frac{1}{1+\cot^2\delta_0} \approx \frac{4\pi a_s^2}{1+(ka_s)^2}. \tag{1.93}$$

In particular, we have

$$\sigma(E=0) = 4\pi a_s^2; \tag{1.94}$$

for the hard sphere with $a_s = a$, we find a fourfold larger scattering cross-section than classically expected, $\sigma_{\mathrm{cl}} = \pi a^2$.

1.9.1 Bound States and Resonances

We want to examine the analytical properties of the scattering matrix (with bound states and scattering resonances) discussed in Chapter 1.8 in more detail using the example of low-energy s-wave scattering. The scattering phase can be expressed in terms of the scattering length a_s as

$$S_0 - 1 = \frac{2i}{\cot\delta_0 - i} \approx \frac{2ka_s}{i - ka_s} \qquad (\text{for } ka \ll 1). \tag{1.95}$$

The scattering matrix $S_0(E)$ has a pole at $k = i/a_s$ or $\kappa = -ik = a_s^{-1} > 0$ as long as $a_s > 0$ and $a \ll a_s$.[14] Thus, one obtains a (weakly) bound state at the energy $E = -E_B = -\hbar^2/2ma_s^2$. One can also reverse the argument and say that a weakly bound state in the potential generates a large positive scattering length $a_s \gg a > 0$, i.e., a weakly bound state repels a low-energy scattering particle. Calculating the total scattering cross-section, cf. (1.93),

$$\sigma \approx \sigma_0 \approx \frac{2\pi\hbar^2/m}{E+E_B}, \quad E_B \gtrsim 0. \tag{1.96}$$

---

[13] For the hard sphere, $R_l(a) = 0$, thus $\alpha_l = \infty$, $a_s = a > 0$ and $\cot\delta_0 = -1/ka$. For small ka, we have $\delta_0 \approx -ka < 0$. The negative phase shift was to be expected, as it is a repulsive potential.

[14] That the condition $a \ll a_s$ must be satisfied is evident from the example of the hard sphere. It holds $a = a_s$ but of course the potential has no bound state and thus $S_0 = e^{2i\delta_0}$ has no pole.

one obtains the remarkable result that the energy of the weakly bound state completely determines the low-energy scattering cross-section.

Analogously, one obtains a resonance in the s-channel, see (1.90), when

$$\cot\delta_0 = 0 \Rightarrow 1 + a\alpha_0(E_r) = 0. \tag{1.97}$$

For a resonance, the condition $\Gamma_r < E_r$ must also hold, which guarantees a (albeit broad) resonance maximum. With

$$\begin{aligned}\cot\delta_0(E) &= \frac{1}{k_r a}\,\frac{\overbrace{1 + a\alpha_0(E_r)}^{=0} + a\alpha_0'(E_r)(E-E_r)}{\underbrace{-a\alpha_0(E_r)}_{=1}} \\ &\approx -\frac{2}{\Gamma_r}(E-E_r) \end{aligned}\tag{1.98}$$

we obtain the condition

$$\Gamma_r = -\frac{2k_r a}{a\alpha_0'(E_r)} = -\frac{2k_r}{\alpha_0'(E_r)} < \frac{\hbar^2 k_r^2}{2m} = E_r, \tag{1.99}$$

$$\Rightarrow \left|\frac{\partial\alpha_0}{\partial k^2}\right| > \frac{2}{k_r} \tag{1.100}$$

for the formation of a resonance in the s-channel.

Since the resonances in the s-channel are usually not very pronounced due to the strict condition (1.100), we next examine the case $l > 0$. We have already seen (1.91), that scattering for $l > 0$ is generally small,

$$\sigma_l = \frac{4\pi}{k^2}\frac{(2l+1)}{1+\cot^2\delta_l} = \frac{4\pi}{k^2}(2l+1)\sin^2\delta_l \overset{(k\to 0)}{\propto} a^2(ak)^{4l}. \tag{1.101}$$

However, near a resonance, $\cot\delta_l \approx 0$ and σ_l goes through a maximum with

$$\sigma_l = \frac{4\pi}{k_r^2}(2l+1). \tag{1.102}$$

According to (1.90), we find resonances at

$$l + 1 + a\alpha_l(E_r) = 0. \tag{1.103}$$

For the width of the resonance, we obtain[15]

$$\Gamma_r = -\frac{2k_r(ak_r)^{2l}}{[(2l-1)!!]^2\alpha_l'(E_r)} \propto k_r^{2l+1}; \tag{1.104}$$

---

[15] We use that the expression $l - a\alpha_l$ in the denominator of

$$\cot\delta_l \approx \frac{(2l+1)!!(2l-1)!!}{(k_r a)^{2l+1}}\,\frac{l+1+a\left[\alpha_l(E_r)+\alpha_l'(E_r)(E-E_r)\right]}{l-a\alpha_l(E_r)} = -\frac{2}{\Gamma_r}(E-E_r)$$

can be replaced by $2l+1$ due to (1.103).

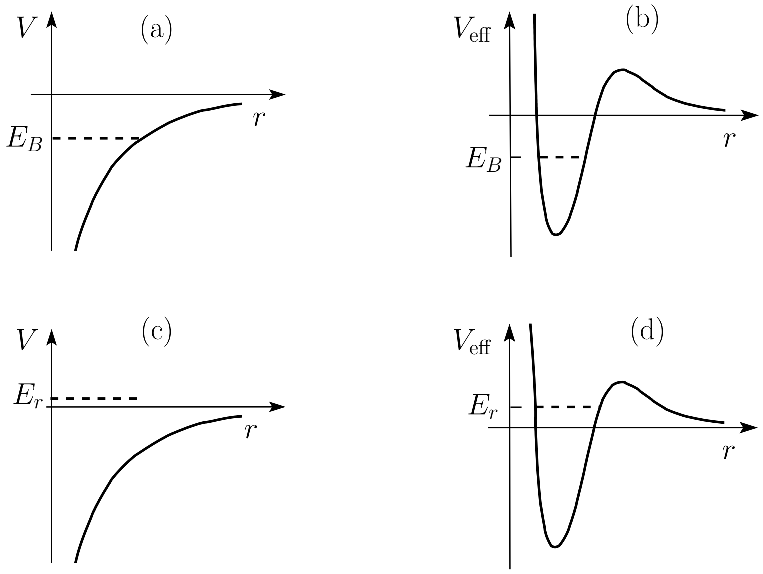

Figure 1.9: Bound states (a,b) and resonances (c,d): (a) Bound state for $l = 0$. (b) Bound state for $l > 0$, with the potential $V(r)$ replaced by the effective potential with centrifugal barrier $\hbar^2 l(l+1)/2mr^2$. (c) In the s-wave sector, the resonances are broad, mostly undefined with $\Gamma_r > E_r$. A defined resonance with $\Gamma_r < E_r$ requires that $|\alpha_0'(E_r)|$ is large. (d) For $l > 0$, sharp resonances arise, as the decay of the state is suppressed by the presence of the centrifugal barrier. The resonances are sharper the smaller k_r, the larger l, and the larger $\alpha_l'(E_r)$ are.

i.e., the smaller k_r, the larger $l \geq 1$ and the larger $\alpha_l'(E_r)$, the sharper the resonance. Note that for $l > 0$, $\Gamma_r \ll E_r \propto k_r^2$ as $k_r \to 0$. For $l = 0$, on the other hand, E_r vanishes faster than Γ_r and thus $\alpha_0'(E_r)$ must become large in the denominator to preserve the visibility of the resonance, cf. (1.100).

Chapter 2

Identical Particles

When we want to describe multiple identical particles in quantum mechanics, we must introduce the principle of 'indistinguishability' of similar particles, which has no counterpart in classical mechanics. In classical mechanics, similar particles, despite having identical physical properties, do not lose their individuality; in principle, we can mark each particle and thus identify them. In fact, the markings are even superfluous since we can follow the trajectories of the particles and therefore identify them—classically, the physics of distinguishable and identical particles is the same.

In quantum mechanics, we can neither mark the particles nor follow their trajectories, a consequence of the Heisenberg uncertainty principle. Thus, in quantum mechanics, there is fundamentally no way to track a single particle among identical particles separately and thereby distinguish the particles. A consistent consideration of the indistinguishability of particles produces astonishing physical effects, which we will describe below.

2.1 Description of N Particles

We start with the problem of describing N (distinguishable) particles. The concepts of wave functions and operators are generalized in the obvious way from single to many-particle systems:

- The wave functions depend on the N particle coordinates, for example, on position and spin coordinates $\boldsymbol{r}_1, s_1; \ldots; \boldsymbol{r}_N, s_N$, or in compact notation $x_1, \ldots, x_N$ with $x_i = (\boldsymbol{r}_i, s_i)$,

  $$\Psi(x_1, \ldots, x_N) = \langle x_1, \ldots, x_N | \Psi \rangle; \tag{2.1}$$

  correspondingly, we define a Hilbert space $\mathcal{H}$ over the complex-valued functions

$\Psi(x_1, \ldots, x_N)$ of N arguments x_N with the inner product

$$\langle \Psi | \Phi \rangle = \int dx_1 \cdots dx_N \, \Psi^*(x_1, \ldots, x_N) \Phi(x_1, \ldots, x_N). \tag{2.2}$$

The canonical basis in $\mathcal{H}$ is the product basis generated from a single-particle basis $\{\varphi_k(x)\}$,

$$\Psi_{k_1,\ldots,k_N}(x_1, \ldots, x_N) = \varphi_{k_1}(x_1) \cdots \varphi_{k_N}(x_N). \tag{2.3}$$

Of course, other bases are also possible.

- The operators act on the N-particle wave functions. The single-particle operators A are given by

$$A = \sum_{i=1}^{N} a_i, \tag{2.4}$$

where a_i acts only on the i-th particle. In the product basis, this looks as follows:

$$\begin{aligned} \langle x_1, \ldots, x_N | A \Psi \rangle &= A \Psi(x_1, \ldots, x_N) \qquad (2.5) \\ &= [a \varphi_{k_1}(x_1)] \varphi_{k_2}(x_2) \ldots \varphi_{k_N}(x_N) \\ &+ \varphi_{k_1}(x_1) [a \varphi_{k_2}(x_2)] \ldots \varphi_{k_N}(x_N) + \cdots . \end{aligned}$$

Mathematically, this means that the operator a_i acts as $\cdots \otimes I \otimes a \otimes I \otimes \cdots$ in the Hilbert space $\mathcal{H}_N = \mathcal{H} \otimes \mathcal{H} \otimes \cdots = \mathcal{H}^{\otimes N}$.

Operators can, of course, also act on two (or more) particles simultaneously, thereby creating interactions between the particles, for example, pair interactions,

$$V = \frac{1}{2} \sum_{i \neq j} v_{ij}, \qquad v_{ij} \text{ acts only on particle pairs } i, j. \tag{2.6}$$

As an example, we consider N particles in $\mathbb{R}^3$ without spin.

- The product basis is constructed from the single-particle basis $\{|\varphi_{\boldsymbol{k}_i}\rangle\}$,

$$|\boldsymbol{k}_1, \ldots, \boldsymbol{k}_N\rangle = |\varphi_{\boldsymbol{k}_1}\rangle \otimes |\varphi_{\boldsymbol{k}_2}\rangle \otimes \cdots |\varphi_{\boldsymbol{k}_N}\rangle; \tag{2.7}$$

in the position representation, we have

$$\begin{aligned} \langle \boldsymbol{r}_i | \varphi_{\boldsymbol{k}_i} \rangle &= \varphi_{\boldsymbol{k}_i}(\boldsymbol{r}_i), \\ \langle \boldsymbol{r}_1, \ldots, \boldsymbol{r}_N | \boldsymbol{k}_1, \ldots, \boldsymbol{k}_N \rangle &= \varphi_{\boldsymbol{k}_1}(\boldsymbol{r}_1) \cdots \varphi_{\boldsymbol{k}_N}(\boldsymbol{r}_N). \end{aligned} \tag{2.8}$$

- The plane wave basis, (Ω is the quantization volume)

$$\begin{aligned}\varphi_{\boldsymbol{k}}(\boldsymbol{r}) &= e^{i\boldsymbol{k}\cdot\boldsymbol{r}}/\sqrt{\Omega},\\ \langle \boldsymbol{r}_1,\ldots,\boldsymbol{r}_N|\boldsymbol{k}_1,\ldots,\boldsymbol{k}_N\rangle &= \prod_i e^{i\boldsymbol{k}_i\cdot\boldsymbol{r}_i}/\sqrt{\Omega},\end{aligned} \tag{2.9}$$

  spans the product Hilbert space

$$\mathcal{H}^{\otimes N} = L^2(\mathbb{R}^3)\otimes\cdots\otimes L^2(\mathbb{R}^3) = L^2(\mathbb{R}^3)^{\otimes N} \tag{2.10}$$

- Examples of operators are (except for the interaction, all are single-particle operators)

  - the (total) momentum

$$\boldsymbol{P} = \sum_i \boldsymbol{p}_i, \quad \boldsymbol{p}_i = \frac{\hbar}{i}\boldsymbol{\nabla}_i, \tag{2.11}$$

  - the (total) energy

$$\begin{aligned} H_0 &= \sum_i \frac{p_i^2}{2m}, \quad \text{for free particles,}\\ H &= H_0 + \frac{1}{2}\sum_{i\neq j} V(\boldsymbol{r}_i-\boldsymbol{r}_j), \quad \text{for interacting particles,}\end{aligned} \tag{2.12}$$

  - the density

$$\rho(\boldsymbol{r}) = \sum_i \delta^{(3)}(\boldsymbol{r}-\boldsymbol{r}_i), \tag{2.13}$$

  - the current density

$$\boldsymbol{j}(\boldsymbol{r}) = \sum_i \left[\frac{\boldsymbol{p}_i}{2m}\delta^{(3)}(\boldsymbol{r}-\boldsymbol{r}_i) + \delta^{(3)}(\boldsymbol{r}-\boldsymbol{r}_i)\frac{\boldsymbol{p}_i}{2m}\right]. \tag{2.14}$$

  - Thus, we form the expectation values

$$\begin{aligned}\langle \boldsymbol{P}\rangle &= \sum_i \int d^3r_1\cdots d^3r_N\, \Psi^*(\boldsymbol{r}_1,\ldots,\boldsymbol{r}_N)\frac{\hbar}{i}\boldsymbol{\nabla}_i\Psi(\boldsymbol{r}_1,\ldots,\boldsymbol{r}_N),\\ &= \sum_i \int d^3r_i\, \varphi^*_{\boldsymbol{k}_i}(\boldsymbol{r}_i)\frac{\hbar}{i}\boldsymbol{\nabla}_i\varphi_{\boldsymbol{k}_i}(\boldsymbol{r}_i) = \sum_i \hbar\boldsymbol{k}_i,\end{aligned} \tag{2.15}$$

$$\begin{aligned}\langle H_0\rangle &= \sum_i \frac{\hbar^2 k_i^2}{2m}, && (2.16)\\ \langle H\rangle &= \langle H_0\rangle + \frac{1}{2}\sum_{i\neq j}\int d^3r_1\cdots d^3r_N \\ &\qquad \times \Psi^*(\boldsymbol{r}_1,\ldots,\boldsymbol{r}_N)V(\boldsymbol{r}_i-\boldsymbol{r}_j)\Psi(\boldsymbol{r}_1,\ldots,\boldsymbol{r}_N)\\ &= \langle H_0\rangle + \frac{1}{2}\sum_{i\neq j}\int d^3r_i\,d^3r_j \\ &\qquad \times \varphi^*_{\boldsymbol{k}_i}(\boldsymbol{r}_i)\varphi^*_{\boldsymbol{k}_j}(\boldsymbol{r}_j)V(\boldsymbol{r}_i-\boldsymbol{r}_j)\varphi_{\boldsymbol{k}_i}(\boldsymbol{r}_i)\varphi_{\boldsymbol{k}_j}(\boldsymbol{r}_j)\\ &= \langle H_0\rangle + \frac{1}{2}\sum_{i\neq j}\int d^3r_i\,d^3r_j\,|\varphi_{\boldsymbol{k}_i}(\boldsymbol{r}_i)|^2V(\boldsymbol{r}_i-\boldsymbol{r}_j)|\varphi_{\boldsymbol{k}_j}(\boldsymbol{r}_j)|^2. && (2.17)\end{aligned}$$

2.2 Description of N Identical Particles

When we write the wave function $\Psi(x_1,\ldots,x_N)$ of a many-particle system, we use the term 'first particle' for the particle that is designated by the first argument, 'second particle' for the particle designated by the second argument, and so on. The question arises whether this does not mark the particles and violate the fundamental indistinguishability. The answer is that we need the markings/names to be able to describe the system mathematically at all. However, this does not necessarily lead to a physical distinguishability. We must simply ensure that we treat all particles as absolutely equivalent. In particular, no (physical) operator may exist that allows for the identification of the particles. This means that all allowed operators are symmetric. In the coordinate representation, the allowed operators are, for example, symmetric in the coordinates,

$$A(x_1,\ldots,x_N) = A(x_{\pi(1)},\ldots,x_{\pi(N)}), \tag{2.18}$$

with $\pi \in S_N$ being any permutation,

$$\begin{pmatrix} 1 & 2 & 3 & \cdots & N \\ \pi(1) & \pi(2) & \pi(3) & \cdots & \pi(N) \end{pmatrix}, \tag{2.19}$$

which maps the upper row to the lower one.

Next, we consider the expectation values of A,

$$\begin{aligned}\langle A\rangle &= \int dx_1\cdots dx_N\,\Psi^*(x_1,\ldots,x_N)A(x_1,\ldots,x_N)\Psi(x_1,\ldots,x_N) && (2.20)\\ &= \int dx_1\cdots dx_N\,\Psi^*(x_1,\ldots,x_N)A(x_{\pi(1)},\ldots,x_{\pi(N)})\Psi(x_1,\ldots,x_N)\\ &= \int dx_1\cdots dx_N\,\Psi^*(x_{\pi^{-1}(1)},\ldots,x_{\pi^{-1}(N)})A(x_1,\ldots,x_N)\Psi(x_{\pi^{-1}(1)},\ldots,x_{\pi^{-1}(N)});\end{aligned}$$

here, π^{-1} is the inverse permutation of π. Clearly, we can interchange the arguments in Ψ arbitrarily, since A is symmetric, $\langle A\rangle$ remains invariant. The invariance of $\langle A\rangle$ thus does not give us any condition on the behavior of the wave functions Ψ under the interchange of arguments.

We can formalize the above discussion somewhat: Analogous to the translation and rotation representations in Hilbert space,

$$\begin{aligned} &\text{Translations:} && U_{\boldsymbol{a}}\,\Psi(\boldsymbol{r}) = e^{-i\boldsymbol{a}\cdot\boldsymbol{p}/\hbar}\Psi(\boldsymbol{r}) = \Psi(\boldsymbol{r}-\boldsymbol{a}), \\ &\text{Rotations:} && U_{\boldsymbol{\omega}}\,\Psi(\boldsymbol{r}) = e^{-i\boldsymbol{\omega}\cdot\boldsymbol{L}/\hbar}\Psi(\boldsymbol{r}) = \Psi(\mathbf{R}_{-\boldsymbol{\omega}}\,\boldsymbol{r}), \end{aligned} \tag{2.21}$$

we introduce the following (unitary) representation of the permutation group S_N [1]

$$U_\pi\,\Psi(x_1,\dots,x_N) = \Psi(x_{\pi(1)},\dots,x_{\pi(N)}). \tag{2.22}$$

With the definition of U_π, we can define symmetric operators as follows: An operator A is symmetric if for all $\pi\in S_N$ it holds that

$$U_\pi A U_\pi^{-1} = A \qquad \Leftrightarrow \qquad [A,U_\pi] \;=\; 0. \tag{2.23}$$

The central question we will address next is how the permuted wave function $U_\pi\Psi$ relates to Ψ. Clearly, U_π defines a representation of S_N in $\mathcal{H}$. Furthermore, for all (allowed, i.e., symmetric) operators A, in particular also for the Hamiltonian H, it holds that $[H,U_\pi]=0$. This means that we can diagonalize every operator A and U_π simultaneously.

Let now $A\Psi_a = a\Psi_a$, then also $AU_\pi\Psi_a = aU_\pi\Psi_a$ and $\{U_\pi\Psi_a|\pi\in S_N\}$ spans the eigenspace Eig_a for A. [2] In the eigenspace Eig_a with $\dim\mathrm{Eig}_a = D_a$, a D_a-dimensional representation of S_N can be generated. This representation can then be decomposed into irreducible representations of S_N. In general, any irreducible representation of dimension $d\le D_a$ can occur. However, if $d>1$, all energy eigenstates of H (and also the eigenstates of any operator A) are d-fold degenerate. This degeneracy is called exchange degeneracy, as it arises solely due to the indistinguishability of the particles. This degeneracy has measurable consequences, as it increases, for example, the specific heat or provides a mixing entropy of two identical gases[3]. It is now an experimental fact that no exchange degeneracy exists for any particle. Therefore, we do not need to apply the entire machinery of group theory to this problem and only need to consider the one-dimensional representations. There are two of these in S_N, namely the symmetric representation S and the antisymmetric representation A. We denote the corresponding invariant Hilbert spaces by $\mathcal{H}_{\mathcal{S}/\mathcal{A}}$.

---

[1] Since S_N is not a continuous group, there is no infinitesimal generator.

[2] In the case $A=H$, we consider Ψ_E with $H\Psi_E = E\Psi_E$ and note that $U_\pi\Psi_E$ also lies in Eig_E.

[3] The absence of exchange degeneracy in mixtures is referred to in statistical mechanics as the Gibbs paradox.

2.3 Fermions and Bosons

Let $\mathcal{H}$ be the Hilbert space of N-particle functions. Only the sectors of $\mathcal{H}$ are relevant:

$$\begin{aligned} \mathcal{H}_{\mathcal{A}} &= \{\mathcal{A}\,\Psi | \Psi \in \mathcal{H}\}, \\ \mathcal{H}_{\mathcal{S}} &= \{\mathcal{S}\,\Psi | \Psi \in \mathcal{H}\}, \end{aligned} \tag{2.24}$$

where

$$\mathcal{A} = \frac{1}{N!} \sum_{\pi \in S_N} (-1)^\pi U_\pi, \tag{2.25}$$

$$\mathcal{S} = \frac{1}{N!} \sum_{\pi \in S_N} U_\pi, \tag{2.26}$$

the (anti-)symmetrization operators with $(-1)^\pi$ being the signature of π, see B.1. The normalization has been chosen such that the operators are projectors with $\mathcal{S}^2 = \mathcal{S}$ and $\mathcal{A}^2 = \mathcal{A}$. For the functions in $\mathcal{H}_{\mathcal{A}}$, it holds that

$$\Psi(x_{\pi(1)}, \ldots, x_{\pi(N)}) = (-1)^\pi \Psi(x_1, \ldots, x_N), \quad \forall \pi \in S_N, \tag{2.27}$$

for those in $\mathcal{H}_{\mathcal{S}}$ it holds

$$\Psi(x_{\pi(1)}, \ldots, x_{\pi(N)}) = \Psi(x_1, \ldots, x_N). \tag{2.28}$$

In nature, only a small part of $\mathcal{H}$ is realized, namely the symmetric and antisymmetric parts. We call particles whose wave functions lie in $\mathcal{H}_{\mathcal{A}}$ ($\mathcal{H}_{\mathcal{S}}$) and are thus antisymmetric (symmetric) under the interchange of arguments fermions (bosons).

$$\begin{array}{ccc} \mathcal{H}_{\mathcal{A}} & & \mathcal{H}_{\mathcal{S}} \\ \text{antisymmetric} & \leftrightarrow & \text{symmetric} \\ \text{Fermions} & & \text{Bosons} \end{array}$$

This leads to the problem of which Hilbert space, $\mathcal{H}_{\mathcal{A}}$ or $\mathcal{H}_{\mathcal{S}}$, one should choose for a particular type of particle, or in other words, whether the particles are fermions or bosons. The answer is given by the spin-statistics theorem.

2.4 Spin and Statistics

The following relationship between particle spin and the symmetry properties of the wave functions under S_N can be proven in relativistic quantum field theory:

$$\begin{array}{ccc} \text{Half-integer spin} & & \text{Integer spin} \\ \text{Fermions} & \leftrightarrow & \text{Bosons} \end{array} \tag{2.29}$$

Examples of particles with the corresponding properties are:

Fermions

- Leptons $e^-,\ \mu,\ \tau$
- Lepton neutrinos $\nu_e,\ \nu_\mu,\ \nu_\tau$
- Baryons $p, n, \Lambda, \Sigma, \Xi, \cdots$ with 3 quarks each
- ^{3}He

All fermions listed here have spin-1/2.

Bosons

- Higgs (spin-0)
- Mesons π, K with spin-0, or ρ, ω with spin-1, each with two quarks.
- Gauge bosons (Yang-Mills) of the
  - electroweak interactions: $\gamma, W^\pm, Z^0$ with spin-1.
  - strong interactions: gluons (spin-1).
- ^{4}He (spin-0).

2.5 Applications

2.5.1 Wave Functions of Two (Spin-1/2) Fermions

We consider two spin-1/2 fermions, e.g., two electrons. Let $\Psi(\boldsymbol{r}_1, s_1; \boldsymbol{r}_2, s_2) \in \mathcal{H}$ be an element of the product basis

$$\Psi_{\mu,\nu}(x_1, x_2) = \varphi_\mu(x_1)\varphi_\nu(x_2). \tag{2.30}$$

The physical states are

$$\begin{aligned}\Psi^{\mathcal{A}}_{\mu,\nu}(x_1, x_2) = \sqrt{2}\mathcal{A}\Psi_{\mu,\nu} &= \frac{1}{\sqrt{2!}} \sum_{\pi \in S_2} (-1)^\pi U_\pi \Psi_{\mu,\nu}(x_1, x_2) \\ &= \frac{1}{\sqrt{2}} \big[\Psi_{\mu,\nu}(x_1, x_2) - \Psi_{\mu,\nu}(x_2, x_1)\big] \\ &= \frac{1}{\sqrt{2}} \big[\varphi_\mu(x_1)\varphi_\nu(x_2) - \varphi_\mu(x_2)\varphi_\nu(x_1)\big]. \end{aligned} \tag{2.31}$$

If $\mu = \nu$, it follows that $\mathcal{A}\Psi_{\mu,\mu} = 0$, thus no two fermions can be in the same state: This is the famous Pauli exclusion principle. The Pauli exclusion principle for fermions also holds generally for N fermions.

2.5.2 Spin and Orbital Wave Functions

Next, we separate the spin and orbital components for the wave function Ψ of two spin-1/2 fermions,

$$\Psi(\boldsymbol{r}_1, s_1; \boldsymbol{r}_2, s_2) = \varphi(\boldsymbol{r}_1, \boldsymbol{r}_2)\chi(s_1, s_2). \tag{2.32}$$

The total wave function Ψ is antisymmetric if

$$\left.\begin{array}{cc} \varphi & \text{symmetric} \\ \chi & \text{antisymmetric} \end{array}\right\} \text{ or } \left\{\begin{array}{cc} \varphi & \text{antisymmetric} \\ \chi & \text{symmetric} \end{array}\right. \tag{2.33}$$

is. The spin part $\chi(s_1, s_2)$ can be reduced according to $\boldsymbol{S} = \boldsymbol{S}_1 + \boldsymbol{S}_2$, $\mathcal{H}_{1/2} \otimes \mathcal{H}_{1/2} = \mathcal{H}_0 \oplus \mathcal{H}_1$. In the spin Hilbert space $\mathcal{H}_0$, the singlet state $\chi_{0,0}(s_1, s_2)$ is antisymmetric in s_1, s_2,[4]

$$\begin{aligned} \chi_{0,0}(s_1, s_2) &= \langle s_1, s_2 | 0, 0\rangle \\ &= \frac{1}{\sqrt{2}}\big[\langle s_1|\uparrow\rangle\langle s_2|\downarrow\rangle - \langle s_1|\downarrow\rangle\langle s_2|\uparrow\rangle\big] \\ &= \frac{1}{\sqrt{2}}\big[\chi_\uparrow(s_1)\chi_\downarrow(s_2) - \chi_\downarrow(s_1)\chi_\uparrow(s_2)\big]. \end{aligned} \tag{2.34}$$

The spin Hilbert space $\mathcal{H}_1$ is spanned by the three states $\chi_{1,1}$, $\chi_{1,0}$, and $\chi_{1,-1}$. These are the symmetric triplet states,

$$\begin{aligned} \chi_{1,1}(s_1, s_2) &= \langle s_1, s_2 | 1, 1\rangle = \chi_\uparrow(s_1)\chi_\downarrow(s_2), \\ \chi_{1,0}(s_1, s_2) &= \langle s_1, s_2 | 1, 0\rangle \\ &= \frac{1}{\sqrt{2}}\big[\chi_\uparrow(s_1)\chi_\downarrow(s_2) + \chi_\downarrow(s_1)\chi_\uparrow(s_2)\big], \\ \chi_{1,-1}(s_1, s_2) &= \langle s_1, s_2 | 1, -1\rangle = \chi_\downarrow(s_1)\chi_\downarrow(s_2). \end{aligned} \tag{2.35}$$

The above symmetric and antisymmetric spin functions χ are combined with appropriately symmetrized orbital functions φ. We thus define the symmetrized combinations

$$\begin{array}{ll} \varphi \text{ symmetric:} & \varphi_{\mathcal{S}} = \big[\varphi_1(\boldsymbol{r}_1)\varphi_2(\boldsymbol{r}_2) + \varphi_2(\boldsymbol{r}_1)\varphi_1(\boldsymbol{r}_2)\big]/\sqrt{2}, \\ \varphi \text{ antisymmetric:} & \varphi_{\mathcal{A}} = \big[\varphi_1(\boldsymbol{r}_1)\varphi_2(\boldsymbol{r}_2) - \varphi_2(\boldsymbol{r}_1)\varphi_1(\boldsymbol{r}_2)\big]/\sqrt{2}. \end{array}$$

Thus, we can simultaneously diagonalize S^2, S_z and S_N and obtain wave functions Ψ with defined spin and defined symmetry. Here, the spin determines the symmetry of χ and of φ:

$$\begin{aligned} S &= 1 \Rightarrow \chi = \text{symmetric}, \quad \varphi = \text{antisymmetric}; \\ S &= 0 \Rightarrow \chi = \text{antisymmetric}, \quad \varphi = \text{symmetric}. \end{aligned} \tag{2.36}$$

A similar principle generally applies for N spin-1/2 fermions, see Appendix B: from Weyl's theorem and the Pauli principle, it follows that the total spin S determines the type (the representation under the permutation group) of the orbital wave function. However, the type essentially determines the value of the 'exchange integrals', i.e., the energy of the state. Thus, the total spin indirectly influences the energy of a state. Magnetic properties such as ferromagnetism are therefore consequences of the relationship between spin and orbital type.

---

[4] It holds that $\chi_\uparrow(s = \uparrow) = 1$ and $\chi_\uparrow(s = \downarrow) = 0$.

Clearly, fermions interfere with each other due to the Pauli principle, and the question arises whether we always need to antisymmetrize all the electrons in the world. Fortunately, this is not the case. Consider two non-interacting electrons in Aachen and Cologne, described by single-particle states $\varphi_A(\boldsymbol{r}_1, s_1)$ and $\varphi_K(\boldsymbol{r}_1, s_1)$ with $\int dx\, \varphi_A^* \varphi_K \approx 0$, which (correctly) are described by the antisymmetric wave function

$$\Psi \approx \frac{1}{\sqrt{2}}\big[\varphi_A(x_1)\varphi_K(x_2) - \varphi_K(x_1)\varphi_A(x_2)\big] \tag{2.37}$$

Let $A(x)$ be a local single-particle operator. Then its expectation value is given by

$$\begin{aligned}\langle A\rangle = \frac{1}{2}\int dx_1 dx_2 \Big[&\varphi_A^*(x_1)\varphi_K^*(x_2)\, A(x_1)\, \varphi_A(x_1)\varphi_K(x_2)\\ &+ \varphi_K^*(x_1)\varphi_A^*(x_2)\, A(x_1)\, \varphi_K(x_1)\varphi_A(x_2)\\ &\left.\begin{aligned}&-\varphi_A^*(x_1)\varphi_K^*(x_2)\, A(x_1)\, \varphi_K(x_1)\varphi_A(x_2)\\ &-\varphi_K^*(x_1)\varphi_A^*(x_2)\, A(x_1)\, \varphi_A(x_1)\varphi_K(x_2)\Big]\end{aligned}\right\} \approx 0\\ \approx \langle A\rangle_A + \langle A\rangle_K.&\end{aligned} \tag{2.38}$$

It is the interference terms that carry the symmetrization properties.[5] For non-overlapping wave functions, these terms vanish, and we can do without (anti-)symmetrization: the results in Aachen depend only on the wave function in Aachen and analogously for Cologne.

2.5.3 Wave Function of Two (Spin-0) Bosons

For two bosons, the product wave function $\Psi_{\mu,\nu}$ must be symmetrized. The allowed wave functions are therefore given by

$$\Psi^{\mathcal{S}}_{\mu,\nu}(x_1,x_2) = \sqrt{2}\mathcal{S}\Psi_{\mu,\nu} = \frac{1}{\sqrt{2}}\big[\varphi_\mu(x_1)\varphi_\nu(x_2) + \varphi_\mu(x_2)\varphi_\nu(x_1)\big]. \tag{2.39}$$

For bosons, $\mu = \nu$ is now allowed, and the wave function of two bosons in the same state is given by (note the new normalization, cf. (2.53) later)

$$\Psi^{\mathcal{S}}_{\mu,\mu}(x_1,x_2) = \varphi_\mu(x_1)\varphi_\mu(x_2) \overset{x_1=x_2=x}{\longrightarrow} \varphi_\mu(x)^2 \neq 0, \tag{2.40}$$

and both bosons are allowed to sit in the same place.

---

[5] Note that for bosons, the last two terms in (2.38) are added.

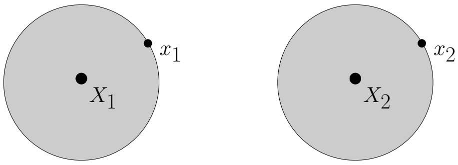

Figure 2.1: On the symmetry of the wave function of two hydrogen atoms: X_1, X_2 denote the coordinates of the protons, x_1, x_2 the coordinates of the electrons.

Note: Fermions avoid each other, bosons like each other

$$\begin{aligned}\Psi^{\mathcal{S}/\mathcal{A}}_{1,2}(x_1,x_2) &= \frac{1}{\sqrt{2}}\Big[\varphi_1(x_1)\varphi_2(x_2) \mp \varphi_2(x_1)\varphi_1(x_2)\Big] \\ &\downarrow x_1 = x_2 = x \\ &= \begin{cases} 0, & \text{Fermions,} \\ \sqrt{2}\varphi_1(x)\varphi_2(x), & \text{Bosons.} \end{cases} \end{aligned} \tag{2.41}$$

□

2.5.4 Composite Particles

Consider two H atoms as sketched in Figure 2.1. The total wave function $\Psi(x_1, X_1, x_2, X_2)$ must be antisymmetric in the electron coordinates x_1, x_2 and also antisymmetric in the coordinates X_1, X_2 of the protons. Interchanges of x_1, X_1; x_1, X_2; x_2, X_1; x_2, X_2 are not subject to any regulations. Since the exchanged particles are not identical, such exchanges are also not physically meaningful. The interchange of the atoms yields (first the electrons, then interchange the protons)

$$\begin{aligned}\Psi(x_2, X_2, x_1, X_1) &= -\Psi(x_1, X_2, x_2, X_1) \\ &= (-1)^2\Psi(x_1, X_1, x_2, X_2).\end{aligned} \tag{2.42}$$

From this, we find that the H atoms, which consist of 2 fermions each, behave like bosons. Note the compatibility with the theorem of spin and statistics from Chapter 2.4,

$$\text{H-atom} \Rightarrow \ \mathcal{H}_{1/2} \otimes \mathcal{H}_{1/2} = \mathcal{H}_0 \oplus \mathcal{H}_1; \tag{2.43}$$

thus, the H atoms have an integer spin and are therefore bosons. A similar treatment applies to other composite particles, for example

$$\begin{aligned} {}^3\text{He} &= 2p + 1n + 2e = \text{Fermion} \to \text{pairing transition,} \\ {}^4\text{He} &= 2p + 2n + 2e = \text{Bosons} \to \lambda - \text{transition;} \end{aligned} \tag{2.44}$$

both He liquids become superfluid at low temperatures. While ^{4}He ‘Bose-condenses’ (at low temperatures $T < 2.17\,\mathrm{K}$ all ^{4}He atoms occupy the same single-particle state), the fermionic ^{3}He atoms must first pair (→ bosons) to then transition into the superfluid state at the lowest temperatures $T \sim 10\,\mathrm{mK}$ via a so-called BCS (Bardeen Cooper Schrieffer) transition.

2.5.5 Symmetry under Time Evolution

Time evolution preserves symmetry, since let

$$U_\pi \Psi = (\pm)^\pi \Psi, \qquad \begin{matrix}\text{Bosons } (+), \\ \text{Fermions } (-),\end{matrix} \tag{2.45}$$

then we have

$$\begin{aligned} U_\pi \Psi(t+dt) &= U_\pi \Psi(t) + U_\pi[\partial_t \Psi(t)]dt \\ &= (\pm)^\pi \Psi - iU_\pi (H/\hbar)\Psi dt \\ &\quad \downarrow_{[H,U_\pi]=0} \\ &= (\pm)^\pi \Psi - i(H/\hbar)U_\pi \Psi dt && (2.46) \\ &= (\pm)^\pi[\Psi + (\partial_t \Psi)dt] = (\pm)^\pi \Psi(t+dt). && (2.47) \end{aligned}$$

2.5.6 Many-particle states of non-interacting identical particles

For non-interacting particles, we can write the Hamiltonian operator as

$$H = \sum_{i=1}^N H_0(x_i), \qquad x_i = (\boldsymbol{r}_i, s_i), \tag{2.48}$$

where H_0 denotes the single-particle Hamiltonian. With the single-particle solutions

$$H_0 \varphi_j = \varepsilon_j \varphi_j, \qquad \{\varphi_j\} \text{ a complete orthonormal system (COS)}, \tag{2.49}$$

we can define N-particle product eigenstates

$$\Psi(x_1, \ldots, x_N) = \varphi_{\alpha_1}(x_1)\varphi_{\alpha_2}(x_2)\cdots\varphi_{\alpha_N}(x_N) \tag{2.50}$$

for H. The total energy is then $E = \sum_i \varepsilon_{\alpha_i}$. Equation (2.50) describes an N-particle system in the states $\varphi_{\alpha_1}, \varphi_{\alpha_2}, \ldots \varphi_{\alpha_N}$, for example for $N = 4$ and V a potential well

$$\Psi_{1356} = \varphi_1(\boldsymbol{r}_1)\varphi_3(\boldsymbol{r}_2)\varphi_5(\boldsymbol{r}_3)\varphi_6(\boldsymbol{r}_4), \tag{2.51}$$

as illustrated in Figure 2.2.

Fermions: For fermions, we must antisymmetrize Ψ,

$$\begin{aligned} \Psi \mapsto \Psi_{\mathcal{A}} &= \frac{1}{\sqrt{N!}} \sum_{\pi \in S_N} (-1)^\pi \varphi_{\alpha_1}(x_{\pi(1)}) \cdots \varphi_{\alpha_N}(x_{\pi(N)}) \\ &= \frac{1}{\sqrt{N!}} \begin{vmatrix} \varphi_{\alpha_1}(x_1) & \cdots & \varphi_{\alpha_1}(x_N) \\ \varphi_{\alpha_2}(x_1) & \cdots & \varphi_{\alpha_2}(x_N) \\ \vdots & \vdots & \\ \varphi_{\alpha_N}(x_1) & \cdots & \varphi_{\alpha_N}(x_N) \end{vmatrix} = \frac{1}{\sqrt{N!}} \det \phi_{\alpha_i}(x_j); \end{aligned} \tag{2.52}$$

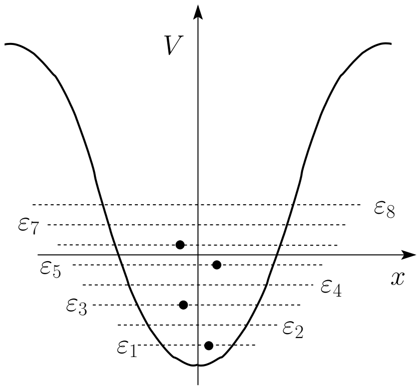

Figure 2.2: Occupation of a fermionic system in the state Ψ_{1356}. The Pauli principle (the symmetry of the wave function) allows at most one particle per state.

Here, the factor $(N!)^{-1/2}$ ensures the normalization of the many-particle wave function. The determinant in expression (2.52) is called the Slater determinant. If there is a pair $i \neq j$ with $\alpha_i = \alpha_j$, then $\Psi_{\mathcal{A}} \equiv 0$. Thus, the Pauli exclusion principle demands that no two fermions occupy the same state in spin and orbital.

Bosons: For bosons, we must symmetrize the wave function Ψ,

$$\Psi \mapsto \Psi_{\mathcal{S}} = \sqrt{\frac{1}{N! \prod_j n_j!}} \sum_{\pi \in S_N} \varphi_{\alpha_1}(x_{\pi(1)}) \cdots \varphi_{\alpha_N}(x_{\pi(N)}); \tag{2.53}$$

it is a simple exercise to show that the prefactor guarantees the normalization of the wave function. The degeneracy n_j indicates how many of the indices α_i have the same value j (where $\sum_j n_j = N$).

2.5.7 Fermi Sea

The electrons in solids are described in the simplest case by

- Core or valence electrons; these are electrons firmly bound to the atoms (or in atomic aggregates) and define full electron bands.
- Conduction electrons. These are quasi-free mobile electrons in partially filled bands, see Figure 2.3.

The bands are filled up to the Fermi level. If the Fermi level lies within a band, it is a metal; if the Fermi level lies within an energy gap, it is a semiconductor or an insulator.

The conduction electrons can be most simply described as a gas of free spin-1/2 fermions with the Hamiltonian operator $H_0 = p^2/2m$. The ground state $|\Phi_0\rangle$ ('Fermi sea') takes the form of a Slater determinant, where the low-energy states with $k \leq k_F$

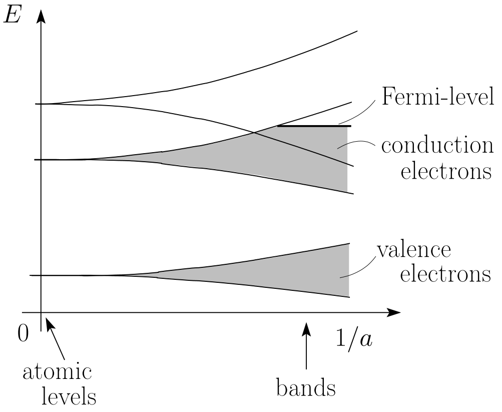

Figure 2.3: Electron states in solids form into bands. Well-separated atoms with $a \to \infty$, a being the lattice spacing, show a discrete spectrum. At finite (small) distances, the electrons can hop between the lattice sites, forming energy bands that are filled up to the Fermi level.

are occupied, with the Fermi sphere having radius k_F. The eigenstates of the single-particle Hamiltonian operator are plane waves $\phi_{\boldsymbol{k}} \propto e^{i\boldsymbol{k}\cdot\boldsymbol{r}}$. For the specific case that the particles are in the volume $\Omega = L^3$ with periodic boundary conditions, one obtains the quantization condition $\boldsymbol{k} = (2\pi/L)\mathbb{Z}^3$. The number of states in the Fermi sphere is

$$N = \frac{\text{Volume of the sphere}}{\text{Volume per lattice point}} = g_s \frac{(4\pi/3)k_F^3}{(2\pi/L)^3} \tag{2.54}$$

where the factor $g_s = 2$ accounts for spin degeneracy.[6] From (2.54), one obtains the relationship between the electron density $n = N/\Omega$ and the parameters $\varepsilon_F = p_F^2/2m$ (Fermi energy), $p_F = \hbar k_F$ (Fermi momentum), $k_F = \sqrt{2m\varepsilon_F}/\hbar$ (Fermi wave vector) of the Fermi gas given by

$$k_F^3 = \frac{6\pi^2}{g_s} n \tag{2.55}$$

The corresponding ground state energy is

$$E_0 = g_s \sum_{k<k_F} \frac{\hbar^2 k^2}{2m} = g_s \frac{L^3}{(2\pi)^3} \int_{k<k_F} d^3k \, \frac{\hbar^2 k^2}{2m} = N \frac{3}{5} \varepsilon_F . \tag{2.56}$$

Thus, one finds for the ground state energy density $e_0 = 3\varepsilon_F n/5$, which corresponds to the Fermi pressure $p = \partial E_0/\partial\Omega = e_0$ of the quantum gas at 0 K. The ground state energy $\propto N\varepsilon_F$ of N fermions is always high, as the particles avoid each other and thus will occupy high-energy states. We find the following energy scale in typical

---

[6] If one assumes infinitely high potential walls instead of periodic boundary conditions, such that $\phi_j(\boldsymbol{r})$ vanishes at the boundary, one obtains the single-particle wave functions $\phi_{\boldsymbol{k}'}(\boldsymbol{r}) = \prod_{i=1}^{3} \sin k_i' r_i$ with $k_i = \pi n_i/L$ and $n_i \in \mathbb{N}$. The number of states in the Fermi sphere is then given by $N = g_s V_{k_F}^{>}/(\pi/L)^3$ where $V_{k_F}^{>}$ is the volume of the Fermi sphere in the first octant with $V_{k_F}^{>} = (4\pi/3)k_F^3/8$. The result (2.54) (and thus also the following results) therefore remain unchanged.

metals: With

$$\begin{aligned} \varepsilon_F &= \frac{\hbar^2 k_F^2}{2m} = 3.81\,\mathrm{eV}\cdot k_F^2\,[\text{Å}^{-2}] \quad \text{and} \\ k_F &\approx \frac{\pi}{a}, \qquad a = \text{lattice constant} \approx 3\text{Å}, \end{aligned} \tag{2.57}$$

we obtain $k_F \sim 1$ Å^{-1} and $\varepsilon_F \sim$ several eV typically, which corresponds to several $10^4\,\mathrm{K}$. Thus, the kinetic energy of electrons in metals at room temperature is not $300\,\mathrm{K}$ but $\sim 30000\,\mathrm{K}$. The Fermi pressure corresponds to $\sim \varepsilon_F/a^3 \sim 10^6$ atm.

2.5.8 Bose Condensate

The ground state of the bosonic many-particle system (with spin-0) looks very different from the Fermi sea. The product state

$$\Psi_0 = \prod_{i=1}^{N} \varphi_0(\boldsymbol{r}_i) \tag{2.58}$$

with φ_0 being the single-particle ground state is already symmetric and $E_0 = N\varepsilon_0$: The bosons condense in the lowest energy state. This condensation phenomenon ultimately leads to the superfluidity of a bosonic system at low temperatures. Fermions can only condense if they first pair, for example, in the form of Cooper pairs during superconductivity in metals.[7]

2.5.9 Scattering of Identical Particles

Consider the collision/scattering of two identical particles. We separate into center-of-mass and relative coordinates $\boldsymbol{R} = \boldsymbol{r}_1 + \boldsymbol{r}_2$ and $\boldsymbol{r} = \boldsymbol{r}_1 - \boldsymbol{r}_2$. Thus, $\boldsymbol{R}$ is symmetric and $\boldsymbol{r}$ is antisymmetric in $\boldsymbol{r}_1$ and $\boldsymbol{r}_2$. We decompose the total wave function into spin and orbital components,

$$\Psi(x_1, x_2) = e^{i\boldsymbol{P}\cdot\boldsymbol{R}}\,\psi(\boldsymbol{r})\chi(s_1, s_2). \tag{2.59}$$

For distinguishable particles, the scattering solution has the asymptotic form

$$\psi(\boldsymbol{r}) \sim e^{i\boldsymbol{k}\cdot\boldsymbol{r}} + f_{\boldsymbol{k}}(\Omega_{\boldsymbol{r}})\frac{e^{ikr}}{r}. \tag{2.60}$$

Spin-0 Bosons: For bosons with spin-0 we have $\chi = 1$ and due to the symmetry of Ψ, it holds that $\psi(\boldsymbol{r}) = \psi(-\boldsymbol{r})$; accordingly, we must symmetrize the scattering solution and obtain

$$\psi \sim \left(e^{i\boldsymbol{k}\cdot\boldsymbol{r}} + e^{-i\boldsymbol{k}\cdot\boldsymbol{r}}\right) + [f_{\boldsymbol{k}}(\Omega_{\boldsymbol{r}}) + f_{\boldsymbol{k}}(\Omega_{-\boldsymbol{r}})]\frac{e^{ikr}}{r}. \tag{2.61}$$

---

[7] This pairing phenomenon is somewhat more complex in nature, and we refer to Chapter 5.2 and the corresponding standard literature on BCS (Bardeen-Cooper-Schrieffer) theory.

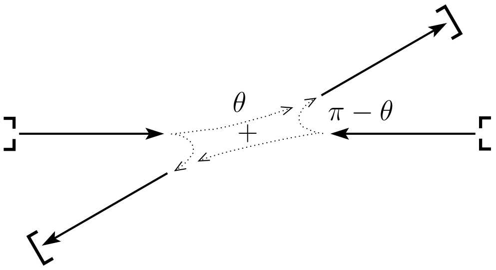

Figure 2.4: The symmetrization of the scattering wave function generates two trajectories with scattering angles θ and $\pi-\theta$ that can be coherently added.

For the differential cross section, we obtain

$$\begin{aligned}\frac{d\sigma}{d\Omega_{\boldsymbol{r}}} &= \left|f_{\boldsymbol{k}}(\Omega_{\boldsymbol{r}})+f_{\boldsymbol{k}}(\Omega_{-r})\right|^2 \\ &= \underbrace{\left|f_{\boldsymbol{k}}(\Omega_{\boldsymbol{r}})\right|^2+\left|f_{\boldsymbol{k}}(\Omega_{-\boldsymbol{r}})\right|^2}_{\text{classical terms}}+\underbrace{2\mathrm{Re}\left[f^*_{\boldsymbol{k}}(\Omega_{\boldsymbol{r}})f_{\boldsymbol{k}}(\Omega_{-\boldsymbol{r}})\right]}_{\text{interference terms}}. \qquad (2.62)\end{aligned}$$

The classical term is the addition of the cross sections for detecting one of the two particles (the detector cannot distinguish which particle arrives). The interference terms arise as a consequence of the symmetrization due to particle statistics.

For a central symmetric potential $V(r)$, the scattering amplitude $f_{\boldsymbol{k}}$ depends only on the scattering angle θ. The inversion $\boldsymbol{r}\mapsto-\boldsymbol{r}$ in polar coordinates is given by $\theta\mapsto\pi-\theta, r\mapsto r$. Thus, equation (2.62) simplifies to

$$\frac{d\sigma}{d\Omega_{\boldsymbol{r}}}=\left|f_{\boldsymbol{k}}(\theta)+f_{\boldsymbol{k}}(\pi-\theta)\right|^2=\left|f_{\boldsymbol{k}}(\theta)\right|^2+\left|f_{\boldsymbol{k}}(\pi-\theta)\right|^2+2\mathrm{Re}\left[f^*_{\boldsymbol{k}}(\theta)f_{\boldsymbol{k}}(\pi-\theta)\right].$$

The angles that arise are illustrated in Figure 2.4. Due to the interference terms, for bosons in the case $\theta=\pi/2$, the cross section doubles compared to the classical result,

$$\theta=\frac{\pi}{2}: \qquad \frac{d\sigma}{d\Omega_{\boldsymbol{r}}}=4\left|f_{\boldsymbol{k}}(\pi/2)\right|^2. \qquad (2.63)$$

In the partial wave representation

$$\begin{aligned}f_{\boldsymbol{k}}(\theta) &= \sum_l i^l(2l+1)f_lP_l(\cos\theta) \\ &\downarrow P_l(\cos\theta) \;=\; (-1)^lP_l(\cos(\pi-\theta)) \\ f_{\boldsymbol{k}}(\theta)+f_{\boldsymbol{k}}(\pi-\theta) &= 2\sum_{l\ \text{even}} i^l(2l+1)f_lP_l(\cos\theta), \qquad (2.64)\end{aligned}$$

we find that only even angular momenta l occur (for odd l, the Legendre polynomial changes sign and the contributions cancel each other out).

Spin-1/2 Fermions: In the case of spin-1/2 fermions, two scenarios are possible:

1. The spin-singlet state $\chi_s = \big[(|\uparrow\downarrow\rangle - |\downarrow\uparrow\rangle\big]/\sqrt{2}$ is antisymmetric, and consequently, the spatial part
$$\psi(\boldsymbol{r}) = \psi(-\boldsymbol{r}) \tag{2.65}$$
must be symmetric. The scattering cross-section is equal to that of spin-0 bosons,
$$\left.\frac{d\sigma}{d\Omega_{\boldsymbol{r}}}\right|_s = \big|f_{\boldsymbol{k}}(\theta) + f_{\boldsymbol{k}}(\pi - \theta)\big|^2. \tag{2.66}$$

2. The symmetric spin-triplet states
$$\chi_t = \begin{cases} |\uparrow\uparrow\rangle \\ \big[|\uparrow\downarrow\rangle + |\downarrow\uparrow\rangle\big]/\sqrt{2} \\ |\downarrow\downarrow\rangle \end{cases} \tag{2.67}$$
enforce an antisymmetric spatial wave function $\psi(\boldsymbol{r}) = -\psi(-\boldsymbol{r})$, and we obtain a scattering amplitude $f_{\boldsymbol{k}}(\theta) \to f_{\boldsymbol{k}}(\theta) - f_{\boldsymbol{k}}(\pi - \theta)$ that contains only odd angular momenta l. Thus, the scattering cross-section results in
$$\left.\frac{d\sigma}{d\Omega_{\boldsymbol{r}}}\right|_t = \big|f_{\boldsymbol{k}}(\theta) - f_{\boldsymbol{k}}(\pi - \theta)\big|^2 \qquad (\,= 0 \text{ for } \theta = \pi/2). \tag{2.68}$$

Note that polarized fermions scatter only in odd angular momentum channels: cold bosonic atoms exhibit a contact potential and scatter mainly in the s-wave channel, cf. (2.64). Cold polarized fermionic atoms, on the other hand, interact much more weakly, as the p-wave channel is the first to appear (the scattering cross-section σ_l behaves like $\sim a^2(ak)^{4l}$ at low energies).

In the case of a statistical ensemble for an unpolarized beam, the weighted average (from 3 triplet states and 1 singlet state) results in
$$\begin{aligned}\frac{d\sigma}{d\Omega_{\boldsymbol{r}}} &= \frac{3}{4}\left.\frac{d\sigma}{d\Omega_{\boldsymbol{r}}}\right|_t + \frac{1}{4}\left.\frac{d\sigma}{d\Omega_{\boldsymbol{r}}}\right|_s \\ &= \big|f_{\boldsymbol{k}}(\theta)\big|^2 + \big|f_{\boldsymbol{k}}(\pi - \theta)\big|^2 - \mathrm{Re}\,\big[f_{\boldsymbol{k}}^*(\theta) f_{\boldsymbol{k}}(\pi - \theta)\big].\end{aligned} \tag{2.69}$$

Chapter 3

Atoms

3.1 Atom with Two Electrons

To begin, we consider the 2-electron atom, helium He ($Z = 2$) or the ions H^- ($Z = 1$), Li^+ ($Z = 3$), and Be^{++} ($Z = 4$) described by the Hamiltonian operator

$$H = H_0 + H_{\mathrm{WW}} = \frac{p_1^2}{2m} + \frac{p_2^2}{2m} - \frac{Ze^2}{r_1} - \frac{Ze^2}{r_2} + \frac{e^2}{|\boldsymbol{r}_1 - \boldsymbol{r}_2|}. \tag{3.1}$$

Here, $\boldsymbol{r}_1$ and $\boldsymbol{r}_2$ describe the positions of the electrons with respect to the atomic nucleus, and $e > 0$ denotes the elementary charge. We have assumed that the nucleus does not move, which is a reasonable approximation due to the mass difference between the electrons and the nucleus. The Hamiltonian operator (3.1) is not exactly solvable because of the interaction term $H_{\mathrm{WW}} = e^2/r_{12}$, $r_{12} = |\boldsymbol{r}_1 - \boldsymbol{r}_2|$, between the two electrons. The simplest approximate solution treats this term perturbatively, meaning we first solve the non-interacting problem $H_0\Psi_0 = E_0\Psi_0$ and then determine the correction $E_1 = \langle\Psi_0|e^2/r_{12}|\Psi_0\rangle$. The solutions of $H_0\Psi_0 = E_0\Psi_0$ are the product wave functions $\Psi_0(\boldsymbol{r}_1, \boldsymbol{r}_2) = \varphi_{\alpha_1}(\boldsymbol{r}_1)\varphi_{\alpha_2}(\boldsymbol{r}_2)$, where $\varphi_\alpha(\boldsymbol{r})$ is a hydrogen wave function for nuclear charge Z with $\alpha = nlm$. The corresponding energies are

$$E_0 = \varepsilon_{\alpha_1} + \varepsilon_{\alpha_2} \tag{3.2}$$

with

$$\varepsilon_\alpha = -\frac{Z^2}{n^2}E_R, \qquad E_R = \frac{e^2}{2a_B} = 1\,\mathrm{Ry} \approx 13.6\,\mathrm{eV}, \qquad a_B = \frac{\hbar^2}{me^2} \approx 0.529\,\text{Å}. \tag{3.3}$$

Additionally, we must consider the Pauli principle for fermions. The total wave function $\Psi(x_1, x_2)$ is antisymmetric in $x_i = (\boldsymbol{r}_i, s_i)$,

$$\Psi(x_1, x_2) = -\Psi(x_2, x_1). \tag{3.4}$$

The separation of spin and orbital parts yields

$$\Psi(x_1, x_2) = \Psi_0(\boldsymbol{r}_1, \boldsymbol{r}_2)\chi_0(s_1, s_2), \tag{3.5}$$

where the antisymmetry of the total wave function can be constructed in two ways, either with

$$\begin{cases} \Psi_0 & \text{symmetrical,} \\ \chi_0 & \text{antisymmetrical,} \quad (S = 0, \quad \text{singlet}) \end{cases} \tag{3.6}$$

thus an antisymmetrical spin function (spin-singlet state), or via

$$\begin{cases} \Psi_0 & \text{antisymmetrical,} \\ \chi_0 & \text{symmetrical,} \quad (S = 1, \quad \text{triplet}) \end{cases} \tag{3.7}$$

with a symmetrical spin function (spin-triplet state). With Ψ_0 antisymmetrical, $\alpha_1 \neq \alpha_2$ must hold, which costs us at least the additional energy

$$\Delta E = Z^2(1 - 1/2^2)E_R \approx Z^2 \times 10\,\mathrm{eV} \tag{3.8}$$

We therefore choose the spin-singlet state as a candidate for the ground state with

$$\begin{aligned} \Psi_0(x_1, x_2) &= \varphi_{100}(\boldsymbol{r}_1)\,\varphi_{100}(\boldsymbol{r}_2)\,\chi_{00}(s_1, s_2), \\ \varphi_{100}(r) &= (Z^3/\pi a_B^3)^{1/2} \exp(-Zr/a_B), \\ \chi_{00}(s_1, s_2) &= [\chi_\uparrow(s_1)\chi_\downarrow(s_2) - \chi_\downarrow(s_1)\chi_\uparrow(s_2)]/\sqrt{2}, \\ E_0 &= -2Z^2 E_R = -Z^2 e^2/a_B. \end{aligned} \tag{3.9}$$

The correction E_1 follows through integration

$$\begin{aligned} E_1 &= \int d^3r_1\, d^3r_2\, \frac{Z^6 e^2}{a_B^6 \pi^2} \frac{\exp[-2Z(r_1 + r_2)/a_B]}{|\boldsymbol{r}_1 - \boldsymbol{r}_2|} \\ &= \frac{5}{8}\frac{Ze^2}{a_B}. \end{aligned} \tag{3.10}$$

We obtain the ground state energy

$$E_G = E_0 + E_1 = -\Big(Z - \frac{5}{8}\Big)\frac{Ze^2}{a_B}. \tag{3.11}$$

in first-order perturbation theory. This energy represents an upper bound for the actual value of the ground state energy because first-order perturbation theory is equivalent to the Rayleigh-Ritz variational principle with the unperturbed ground state wave function as a test function.

For the He atom ($Z = 2$), we obtain $E_G \approx -5.5\,\mathrm{Ry}$. The experimentally measured value is $E_G^{\mathrm{He}} \approx -5.8\,\mathrm{Ry}$, about 4 eV lower than our calculated value. With a variational approach $Z \mapsto \alpha$ (α variational parameter)[1] we find the estimate

$$\begin{aligned} E_G &= \min_\alpha \Big(\alpha - 2Z + \frac{5}{8}\Big)\frac{\alpha\, e^2}{a_B} = -\Big(Z - \frac{5}{16}\Big)^2 \frac{e^2}{a_B} \qquad {\scriptstyle (\alpha = Z - 5/16)} \\ &\approx -5.7 \text{ Ry}, \end{aligned} \tag{3.12}$$

an improvement of $\approx 2.7\,\mathrm{eV}$; about $1.4\,\mathrm{eV}$ are still missing from a total of $79\,\mathrm{eV}$, a respectable result. The improvement provided by $Z \mapsto \alpha$ is a consequence of considering screening effects: each electron 'sees' only a charge of $2 - 5/16 = 27/16$ instead of $Z = 2$.

For the hydrogen ion H^- ($Z = 1$) we obtain

$$E_G = -\Big(\frac{11}{16}\Big)^2 \frac{e^2}{a_B} \approx -12.86\,\mathrm{eV}. \tag{3.13}$$

The configuration $\mathrm{H} + \mathrm{e}^-$ corresponds to the energy -13.6 eV, which would make H^- unstable; however, experimentally H^- is stable, which means our result must be at least $(3/4)\,\mathrm{eV}$ wrong.

3.2 Hartree and Hartree-Fock Approximation

When we move to larger atoms, we are confronted with a complicated electronic many-body problem. The general form of this many-body problem can be described by the Hamiltonian operator

$$H = \sum_{i=1}^{N}\Big[\frac{p_i^2}{2m} + U(\boldsymbol{r}_i)\Big] + \underbrace{\frac{1}{2}\sum_{i\neq j} \overbrace{\frac{e^2}{|\boldsymbol{r}_i - \boldsymbol{r}_j|}}^{V_{\text{int}}^{ij}}}_{V_{\text{int}}} \tag{3.14}$$

(we neglect here interactions that involve spin). The potential $U(\boldsymbol{r})$ is a given (external) potential; for atoms of charge Z, $U(\boldsymbol{r}) = -Ze^2/r$. Naively, we could again first solve the one-particle problem

$$h = \frac{p^2}{2m} + U(\boldsymbol{r}), \qquad\qquad h\varphi_j(\boldsymbol{r}) = \varepsilon_j \varphi_j(\boldsymbol{r}), \tag{3.15}$$

assume the many-body function as an antisymmetrized product wave function [i.e., as a Slater determinant (2.52)] and treat the interaction term in the Hamiltonian as a perturbation. The expected results are mediocre, as we have seen in the example of the He atom. The problem is that the electrons are not only subjected to the potential $U(\boldsymbol{r})$, but also move in the (mean) field of the other electrons, leading to

---

[1] One replaces $Z \mapsto \alpha$ only in the wave function, not in the Hamiltonian!

a screening of U. This screening, in turn, depends on the orbits of the electrons, so we must determine the orbits and the screening effects self-consistently. This is precisely the strength of the Hartree and Hartree-Fock approximations: The Hartree approximation considers (only) the screening effects and not the exchange effects due to the fermionic nature of the electrons. The complete Hartree-Fock theory also takes into account the antisymmetry of the wave function.

3.2.1 Hartree Approximation

In the Hartree approximation, the task is to find the optimal product wave function

$$\Psi_{\text{H}} = \varphi_1(\boldsymbol{r}_1)\,\varphi_2(\boldsymbol{r}_2)\cdots\varphi_N(\boldsymbol{r}_N). \tag{3.16}$$

We can at least partially consider the Pauli principle by orthogonalizing the φ_i and allowing each state to be occupied at most twice (due to $g_s = 2$). Mathematically, we seek single-particle functions φ_i such that the expectation value of the energy $\langle H\rangle_{\text{H}} = \langle\Psi_{\text{H}}|H|\Psi_{\text{H}}\rangle$ is minimal; the wave functions should be normalized, $\|\varphi_i\| = 1$. With these constraints, which we consider through Lagrange multipliers, we have the following functional to minimize:[2]

$$\begin{aligned}\mathcal{F}[\varphi_1(x_1),\ldots,\varphi_N(x_N)] &= \langle H\rangle_{\text{H}} - \sum_{i=1}^{N}\lambda_i\langle\varphi_i|\varphi_i\rangle \qquad (3.17)\\ &= \int\prod_{i=1}^{N} d^3r_i\,(\varphi_1^*\cdots\varphi_N^* H\varphi_1\cdots\varphi_N) - \sum_{i=1}^{N}\lambda_i\int dr_i^3\,\varphi_i^*\varphi_i\\ &= \sum_{i=1}^{N}\int dr_i^3\,\varphi_i^*\left[\frac{p_i^2}{2m} + U(\boldsymbol{r}_i) + \frac{1}{2}\sum_j{}'\int d^3r_j\,\varphi_j^*\frac{e^2}{|\boldsymbol{r}_i-\boldsymbol{r}_j|}\varphi_j - \lambda_i\right]\varphi_i.\end{aligned}$$

At the minimum of $\mathcal{F}$, the variation $\delta\mathcal{F} = 0$ vanishes, and we find the condition ($\delta\mathcal{F}/\delta\varphi_i^* = 0$)

$$\left[-\frac{\hbar^2}{2m}\nabla^2 + U(\boldsymbol{r}) + \int d^3r'\frac{e}{|\boldsymbol{r}-\boldsymbol{r}'|}\sum_j{}'e|\varphi_j(\boldsymbol{r}')|^2\right]\varphi_i(\boldsymbol{r}) = \lambda_i\varphi_i(\boldsymbol{r}). \tag{3.18}$$

The sum $n_i(\boldsymbol{r}') = \sum_j' |\varphi_j(\boldsymbol{r}')|^2$ describes the average charge distribution $-e\,n_i(\boldsymbol{r}')$ of the other electrons $j \neq i$. The system (3.18) defines the Hartree equations; the optimization of the single-particle wave functions φ_i takes into account the presence of the other electrons through the interaction term

$$V_{\text{H}}(\boldsymbol{r}) = \int d^3r'\,\frac{e^2 n_i(\boldsymbol{r}')}{|\boldsymbol{r}-\boldsymbol{r}'|}. \tag{3.19}$$

---

[2] The symbol $\sum_j'$ describes the sum over j without the term $j = i$.

Note that the φ_i are generally not orthogonal, as $n_i(\boldsymbol{r})$ depends on i. Therefore, one usually writes $n_i(\boldsymbol{r}) \approx n(\boldsymbol{r})$ for the particle density, as one electron represents only a small disturbance of the $N \gg 1$ electron cloud. The density $-e\,n(\boldsymbol{r})$ then describes the charge distribution that an external test charge perceives, and the φ_i become orthogonal. The (Hartree) expectation value of the ground state energy $E_{\mathrm{H}} = \langle H \rangle_{\mathrm{H}} = \sum_i \lambda_i - \langle V_{\mathrm{int}} \rangle_{\mathrm{H}}$ represents an upper bound for the exact ground state energy.

The Lagrange multipliers λ_i appear in the Hartree equation like single-particle energies ε_i. To determine their physical significance, we multiply (3.18) by φ_i^* and integrate over $\boldsymbol{r}$. We obtain

$$\lambda_i = \int d^3r \left[\frac{p^2}{2m} + U(\boldsymbol{r})\right] |\varphi_i(\boldsymbol{r})|^2 + \sum_j{}' \int d^3r\, d^3r'\, \frac{e^2 |\varphi_i(\boldsymbol{r})|^2 |\varphi_j(\boldsymbol{r}')|^2}{|\boldsymbol{r} - \boldsymbol{r}'|}. \tag{3.20}$$

Since λ_i takes into account precisely those terms of $\langle H \rangle_{\mathrm{H}}$ (see (3.17)) that contain φ_i, $-\lambda_i$ corresponds to the ionization energy under the assumption that the other wave functions do not change (Koopmans Theorem). In reality, the other wave functions relax, i.e., the relaxed state $\Psi_{\mathrm{H},i}^{(N-1)}$ (with $N-1$ particles) contains modified single-particle waves. However, the 'knocking out' of the i-th electron, for example in a photoemission experiment, leaves an exchange hole that is only filled after a finite relaxation time. A rapid ionization process (e.g., via photoemission) therefore involves the unrelaxed ionization energy $-\lambda_i$ and not the relaxed quantity $\lambda_i^{\mathrm{ion}} = \langle H \rangle_{\mathrm{H}} - \langle \Psi_{\mathrm{H},i} | H | \Psi_{\mathrm{H},i} \rangle$.

3.2.2 Hartree-Fock Approximation

The Hartree-Fock theory goes a step further and minimizes

$$\langle \Psi_{\mathrm{HF}} | H | \Psi_{\mathrm{HF}} \rangle - \sum_i \lambda_i \langle \varphi_i | \varphi_i \rangle \tag{3.21}$$

in the variational space spanned by the Slater determinant[3]

$$\Psi_{\mathrm{HF}} = \frac{1}{\sqrt{N!}} \begin{vmatrix} \varphi_1(\boldsymbol{r}_1)\chi_{\sigma_1}(s_1) & \cdots & \varphi_1(\boldsymbol{r}_N)\chi_{\sigma_1}(s_N) \\ \vdots & \ddots & \vdots \\ \varphi_N(\boldsymbol{r}_1)\chi_{\sigma_N}(s_1) & \cdots & \varphi_N(\boldsymbol{r}_N)\chi_{\sigma_N}(s_N) \end{vmatrix}. \tag{3.22}$$

The single-particle expectation values of p_i^2 and $U(\boldsymbol{r}_i)$ remain unchanged, while the interaction term now produces two terms,

$$\begin{aligned} \langle V_{\mathrm{int}} \rangle_{\mathrm{HF}} = \frac{1}{2} \int d^3r\, d^3r'\, \frac{e^2}{|\boldsymbol{r} - \boldsymbol{r}'|} \sum_{i \neq j} \Big[& \varphi_i^*(\boldsymbol{r}) \varphi_j^*(\boldsymbol{r}') \varphi_j(\boldsymbol{r}') \varphi_i(\boldsymbol{r}) \\ & - \delta_{\sigma_i \sigma_j} \varphi_i^*(\boldsymbol{r}) \varphi_j^*(\boldsymbol{r}') \varphi_j(\boldsymbol{r}) \varphi_i(\boldsymbol{r}') \Big]. \end{aligned} \tag{3.23}$$

---

[3] Note that the Slater determinant Ψ_{HF} actually depends only on the variational space $\mathrm{span}\{\varphi_1, \ldots, \varphi_N\}$ and not on the choice of basis functions φ that span this space.

The spin-dependent term $\propto \delta_{\sigma_i\sigma_j}$ is called the Fock or exchange term.

Its derivation involves the following steps: Starting from the product state $\Psi_{\mathrm{H}} = \prod_i \varphi_i(\boldsymbol{r}_i)\chi_{\sigma_i}(s_i)$, we define the antisymmetrized state $\Psi_{\mathrm{HF}} = \sqrt{N!}\mathcal{A}\Psi_{\mathrm{H}} = 1/\sqrt{N!}\sum_{\pi\in S_N}(-1)^\pi U_\pi \Psi_{\mathrm{H}}$ and calculate the matrix element[4]

$$\begin{aligned}
\langle V_{\text{int}}\rangle_{\mathrm{HF}} &= N!\langle \Psi_{\mathrm{H}}\mathcal{A}V_{\text{int}}\mathcal{A}\Psi_{\mathrm{H}}\rangle \\
&\downarrow \qquad\qquad \scriptstyle (\mathcal{A}V_{\text{int}}\mathcal{A}=V_{\text{int}}\mathcal{A}^2=V_{\text{int}}\mathcal{A}, \quad \text{since } [\mathcal{A},V_{\text{int}}]=0) \\
&= \frac{1}{2}\sum_{j\neq i}\sum_{\pi\in S_N}(-1)^\pi\langle\Psi_{\mathrm{H}}V_{\text{int}}^{ij}U_\pi\Psi_{\mathrm{H}}\rangle \quad \scriptstyle [\text{only } \pi=1 \text{ and } \pi=(i\leftrightarrow j) \text{ do not vanish}] \\
&= \frac{1}{2}\sum_{i\neq j}\langle\Psi_{\mathrm{H}}|V_{\text{int}}^{ij}[1-(i\leftrightarrow j)]|\Psi_{\mathrm{H}}\rangle\,. \qquad (3.24)
\end{aligned}$$

Now, $\langle\chi_{\mathrm{H}}|\chi_{\mathrm{H}}\rangle = 1$ and

$$\langle\chi_{\mathrm{H}}|(i\leftrightarrow j)|\chi_{\mathrm{H}}\rangle = \delta_{s_is_j}\,. \qquad (3.25)$$

with $\chi_{\mathrm{H}} = \prod_i \chi_{\sigma_i}$ in spin space. The two terms in (3.24) then describe the Hartree and exchange contributions in equation (3.23).

Analogous to (3.18), we vary $\delta\mathcal{F}/\delta\varphi_i^* = 0$ and thus generate the Hartree-Fock integro-differential equations

$$\begin{aligned}
&\left[-\frac{\hbar^2}{2m}\nabla^2 + U(\boldsymbol{r}) + \int d^3r'\,\frac{e^2 n_i(\boldsymbol{r}')}{|\boldsymbol{r}-\boldsymbol{r}'|}\right]\varphi_i(\boldsymbol{r}) \qquad (3.26)\\
&\quad -\sum_j \delta_{\sigma_i\sigma_j}\int d^3r'\left[\varphi_j^*(\boldsymbol{r}')\frac{e^2}{|\boldsymbol{r}-\boldsymbol{r}'|}\varphi_i(\boldsymbol{r}')\right]\varphi_j(\boldsymbol{r}) = \lambda_i\varphi_i(\boldsymbol{r}).
\end{aligned}$$

In the second line, integration is performed over the sought eigenfunction φ_i; accordingly, the electron is subjected to a non-local potential. The formulas (3.18) and (3.26) must be solved numerically through iteration.

Note that the Hartree-Fock approximation does not yet take correlation effects[5] into account, and therefore neither (3.18) nor (3.26) are exact. The ground state energy $E_{\mathrm{HF}} = \langle H\rangle_{\mathrm{HF}}$ of the system includes the terms

$$E_{\mathrm{HF}} = \underbrace{\underbrace{\underbrace{E_0}_{\text{Single-particle}} + E_{\mathrm{WW}}}_{\text{Hartree}} + E_{\text{Exchange.}}}_{\text{Hartree-Fock}} \qquad (3.27)$$

---

[4] See (2.26) for the definition of the antisymmetrization operator.

[5] Correlation energy: An electron at position $\boldsymbol{r}$ reduces the probability of finding another electron there. In particular, an electron with spin-$|\uparrow\rangle$ creates an exchange and correlation hole for other spin-$|\uparrow\rangle$ electrons. The HF theory accounts for the exchange part; any contributions to the exchange hole that go beyond the molecular field HF theory are referred to as correlation effects.

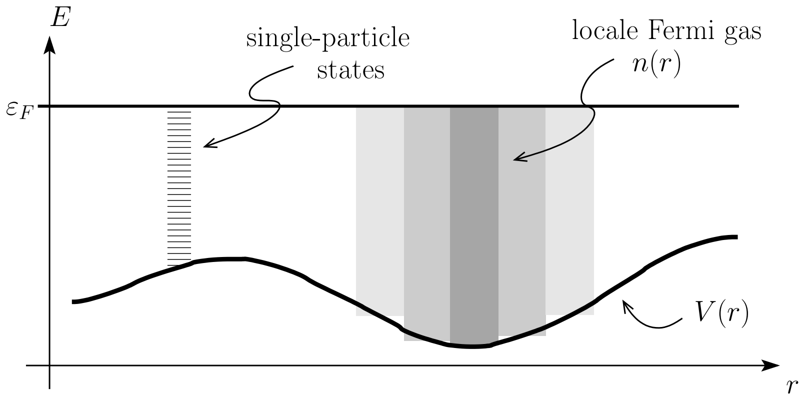

Figure 3.1: Thomas-Fermi screening: The inhomogeneous Fermi gas is approximated by a local Fermi gas of density $n(\boldsymbol{r}) = k_F^3(\boldsymbol{r})/3\pi^2$. The position-dependent Fermi wave number $k_F(\boldsymbol{r})$ results from the local potential $V(\boldsymbol{r})$ taking screening effects into account, see (3.30).

Additionally, there is a correlation energy $E_{\text{Correlation}}$ that can be found within the framework of many-body physics/quantum field theory via systematic development in a perturbation theory. For atoms, the Hartree-Fock approximation provides results that are accurate up to typical correlation energies of the order of $\simeq 0.5\,\text{eV}$ per electron.

3.3 Thomas-Fermi Screening

We consider electrons in a slowly varying potential $U(\boldsymbol{r})$, which we can treat as locally constant, see also Figure 3.1. The electrons then locally form a Fermi gas of density [cf. (2.55) with $g_s = 2$]

$$n(\boldsymbol{r}) = \frac{k_F^3(\boldsymbol{r})}{3\pi^2}. \tag{3.28}$$

A test charge at position $\boldsymbol{r}$ feels a local potential composed of the ‘bare’ potential $U(\boldsymbol{r})$ and the potential generated by the inhomogeneous electron gas,

$$V(\boldsymbol{r}) = U(\boldsymbol{r}) + \int d^3r'\,\frac{e^2\,n(\boldsymbol{r}')}{|\boldsymbol{r}-\boldsymbol{r}'|}. \tag{3.29}$$

The second term corresponds exactly to the Hartree potential that we learned about in the last chapter.

The electrons in the Fermi gas distribute themselves in equilibrium such that the addition of a test electron at any position $\boldsymbol{r}$ costs the identical energy ε_F, thus we have

$$\varepsilon_F = \frac{\hbar^2 k_F^2(\boldsymbol{r})}{2m} + V(\boldsymbol{r}); \tag{3.30}$$

the first term describes the kinetic energy of the added electron while the second term describes its potential energy $V(\boldsymbol{r})$. The combination of (3.28) and (3.30) provides the relationship between the local density $n(\boldsymbol{r})$ and the effective potential $V(\boldsymbol{r})$,

$$n(\boldsymbol{r}) = \frac{1}{3\pi^2}\left[\frac{2m}{\hbar^2}\big(\varepsilon_F - V(\boldsymbol{r})\big)\right]^{3/2}; \tag{3.31}$$

note that this represents an integral equation for the density $n(\boldsymbol{r})$. The equation (3.31) for $n(\boldsymbol{r})$ can be transformed into a differential equation for $V(\boldsymbol{r})$: applying the Laplace operator ∇^2 to (3.29) using $\nabla^2 1/|\boldsymbol{r}-\boldsymbol{r}'| = -4\pi\delta^{(3)}(\boldsymbol{r}-\boldsymbol{r}')$ yields

$$\begin{aligned}\nabla^2 V(\boldsymbol{r}) &= \nabla^2 U(\boldsymbol{r}) - 4\pi e^2 n(\boldsymbol{r})\\ &= -4\pi e^2\left[-\rho_{\rm ext}(\boldsymbol{r})/e + n(\boldsymbol{r})\right],\end{aligned} \tag{3.32}$$

where $\rho_{\rm ext}(\boldsymbol{r})$ denotes the charge density generating the external potential $U(\boldsymbol{r})$ and $n(\boldsymbol{r})$ denotes the screening electron density. With the usual definition of the dielectric constant

$$\varepsilon(\boldsymbol{q}) = \frac{U(\boldsymbol{q})}{V(\boldsymbol{q})} \tag{3.33}$$

we obtain [with $q^2[V(\boldsymbol{q}) - U(\boldsymbol{q})] = 4\pi e^2 n(\boldsymbol{q})$ from (3.32)]

$$\varepsilon(\boldsymbol{q}) = \frac{q^2(V-V+U)}{q^2 V} = 1 - \frac{(V-U)q^2}{q^2 V} = 1 - \frac{4\pi e^2}{q^2}\frac{n}{V}; \tag{3.34}$$

for small $V(\boldsymbol{q})$, $\boldsymbol{q} \neq 0$, the screening (induced) charge density is given by $n \approx (\partial n/\partial V)V = (-\partial n/\partial \varepsilon_F)_{V=0}V$. Substituting into (3.33) yields the Thomas-Fermi result for the dielectric constant of a metal,

$$\varepsilon(\boldsymbol{q}) = 1 + \frac{4\pi e^2}{q^2}\frac{\partial n}{\partial \varepsilon_F} \equiv 1 + \frac{q_{\rm TF}^2}{q^2}. \tag{3.35}$$

To see that the result (3.35) describes screening, we calculate the inverse transformation of (3.33)

$$V(\boldsymbol{r}) = \int d^3r' \frac{e^{-q_{\rm TF}|\boldsymbol{r}-\boldsymbol{r}'|}}{4\pi|\boldsymbol{r}-\boldsymbol{r}'|}U(\boldsymbol{r}'). \tag{3.36}$$

Indeed, the external potential U is screened over the length $q_{\rm TF}^{-1}$. The Thomas-Fermi wave number is determined by the electron density via k_F,

$$q_{\rm TF}^2 = 4\pi e^2\frac{\partial n}{\partial \varepsilon_F} = \frac{4e^2 m k_F}{\pi\hbar^2} = \frac{4}{\pi}\frac{k_F}{a_B}. \tag{3.37}$$

In a typical metal, $k_F \approx 1\,\text{Å}^{-1}$, and thus $q_{\rm TF} \simeq 1\,\text{Å}^{-1}$: a charge in a metal is screened by other electrons within $\simeq 1\,\text{Å} = 10^{-10}\,\text{m}$.

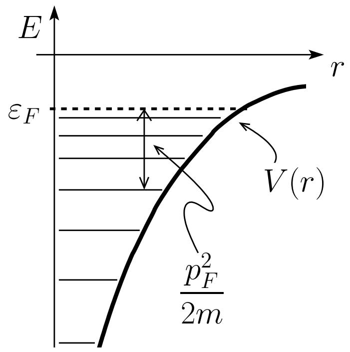

Figure 3.2: Potential with bound states in the Thomas-Fermi atom. The states are filled up to the Fermi level ε_F; their charge contributes, via screening, to the effective potential.

3.4 Thomas-Fermi Atom

We want to investigate atoms with nuclear charge $Z \gg 1$. The solution of the hydrogen problem (with only one electron) yields the radius $r_K = a_B/Z$. This result is applicable for describing the innermost $1s$ shell. The reason is that the nuclear potential there is still 'bare' and not yet screened by the presence of other electrons. For the last electron (in the outermost shell), however, only an effective nuclear charge $Z_{\text{eff}} \approx 1$ remains. Thus, the last shell has the radius $R = a_B$ (independent of the nuclear charge). For the treatment of the electron cloud of the 'middle' shells with typical radius $\bar{r}$, we need to consider the screening effects more accurately. The simplest model for this is the Thomas-Fermi atom.

We apply the principle of Thomas-Fermi screening to the treatment of atoms and start from (3.32) with $\rho_{\text{ext}}(\boldsymbol{r})/e = Z\delta^{(3)}(\boldsymbol{r})$ (due to the nuclear charge). We approximate $V(\boldsymbol{r})$ as spherically symmetric and obtain for $r > 0$

$$\nabla^2 V(r) = \frac{1}{r^2}\partial_r r^2 \partial_r V(r) = -\frac{4e^2}{3\pi\hbar^3}\Big[2m\big(\varepsilon_F - V(r)\big)\Big]^{3/2}. \tag{3.38}$$

For $r \to 0$, the screening must disappear, and the electrons should be exposed to the 'bare' nuclear potential with $V(r) \sim -Ze^2/r$; this provides a boundary condition for (3.38). The atomic radius R is determined by the condition $n(R) = 0$. From this, with (3.31), follows the second boundary condition $V(R) = \varepsilon_F$. For a neutral atom, $V(r > R) = \text{const.} = 0$, and thus $\varepsilon_F = 0$; for a charged ion, $V(r > R) = -(Z - N)e^2/r$, with N being the number of electrons, cf. Figure 3.2.

In the following, we consider the neutral case with $N = Z$ and define the dimensionless scales x and Φ for length and for energy (the potential),

$$r = \left(\frac{3\pi}{4\sqrt{Z}}\right)^{2/3}\frac{a_B x}{2} = \beta\frac{a_B x}{Z^{1/3}}, \quad V(r) = -\frac{Ze^2}{r}\Phi(x) \qquad (\text{with } \beta = 0.8853). \tag{3.39}$$

The universal atom[6] is then characterized by a dimensionless potential $\Phi(x)$, which

---

[6] The potential $\Phi(x)$ is independent of Z.

solves the Thomas-Fermi equation

$$\sqrt{x}\,\frac{d^2\Phi(x)}{dx^2} = \Phi(x)^{3/2}, \qquad \Phi(0) \;=\; 1, \tag{3.40}$$

The potential satisfies the asymptotics

$$\Phi(x) = \begin{cases} 1 - 1.59\,x, & x \to 0, \\ \;144/x^3, & x \to \infty, \end{cases} \tag{3.41}$$

and is otherwise found through numerical integration of the differential equation (3.40). Note that the potential of the universal Thomas-Fermi atom extends to infinity since $\Phi(x)$ only decays algebraically.

In fact, the Thomas-Fermi approximation is only applicable for intermediate radii (with $r_{\text{min}} \ll r \ll r_{\text{max}}$). The local density approximation assumes that the potential does not change significantly over the (local) Fermi wavelength. The typical scale d of the potential change is given by the distance r, since $d \simeq V/\partial_r V \simeq r$. On the other hand, the Fermi wave number is approximately given by $k_F^2 \simeq 2mV(r)/\hbar^2 \simeq Z\Phi(x)/a_B r$. Thus, we obtain the condition

$$1 \ll (k_F d)^2 \qquad \Leftrightarrow \qquad 1 \ll Z\,\Phi(x)\,r/a_B \tag{3.42}$$

for the applicability of the Thomas-Fermi approximation. For small distances, $\Phi(x) \approx 1$, and thus $r_{\text{min}} \simeq r_K = a_B/Z$. For large distances, we use $\Phi(x) \sim x^{-3} \simeq (a_B/r)^3/Z$ and find that $r_{\text{max}} \simeq R = a_B$ (independent of Z). Thus, the Thomas-Fermi approximation holds from the innermost shell $r_K = a_B/Z$ to the outermost shell $R = a_B$. In this range, we have

$$\begin{aligned} \int_{r_K \le r \le R} d^3r\, n(r) &= -\frac{1}{e^2}\int_{r_K}^{R} dr\, r^2\, \nabla^2 V(\boldsymbol{r}) = \left.\frac{r^2 \partial_r V(r)}{e^2}\right|_{r=R}^{r_K} \\ &\simeq -\frac{r_K\, V(r_K)}{e^2} \simeq Z\Phi(1) \propto Z \end{aligned}$$

electrons. Thus, the majority of electrons (except those in the outer and inner shells) contribute to the formation of the Thomas-Fermi atom.

We find the following scaling laws as a function of Z for the Thomas-Fermi atom:

- Radius: $\bar{r} \simeq Z^{-1/3} a_B$, heavier atoms are smaller,[7]
- Potential: $V \simeq Ze^2\Phi(x)/r \simeq Z^{4/3} E_R \Phi(x)/x \propto Z^{4/3}$ at fixed $x \propto Z^{1/3} r$,
- e^- density: $n \simeq \nabla^2 V/e^2 \simeq V/e^2 r^2 \simeq Z\Phi(x)/r^3 \simeq (Z^2/a_B^3)\Phi(x)/x^3 \propto Z^2$ at fixed x,

---

[7] Numerically, it is found that 50% of the atoms are found within a radius $1.33\,Z^{-1/3} a_B$.

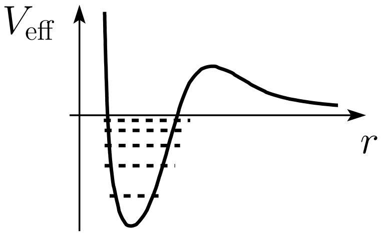

Figure 3.3: Effective potential of the Thomas-Fermi atom including the centrifugal barrier. The TF atom binds a state with angular momentum l if V_{eff} has a minimum with negative energy.

- Kinetic energy: $p^2/2m = \hbar^2 k_F^2/2m \simeq \hbar^2 n^{2/3}/m \simeq Z^{4/3} E_R$,
- Velocity:[8] $v \simeq p/m \simeq Z^{2/3} e^2/\hbar \propto Z^{2/3}$.

The electrons arrange themselves in shells in the Thomas-Fermi atom. The Thomas-Fermi atom binds a state with angular momentum l if the effective potential [including the centrifugal potential $\hbar^2 l(l+1)/2mr^2$]

$$V_{\text{eff}}(r) = V(r) + \frac{\hbar^2 l(l+1)}{2mr^2} = \frac{Z^{2/3}e^2}{\beta\, a_B}\left[-Z^{2/3}\frac{\Phi(x)}{x} + \frac{l(l+1)}{2\beta\, x^2}\right] \tag{3.43}$$

has a local minimum with $V_{\text{eff}} < 0$, see Figure 3.3.

With the TF potential $\Phi(x)$ according to (3.40), one finds for the Thomas-Fermi atom shells for the following l and Z ranges:

	$l = 0$	$l \leq 1$	$l \leq 2$	$l \leq 3$
TF-Atom	$Z \leq 4$	$5 \leq Z \leq 19$	$20 \leq Z \leq 53$	$54 \leq Z$
	only s	$s\,\&\,p$	$s,\ p\,\&\,d$	$s,\ p,\ d\,\&\,f$
Experimentally		p-electrons	d-e^-	f-e^-
		for $Z \geq 5$	for $Z \geq 20$	for $Z \geq 58$

Shells in the Thomas-Fermi atom

Note that due to $V_{\text{eff}}(r) \neq Ze^2/r$, the single-particle energies ε_i in the Thomas-Fermi approximation depend on n and l (but, due to radial symmetry, not on m). In particular, there are the shells nl in an atom with energy ϵ_{nl} with degeneracy $(2l+1)(2s+1) = 4l+2$, that is

$$s\text{-shell (deg. 2)}, \qquad p\text{- (deg. 6)}, \qquad d\text{- (deg. 10)} \quad \text{and} \quad f\text{- (deg. 14)}. \tag{3.44}$$

The determination of the shell sequence (increase of l or of n) requires a numerical analysis. One finds the sequence

$$\begin{aligned} 1s < 2s < 2p < 3s < 3p < 4s < 3d < 4p < 5s < 4d < 5p \\ < 6s < 4f < 5d < 6p < 7s < 5f. \end{aligned} \tag{3.45}$$

This arrangement can be memorized using the scheme 3.4. Accordingly, one finds the

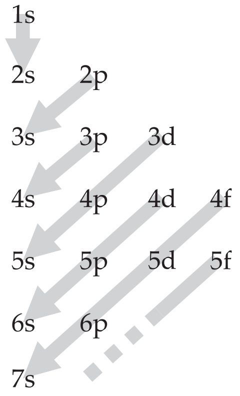

Figure 3.4: Sequence of the shells nl for the energy of the last added electron in the Thomas-Fermi atom. n = principal quantum number, l = angular momentum quantum number. Note that the energetically lower/inner electrons have a different sequence (namely the trivial one): The sequence of the so-called X-ray shells is $1s$ (the 1K shell), $2s$, $2p$ (2L shell), $3s$, $3p$, $3d$ (3M shell), $4s$, $4p$, $4d$, $4f$ (4N shell), etc.

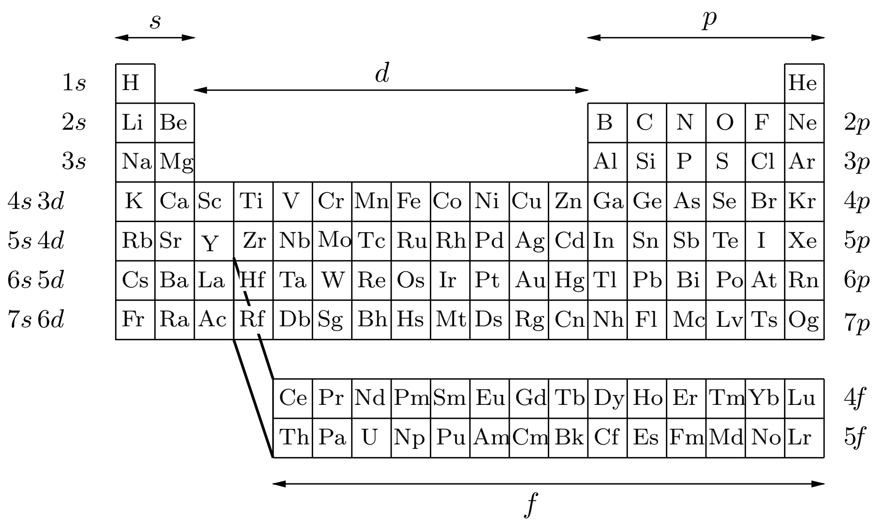

$1s$	H																	He	
$2s$	Li	Be											B	C	N	O	F	Ne	$2p$
$3s$	Na	Mg											Al	Si	P	S	Cl	Ar	$3p$
$4s\,3d$	K	Ca	Sc	Ti	V	Cr	Mn	Fe	Co	Ni	Cu	Zn	Ga	Ge	As	Se	Br	Kr	$4p$
$5s\,4d$	Rb	Sr	Y	Zr	Nb	Mo	Tc	Ru	Rh	Pd	Ag	Cd	In	Sn	Sb	Te	I	Xe	$5p$
$6s\,5d$	Cs	Ba	La	Hf	Ta	W	Re	Os	Ir	Pt	Au	Hg	Tl	Pb	Bi	Po	At	Rn	$6p$
$7s\,6d$	Fr	Ra	Ac	Rf	Db	Sg	Bh	Hs	Mt	Ds	Rg	Cn	Nh	Fl	Mc	Lv	Ts	Og	$7p$
					Ce	Pr	Nd	Pm	Sm	Eu	Gd	Tb	Dy	Ho	Er	Tm	Yb	Lu	$4f$
					Th	Pa	U	Np	Pu	Am	Cm	Bk	Cf	Es	Fm	Md	No	Lr	$5f$

Figure 3.5: Periodic table of elements.

periodic table of elements in the form 3.5.

We go through the periodic table with some comments:

- H, He: the $1s$ shell is filled
- Li, Be: the $2s$ shell, Be–Ne: the $2p$ shell is filled. $2s$ and $2p$ have different energies; the orbitals with small l are closer to the nucleus and therefore have lower energies, $\varepsilon_{2s} < \varepsilon_{2p}$.
- Na–A: as before, the $3s$ is filled first, then the $3p$ shell.
- K–Kr: the energies of $4s$ are almost equal to those of $3d$. This results in the complicated filling (we only indicate the number of electrons in the $4s$ shell):

---

[8] It holds that $e^2/\hbar = \alpha c$ with $\alpha \approx 1/137$ being the fine-structure constant.

$$\mathrm{K}\ 4s^1,\ \mathrm{Ca}\ 4s^2,\ \cdots,\ \mathrm{V}\ 4s^2,\ \mathrm{Cr}\ 4s^1,\ \mathrm{Mn}\ 4s^2, \cdots,\ \mathrm{Ni}\ 4s^2,\ \mathrm{Cu}\ 4s^1,\ \mathrm{Zn}\ 4s^2$$

With Ga–Kr, the p-shell is filled. The $3d$ shells are compact, thus less chemically important; however, they provide the magnetic moments that generate the ferro- or antiferromagnetism of the elements Cr–Ni.

- Rb–Xe: essentially a repetition of the sequence K–Kr. Again, the s-orbitals have about the same energy as the d-orbitals of the previous shell, leading to the unusual filling

$$\mathrm{Rb}\ 5s^1,\ \mathrm{Sr}\ 5s^2,\ \cdots,\ \mathrm{Zr}\ 5s^2,\ \mathrm{Nb}\ 5s^1, \cdots,\ \mathrm{Rh}\ 5s^1,\ \mathrm{Pd}\ 4d^{10}\,5s^0, \\ \mathrm{Ag}\ 4d^{10}\,5s^1,\ \mathrm{Cd}\ 4d^{10}\,5s^2$$

With In–Xe, the p-shell is filled.

- Cs–Rn: Cs and Ba fill the $6s$ orbital. La fills the first $5d^1$ orbital, then the lanthanides (rare earths) La–Lu follow with the filling of the $4f$ shell, which is energetically close to $5d$. Again, there are shifts in the occupations,

$$\mathrm{Ce}\ 5d^0\,4f^2, \cdots,\ \mathrm{Eu}\ 5d^0\,4f^7,\ \mathrm{Gd}\ 5d^1\,4f^7,\ \mathrm{Tb}\ 5d^0\,4f^9, \cdots,\ \mathrm{Yb}\ 5d^0\,4f^{14}.$$

The compact f-orbitals are passive in chemical bonding, but yield large magnetic moments, especially in the case of Ce, Pr, Nd, Sm–Yb. Following the filling of the f-shell, the $5d$ and $6p$ shells are filled; Pt and Au again show a reoccupation with $5s^1$.

- Fr–Rg: Fr and Ra fill the $7s$ orbital, Ac has the configuration $6d^1$, then the actinides follow with the filling of the f-orbital. The energies of $6d$ and $5f$ are close together, leading to corresponding reoccupations with $6d^{0,1}$ up to Lr and $6d^{2,3}$ for Rf and Db. There are no stable elements with filled $6d$, $7p$ orbitals.

For the chemical properties of the elements, the respective outer electrons are relevant. Accordingly, elements in a column of the periodic table have similar chemical properties. For example,

- the noble gases He–Rn with their full orbitals are very inert,
- the alkali metals (H), Li–Fr with one electron, and
- the halogens F–At with a 'hole' are very reactive.

3.5 Hund's Rules

For electrons in partially filled p-, d- or f-shells, the question arises as to how the electrons of these shells arrange themselves in the ground state. This question can be illustrated using the example of the carbon atom ($1s^2\,2s^2\,2p^2$) with two $2p$ electrons. The electrons in the p shell have the 6 states $\{\phi_{p_x}, \phi_{p_y}, \phi_{p_z}\} \otimes \{\chi_\uparrow, \chi_\downarrow\}$ available. The two electrons can 'choose' among $\binom{6}{2} = 15$ different configurations. The energy of the states is determined by the Hamiltonian $H = H_0 + H_{\text{WW}} + H_{\text{SO}}$, where

$$H_0 = \sum_{i=1}^{N} \left[\frac{p_i^2}{2m} + V_{\text{H}}(\boldsymbol{r}_i) - \frac{Ze^2}{r_i} \right] \tag{3.46}$$

with $V_{\text{H}}(\boldsymbol{r})$ being the effective potential in the Hartree approximation, see equation (3.19). Due to rotational symmetry, the $2p$ states of H_0 are degenerate.

The additional terms partially lift this degeneracy: The (residual) interaction energy is given by

$$H_{\text{WW}} = \frac{1}{2} \sum_{i \neq j} \frac{e^2}{|\boldsymbol{r}_i - \boldsymbol{r}_j|} - \sum_{i=1}^{N} V_{\text{H}}(\boldsymbol{r}_i) \tag{3.47}$$

and the (relativistic) spin-orbit (Russell-Saunders or LS coupling) takes the form

$$H_{\text{SO}} = \frac{1}{2m^2c^2} \frac{1}{r} \frac{dV}{dr} \sum_{i=1}^{N} \boldsymbol{l}_i \cdot \boldsymbol{s}_i \tag{3.48}$$

with $\boldsymbol{l}_i$ and $\boldsymbol{s}_i$ being the orbital angular momentum and spin of the i-th electron. Counting these energies, the 15 states split. This raises the question of which resulting ground state occurs and how large its remaining degeneracy is.

To solve this question, we treat the terms H_{WW} and H_{SO} in perturbation theory. $H_0 + H_{\text{WW}}$ is still $SO(3)$-symmetric and spin-independent. Thus, we define $\boldsymbol{L} = \sum_i \boldsymbol{l}_i$ and $\boldsymbol{S} = \sum_i \boldsymbol{s}_i$ as good quantum numbers.[9] The spin-orbit coupling destroys this symmetry, and $\boldsymbol{L}$, $\boldsymbol{S}$ are no longer individually conserved. Therefore, we switch to the total angular momentum $\boldsymbol{J}$ with

$$\boldsymbol{J} = \sum_i \boldsymbol{j}_i, \qquad \boldsymbol{j}_i = \boldsymbol{l}_i + \boldsymbol{s}_i, \tag{3.49}$$

which is still conserved.

The symmetry in the problem is $SO(3)$. We combine the degenerate configuration states into states with sharp angular momenta and spins $\boldsymbol{L}^2$, L_z, $\boldsymbol{S}^2$, S_z and find the state with the lowest energy. This state is still $(2L+1)(2S+1)$-fold degenerate. In

---

[9] Note that the total wave function Ψ must be antisymmetric, meaning that the mixing of the spin wave functions causes the individual spins $\boldsymbol{s}_i$ to not be good quantum numbers. For example, for $n = 2$ the singlet spin function $\chi_S = [|\uparrow\downarrow\rangle + |\downarrow\uparrow\rangle] / \sqrt{2}$ has $S_z \chi_S = 0$ but $s_{1z} \chi_S \not\propto \chi_S$.

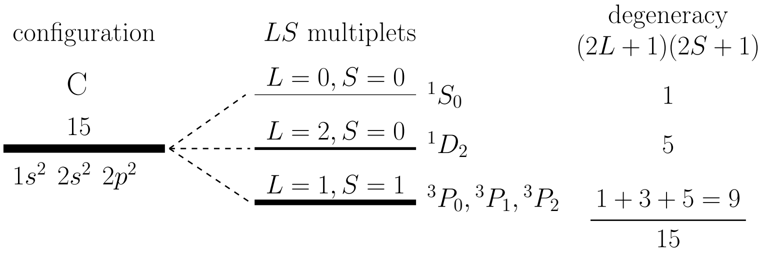

Figure 3.6: Configuration of the carbon atom C with splitting into LS multiplets and their degeneracy. The splitting of the highly degenerate configuration level involves that part of the Coulomb energy that has not already been accounted for in the one-particle energies.

our specific example of carbon C with the configuration $1s^2\,2s^2\,2p^2$ the $2p$ orbitals can be combined into

$$L_{\max} = 2 \text{ to } L_{\min} = 0 \qquad (\mathcal{H}_1 \otimes \mathcal{H}_1 = \mathcal{H}_0 \oplus \mathcal{H}_1 \oplus \mathcal{H}_2), \tag{3.50}$$

$$S_{\max} = 1 \text{ to } S_{\min} = 0 \qquad (\mathcal{H}_{1/2} \otimes \mathcal{H}_{1/2} = \mathcal{H}_0 \oplus \mathcal{H}_1). \tag{3.51}$$

The Pauli principle then allows the combinations

$$\begin{array}{llllll} L=2 & \text{symmetric} & \mapsto & S=0 & \text{antisymm.} & \mapsto J=2, \\ L=0 & \text{symmetric} & \mapsto & S=0 & \text{antisymm.} & \mapsto J=0, \\ L=1 & \text{antisymm.} & \mapsto & S=1 & \text{symmetric} & \mapsto J=0,1,2; \end{array}$$

the so-called LS multiplets. To characterize them, one uses the so-called term symbol

$$^{2S+1}L_J. \tag{3.52}$$

Here, S is the spin, L is the orbital angular momentum, and J is the total angular momentum of the atom; the latter can take different values for a fixed LS multiplet.

Under H_{WW}, the configuration states split. In Figure 3.6, this splitting is illustrated using the example of carbon C. The sequence of this splitting is nontrivial — the L, S, (J) quantum numbers for the atomic ground state are given by the Hund's rules, see Section 3.5.2.

In the next step, we consider the spin-orbit coupling H_{SO}. H_{SO} couples $\boldsymbol{L}$ and $\boldsymbol{S}$ and only the total angular momentum $\boldsymbol{J}$ remains as a good quantum number. Therefore, we transition from the $(2L+1)(2S+1)$ dimensional LS multiplet to the $\boldsymbol{J}$ basis (the 'quantum number' K symbolizes the not further described electron configuration) with

$$|K\,L\,S\,M_L\,M_S\rangle \mapsto |K\,L\,S\,J\,M\rangle \tag{3.53}$$

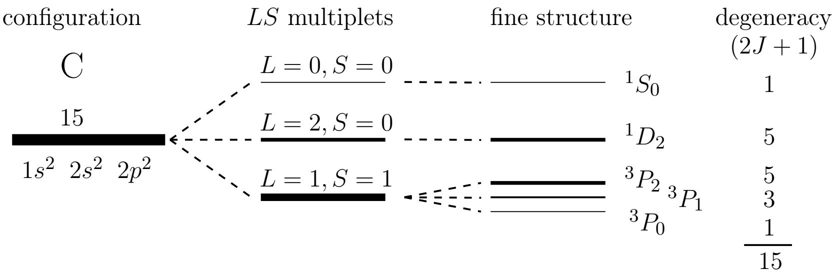

Figure 3.7: Configuration of the carbon atom C with splitting into LS multiplets and their fine structure (splitting in the range of 10 meV). The latter is induced by the (relativistic) spin-orbit coupling which mixes the orbital and spin angular momentum and thus only respects the total angular momentum J as a symmetry quantum number.

When we express H_{SO} in the LS multiplet basis, we obtain[10]

$$a\sum_{i=1}^{N}\boldsymbol{l}_i\cdot\boldsymbol{s}_i\mapsto A\,\boldsymbol{L}\cdot\boldsymbol{S}=\frac{A}{2}\big(\boldsymbol{J}^2-\boldsymbol{L}^2-\boldsymbol{S}^2\big) \tag{3.54}$$

$$=\frac{A}{2}\big[J(J+1)\underbrace{-L(L+1)-S(S+1)}_{\text{Constant in the } LS \text{ multiplet}}\big] \tag{3.55}$$

where A depends on L and S. One finds that A is positive in our case and therefore $J=0$ corresponds to the lowest energy state. Thus, we obtain the splitting of the LS multiplet into levels separated by typical energies $\simeq(\mathrm{Ry}^2/mc^2)Z^2\cdot J$ in the sub-eV range. The term scheme for carbon with the LS splitting and the fine structure of the spin-orbit coupling is sketched in Figure 3.7.

The remaining $(2J+1)$-fold degeneracy can be lifted by a (weak) magnetic field, see the discussion in Section 3.6. The resulting Zeeman splitting for the carbon atom is sketched in Figure 3.8.

3.5.1 Atoms heavier than Pb

For heavy atoms, we first treat H_0+H_{SO} and consider H_{WW} as a perturbation. We combine the one-particle orbitals $|n\,l\,m\,s\rangle=\varphi_{nlm}\chi_s=R_{nl}Y_{lm}\chi_s$ to fixed l and s into those with fixed $\boldsymbol{j}$, $j=l\pm1/2$, and obtain the new orbitals $|n\,l\,j\,m_j\rangle$. The new orbitals already take into account the spin-orbit interaction at the one-particle level. Finally, we consider H_{WW} by combining states with fixed total angular momentum $\boldsymbol{J}$[11] and diagonalize H_{WW} in each of these $(2J+1)$-dimensional spaces, yielding a ground state with fixed j_i^2, J^2, J_z.

---

[10] We will later argue that $a\sum_i\boldsymbol{l}_i\cdot\boldsymbol{s}_i=A\,\boldsymbol{L}\cdot\boldsymbol{S}$. A proof follows from the Wigner-Eckart theorem, see G. Baym.

[11] Accordingly, we construct Slater determinants with fixed J instead of fixed L & S.

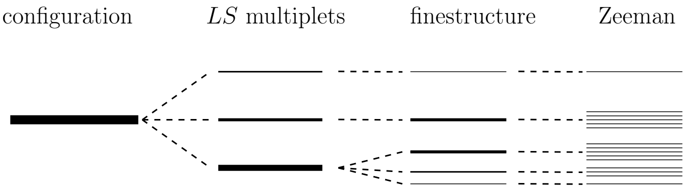

Figure 3.8: Configuration of the carbon atom C with splitting into LS multiplets, their fine structure, and the Zeeman splitting in a magnetic field. The corresponding Hamiltonian operator with the various splitting terms is given by $H_0 + H_{\mathrm{WW}} + H_{\mathrm{SO}} + \mu_B \sum_i \boldsymbol{H} \cdot (\boldsymbol{l}_i + 2\boldsymbol{s}_i)/\hbar$. In addition to the splitting in the external magnetic field (Zeeman), the nuclear spin also generates an effective magnetic field for the electrons, leading to hyperfine structure.

The exact calculation of the term schemes and the ground state ${}^{2S+1}L_J$ involves a complicated calculation. On the other hand, the task of finding the ground state configurations (resp. the corresponding term symbol ${}^{2S+1}L_J$) for light atoms can be easily found using the empirical Hund's rules.

3.5.2 Hund's Rules

1. Full shells do not contribute to the orbital/spin angular momenta L and S.
2. The LS multiplet with the largest S has the lowest energy.
3. For multiple L with the same S, the largest L has the lowest energy.
4. If the shell is less than half full or half full, then

$$J = |L - S|, \text{ i.e., minimal,}$$

if the shell is more than half filled, then

$$J = L + S, \text{ i.e., maximal.}$$

These empirical rules are supported by experimental observations and the following arguments:

1. In full shells, the angular momenta compensate to zero and the ground state configuration corresponds to the term symbol ${}^1S_0$.
2. If the total spin S is maximal, then the spin function χ_{Spin} is symmetric, the orbital function φ_{Bahn} must be antisymmetric due to the Pauli principle, and the electrons avoid each other. Accordingly, this configuration yields the lowest Coulomb energy.

3. If the orbital angular momentum L is maximal, then the radii of the electron orbits are large and the electron density is correspondingly low, which again minimizes the Coulomb energy.

4. For the spin-orbit coupling, we first consider the case where the shell is half or less than half filled. Then all spins are parallel, i.e., for this Hilbert subspace, we have

$$a \sum_{i=1}^{N} \boldsymbol{l}_i \cdot \boldsymbol{s}_i \approx a \sum_{i=1}^{N} \boldsymbol{l}_i \cdot \frac{\boldsymbol{S}}{N} \approx \frac{a}{N} \boldsymbol{L} \cdot \boldsymbol{S} \tag{3.56}$$

so that $A \approx a/N > 0$ and $J = |L - S|$ minimizes the energy ($2S = N =$ Number of electrons in the shell). For more than half-filled shells, we can apply the following consideration: We add the contribution of the missing (unoccupied) spins, so that formally a completely filled shell results, and then subtract this contribution again. Since the filled shell has a vanishing spin-orbit coupling (spin singlet), only the subtracted term $-a \sum_i \boldsymbol{l}_i \cdot \boldsymbol{s}_i$ remains. Now the spins and angular momenta can be viewed as 'hole'-spin and -angular momentum with $\boldsymbol{S} = -\sum_i \boldsymbol{s}_i$ and $\boldsymbol{L} = -\sum_i \boldsymbol{l}_i$. Since these are again aligned, we obtain $A \approx -a/N < 0$ with (2S = N = number of missing electrons in the shell). Thus, $J = L + S$ is the total angular momentum of minimal energy.

These arguments are based on the perspective for light atoms. The Hund's rules, however, apply to all atoms. We apply them here for two examples:

Nitrogen (N) with the electron configuration $1s^2\,2s^2\,2p^3$ ($Z = 7$): This is a half-filled p shell. (2) the maximum spin is $S = 3/2$ and (3) the maximum possible angular momentum is $L = 0$ $(= 1+0-1)$. From this, we find with the spin-orbit coupling (4) $J = |L - S| = 3/2$. The resulting configuration is ${}^4S_{3/2}$.

Promethium (Pm) with the electron configuration [Xe] $6s^2\,4f^5$ ($Z = 61$): This is a less than half-filled shell. (2) the maximum spin is $S = 5 \times 1/2 = 5/2$ and (3) the maximum possible angular momentum is $L = 5$ $(= 3 + 2 + 1 + 0 - 1)$. (4) the spin-orbit coupling yields $J = |L - S| = 5/2$. The configuration is therefore ${}^6H_{5/2}$.

3.6 Zeeman Splitting in a Magnetic Field

We consider atoms in a weak ($< 10^5$ Gauss) magnetic field $\boldsymbol{H} = (0, 0, H_z)$; the term generated by the magnetic field (with the elementary charge $e > 0$; it is $H_Z = -\boldsymbol{\mu} \cdot \boldsymbol{H}$, $\boldsymbol{\mu}_L = -(e/2mc)\boldsymbol{L}$, $\boldsymbol{\mu}_S = -g_e(e/2mc)\boldsymbol{S}, g_e = 2$)

$$H_Z = \frac{e}{2mc}(\boldsymbol{L} + 2\boldsymbol{S}) \cdot \boldsymbol{H} = \frac{e}{2mc}(\boldsymbol{J} + \boldsymbol{S}) \cdot \boldsymbol{H} \tag{3.57}$$

we treat in perturbation theory. The $(2J+1)$-fold degeneracy remaining in the fine structure is lifted by the magnetic field. The term proportional to $\boldsymbol{J}$ in (3.57) gives the contribution $e\hbar\, M\, H_z/2mc$ with M the magnetic quantum number for J_z. It remains to calculate $\langle S_z\rangle = \langle K\, L\, S\, J\, M|S_z|K\, L\, S\, J\, M\rangle$. It turns out that $\langle S_z\rangle \propto \langle J_z\rangle = M$. The result follows directly from the Wigner-Eckart theorem (which we do not want to introduce here). For an alternative proof, we use that $\boldsymbol{L}\cdot\boldsymbol{S}$ commutes with $\boldsymbol{J}$, so that the states $|K\, L\, S\, J\, M\rangle$ are eigenstates of $\boldsymbol{L}\cdot\boldsymbol{S}$ [the result follows immediately from $\boldsymbol{L}\cdot\boldsymbol{S} = \frac{1}{2}(\boldsymbol{J}^2 - \boldsymbol{L}^2 - \boldsymbol{S}^2)$]. Note also the following relation

$$[\boldsymbol{S}, \boldsymbol{L}\cdot\boldsymbol{S}] = \boldsymbol{S}(\boldsymbol{L}\cdot\boldsymbol{S}) - (\boldsymbol{L}\cdot\boldsymbol{S})\boldsymbol{S} \overset{12}{=} \boldsymbol{L}\times(\boldsymbol{S}\times\boldsymbol{S}) = i\hbar\boldsymbol{L}\times\boldsymbol{S}, \tag{3.58}$$

where we have used that $\boldsymbol{S}\times\boldsymbol{S} = i\hbar\boldsymbol{S}$ (angular momentum algebra) and $[\boldsymbol{L}, \boldsymbol{S}] = 0$. By taking the vector product with $\boldsymbol{J}$ (from the right), we obtain

$$\begin{aligned}(\boldsymbol{S}\times\boldsymbol{J})(\boldsymbol{L}\cdot\boldsymbol{S}) - (\boldsymbol{L}\cdot\boldsymbol{S})(\boldsymbol{S}\times\boldsymbol{J}) &= i\hbar(\boldsymbol{L}\times\boldsymbol{S})\times\boldsymbol{J} \overset{13}{=} i\hbar[\overbrace{\boldsymbol{S}(\boldsymbol{L}\cdot\boldsymbol{J})}^{+\boldsymbol{S}(\boldsymbol{S}\cdot\boldsymbol{J})} - \overbrace{\boldsymbol{L}(\boldsymbol{S}\cdot\boldsymbol{J})}^{+\boldsymbol{S}(\boldsymbol{S}\cdot\boldsymbol{J})}] \\ &= i\hbar[\boldsymbol{S}\boldsymbol{J}^2 - \boldsymbol{J}(\boldsymbol{S}\cdot\boldsymbol{J})].\end{aligned} \tag{3.59}$$

Since $|K\, L\, S\, J\, M\rangle$ is an eigenstate of $\boldsymbol{L}\cdot\boldsymbol{S}$, the expectation value of (3.58) (and thus also of (3.59)) must vanish. It follows that

$$\underbrace{\langle \boldsymbol{S}\boldsymbol{J}^2\rangle}_{=\hbar^2 J(J+1)\langle\boldsymbol{S}\rangle} = \langle \boldsymbol{J}(\boldsymbol{S}\cdot\boldsymbol{J})\rangle. \tag{3.60}$$

With $\boldsymbol{J}\cdot\boldsymbol{S} = \boldsymbol{S}^2 + \boldsymbol{L}\cdot\boldsymbol{S} = \frac{1}{2}(\boldsymbol{J}^2 + \boldsymbol{S}^2 - \boldsymbol{L}^2)$ we obtain the desired relation

$$\langle S_z\rangle = \langle J_z\rangle \frac{J(J+1) + S(S+1) - L(L+1)}{2J(J+1)}\,. \tag{3.61}$$

For the Zeeman splitting, we find

$$\langle H_Z\rangle = g\,\frac{e\hbar}{2mc} M H_z = g\mu_B M H_z \tag{3.62}$$

with the gyromagnetic factor g [also Landé-g-factor]

$$g = 1 + \frac{J(J+1) - L(L+1) + S(S+1)}{2J(J+1)}. \tag{3.63}$$

The elementary moment of the atom is

$$g\,\mu_B = g\frac{e\hbar}{2mc}. \tag{3.64}$$

---

[12] For operators, the Grassmann identity $\boldsymbol{a}\times(\boldsymbol{b}\times\boldsymbol{c}) = \boldsymbol{b}(\boldsymbol{a}\cdot\boldsymbol{c}) - (\boldsymbol{a}\cdot\boldsymbol{b})\boldsymbol{c}$, if $[a_j, b_k] = 0$.

[13] Here we use the Grassmann identity in the form $(\boldsymbol{a}\times\boldsymbol{b})\times\boldsymbol{c} = \boldsymbol{b}(\boldsymbol{a}\cdot\boldsymbol{c}) - \boldsymbol{a}(\boldsymbol{b}\cdot\boldsymbol{c})$, if $[a_j, b_k] = 0$.

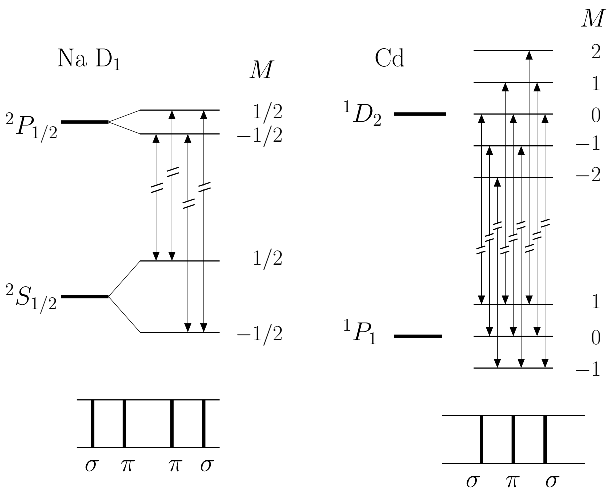

Figure 3.9: Anomalous and normal Zeeman effect for the Na D$_1$ transition [$^2S_{1/2}$ $(g = 2)$ – $^2P_{1/2}$ $(g = 2/3)$] and for the Cd [$^1P_1$ $(g = 1)$ – $^1D_2$ $(g = 1)$] transition. The π and σ transitions belong to the selection rules $\Delta m = 0$ and $\Delta m = \pm 1$.

For $S = 0$, $L = J$ and $g = 1$; conversely, for $L = 0$, the total momentum is given by the spin, $J = S$ and $g = 2$, which corresponds to the g-factor of the electron spin. Note that $g < 1$ is also possible; for example, promethium has $g = 2/7$.[14] The LSJ multiplet splits into $2J + 1$ sublevels with

$$\Delta E_Z = \mu_B g H_z, \tag{3.65}$$

Since the g-factor depends on the quantum numbers LSJ, complicated line splittings can arise in the spectrum. One distinguishes between normal and anomalous Zeeman effect, with the anomalous Zeeman effect being the normal case. In the normal Zeeman effect, the special case occurs where for both involved levels $S = 0$ and therefore $g = 1$, thus an optical line splits into three and one finds a ‘Zeeman triplet’. In the anomalous Zeeman effect, the g-factors of the two levels are different. Accordingly, more complicated line splittings result. In Figure 3.9, the two cases for the Na D$_1$ transition [$^2S_{1/2}$ $(g = 2)$ – $^2P_{1/2}$ $(g = 2/3)$], anomalous Zeeman effect, and for the Cd transition $^1P_1$ $(g = 1)$ – $^1D_2$ $(g = 1)$, normal Zeeman effect, are shown.

For strong magnetic fields ($> 10^5$ Gauss), we start directly from the LS multiplet since $H_Z > H_{\mathrm{SO}}$. The spin-orbit coupling H_{SO} is then included as a perturbation at the end. With the basis $|KLSM_LM_S\rangle$ in the LS multiplet, we immediately obtain the Zeeman splitting

$$\langle H_Z \rangle = \frac{e\hbar}{2mc}(M_L + 2M_S)H_z. \tag{3.66}$$

---

[14] Negative g factors are also possible (e.g., in the term scheme $^6F_{1/2}$). However, this does not correspond to a ground state of a neutral atom according to Hund’s rules.

The perturbation term H_{SO} generates the correction

$$\langle H_{\mathrm{SO}} \rangle = A M_L M_S, \tag{3.67}$$

and the resulting splitting

$$\langle H_Z + H_{\mathrm{SO}} \rangle \approx \mu_B (M_L + 2M_S) H_z \pm |A| M_L M_S, \tag{3.68}$$

where the upper (lower) sign applies for $\leq$ ($>$) half-filled shells. This is the Paschen-Back effect for the splitting of the levels in a strong magnetic field; the mixing of the angular momenta $\boldsymbol{L}$ and $\boldsymbol{S}$ by the spin-orbit coupling H_{SO} is suppressed by the strong magnetic field, and both angular momenta behave classically[15] (except for the $g = 2$ factor of the spin). Both, normal and anomalous Zeeman effect transition into the Paschen-Back effect at high magnetic fields. Conversely, the nontrivial anomalous Zeeman effect at weak fields arises from the mixing of $\boldsymbol{S}$ and $\boldsymbol{L}$ into $\boldsymbol{J}$ by H_{SO}.

---

[15] The angular momenta $\boldsymbol{L}$ and $\boldsymbol{S}$ precess independently in the field.

Chapter 4

Second Quantization

Second quantization is a new formalism that provides us with an elegant and compact formulation of many-body problems. Second quantization has nothing to do with 'quantizing a second time';[1] all of quantum mechanics is already contained in the theory we know, which consists of wave functions, Schrödinger equations (for dynamics), and symmetrization conditions for bosons and fermions. In second quantization, however, one transitions from the product wave function basis to a occupation basis: It is no longer specified which particle is in which state, but only how many particles are in a certain single-particle state. This way, a large part of the indistinguishability of the particles is already taken into account by the choice of basis. The rest, particularly the statistics, is expressed through the commutation relations of the creation and annihilation operators.

As the name suggests, the creation and annihilation operators effect the creation and annihilation of particles. The theory cannot therefore be formulated in Hilbert space with a fixed number of particles, but one must go to the so-called Fock space, which is already known from the grand canonical description of statistical physics. Formally, processes that do not conserve the number of particles become possible. The formalism of second quantization leads to a significant simplification, but ultimately only represents a reformulation of the many-body problem and does not yet provide a complete solution concept. We already know an example of second quantization: We have found the spectrum of the harmonic oscillator in two alternative ways,

---

[1] The name is therefore somewhat misleading.

a) Conventional Way → First Quant.

$$\begin{aligned} &H = p^2/2m + f\,q^2/2,\\ &\big[p, q\big] = -i\hbar;\\ &H\psi(q) = E\psi(q),\\ &E_n = \hbar\omega(n + \tfrac{1}{2}),\\ &\omega = \sqrt{f/m},\\ &\Psi_n(q) = N_n\, H_n(q) e^{-m\omega q^2/2\hbar}. \end{aligned}$$

b) Elegant Way → Operator Technique → Second Quant.

$$\begin{aligned} &H = \hbar\omega(a^\dagger a + 1/2)\\ &\big[a, a^\dagger\big] = 1;\\ &\text{Vacuum } |0\rangle,\ a|0\rangle = 0,\\ &\text{States, } |n\rangle = \frac{(a^\dagger)^n}{\sqrt{n!}}|0\rangle,\\ &E_n = \hbar\omega(n + \tfrac{1}{2}),\\ &\Psi_n(q) = \langle q|n\rangle. \end{aligned}$$

Instead of the wave function Ψ_n, we have introduced the creation and annihilation operators $a^\dagger$ and a and expressed the entire theory through the latter. The 'quanta' that are created and annihilated by $a^\dagger$ and a play the same role as 'particles'.[2]

In the following, we will first introduce the occupation number representation and then the formalism of second quantization for both bosons and fermions.

4.1 Representation of the Problem in First Quantization

In this section, we want to briefly summarize the results from Chapter **??**. The Hamiltonian operator is given by

$$H = \sum_{i=1}^{N} h_i + \frac{1}{2}\sum_{i\neq j}^{N} v_{ij}\,. \tag{4.1}$$

Here, h_i is a single-particle operator (QM) and v_{ij} describes the interaction between particles i and j. Due to the indistinguishability of the particles, the Hamiltonian operator must be symmetric under the exchange of particles, see (2.18).

Let $\{|\varphi_j\rangle\}$ be a vONS. Then the product states $|\varphi_{j_1}, \ldots, \varphi_{j_N}\rangle = |\varphi_{j_1}\rangle \otimes \cdots \otimes |\varphi_{j_N}\rangle$ span the Hilbert space $\mathcal{H}^{\otimes N}$ of distinguishable particles. The Hilbert space for indistinguishable particles $\mathcal{H}_{\mathcal{S},\mathcal{A}}$ is obtained by projecting onto the respective subspace. We write the projectors compactly as (vgl. (2.26))

$$\mathcal{P}_\pm = \frac{1}{N!}\sum_{\pi\in S_N} \zeta^\pi \pi \tag{4.2}$$

---

[2] In general, the number of particles in non-relativistic quantum mechanics is conserved. However, here the number of particles n can be changed by $a^\dagger$ and a; thus, the 'particles' corresponding to the excitations are not conserved in the case of the harmonic oscillator.

with $\pi|\varphi_{j_1},\dots,\varphi_{j_N}\rangle = |\varphi_{j_{\pi(1)}},\dots,\varphi_{j_{\pi(N)}}\rangle$, i.e., π acts by permuting the wave functions.[3] For bosons, $\zeta = +1$, so that the states are symmetrized, and for fermions, $\zeta = -1$, leading to anti-symmetrized states.

We then define basis states in $\mathcal{H}_{\mathcal{S},\mathcal{A}}$ by

$$|\varphi_{j_1},\dots,\varphi_{j_N}\} = \sqrt{N!}\,\mathcal{P}_\pm|\varphi_{j_1},\dots,\varphi_{j_N}\rangle \tag{4.3}$$

Due to the (anti-)symmetrization, we have

$$|\cdots,\varphi_{j_k},\cdots,\varphi_{j_l},\cdots\} = \zeta\,|\cdots,\varphi_{j_l},\cdots,\varphi_{j_k},\cdots\} \tag{4.4}$$

for arbitrary k and l. These states are not normalized for bosons. We will determine the normalization factor in the next section. However, for the proofs and derivations in this chapter, it is advantageous to occasionally work with the unnormalized states $|\cdot\}$.

4.2 Occupation Number Representation and Fock Space

Analogous to the example of the harmonic oscillator, we want to introduce the occupation number basis. To do this, we first establish an order of the (orthonormalized) single-particle states with $\varphi_1, \varphi_2, \dots$. [4] A state in $\mathcal{H}_{\mathcal{S},\mathcal{A}}$ is completely described by specifying how many particles are in the states φ_j. As an example, consider the $N = 10$ particle state[5]

$$|\underbrace{\varphi_1,\varphi_1,\varphi_1,\varphi_1,\varphi_1,\varphi_1,}_{\text{6-times}}\ \underbrace{\varphi_2,\varphi_2,\varphi_2,\varphi_2}_{\text{4-times}}\}\,. \tag{4.5}$$

This state is determined by the specification n_j, how many particles are in the states φ_j. In this example, $n_1 = 6$ and $n_2 = 4$.

In general, we define the occupation number representation by

$$|n_1, n_2, \cdots\rangle = \mathcal{N}|\overbrace{\varphi_1,\cdots,\varphi_1,}^{n_1\text{-times}}\overbrace{\varphi_2,\cdots,\varphi_2,}^{n_2\text{-times}}\cdots\} \tag{4.6}$$

with $\sum_j n_j = N$. Note the order of the states on the right side: the states φ_j are ordered by the index j. The Pauli principle for fermions requires $n_j = 0, 1$ while for bosons all occupation numbers $n_j = 0, 1, \dots$ are allowed. To determine the

---

[3] This corresponds to a permutation of the positions x with the inverse permutation π^{-1}.

[4] We need a discrete and ordered basis, i.e., the basis functions φ_j of the vONS can be numbered by natural numbers. A typical example is the plane waves e^{ikx} with $k \in (2\pi/L)\mathbb{Z}$. In the end, one lets the length L of the system go to infinity, with the 'usual' continuum limit $\sum_k \mapsto (L/2\pi)\int dk$.

[5] We use the (anti-)symmetry to order the particles according to the states φ_j.

correct normalization factor $\mathcal{N}$, we calculate the overlap between two states using the projector property $\mathcal{P}_\pm^2 = \mathcal{P}_\pm$

$$\begin{aligned}\{\varphi_{i_1}, \dots, \varphi_{i_N} | \varphi_{j_1}, \dots, \varphi_{j_N}\} &= N!\, \langle \varphi_{i_1}, \dots, \varphi_{i_N} | \mathcal{P}_\pm | \varphi_{j_1}, \dots, \varphi_{j_N} \rangle \\ &= \sum_{\pi \in S_N} \zeta^\pi \langle \varphi_{i_1} | \varphi_{j_{\pi(1)}} \rangle \cdots \langle \varphi_{i_N} | \varphi_{j_{\pi(N)}} \rangle . \end{aligned} \tag{4.7}$$

Due to the orthonormality of $|\varphi_j\rangle$, the only non-vanishing terms in the sum are those for which $(i_1, \dots, i_N)$ is a permutation of $(j_1, \dots, j_N)$. There are $\prod_j n_j!$ of these (one can permute the n_j states φ_j with fixed j arbitrarily), and thus it follows

$$\mathcal{N} = \frac{1}{\sqrt{\prod_j n_j!}} \tag{4.8}$$

Note that for fermions, $\mathcal{N} = 1$ regardless of the state.

Thus, every state in $\mathcal{H}_{\mathcal{S},\mathcal{A}}$ can be written as

$$|\Psi\rangle = \sum_{\substack{n_1, n_2, \dots \\ \sum_i n_i = N}} c_{n_1, n_2, \dots} |n_1, n_2, \dots \rangle . \tag{4.9}$$

with

$$\langle n_1', n_2', \dots | n_1, n_2, \dots \rangle = \delta_{n_1', n_1} \delta_{n_2', n_2} \cdots , \tag{4.10}$$

In order to work with creation and annihilation operators, analogous to the harmonic oscillator, we need to abandon the requirement of a fixed particle number N and introduce the Fock space

$$\mathcal{F} = \bigoplus_{N=0}^{\infty} \mathcal{H}^{\otimes N} ; \tag{4.11}$$

The corresponding (anti-)symmetric subspace $\mathcal{F}_{\mathcal{S},\mathcal{A}}$ is then the correct Hilbert space for the description of bosons (fermions) in a grand canonical description without a fixed particle number. States with different particle numbers are orthogonal to each other by construction. The above direct sum includes the 1-dimensional space $\mathcal{H}^{\otimes 0}$ (for $N = 0$), which consists only of the vacuum state $|0\rangle$ without particles. The occupation number states span the Fock space $\mathcal{F}_{\mathcal{S},\mathcal{A}}$ with the completeness relation

$$\sum_{n_1, n_2, \dots} |n_1, n_2, \dots \rangle \langle n_1, n_2, \dots | = I_{\mathcal{F}_{\mathcal{S},\mathcal{A}}} . \tag{4.12}$$

4.3 Creation and Annihilation Operators

All states in the Fock space can be traced back to the vacuum state through the introduction of creation and annihilation operators. For each single-particle state φ_j, we define the creation operator $a_j^\dagger\colon \mathcal{H}^{\otimes N} \to \mathcal{H}^{\otimes(N+1)}$ by its action

$$a_j^\dagger |\varphi_{i_1}\varphi_{i_2}\dots\} = |\varphi_j\ \varphi_{i_1}\varphi_{i_2}\dots\}. \tag{4.13}$$

on the (anti-)symmetric basis. The operator adds a particle 'in the first entry', while the state remains (anti-)symmetric. The action of $a_j^\dagger$ in the occupation number representation is then given by

$$a_j^\dagger |n_1,\dots,n_j,\dots\rangle = \zeta^{S_j}\ \sqrt{n_j+1}\,|n_1,\dots,n_j+1,\dots\rangle, \qquad S_j = \sum_{i=1}^{j-1} n_i. \tag{4.14}$$

The factor $\sqrt{n_j+1} = \sqrt{(n_j+1)!/n_j!}$ follows from the normalization of the occupation number states.

The sign factor ζ^{S_k} arises because the added state φ_j is at the beginning of $|\cdots\}$ and must be brought to the correct position in the occupation number representation. For this, it must be exchanged with the n_1 wave functions φ_1, the n_2 wave functions φ_2, ... and the n_{k-1} wave functions φ_{k-1}, see (4.4).

From equation (4.14), it follows that every state in the Fock space can be generated by repeated application of creation operators on the vacuum state $|0\rangle$[6]

$$|n_1,n_2,\dots\rangle = \frac{(a_1^\dagger)^{n_1}}{\sqrt{n_1!}}\frac{(a_2^\dagger)^{n_2}}{\sqrt{n_2!}}\cdots\ |0\rangle \tag{4.15}$$

Equation (4.15) is a strong statement: One can generate the complicated (anti-)symmetric many-body state (on the left) by successive application of the linear creation operators (on the right) to a single reference state (see exercise).

It may now turn out that constraints (in particular, that $n_j = 0, 1$ for fermions) lead to complicated relations between the various $a_j^\dagger$. We will now show that this is not the case. Consider the action of two creation operators $a_i^\dagger$ and $a_j^\dagger$ with $i \neq j$ on an arbitrary basis state

$$\begin{aligned} a_i^\dagger a_j^\dagger |\varphi_{j_1},\varphi_{j_2},\cdots\} &= |\varphi_i,\varphi_j,\ \varphi_{j_1},\varphi_{j_2},\cdots\} \\ &= \zeta|\varphi_j,\varphi_i,\ \varphi_{j_1},\varphi_{j_2},\cdots\} \\ &= \zeta a_j^\dagger a_i^\dagger |\varphi_{j_1},\varphi_{j_2},\cdots\}. \end{aligned} \tag{4.16}$$

Thus, it follows that $(i \neq j)$

$$\begin{aligned} [a_i^\dagger, a_j^\dagger]_+ &= [a_i^\dagger, a_j^\dagger] = a_i^\dagger a_j^\dagger - a_j^\dagger a_i^\dagger = 0, \qquad \text{(Bosons)}, \\ [a_i^\dagger, a_j^\dagger]_- &= \{a_i^\dagger, a_j^\dagger\} = a_i^\dagger a_j^\dagger + a_j^\dagger a_i^\dagger = 0, \qquad \text{(Fermions)}. \end{aligned} \tag{4.17}$$

---

[6] The order of the operators is important for fermions! In the form given here, no signs arise, as we first 'fill' the backmost state with a particle.

Thus, only the question of $i = j$ remains. For bosons ($\zeta = 1$), we have naturally $[a_j^\dagger, a_j^\dagger] = 0$ (the same operators commute). For fermions, the Pauli principle comes into play, which prohibits occupying a state more than once. This is expressed by the operator identity $(a_j^\dagger)^2 = 0$ (nilpotency), from which $\{a_j^\dagger, a_j^\dagger\} = 0$ follows. Overall, the creation operators thus satisfy the algebra

$$[a_i^\dagger, a_j^\dagger]_\zeta = 0. \tag{4.18}$$

Next, we turn to the adjoint operator $a_j = (a_j^\dagger)^\dagger$. The general matrix elements of (4.14) have the form

$$\langle n_1, \dots, n_j, \dots | a_j^\dagger | n_1', \dots, n_j', \dots \rangle = \zeta^{S_j} \sqrt{n_j' + 1}\, \delta_{n_1, n_1'} \cdots \delta_{n_j, n_j'+1} \cdots . \tag{4.19}$$

A complex conjugation of the above equation leads to the relation

$$\langle n_1', \dots, n_j', \dots | a_j | n_1, \dots, n_j, \dots \rangle = \zeta^{S_j} \sqrt{n_j}\, \delta_{n_1', n_1} \cdots \delta_{n_j', n_j - 1} \cdots . \tag{4.20}$$

Thus, for the adjoint operator a_i, we have

$$a_j | n_1, \dots, n_j, \dots \rangle = \zeta^{S_j} \sqrt{n_j}\, | n_1, \dots, n_j - 1, \dots \rangle. \tag{4.21}$$

Since a_i decreases the number of particles, it is called an annihilation operator. Adjointing (4.18) immediately yields $[a_i, a_j]_\zeta = 0$. From (4.21), we obtain the relation[7]

$$a_j |0\rangle = 0, \tag{4.22}$$

which uniquely determines the vacuum state.

To complete the algebra, we still need the (anti-)commutation relations between a_i and $a_j^\dagger$. For this, we consider the action of a_i and $a_j^\dagger$ on an arbitrary state in the occupation number representation. For $i < j$, we have

$$\begin{aligned} a_i a_j^\dagger | \dots, n_i, \dots, n_j, \dots \rangle =& a_i \zeta^{S_j} \sqrt{n_j + 1}\, | \dots, n_i, \dots, n_j + 1, \dots \rangle \\ =& \zeta^{S_j + S_i} \sqrt{(n_j + 1) n_i}\, | \dots, n_i - 1, \dots, n_j + 1, \dots \rangle \end{aligned}$$

and analogously

$$\begin{aligned} a_j^\dagger a_i | \dots, n_i, \dots, n_j, \dots \rangle =& a_j^\dagger \zeta^{S_i} \sqrt{n_i}\, | \dots, n_i - 1, \dots, n_j, \dots \rangle \\ =& \zeta^{(S_j - 1) + S_i} \sqrt{(n_j + 1) n_i}\, | \dots, n_i - 1, \dots, n_j + 1, \dots \rangle. \end{aligned}$$

Combining these two equations gives $(a_i a_j^\dagger - \zeta a_j^\dagger a_i) | n_1, n_2, \cdots \rangle = 0$ and thus $[a_i, a_j^\dagger]_\zeta = 0$ for $i < j$. The proof of this relation for $i > j$ follows analogously.

---

[7] It is important not to confuse the basis state $|0\rangle$ in the Hilbert space without particles (vacuum) with the number 0.

Finally, we consider the case $i = j$: For bosons, we have

$$a_j a_j^\dagger | \dots, n_j, \dots \rangle = (n_j + 1) | \dots, n_j, \dots \rangle$$

while

$$a_j^\dagger a_j | \dots, n_j, \dots \rangle = n_j | \dots, n_j, \dots \rangle.$$

From the difference of the two equations, we obtain $(a_j a_j^\dagger - a_j^\dagger a_j)|n_1, n_2, \cdots\rangle = |n_1, n_2, \cdots\rangle$ and thus $[a_j, a_j^\dagger] = 1$. For fermions, one must note that $n_j = 0, 1$. Thus, we have $a_j a_j^\dagger | \dots, n_j, \dots \rangle = (1 - n_j) | \dots, n_j, \dots \rangle$, $a_j^\dagger a_j | \dots, n_j, \dots \rangle = n_j | \dots, n_j, \dots \rangle$, from which $\{a_i^\dagger, a_i\} = 1$ follows.

In summary, the creation and annihilation operators satisfy the canonical commutation relations

$$\begin{aligned} &\text{Bosons:} && \text{Fermions:} \\ &[a_i, a_j^\dagger] = \delta_{ij}, && \{a_i, a_j^\dagger\} = \delta_{ij}, \\ &[a_i, a_j] = 0, && \{a_i, a_j\} = 0, \\ &[a_i^\dagger, a_j^\dagger] = 0, && \{a_i^\dagger, a_j^\dagger\} = 0, \end{aligned} \tag{4.23}$$

which each form a closed algebra. Considering that the full complexity of the Fock space is generated by repeatedly applying $a_j^\dagger$, the simplicity of the commutation relations is astonishing.

4.4 Basis Transformation

The creation and annihilation operators directly refer to a basis. Therefore, it is important to understand how the formalism behaves under a basis transformation. Let the single-particle states $\{|\varphi_i\rangle\}$ and $\{|\psi_j\rangle\}$ be two vONS. A change between the two basis systems is described in QM by the unitary basis transformation

$$\begin{aligned} |\varphi_i\rangle &= \sum_j \langle\psi_j|\varphi_i\rangle \, |\psi_j\rangle, \\ |\psi_j\rangle &= \sum_i \langle\varphi_i|\psi_j\rangle \, |\varphi_i\rangle \end{aligned} \tag{4.24}$$

In the language of second quantization, this basis change corresponds to a transformation of the annihilation operators a_i (to φ_i) to b_j (to ψ_j). From the relation $|\varphi_i\rangle = a_i^\dagger|0\rangle$, we obtain

$$a_i^\dagger|0\rangle = |\varphi_i\rangle \overset{(4.24)}{=} \sum_j \langle\psi_j|\varphi_i\rangle \, |\psi_j\rangle = \sum_j \langle\psi_j|\varphi_i\rangle \, b_j^\dagger \, |0\rangle. \tag{4.25}$$

A comparison of coefficients then leads to the transformation rules

$$\begin{aligned} a_i^\dagger &= \sum_j \langle\psi_j|\varphi_i\rangle b_j^\dagger, & b_j^\dagger &= \sum_i \langle\varphi_i|\psi_j\rangle a_i^\dagger, \\ a_i &= \sum_j \langle\varphi_i|\psi_j\rangle b_j, & b_j &= \sum_i \langle\psi_j|\varphi_i\rangle a_i. \end{aligned} \tag{4.26}$$

The commutation relations of the new operators $b_j, b_j^\dagger$ follow directly from those of a_i, $a_i^\dagger$. In particular, we have

$$[b_i, b_j]_\zeta \overset{(4.26)}{=} \sum_{k,k'} \langle\psi_i|\varphi_k\rangle\langle\psi_j|\varphi_{k'}\rangle \underbrace{[a_k, a_{k'}]_\zeta}_{=0} = 0$$

Furthermore, with the completeness of $\{|\varphi_k\rangle\}$

$$\begin{aligned} [b_i, b_j^\dagger]_\zeta &\overset{(4.26)}{=} \sum_{k,k'} \langle\psi_i|\varphi_k\rangle\langle\varphi_{k'}|\psi_j\rangle \overbrace{[a_k, a_{k'}^\dagger]_\zeta}^{=\delta_{kk'}} \\ &= \sum_k \langle\psi_i|\varphi_k\rangle\langle\varphi_k|\psi_j\rangle = \langle\psi_i|\psi_j\rangle = \delta_{ij}\,. \end{aligned} \tag{4.27}$$

Thus, $b_j, b_j^\dagger$ also satisfy the canonical commutation relations.

As an application example of the basis transformations, we consider fermions on a lattice. The operators $c_i^\dagger$, c_i create or annihilate a fermion at position i. On the other hand, the operators $c_{\boldsymbol{k}}^\dagger$, and $c_{\boldsymbol{k}}$ create/annihilate plane waves with wave vector $\boldsymbol{k}$. Then we have

$$\begin{aligned} c_{\boldsymbol{k}}^\dagger &= \sum_i \langle i|\boldsymbol{k}\rangle\, c_i^\dagger = \sum_i \frac{e^{i\boldsymbol{k}\cdot\boldsymbol{r}_i}}{\sqrt{\Omega}}\, c_i^\dagger, \\ c_i^\dagger &= \sum_{\boldsymbol{k}} \frac{e^{-i\boldsymbol{k}\cdot\boldsymbol{r}_i}}{\sqrt{\Omega}}\, c_{\boldsymbol{k}}^\dagger. \end{aligned} \tag{4.28}$$

Next, we are interested in the two-particle state $|\boldsymbol{kq}\rangle$, in particular its representation in the position basis on the lattice, which is given by the matrix elements $\langle ij|\boldsymbol{kq}\rangle$. To do this, we use the definitions

$$|ij\rangle = c_i^\dagger c_j^\dagger\,|0\rangle, \qquad |\boldsymbol{kq}\rangle = c_{\boldsymbol{k}}^\dagger c_{\boldsymbol{q}}^\dagger|0\rangle, \tag{4.29}$$

$$\begin{aligned} \Rightarrow \langle ij|\boldsymbol{kq}\rangle &= \langle 0|c_j c_i c_{\boldsymbol{k}}^\dagger c_{\boldsymbol{q}}^\dagger|0\rangle \\ &= \frac{1}{\Omega}\sum_{lm} \langle 0|c_j c_i e^{i\boldsymbol{k}\cdot\boldsymbol{r}_l} c_l^\dagger e^{i\boldsymbol{q}\cdot\boldsymbol{r}_m} c_m^\dagger|0\rangle \\ &= \frac{1}{\Omega}\sum_{lm} e^{i\boldsymbol{k}\cdot\boldsymbol{r}_l} e^{i\boldsymbol{q}\cdot\boldsymbol{r}_m} \langle 0|c_j c_i c_l^\dagger c_m^\dagger|0\rangle. \end{aligned} \tag{4.30}$$

The calculation of the matrix elements $\langle 0|c_j c_i c_l^\dagger c_m^\dagger|0\rangle$ shows how calculations are performed in the second quantized formalism: One uses the commutation relations (4.23) and the definition of the vacuum (4.22),

$$\begin{aligned}
\langle 0|c_j c_i c_l^\dagger c_m^\dagger|0\rangle &= \langle 0|c_j(\{c_i, c_l^\dagger\} - c_l^\dagger c_i)c_m^\dagger|0\rangle \\
&= \langle 0|c_j(\delta_{il} - c_l^\dagger c_i)c_m^\dagger|0\rangle \\
&= \delta_{il}\underbrace{\langle 0|c_j c_m^\dagger|0\rangle}_{\langle 0|\underbrace{\{c_j, c_m^\dagger\}}_{\delta_{jm}} - c_m^\dagger \underbrace{c_j|0\rangle}_{0}} - \langle 0|c_j c_l^\dagger \underbrace{c_i c_m^\dagger}_{\underbrace{\{c_i, c_m^\dagger\}}_{\delta_{im}} - c_m^\dagger c_i}|0\rangle \\
&= \delta_{il}\delta_{jm} - \langle 0|c_j c_l^\dagger(\delta_{im} - c_m^\dagger \underbrace{c_i)|0\rangle}_{0} \\
&= \delta_{il}\delta_{jm} - \delta_{im}\langle 0|\underbrace{\{c_j, c_l^\dagger\}}_{\delta_{jl}} - c_l^\dagger \underbrace{c_j|0\rangle}_{0} \\
&= \delta_{il}\delta_{jm} - \delta_{im}\delta_{jl}. \qquad (4.31)
\end{aligned}$$

We substitute the result into (4.30) and obtain the two-particle matrix element,

$$\begin{aligned}
\langle ij|\boldsymbol{kq}\rangle &= \frac{1}{\Omega}\sum_{lm}(\delta_{il}\delta_{jm} - \delta_{im}\delta_{jl})e^{i\boldsymbol{k}\cdot\boldsymbol{r}_j}e^{i\boldsymbol{q}\cdot\boldsymbol{r}_m} \\
&= \frac{1}{\Omega}\begin{vmatrix} e^{i\boldsymbol{k}\cdot\boldsymbol{r}_i} & e^{i\boldsymbol{k}\cdot\boldsymbol{r}_j} \\ e^{i\boldsymbol{q}\cdot\boldsymbol{r}_i} & e^{i\boldsymbol{q}\cdot\boldsymbol{r}_j} \end{vmatrix}. \qquad (4.32)
\end{aligned}$$

Thus, $\langle ij|\boldsymbol{kq}\rangle$ is precisely the Slater determinant of the plane wave product function $\varphi_{\boldsymbol{k}}(\boldsymbol{r}_i)\,\varphi_{\boldsymbol{q}}(\boldsymbol{r}_j)$. Accordingly, $\langle ij|\boldsymbol{kq}\rangle$ is already correctly antisymmetrized.

4.5 Operators in Second Quantization

In quantum mechanics, one needs operators in addition to states. The operators can also be compactly represented in the formalism of second quantization. As an introduction, we introduce an alternative representation of the annihilation operator a_j (to φ_j). Let $|\Psi\rangle = |\psi_1, \psi_2, \cdots, \psi_N\rangle$ be a general N-particle product state. We define the annihilation operator without considering symmetry as

$$a_j|\Psi\rangle = a_j|\psi_1, \psi_2, \cdots, \psi_N\rangle = \sqrt{N}\langle\varphi_j|\psi_1\rangle|\psi_2, \cdots, \psi_N\rangle\,. \qquad (4.33)$$

Now we show that the defined a_j agrees with (4.21) in the relevant subspace $\mathcal{H}_{\mathcal{S},\mathcal{A}}$. Due to linearity, we only need to show this for the states $|n_1, \ldots, n_j \ldots\rangle$. It holds (with $\langle\varphi_i|\varphi_j\rangle = \delta_{ij}$ and with the definition (4.33))

$$a_j \sum_{\pi\in S_N}(-1)^\pi \pi|\cdots,\overbrace{\varphi_j,\cdots,\varphi_j}^{n_j\text{-times}},\cdots\rangle = n_j\zeta^{S_j} a_j \sum_{\substack{\pi\in S_{N-1}\subset S_N\\ \pi(1)=1}}(-1)^\pi\pi|\varphi_j,\varphi_1,\cdots,\overbrace{\varphi_j,\cdots,\varphi_j}^{(n_j-1)\text{-times}},\cdots\rangle$$

$$= n_j\zeta^{S_j}\sqrt{N}\sum_{\pi\in S_{N-1}}(-1)^\pi\pi|\varphi_1,\cdots,\underbrace{\varphi_j,\cdots,\varphi_j}_{(n_j-1)\text{-times}},\cdots\rangle,$$

where we have utilized in the first line that only the permutations that place a φ_j in the first position contribute (where there are n_j possibilities), while the permutation over the remaining $N-1$ particles remains free. Since a_j only acts on the first entry, it commutes in a second step with the permutations restricted to $\pi(1)=1$. Thus, we obtain from (4.33) the action on the occupation number states

$$\begin{aligned} a_j|n_1,\ldots,n_j,\ldots\rangle &= \sqrt{\frac{1}{N!\prod_i n_i!}}\,a_j\sum_{\pi\in S_N}(-1)^\pi\pi|\cdots,\overbrace{\varphi_j,\cdots,\varphi_j}^{n_j\text{-times}},\cdots\rangle \\ &= \zeta^{S_j}\sqrt{\frac{1}{N!\prod_i n_i!}}n_j\sqrt{N}\sum_{\pi\in S_{N-1}}(-1)^\pi\pi|\cdots,\overbrace{\varphi_j,\cdots,\varphi_j}^{(n_j-1)\text{-times}},\cdots\rangle \\ &= \zeta^{S_j}\sqrt{n_j}\,|n_1,\ldots,n_j-1,\ldots\rangle, \end{aligned} \tag{4.34}$$

which agrees with (4.21). In particular, (4.33) remains valid in the subspace with the corresponding symmetry.

4.5.1 Single-Particle Operators

Let b be a general operator on $\mathcal{H}$ with the matrix elements $b_{\alpha\beta} = \langle\varphi_\alpha|b|\varphi_\beta\rangle$.[8] The corresponding single-particle operator B in the Fock space $\mathcal{F}$ is defined as

$$B = \bigoplus_{N=0}^{\infty} B_N = 0\oplus B_1\oplus B_2\oplus\cdots \tag{4.35}$$

with

$$B_1 = b, \qquad B_2 = b_1 + b_2 = b\otimes I + I\otimes b, \qquad B_N = \sum_{i=1}^{N} b_i \tag{4.36}$$

see (2.4). This operator is expressed in second quantization by

$$B = \sum_{\alpha,\beta} b_{\alpha\beta}\,a_\alpha^\dagger a_\beta = \sum_{\alpha,\beta}\langle\varphi_\alpha|b|\varphi_\beta\rangle\,a_\alpha^\dagger a_\beta \tag{4.37}$$

---

[8] In this section, we use Greek indices α,β for the sums over the basis states to distinguish them from i, the sum over the particles.

To prove this, we calculate in the N-particle subspace ($|\boldsymbol{\psi}\} = |\psi_1, \cdots\}$)

$$\{\boldsymbol{\psi}'|\sum_{i=1}^{N} b_i|\boldsymbol{\psi}\} = N\{\boldsymbol{\psi}'|b_1|\boldsymbol{\psi}\} = N\sum_{\alpha,\beta} b_{\alpha\beta}\{\boldsymbol{\psi}'|(|\varphi_\alpha\rangle\langle\varphi_\beta|)_1|\boldsymbol{\psi}\} \overset{(4.33)}{=} \sum_{\alpha,\beta} b_{\alpha\beta}\{a_\alpha\boldsymbol{\psi}'|a_\beta\boldsymbol{\psi}\}$$
$$= \{\boldsymbol{\psi}'|\sum_{\alpha,\beta} b_{\alpha\beta}a^\dagger_\alpha a_\beta|\boldsymbol{\psi}\}; \tag{4.38}$$

In the first step, we have used the symmetry of $|\boldsymbol{\psi}\}, |\boldsymbol{\psi}'\}$. Thus, it holds $B_N = \sum_{\alpha,\beta} b_{\alpha\beta}\, a^\dagger_\alpha a_\beta$ for all N and B is represented in the (anti-)symmetric Fock space by (4.37).

An important single-particle operator is the particle number. This corresponds to the operator $b = I$ with $N = B = \sum_\alpha a^\dagger_\alpha a_\alpha$. The operator N acts in the Fock space by simply returning N, i.e.

$$N = 0 \oplus 1 \oplus 2 \oplus 3 \oplus \cdots\,. \tag{4.39}$$

If a Hamiltonian operator is a single-particle operator, i.e. $H = \sum_i h_i$, it is called quadratic. All single-particle problems that have been treated in QM fall into this category. In many-body theory, quadratic Hamiltonians are called solvable, as one can immediately determine all many-body eigenstates with the (complete) solution of the single-particle problem

$$h|\psi_\alpha\rangle = \varepsilon_\alpha|\psi_\alpha\rangle \tag{4.40}$$

By defining the creation and annihilation operators b_α with respect to the energy eigenbasis (see section 4.4), one obtains

$$H = \sum_\alpha \varepsilon_\alpha b^\dagger_\alpha b_\alpha\,. \tag{4.41}$$

The many-body eigenstates with $H|\boldsymbol{n}\rangle = E_{\boldsymbol{n}}|\boldsymbol{n}\rangle$ are simply occupation number states $|\boldsymbol{n}\rangle = |n_1, n_2, \dots\rangle$ corresponding to the single-particle solutions $|\alpha\rangle$. The energy of the many-body states is given by

$$E_{\boldsymbol{n}} = \sum_\alpha n_\alpha \varepsilon_\alpha. \tag{4.42}$$

The statistics of the particles only appears through the occupation numbers $n_\alpha = 0, 1, \dots$ for bosons and $n_\alpha = 0, 1$ for fermions.

However, many-body Hamiltonians are mostly given by a sum of a single-particle and a two-particle part. Then the solution of the single-particle problem is not sufficient to solve the complete many-body problem. Rather, one usually uses the single-particle solution as a basis to treat the many-body problem perturbatively with the two-particle operator as the perturbation. An exact solution of the many-body problem is then usually not possible, and the computational effort, e.g., on a computer grows exponentially with the number of particles N.

4.5.2 Two-Particle Operators

For a general two-particle operator $B = \frac{1}{2}\sum_{i\neq j} b_{ij}$, the derivation of the second quantized representation works analogously to the case for single-particle operators. The matrix elements are given by

$$b_{\alpha_1\alpha_2,\beta_1\beta_2} = \langle\varphi_{\alpha_1}\varphi_{\alpha_2}|b|\varphi_{\beta_1}\varphi_{\beta_2}\rangle\,. \tag{4.43}$$

We calculate

$$\begin{aligned}
\{\boldsymbol{\psi}'|\tfrac{1}{2}\textstyle\sum_{i\neq j} b_{ij}|\boldsymbol{\psi}\} &= \frac{N(N-1)}{2}\{\boldsymbol{\psi}'|b_{12}|\boldsymbol{\psi}\} \\
&= \frac{N(N-1)}{2}\sum_{\substack{\alpha_1,\alpha_2\\ \beta_1,\beta_2}} b_{\alpha_1\alpha_2,\beta_1\beta_2}\{\boldsymbol{\psi}'|(|\varphi_{\alpha_1},\varphi_{\alpha_2}\rangle\langle\varphi_{\beta_1},\varphi_{\beta_2}|)_{12}|\boldsymbol{\psi}\} \\
&\overset{(4.33)}{=} \frac{1}{2}\sum_{\alpha,\beta} b_{\alpha_1\alpha_2,\beta_1\beta_2}\{a_{\alpha_2}a_{\alpha_1}\boldsymbol{\psi}'|a_{\beta_2}a_{\beta_1}\boldsymbol{\psi}\} \\
&= \{\boldsymbol{\psi}'|\tfrac{1}{2}\textstyle\sum_{\alpha,\beta} b_{\alpha_1\alpha_2,\beta_1\beta_2}a^\dagger_{\alpha_1}a^\dagger_{\alpha_2}a_{\beta_2}a_{\beta_1}|\boldsymbol{\psi}\};
\end{aligned}$$

Note that the annihilation operator forms a matrix element with the first entry according to (4.33). This defines the order in the third line. Thus, we obtain the representation

$$B = \frac{1}{2}\sum_{\substack{\alpha_1,\alpha_2\\ \beta_1,\beta_2}} b_{\alpha_1\alpha_2,\beta_1\beta_2}a^\dagger_{\alpha_1}a^\dagger_{\alpha_2}a_{\beta_2}a_{\beta_1} = \frac{1}{2}\sum_{\substack{\alpha_1,\alpha_2\\ \beta_1,\beta_2}} \langle\varphi_{\alpha_1}\varphi_{\alpha_2}|b|\varphi_{\beta_1}\varphi_{\beta_2}\rangle\, a^\dagger_{\alpha_1}a^\dagger_{\alpha_2}a_{\beta_2}a_{\beta_1}$$

of any two-particle operator in the Fock space. Note particularly the reversed order of the creation and annihilation operators. The particles are first 'removed' and then reinserted in reverse order.

The derivation presented here can be easily extended to the case of a ν-particle operator. This generally has the form

$$B = \frac{1}{\nu!}\sum_{\substack{\alpha_1,\ldots,\alpha_\nu\\ \beta_1,\ldots,\beta_\nu}} \langle\varphi_{\alpha_1},\ldots,\varphi_{\alpha_\nu}|b|\varphi_{\beta_1},\ldots,\varphi_{\beta_\nu}\rangle\, a^\dagger_{\alpha_1}\cdots a^\dagger_{\alpha_\nu}a_{\beta_\nu}\cdots a_{\beta_1}. \tag{4.44}$$

4.6 Field Operators

By performing a basis transformation to the position basis $\{|\boldsymbol{r}s\rangle\}$, we obtain the field operators, $\Psi_s(\boldsymbol{r})$ (where s denotes the spin quantum number). The field operators are practical because they are independent of the system and thus allow for a unified description. Let $\{\varphi_\alpha\}$ be any vONS in the single-particle Hilbert space. The completeness provides the expansion

$$|\boldsymbol{r}s\rangle = \sum_\alpha |\varphi_\alpha\rangle\,\underbrace{\langle\varphi_\alpha|\boldsymbol{r}s\rangle}_{\varphi^*_{\alpha,s}(\boldsymbol{r})}\,. \tag{4.45}$$

It holds that $|\varphi_\alpha\rangle = a_\alpha^\dagger|0\rangle$ and we define analogously $|\boldsymbol{r}s\rangle = \Psi_s^\dagger(\boldsymbol{r})|0\rangle$, i.e., the field operator $\Psi_s^\dagger(\boldsymbol{r})$ creates a particle with spin s at position $\boldsymbol{r}$. The relation (4.45) can then be written as

$$\Psi_s^\dagger(\boldsymbol{r})|0\rangle = \sum_\alpha \varphi_{\alpha,s}^*(\boldsymbol{r})\, a_\alpha^\dagger|0\rangle \tag{4.46}$$

and we obtain the transformation to the field operators (cf. (4.26))

$$\Psi_s^\dagger(\boldsymbol{r}) = \sum_\alpha \varphi_{\alpha,s}^*(\boldsymbol{r})\, a_\alpha^\dagger, \qquad \Psi_s(\boldsymbol{r}) = \sum_\alpha \varphi_{\alpha,s}(\boldsymbol{r})\, a_\alpha. \tag{4.47}$$

The notation for the so-called field operators $\Psi_s^\dagger(\boldsymbol{r})$, $\Psi_s(\boldsymbol{r})$ is historically conditioned and is meant to remind one of the wave function $\psi_s(\boldsymbol{r})$.

The commutation relations of the field operators follow from completeness and from the canonical relations of the a_α and $a_\alpha^\dagger$ operators. The only non-trivial case is

$$\begin{aligned}[\Psi_s(\boldsymbol{r}), \Psi_{s'}^\dagger(\boldsymbol{r}')]_\zeta &= \sum_{\alpha,\alpha'} \varphi_{\alpha,s}(\boldsymbol{r})\varphi_{\alpha',s'}^*(\boldsymbol{r}')\, \overbrace{[a_\alpha, a_{\alpha'}^\dagger]_\zeta}^{\delta_{\alpha,\alpha'}} = \sum_\alpha \langle \boldsymbol{r}, s|\varphi_\alpha\rangle\langle\varphi_\alpha|\boldsymbol{r}', s'\rangle \\ &= \delta^{(3)}(\boldsymbol{r}-\boldsymbol{r}')\delta_{ss'}\end{aligned} \tag{4.48}$$

For bosons, this yields

For fermions, we obtain

$$\begin{aligned}
&[\Psi_s(\boldsymbol{r}), \Psi_{s'}(\boldsymbol{r}')] = 0, && \{\Psi_s(\boldsymbol{r}), \Psi_{s'}(\boldsymbol{r}')\} = 0, \\
&[\Psi_s^\dagger(\boldsymbol{r}), \Psi_{s'}^\dagger(\boldsymbol{r}')] = 0, && \{\Psi_s^\dagger(\boldsymbol{r}), \Psi_{s'}^\dagger(\boldsymbol{r}')\} = 0, \\
&[\Psi_s(\boldsymbol{r}), \Psi_{s'}^\dagger(\boldsymbol{r}')] = \delta^{(3)}(\boldsymbol{r}-\boldsymbol{r}')\delta_{ss'}. && \{\Psi_s(\boldsymbol{r}), \Psi_{s'}^\dagger(\boldsymbol{r}')\} = \delta^{(3)}(\boldsymbol{r}-\boldsymbol{r}')\delta_{ss'}.
\end{aligned} \tag{4.49}$$

4.6.1 The Many-Body Position Basis

In the following, we suppress the spin index s to keep the notation simple. We define the states of the many-body position basis by

$$|\boldsymbol{r}_1, \boldsymbol{r}_2, \ldots, \boldsymbol{r}_N\} = \Psi^\dagger(\boldsymbol{r}_1)\Psi^\dagger(\boldsymbol{r}_2)\cdots\Psi^\dagger(\boldsymbol{r}_N)|0\rangle \tag{4.50}$$

By construction, the states are (anti-)symmetric upon exchanging two particles. $\Psi^\dagger(\boldsymbol{r})$ adds a particle at $\boldsymbol{r}$ while $\Psi(\boldsymbol{r})$ annihilates a particle at $\boldsymbol{r}$. The action of the field operators on an (anti-)symmetric position state is therefore

$$\Psi^\dagger(\boldsymbol{r})|\boldsymbol{r}_1, \ldots, \boldsymbol{r}_N\} = |\boldsymbol{r}, \boldsymbol{r}_1, \ldots, \boldsymbol{r}_N\} \tag{4.51}$$

$$\begin{aligned}\Psi(\boldsymbol{r})\,|\boldsymbol{r}_1, \ldots, \boldsymbol{r}_N\} &= \Psi(\boldsymbol{r})\Psi^\dagger(\boldsymbol{r}_1)\cdots\Psi^\dagger(\boldsymbol{r}_N)|0\rangle \\ &= \sum_{i=1}^N \zeta^{i-1}\delta(\boldsymbol{r}-\boldsymbol{r}_i)|\boldsymbol{r}_1, \ldots, \boldsymbol{r}_{i-1}, \boldsymbol{r}_{i+1}, \ldots, \boldsymbol{r}_N\}.\end{aligned} \tag{4.52}$$

The equivalence in the last line follows by permuting $\Psi(\boldsymbol{r})$ through all $\Psi^\dagger(\boldsymbol{r}_i)$. The physical interpretation is that the particle at $\boldsymbol{r}$ can only be removed if one of the N coordinates $\boldsymbol{r}_1, \ldots, \boldsymbol{r}_N$ is equal to $\boldsymbol{r}$.

The overlap of two states in the many-body position basis is determined analogously to equation (4.7) by

$$\begin{aligned}\{\boldsymbol{r}'_1, \ldots, \boldsymbol{r}'_{N'}|\boldsymbol{r}_1, \ldots, \boldsymbol{r}_N\} = \delta_{NN'} \sum_{\pi \in S_n} \zeta^\pi \delta(\boldsymbol{r}_1 - \boldsymbol{r}'_{\pi(1)}) \\ \times \delta(\boldsymbol{r}_2 - \boldsymbol{r}'_{\pi(2)}) \cdots \delta(\boldsymbol{r}_N - \boldsymbol{r}'_{\pi(N)}). \quad (4.53)\end{aligned}$$

The identity in the Fock space can also be written in the many-body position basis. To do this, one starts with the identity in the Hilbert space of distinguishable particles and applies the (anti-)symmetrizer as an operator transformation

$$\begin{aligned}I_{\mathcal{F}} &= \sum_N \int d^3r_1 \ldots d^3r_N \, \mathcal{P}_\pm |\boldsymbol{r}_1, \ldots, \boldsymbol{r}_N \rangle\langle \boldsymbol{r}_1, \ldots, \boldsymbol{r}_N | \mathcal{P}_\pm \\ &= \sum_N \frac{1}{N!} \int d^3r_1 \ldots d^3r_N |\boldsymbol{r}_1, \ldots, \boldsymbol{r}_N\}\{\boldsymbol{r}_1, \ldots, \boldsymbol{r}_N| \qquad (4.54)\end{aligned}$$

With this representation of the identity, arbitrary states in the many-body position basis can be developed as usual:

$$|\Phi\rangle = \sum_N \frac{1}{N!} \int d^3r_1 \ldots d^3r_N \, \varphi(\boldsymbol{r}_1, \ldots, \boldsymbol{r}_N) |\boldsymbol{r}_1, \ldots, \boldsymbol{r}_N\} \qquad (4.55)$$

$|\Phi\rangle$ has the correct symmetry for arbitrary wave functions $\varphi(\boldsymbol{r}_1, \ldots, \boldsymbol{r}_N)$, including those that are not (anti-)symmetrized. This is easiest to see by considering equation (4.55) for φ with fixed N

$$\begin{aligned}\{\boldsymbol{r}'_1, \ldots, \boldsymbol{r}'_N|\Phi\rangle &\overset{(4.53)}{=} \frac{1}{N!} \int d^3r_1 \ldots d^3r_N \, \varphi(\boldsymbol{r}_1, \ldots, \boldsymbol{r}_N)\{\boldsymbol{r}'_1, \ldots, \boldsymbol{r}'_N|\boldsymbol{r}_1, \ldots, \boldsymbol{r}_N\} \\ &= \frac{1}{N!} \sum_\pi \zeta^\pi \varphi(\boldsymbol{r}'_{\pi(1)}, \ldots, \boldsymbol{r}'_{\pi(N)}) = \varphi(\boldsymbol{r}'_1, \ldots, \boldsymbol{r}'_N),\end{aligned}$$

Here, the last equation holds if φ is already (anti-)symmetrized. If φ is also normalized, i.e., $\int d^3r_1 \cdots d^3r_N \, |\varphi(\boldsymbol{r}_1, \ldots, \boldsymbol{r}_N)|^2 = 1$, then $|\Phi\rangle$ is also normalized, $\langle\Phi|\Phi\rangle = 1$.

4.6.2 Operators Expressed Through Field Operators

As already mentioned, the field operators are particularly well-suited for deriving the representation of various operators in second quantization. We want to demonstrate this in this section with a series of important examples. We start with the single-particle operators.

The representation of a single-particle operator B in the field operators is obtained from equation (4.26) by expressing the operators a_α using (4.47) in terms of the field operators. Starting from a single-particle operator $b = \iint d^3r' d^3r\, B(\boldsymbol{r}', \boldsymbol{r})|\boldsymbol{r}'\rangle\langle\boldsymbol{r}|$ in the position basis, we obtain the general expression of the single-particle operator

$$\begin{aligned} B &= \sum_{\alpha,\beta} \langle\varphi_\alpha|b|\varphi_\beta\rangle\, a^\dagger_\alpha a_\beta = \sum_{\alpha,\beta} \iint d^3r' d^3r\, \varphi^*_\alpha(\boldsymbol{r}')B(\boldsymbol{r}', \boldsymbol{r})\varphi_\beta(\boldsymbol{r})a^\dagger_\alpha a_\beta \\ &= \iint d^3r' d^3r\, \Psi^\dagger(\boldsymbol{r}')B(\boldsymbol{r}', \boldsymbol{r})\Psi(\boldsymbol{r}). \end{aligned} \tag{4.56}$$

It is interesting to compare this second-quantized form with the first-quantized form of the expectation value in the state $\varphi(\boldsymbol{r})$,

$$\langle b\rangle_\varphi = \iint d^3r' d^3r\, \varphi^*(\boldsymbol{r}')B(\boldsymbol{r}', \boldsymbol{r})\varphi(\boldsymbol{r}). \tag{4.57}$$

If one replaces the wave function $\varphi(\boldsymbol{r})$ in the expression for $\langle b\rangle_\varphi$ with the field operator $\Psi(\boldsymbol{r})$, one obtains the operator in second-quantized form! This formal similarity is the reason why the formalism with creation and annihilation operators is called "second quantization"; single-particle wave functions have seemingly become operators that create and annihilate particles. However, this is only a formal relationship. We have derived the second-quantized formalism from the first-quantized many-body quantum mechanics without additional assumptions. The formal relationship is therefore more an expression of the 'naturalness' of second quantization.

Example Density Operator: The expectation value of the single-particle density operator

$$\begin{aligned} \langle\rho(\boldsymbol{r})\rangle_\varphi &= \int d^3r'\, \varphi^*(\boldsymbol{r}')\delta^{(3)}(\boldsymbol{r} - \boldsymbol{r}')\varphi(\boldsymbol{r}') \\ &= \varphi^*(\boldsymbol{r})\varphi(\boldsymbol{r}), \end{aligned} \tag{4.58}$$

when rewritten in second-quantized form becomes the density operator of the many-body system

$$\rho(\boldsymbol{r}) = \Psi^\dagger(\boldsymbol{r})\Psi(\boldsymbol{r}). \tag{4.59}$$

The particle number operator, which can be obtained in first-quantized form by integrating over the density $\rho(\boldsymbol{r})$, has in second quantization the form

$$N = \int d^3r\, \Psi^\dagger(\boldsymbol{r})\Psi(\boldsymbol{r}). \tag{4.60}$$

For translation-invariant systems, it is often useful to work with quantities in momentum space. For this, we define the Fourier transform of the density as

$\rho(\boldsymbol{q}) = \int d^3r\, e^{-i\boldsymbol{q}\cdot\boldsymbol{r}}\rho(\boldsymbol{r})$ and use the representation $\Psi(\boldsymbol{r}) = \Omega^{-1/2}\sum_{\boldsymbol{k}} e^{i\boldsymbol{k}\cdot\boldsymbol{r}}c_{\boldsymbol{k}}$. This gives us

$$\begin{aligned}\rho(\boldsymbol{q}) = \int d^3r\, e^{-i\boldsymbol{q}\cdot\boldsymbol{r}}\rho(\boldsymbol{r}) &= \sum_{\boldsymbol{k}\boldsymbol{k}'}\frac{1}{\Omega}\int d^3r\, e^{-i\boldsymbol{q}\cdot\boldsymbol{r}}e^{-i\boldsymbol{k}\cdot\boldsymbol{r}}e^{i\boldsymbol{k}'\cdot\boldsymbol{r}}c^\dagger_{\boldsymbol{k}}\,c_{\boldsymbol{k}'} \\ &= \sum_{\boldsymbol{k}} c^\dagger_{\boldsymbol{k}}c_{\boldsymbol{k}+\boldsymbol{q}}.\end{aligned} \tag{4.61}$$

Example Current Density Operator: The expression for the current density in first quantization

$$\langle \boldsymbol{j}(\boldsymbol{r})\rangle = \frac{\hbar}{2mi}\left[\varphi^*(\boldsymbol{r})\boldsymbol{\nabla}\varphi(\boldsymbol{r}) - \varphi(\boldsymbol{r})\boldsymbol{\nabla}\varphi^*(\boldsymbol{r})\right] \tag{4.62}$$

becomes in the Fock space the current density operator of the many-body system

$$\boldsymbol{j}(\boldsymbol{r}) = \frac{\hbar}{2mi}\left[\Psi^\dagger(\boldsymbol{r})\boldsymbol{\nabla}\Psi(\boldsymbol{r}) - \big(\boldsymbol{\nabla}\Psi^\dagger(\boldsymbol{r})\big)\Psi(\boldsymbol{r})\right]. \tag{4.63}$$

Note the order of the operators: First, $\Psi(\boldsymbol{r})$ must "remove" a particle from the state $|\Phi\rangle$, then the operator acts at that location, and finally the particle is added back to the system by $\Psi^\dagger(\boldsymbol{r})$.

The Fourier representation of the current density operator is determined completely analogously to that of the density operator with the result

$$\boldsymbol{j}(\boldsymbol{q}) \;= \frac{\hbar}{2m}\sum_{\boldsymbol{k}}(2\boldsymbol{k}+\boldsymbol{q})\,c^\dagger_{\boldsymbol{k}}c_{\boldsymbol{k}+\boldsymbol{q}}. \tag{4.64}$$

Example Kinetic Energy: The expectation value of the kinetic energy in first quantization

$$\langle T\rangle_\varphi = \int d^3r\,\varphi^*(\boldsymbol{r})\frac{-\hbar^2\nabla^2}{2m}\varphi(\boldsymbol{r}) = \frac{\hbar^2}{2m}\int d^3r\;\boldsymbol{\nabla}\varphi^*(\boldsymbol{r})\cdot\boldsymbol{\nabla}\varphi(\boldsymbol{r}),$$

leads in second quantization to the kinetic energy operator

$$T = \frac{\hbar^2}{2m}\int d^3r\;\boldsymbol{\nabla}\Psi^\dagger(\boldsymbol{r})\cdot\boldsymbol{\nabla}\Psi(\boldsymbol{r}). \tag{4.65}$$

In momentum space, one obtains the result

$$T = \sum_{\boldsymbol{k}}\frac{\hbar^2k^2}{2m}c^\dagger_{\boldsymbol{k}}c_{\boldsymbol{k}} \tag{4.66}$$

Example Spin Density: The spin density of a spin-1/2 particle in first quantization

$$\langle \boldsymbol{s}(\boldsymbol{r})\rangle_\varphi = \frac{\hbar}{2}\sum_{s,s'} \varphi_s^*(\boldsymbol{r})\boldsymbol{\sigma}_{ss'}\varphi_{s'}(\boldsymbol{r}) \tag{4.67}$$

defines the many-body spin density operator

$$\boldsymbol{s}(\boldsymbol{r}) = \frac{\hbar}{2}\sum_{ss'} \Psi_s^\dagger(\boldsymbol{r})\,\boldsymbol{\sigma}_{ss'}\,\Psi_{s'}(\boldsymbol{r}). \tag{4.68}$$

Two-Particle Operator

The interaction $V(\boldsymbol{r}_1, \boldsymbol{r}_2)$ is a two-particle operator. In second quantization, it has the form

$$\begin{aligned} H_{\text{ww}} &= \frac{1}{2}\sum_{\alpha,\beta} \langle \varphi_{\alpha_1}\varphi_{\alpha_2}|V(\boldsymbol{r}_1,\boldsymbol{r}_2)|\varphi_{\beta_1}\varphi_{\beta_2}\rangle a_{\alpha_1}^\dagger a_{\alpha_2}^\dagger a_{\beta_2} a_{\beta_1} \\ &= \frac{1}{2}\int d^3r\, d^3r'\, \Psi^\dagger(\boldsymbol{r})\Psi^\dagger(\boldsymbol{r}')V(\boldsymbol{r},\boldsymbol{r}')\Psi(\boldsymbol{r}')\Psi(\boldsymbol{r}). \end{aligned} \tag{4.69}$$

One should note the correct order $\Psi(\boldsymbol{r})^\dagger\Psi(\boldsymbol{r}')^\dagger\Psi(\boldsymbol{r}')\Psi(\boldsymbol{r})$ of the operators. Here, the relationship between the expectation value also holds

$$\langle \varphi_\alpha\varphi_\beta|V(\boldsymbol{r}_1,\boldsymbol{r}_2)|\varphi_\alpha\varphi_\beta\rangle = \int d^3r d^3r'\, V(\boldsymbol{r},\boldsymbol{r}')|\varphi_\alpha(\boldsymbol{r})|^2\,|\varphi_\beta(\boldsymbol{r}')|^2 \tag{4.70}$$

and the operator under the replacement $\varphi \mapsto \Psi$, modulo the "correct" order of the operators.

Example Hamilton Operator: The typical Hamilton operator for interacting particles with spin has the form (with spin-independent interaction)

$$\begin{aligned} H = &\frac{\hbar^2}{2m}\int d^3r \sum_s \boldsymbol{\nabla}\Psi_s^\dagger(\boldsymbol{r})\cdot\boldsymbol{\nabla}\Psi_s(\boldsymbol{r}) \\ &+ \frac{1}{2}\int d^3r\, d^3r' \sum_{s,s'} \Psi_s^\dagger(\boldsymbol{r})\Psi_{s'}^\dagger(\boldsymbol{r}')V(\boldsymbol{r}-\boldsymbol{r}')\Psi_{s'}(\boldsymbol{r}')\Psi_s(\boldsymbol{r}). \end{aligned} \tag{4.71}$$

For an electron gas, $s = \pm 1/2$, $m = m_e$, $V(r) = e^2/r$ and $\Psi_s^\dagger(\boldsymbol{r})$, $\Psi_s(\boldsymbol{r})$ are fermionic field operators. In momentum space, the Hamilton operator has the form

$$H = \sum_{\boldsymbol{k}s} \frac{\hbar^2k^2}{2m} c_{\boldsymbol{k}s}^\dagger c_{\boldsymbol{k}s} + \frac{1}{2}\sum_{\boldsymbol{k}\boldsymbol{k}'\boldsymbol{q}}\sum_{s's} V_{\boldsymbol{q}}\, c_{\boldsymbol{k}+\boldsymbol{q}s}^\dagger c_{\boldsymbol{k}'-\boldsymbol{q}s'}^\dagger c_{\boldsymbol{k}'s'} c_{\boldsymbol{k}s}. \tag{4.72}$$

where $V_{\boldsymbol{q}} = 4\pi e^2/q^2$ is the Fourier transform of the Coulomb potential. As in the first-quantized picture, the Hamilton operator generates the dynamics of the states, see later.

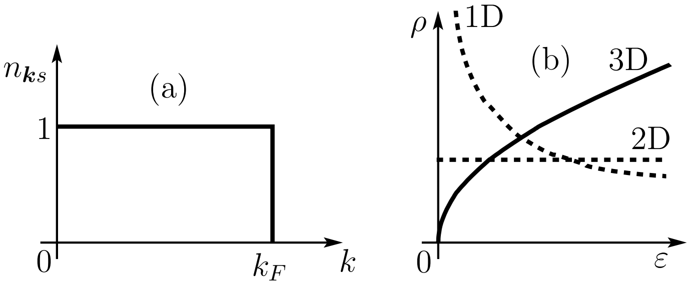

Figure 4.1: (a) Occupation numbers $n_{\boldsymbol{k}s}$ of the electron states with wave vector $\boldsymbol{k}$ and spin s for the Fermi sea. (b) Density of states $\rho(\varepsilon)$ for free fermions in 3D (solid line) and in 2D and 1D.

4.7 Correlations in the Fermi Gas

We briefly summarize the description of the Fermi gas (cf. section 2.5.7). Due to the translational invariance of the system, we define creation operators

$$\langle x|c^\dagger_{\boldsymbol{k}\sigma}|0\rangle = \langle \boldsymbol{r}, s|c^\dagger_{\boldsymbol{k}\sigma}|0\rangle = \varphi_{\boldsymbol{k}}(\boldsymbol{r})\chi_\sigma(s) \tag{4.73}$$

for the plane waves

$$\varphi_{\boldsymbol{k}}(\boldsymbol{r})\chi_\sigma(s) = \frac{1}{\sqrt{\Omega}}\, e^{i\boldsymbol{k}\cdot\boldsymbol{r}}\, \delta_{\sigma s}. \tag{4.74}$$

The field operator then has the form

$$\Psi_s(\boldsymbol{r}) = \frac{1}{\sqrt{\Omega}}\sum_{\boldsymbol{k}} e^{i\boldsymbol{k}\cdot\boldsymbol{r}}\, c_{\boldsymbol{k}s}\,. \tag{4.75}$$

The Fermi sea (where all states up to the Fermi wave number k_F are filled)

$$|\Phi_0\rangle = \prod_{\substack{k\le k_F\\ s\in\{\uparrow,\downarrow\}}} c^\dagger_{\boldsymbol{k}s}|0\rangle, \tag{4.76}$$

is the ground state of the Hamilton operator

$$H = \sum_{\boldsymbol{k},s} \varepsilon_{\boldsymbol{k}} c^\dagger_{\boldsymbol{k}s} c_{\boldsymbol{k}s} = \sum_{\boldsymbol{k},s} \frac{\hbar^2 k^2}{2m} c^\dagger_{\boldsymbol{k}s} c_{\boldsymbol{k}s}. \tag{4.77}$$

at fixed particle density $n = N/\Omega$.[9] The Fermi sea is defined by the occupation numbers (Fermi statistics, Pauli exclusion principle, cf. Figure 4.1)

$$n_{\boldsymbol{k}\sigma} = \langle\Phi_0|c^\dagger_{\boldsymbol{k}s} c_{\boldsymbol{k}s}|\Phi_0\rangle = \begin{cases} 1, & k \le k_F, \\ 0, & \text{otherwise.} \end{cases} \tag{4.78}$$

---

[9] Alternatively, one can also introduce the grand canonical Hamiltonian $H_{\text{gk}} = H - \mu \sum_{\boldsymbol{k}\sigma} c^\dagger_{\boldsymbol{k}\sigma} c_{\boldsymbol{k}\sigma}$ such that Φ_0 with $\epsilon_F = \mu$ is the ground state in the entire Fock space.

The parameters k_F and ε_F (Fermi wave number and energy) are determined by the density n of the Fermi gas with

$$k_F = (3\pi^2 n)^{1/3}, \qquad \varepsilon_F = \frac{\hbar^2 k_F^2}{2m}. \tag{4.79}$$

As already discussed, typical values for $k_F \simeq 1\,\text{Å}^{-1}$ (for $n = N/\Omega \simeq 10^{23}\text{cm}^{-3}$ in metals) and correspondingly $\varepsilon_F \simeq$ eV. The density of states (per spin) $\rho(\varepsilon) = \Omega^{-1}\sum_{\boldsymbol{k}} \delta(\varepsilon - \varepsilon_{\boldsymbol{k}})$ is given by (cf. Figure 4.1(b))

$$\rho(\varepsilon) = \frac{4\pi k^2}{(2\pi)^3 (d\epsilon/dk)} = \frac{m}{2\pi^2\hbar^3}\sqrt{2m\varepsilon} = \frac{3}{4}\frac{n}{\varepsilon_F}\left(\frac{\varepsilon}{\varepsilon_F}\right)^{1/2} \tag{4.80}$$

and its value at the Fermi edge is

$$\rho_0 = \rho(\varepsilon_F) = \frac{3}{4}\frac{n}{\varepsilon_F} \quad \text{(density of states/spin)}, \qquad 2\rho_0 = \text{density of states}. \tag{4.81}$$

As an exercise, one can determine the density of states for the Fermi gases in one dimension ($\rho_{1\text{D}} \propto 1/\sqrt{\varepsilon}$) and in two dimensions ($\rho_{2\text{D}} \propto$ const.). In the following, we will calculate the density matrix $\langle\Phi_0|\Psi_s^\dagger(\boldsymbol{r})\Psi_s(\boldsymbol{r}')|\Phi_0\rangle$ and the pair correlations $\langle\Phi_0|\Psi_s^\dagger(\boldsymbol{r})\Psi_{s'}^\dagger(\boldsymbol{r}')\Psi_{s'}(\boldsymbol{r}')\Psi_s(\boldsymbol{r})|\Phi_0\rangle$ in the Fermi gas.

4.7.1 Density Matrix

The local density operator for electrons with spin s is given by $\rho_s(\boldsymbol{r}) = \Psi_s^\dagger(\boldsymbol{r})\Psi_s(\boldsymbol{r})$. The density matrix of the Fermi sea involves the generalization to different positions $\boldsymbol{r}'$ and $\boldsymbol{r}'$ (non-diagonal density operator),

$$G_s(\boldsymbol{r}-\boldsymbol{r}') \equiv \langle\Phi_0|\Psi_s^\dagger(\boldsymbol{r})\Psi_s(\boldsymbol{r}')|\Phi_0\rangle \tag{4.82}$$

$$= \sum_{\boldsymbol{k},\boldsymbol{k}'} \frac{\exp(-i\boldsymbol{k}\cdot\boldsymbol{r})}{\sqrt{\Omega}}\frac{\exp(i\boldsymbol{k}\cdot\boldsymbol{r}')}{\sqrt{\Omega}} \underbrace{\langle\Phi_0|c_{\boldsymbol{k}s}^\dagger c_{\boldsymbol{k}'s}|\Phi_0\rangle}_{\delta_{\boldsymbol{k}\boldsymbol{k}'}n_{\boldsymbol{k}s}}\ . \tag{4.83}$$

The quantity $G_s(\boldsymbol{r}-\boldsymbol{r}')$ is the probability amplitude to remove an electron at $\boldsymbol{r}$ from the system and add it back at $\boldsymbol{r}'$. Evaluating the Kronecker $\delta_{\boldsymbol{k}\boldsymbol{k}'}$ symbol and transitioning to the continuum leads to,

$$\begin{aligned} G_s(\boldsymbol{r}-\boldsymbol{r}') &= \frac{1}{\Omega}\sum_{\boldsymbol{k}} e^{-i\boldsymbol{k}\cdot(\boldsymbol{r}-\boldsymbol{r}')} n_{\boldsymbol{k}s} \\ &= \int \frac{d^3k}{(2\pi)^3}\, e^{-i\boldsymbol{k}\cdot(\boldsymbol{r}-\boldsymbol{r}')}\Theta(k_F - k) \\ &= \frac{1}{4\pi^2}\int_0^{k_F} dk\, k^2 \int_{-1}^{1} dz\, e^{-ik|\boldsymbol{r}-\boldsymbol{r}'|z} \\ &= \frac{3n}{2}\frac{\sin x - x\cos x}{x^3}\bigg|_{x=k_F|\boldsymbol{r}-\boldsymbol{r}'|} = \frac{3n}{2}\frac{j_1(k_F|\boldsymbol{r}-\boldsymbol{r}'|)}{k_F|\boldsymbol{r}-\boldsymbol{r}'|}, \end{aligned} \tag{4.84}$$

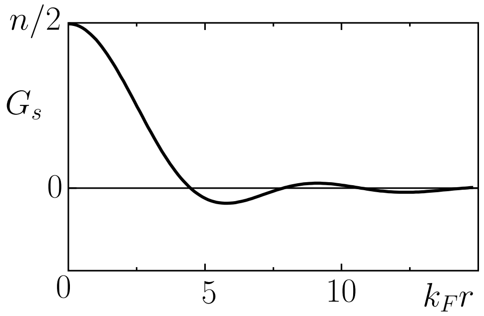

Figure 4.2: Density matrix $G_s(k_F r)$.

with the spherical Bessel function j_1. The result is shown in Figure 4.2; the limits $x = k_F r \to 0, \infty$ are given by

$$\begin{aligned} x \to 0 &: (x - x^3/6 - x + x^3/2)/x^3|_{x\to 0} = 1/3 \Rightarrow G_s(0) = n/2 \\ x \to \infty &: G_s(x) \sim 3n(\cos x)/2x^2. \end{aligned} \tag{4.85}$$

With $G_s(0) = n/2$, we find a homogeneous density $n = G_\uparrow(0) + G_\downarrow(0)$ of particles in the Fermi gas.

4.8 Pair Correlation

The pair correlation

$$\left(\frac{n}{2}\right)^2 g_{ss'}(\boldsymbol{r} - \boldsymbol{r}') = \langle \Phi_0 | \Psi_s^\dagger(\boldsymbol{r}) \Psi_{s'}^\dagger(\boldsymbol{r}') \Psi_{s'}(\boldsymbol{r}') \Psi_s(\boldsymbol{r}) | \Phi_0 \rangle. \tag{4.86}$$

gives us the relative probability of finding an electron at $\boldsymbol{r}', s'$ when there is already an electron at $\boldsymbol{r}, s$. The calculation of the pair correlator is a nice exercise in dealing with the second-quantized formalism. We first express the field operators $\Psi_s(\boldsymbol{r})$ in terms of the annihilation operators $c_{\boldsymbol{k}s}$,

$$\left(\frac{n}{2}\right)^2 g_{ss'}(\boldsymbol{r} - \boldsymbol{r}') = \frac{1}{\Omega^2} \sum_{\boldsymbol{p},\boldsymbol{p}',\boldsymbol{q},\boldsymbol{q}'} e^{-i(\boldsymbol{p}-\boldsymbol{p}')\cdot\boldsymbol{r}} e^{-i(\boldsymbol{q}-\boldsymbol{q}')\cdot\boldsymbol{r}'} \langle \Phi_0 | c_{\boldsymbol{p}s}^\dagger c_{\boldsymbol{q}s'}^\dagger c_{\boldsymbol{q}'s'} c_{\boldsymbol{p}'s} | \Phi_0 \rangle.$$

We start with the case $s \neq s'$: Then $\boldsymbol{q}' = \boldsymbol{q}$ and $\boldsymbol{p}' = \boldsymbol{p}$ must hold, otherwise the expectation value $\langle \cdots \rangle = 0$ vanishes.[10] The expectation value $\langle \cdots \rangle$ leads to

$$\begin{aligned} \langle \Phi_0 | c_{\boldsymbol{p}s}^\dagger c_{\boldsymbol{q}s'}^\dagger c_{\boldsymbol{q}'s'} c_{\boldsymbol{p}'s} | \Phi_0 \rangle &= \delta_{\boldsymbol{p}\boldsymbol{p}'} \delta_{\boldsymbol{q}\boldsymbol{q}'} \langle \Phi_0 | c_{\boldsymbol{p}s}^\dagger c_{\boldsymbol{q}s'}^\dagger c_{\boldsymbol{q}s'} c_{\boldsymbol{p}s} | \Phi_0 \rangle = \delta_{\boldsymbol{p}\boldsymbol{p}'} \delta_{\boldsymbol{q}\boldsymbol{q}'} \langle \Phi_0 | c_{\boldsymbol{p}s}^\dagger n_{\boldsymbol{q}s'} c_{\boldsymbol{p}s} | \Phi_0 \rangle \\ &= \delta_{\boldsymbol{p}\boldsymbol{p}'} \delta_{\boldsymbol{q}\boldsymbol{q}'} n_{\boldsymbol{p}s} n_{\boldsymbol{q}s'}, \end{aligned} \tag{4.87}$$

$$\left(\frac{n}{2}\right)^2 g_{s\neq s'}(\boldsymbol{r}) = \frac{1}{\Omega^2} \sum_{\boldsymbol{p}\boldsymbol{q}} n_{\boldsymbol{p}s} n_{\boldsymbol{q}s'} = n_s n_{s'} \overset{n_s = \frac{n}{2}}{=} \left(\frac{n}{2}\right)^2 \cdot 1, \tag{4.88}$$

$$\Rightarrow g_{s\neq s'}(\boldsymbol{r}) = 1; \tag{4.89}$$

---

[10] The expectation value $\langle \cdots \rangle$ vanishes for $\boldsymbol{q}' \neq \boldsymbol{q}$ or $\boldsymbol{p}' \neq \boldsymbol{p}$ since different states are occupied in $|\Phi_0\rangle$ and in $c_{\boldsymbol{p}s}^\dagger c_{\boldsymbol{q}s'}^\dagger c_{\boldsymbol{q}'s'} c_{\boldsymbol{p}'s} |\Phi_0\rangle$.

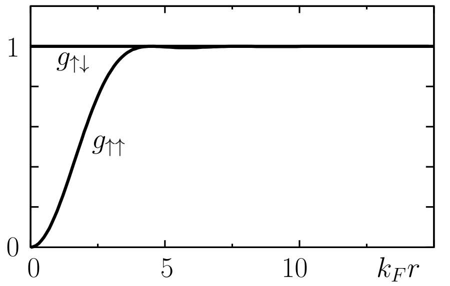

Figure 4.3: Pair correlators $g_{\uparrow\uparrow}(k_F r)$ (with exchange hole due to the Pauli principle) and $g_{\uparrow\downarrow}(k_F r)$ (uncorrelated, since spin ↑ and spin ↓ are distinguishable).

thus we find for $s \neq s'$ a constant value $g_{s\neq s'}(k_F|\boldsymbol{r}-\boldsymbol{r}'|) = 1$. Next, we calculate the case $s = s'$. Here we obtain contributions for $\boldsymbol{p}' = \boldsymbol{p}$ and $\boldsymbol{q}' = \boldsymbol{q}$ or for $\boldsymbol{p}' = \boldsymbol{q}$ and $\boldsymbol{q}' = \boldsymbol{p}$,

$$\begin{aligned}\langle\Phi_0|c^\dagger_{\boldsymbol{p}s}c^\dagger_{\boldsymbol{q}s}c_{\boldsymbol{q}'s}c_{\boldsymbol{p}'s}|\Phi_0\rangle &= \delta_{\boldsymbol{p}\boldsymbol{p}'}\delta_{\boldsymbol{q}\boldsymbol{q}'}\langle\Phi_0|c^\dagger_{\boldsymbol{p}s}c^\dagger_{\boldsymbol{q}s}c_{\boldsymbol{q}s}c_{\boldsymbol{p}s}|\Phi_0\rangle + \delta_{\boldsymbol{q}\boldsymbol{p}'}\delta_{\boldsymbol{p}\boldsymbol{q}'}\langle\Phi_0|c^\dagger_{\boldsymbol{p}s}c^\dagger_{\boldsymbol{q}s}\overbrace{c_{\boldsymbol{p}s}c_{\boldsymbol{q}s}}^{-c_{\boldsymbol{q}s}c_{\boldsymbol{p}s}}|\Phi_0\rangle \\ &= \left(\delta_{\boldsymbol{p}\boldsymbol{p}'}\delta_{\boldsymbol{q}\boldsymbol{q}'} - \delta_{\boldsymbol{p}'\boldsymbol{q}}\delta_{\boldsymbol{q}'\boldsymbol{p}}\right) n_{\boldsymbol{p}s}n_{\boldsymbol{q}s}, \qquad (4.90)\end{aligned}$$

$$\begin{aligned}\left(\frac{n}{2}\right)^2 g_{ss}(\boldsymbol{r}) = \frac{1}{\Omega^2}\sum_{\boldsymbol{p}\boldsymbol{q}}\left(1 - e^{-i(\boldsymbol{p}-\boldsymbol{q})\cdot\boldsymbol{r}}\right) n_{\boldsymbol{p}s}n_{\boldsymbol{q}s} &= \left(\frac{n}{2}\right)^2 - \left(\frac{1}{\Omega}\sum_{\boldsymbol{p}} e^{-i\boldsymbol{p}\cdot\boldsymbol{r}} n_{\boldsymbol{p}s}\right)^2 \\ &= \left(\frac{n}{2}\right)^2 - G_s^2(\boldsymbol{r}) \qquad (4.91) \\ &\overset{x\,=\,k_F r}{=} \left(\frac{n}{2}\right)^2\left[1 - \frac{9}{x^6}\left(\sin x - x\cos x\right)^2\right],\end{aligned}$$

The correlator $g_{ss}(\boldsymbol{r}-\boldsymbol{r}')$ shows an exchange hole. Two fermions with identical spin avoid each other according to the Pauli exclusion principle; the exchange hole exactly displaces one electron with spin s from the vicinity of a spin s electron, since

$$\frac{n}{2}\int d^3r\left[g_{ss}(\boldsymbol{r}) - 1\right] = -\underbrace{\frac{2\pi n}{k_F^3}}_{2/3\pi}\underbrace{\int_0^\infty dx\, x^2\,\frac{9}{x^6}\left(\sin x - x\cos x\right)^2}_{3\pi/2} = -1 \qquad (4.92)$$

The two results are graphically represented in Figure 4.3. The pair correlator $g(\boldsymbol{r}) = \frac{1}{2}\left(g_{\uparrow\uparrow}(\boldsymbol{r}) + g_{\uparrow\downarrow}(\boldsymbol{r})\right)$ of the total system is drawn in Figure 4.4.

The above results were calculated at Hartree-Fock level: Optimal Slater determinants for the homogeneous Fermi gas are constructed from translationally invariant single-particle states. The state $|\Phi_0\rangle$ is thus just an optimized Slater determinant. If one additionally takes correlations into account, one finds corrections as schematically shown in Figure 4.5.

One can also easily calculate the result using the Wick theorem. The correlator $g_{ss'}(\boldsymbol{r}-\boldsymbol{r}')$ is determined by "contractions" of the field operators (the contraction

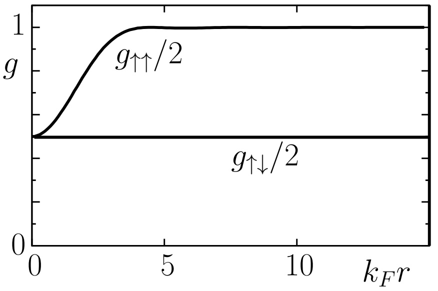

Figure 4.4: Pair correlator $g = [g_{\uparrow\uparrow} + g_{\uparrow\downarrow}]/2$ of the entire electronic system.

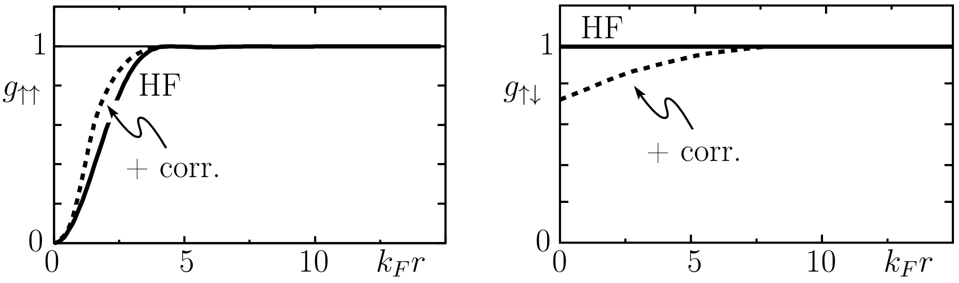

Figure 4.5: Corrections (schematically) to the pair correlators $g_{\uparrow\uparrow}$ and $g_{\uparrow\downarrow}$ considering correlation effects.

indicated by corresponding brackets). For the first term in (4.90)

$$\langle\Phi_0|\underbrace{\Psi_s^\dagger(\boldsymbol{r})\overbrace{\Psi_{s'}^\dagger(\boldsymbol{r}')\Psi_{s'}}(\boldsymbol{r}')\Psi_s}(\boldsymbol{r})|\Phi_0\rangle$$

and for the second term

$$\langle\Phi_0|\underbrace{\Psi_s^\dagger(\boldsymbol{r})\Psi_{s'}^\dagger\mathrlap{\overbrace{\phantom{(\boldsymbol{r}')\Psi_{s'}(\boldsymbol{r}')\Psi_s}}}(\boldsymbol{r}')\Psi_{s'}}(\boldsymbol{r}')\Psi_s(\boldsymbol{r})|\Phi_0\rangle.$$

The contractions correspond to expectation values in the ground state. Thus, one obtains the two terms[11]

$$\begin{aligned}\left(\frac{n}{2}\right)^2 g_{ss'}(\boldsymbol{r}-\boldsymbol{r}') &= \langle\Phi_0|\Psi_s^\dagger(\boldsymbol{r})\Psi_{s'}^\dagger(\boldsymbol{r}')\Psi_{s'}(\boldsymbol{r}')\Psi_s(\boldsymbol{r})|\Phi_0\rangle \\ &= \langle\Phi_0|\Psi_s^\dagger(\boldsymbol{r})\Psi_s(\boldsymbol{r})|\Phi_0\rangle\langle\Phi_0|\Psi_{s'}^\dagger(\boldsymbol{r}')\Psi_{s'}(\boldsymbol{r}')|\Phi_0\rangle \\ &\quad - \langle\Phi_0|\Psi_s^\dagger(\boldsymbol{r})\Psi_{s'}(\boldsymbol{r}')|\Phi_0\rangle\langle\Phi_0|\Psi_{s'}^\dagger(\boldsymbol{r}')\Psi_s(\boldsymbol{r})|\Phi_0\rangle.\end{aligned} \tag{4.93}$$

Thus, one obtains the result directly from $\langle\Phi_0|\Psi_s^\dagger(\boldsymbol{r})\ \Psi_{s'}(\boldsymbol{r}')|\Phi_0\rangle = \delta_{ss'}G_s(\boldsymbol{r}-\boldsymbol{r}')$. One finds $(n/2)^2 g_{s\neq s'} = (n/2)^2 - 0$ (for $s \neq s'$) and $(n/2)^2 g_{ss} = (n/2)^2 - G_s^2$ (for $s = s'$).

The above factorization of $\langle\Phi_0|\Psi_s^\dagger\Psi_{s'}^\dagger\Psi_{s'}\Psi_s|\Phi_0\rangle$ is exact for the ground state $|\Phi_0\rangle$ in Hartree-Fock form (i.e., for a Slater determinant). Accordingly, the factorization is

---

[11] The minus sign in the 2nd term comes from the swapping of the operators $\Psi_{s'}^\dagger(\boldsymbol{r}')\Psi_{s'}(\boldsymbol{r}')$ so that the two contracted operators are directly next to each other.

valid for the non-interacting system. When considering the interaction between the particles, the Hartree-Fock ground state is only an approximation. Accordingly, the expectation value $\langle\Phi|\Psi_s^\dagger\Psi_{s'}^\dagger\Psi_{s'}^\dagger\Psi_s|\Phi\rangle$ in the true ground state $|\Phi\rangle$ is only approximately given by

$$\begin{aligned}\langle\Phi|\Psi_s^\dagger\Psi_{s'}^\dagger\Psi_{s'}^\dagger\Psi_s|\Phi\rangle \overset{\text{in HF}}{\approx} \langle\Phi|\Psi_s^\dagger\Psi_s|\Phi\rangle\langle\Phi|\Psi_{s'}^\dagger\Psi_{s'}|\Phi\rangle \\ - \langle\Phi|\Psi_s^\dagger\Psi_{s'}|\Phi\rangle\langle\Phi|\Psi_{s'}^\dagger\Psi_s|\Phi\rangle. \quad (4.94)\end{aligned}$$

4.9 Equation of Motion

As usual in the first-quantized form of quantum mechanics, we can also choose between Schrödinger, Heisenberg, and interaction pictures in the second-quantized form. In the Heisenberg picture, the operators (and thus also the field operators $\Psi_s^\dagger(\boldsymbol{r})$ and $\Psi_s(\boldsymbol{r})$) become time-dependent. For the time-independent Hamilton operator H, the Heisenberg picture of any operator $A(t)$ is given by

$$A_H(t) = U^\dagger A(t) U = e^{iHt/\hbar} A(t)\, e^{-iHt/\hbar} \qquad (\text{note } H_H(t) = H). \quad (4.95)$$

The equation of motion for the operator $A_H(t)$ is

$$\begin{aligned} i\hbar\frac{dA_H(t)}{dt} &= \big[A_H(t), H\big] + i\hbar(\partial_t A)_H(t) \\ &= \big[A, H\big]_H(t) + i\hbar(\partial_t A)_H(t) \\ &\overset{\partial_t A = 0}{=} \big[A, H\big]_H(t). \end{aligned} \quad (4.96)$$

Here, $(\partial_t A)_H(t) = U^\dagger \dot{A}(t) U$ and $[A, H]_H(t) = U^\dagger[A(t), H]U$.

We calculate the time derivative of the field operator $\Psi(\boldsymbol{r};t) \equiv \Psi(\boldsymbol{r})_H(t) = U^\dagger\Psi(\boldsymbol{r})U$ for a Hamilton operator H of the form

$$\begin{aligned} H = &\int d^3r\, \Psi^\dagger(\boldsymbol{r}) \frac{-\hbar^2\nabla^2}{2m}\Psi(\boldsymbol{r}) \\ &+ \frac{1}{2}\int d^3r\, d^3r'\, \Psi^\dagger(\boldsymbol{r})\Psi^\dagger(\boldsymbol{r}')V(\boldsymbol{r}-\boldsymbol{r}')\Psi(\boldsymbol{r}')\Psi(\boldsymbol{r}) \end{aligned} \quad (4.97)$$

where we have suppressed the spin quantum numbers in the field operator Ψ. From (4.96) we obtain

$$i\hbar\,\frac{\partial\Psi(\boldsymbol{r};t)}{\partial t} = \Big[\Psi(\boldsymbol{r};t), H\Big] = e^{iHt/\hbar}\Big[\Psi(\boldsymbol{r}), H\Big]e^{-iHt/\hbar}, \quad (4.98)$$

$$\begin{aligned} \Big[\Psi(\boldsymbol{r}), H\Big] = &\int d^3r' \Big[\Psi(\boldsymbol{r}), \Psi^\dagger(\boldsymbol{r}')\frac{-\hbar^2\nabla'^2}{2m}\Psi(\boldsymbol{r}')\Big] \quad (4.99) \\ &+ \frac{1}{2}\int d^3r'\, d^3r'' V(\boldsymbol{r}'-\boldsymbol{r}'')\Big[\Psi(\boldsymbol{r}), \Psi^\dagger(\boldsymbol{r}')\Psi^\dagger(\boldsymbol{r}'')\Psi(\boldsymbol{r}'')\Psi(\boldsymbol{r}')\Big]. \end{aligned}$$

To calculate the commutators $[A, BC]$, we use the relationships

$$[A, BC] = \begin{cases} [A, B]C + B[A, C], & \text{for bosons,} \\ \{A, B\}C - B\{A, C\}, & \text{for fermions.} \end{cases} \tag{4.100}$$

Thus, for fermions we find

$$\begin{aligned}
[\Psi(\boldsymbol{r}), \Psi^\dagger(\boldsymbol{r}')\Psi(\boldsymbol{r}')] &= \underbrace{\{\Psi(\boldsymbol{r}), \Psi^\dagger(\boldsymbol{r}')\}}_{\delta^{(3)}(\boldsymbol{r}-\boldsymbol{r}')} \Psi(\boldsymbol{r}') - \Psi^\dagger(\boldsymbol{r}') \underbrace{\{\Psi(\boldsymbol{r}), \Psi(\boldsymbol{r}')\}}_{0} \\
[\Psi(\boldsymbol{r}), \Psi^\dagger(\boldsymbol{r}')\Psi^\dagger(\boldsymbol{r}'')\Psi(\boldsymbol{r}'')\Psi(\boldsymbol{r}')] &= \underbrace{\{\Psi(\boldsymbol{r}), \Psi^\dagger(\boldsymbol{r}')\}}_{\delta^{(3)}(\boldsymbol{r}-\boldsymbol{r}')} \Psi^\dagger(\boldsymbol{r}'')\Psi(\boldsymbol{r}'')\Psi(\boldsymbol{r}') \\
&\quad - \Psi^\dagger(\boldsymbol{r}') \underbrace{\{\Psi(\boldsymbol{r}), \Psi^\dagger(\boldsymbol{r}'')\Psi(\boldsymbol{r}'')\Psi(\boldsymbol{r}')\}}_{\underbrace{\{\Psi(\boldsymbol{r}), \Psi^\dagger(\boldsymbol{r}'')\}}_{\delta^{(3)}(\boldsymbol{r}-\boldsymbol{r}'')} \Psi(\boldsymbol{r}'')\Psi(\boldsymbol{r}')} \\
&= \delta^{(3)}(\boldsymbol{r}-\boldsymbol{r}')\Psi^\dagger(\boldsymbol{r}'')\Psi(\boldsymbol{r}'')\Psi(\boldsymbol{r}') - \delta^{(3)}(\boldsymbol{r}-\boldsymbol{r}'')\Psi^\dagger(\boldsymbol{r}')\Psi(\boldsymbol{r}'')\Psi(\boldsymbol{r}').
\end{aligned} \tag{4.101}$$

The combination of (4.99) to (4.101) yields

$$\begin{aligned}
[\Psi(\boldsymbol{r}), H] = -\frac{\hbar^2}{2m}\nabla^2\Psi(\boldsymbol{r}) + \frac{1}{2}\int d^3r' \int d^3r''\, V(\boldsymbol{r}' - \boldsymbol{r}'') \\
\times [\delta^{(3)}(\boldsymbol{r}-\boldsymbol{r}')\Psi^\dagger(\boldsymbol{r}'')\Psi(\boldsymbol{r}'')\Psi(\boldsymbol{r}') - \delta^{(3)}(\boldsymbol{r}-\boldsymbol{r}')\Psi^\dagger(\boldsymbol{r}'')\Psi(\boldsymbol{r}')\Psi(\boldsymbol{r}'')]
\end{aligned} \tag{4.102}$$

Swapping $\Psi(\boldsymbol{r}')\Psi(\boldsymbol{r}'') = -\Psi(\boldsymbol{r}'')\Psi(\boldsymbol{r}')$ in the last term and using (4.98) gives the final result

$$i\hbar\frac{\partial\Psi(\boldsymbol{r};t)}{\partial t} = -\frac{\hbar^2}{2m}\nabla^2\Psi(\boldsymbol{r};t) + \left(\int d^3r'\, \Psi^\dagger(\boldsymbol{r}';t)V(\boldsymbol{r}-\boldsymbol{r}')\Psi(\boldsymbol{r}';t)\right)\Psi(\boldsymbol{r};t);$$

an analogous calculation for bosons yields the same result.[12] Note that the calculation of the commutators at the same times $t = t'$ yields the results

$$\begin{aligned}
[\Psi(\boldsymbol{r};t), \Psi^\dagger(\boldsymbol{r}';t)]_\pm &= \delta^{(3)}(\boldsymbol{r}-\boldsymbol{r}'), \\
[\Psi(\boldsymbol{r};t), \Psi(\boldsymbol{r}';t)]_\pm &= 0, \\
[\Psi^\dagger(\boldsymbol{r};t), \Psi^\dagger(\boldsymbol{r}';t)]_\pm &= 0,
\end{aligned} \tag{4.103}$$

but the same problem for different times t and t' is a difficult many-body problem

$$\left.\begin{aligned}
[\Psi(\boldsymbol{r};t), \Psi^\dagger(\boldsymbol{r}';t')]_\pm \\
[\Psi(\boldsymbol{r};t), \Psi(\boldsymbol{r}';t')]_\pm \\
[\Psi^\dagger(\boldsymbol{r};t), \Psi^\dagger(\boldsymbol{r}';t')]_\pm
\end{aligned}\right\} \text{'Many-body problem'}, \tag{4.104}$$

which cannot generally be solved exactly, see e.g. Fetter-Walecka.

---

[12] The reason for this lies in the equations (4.100), which lead a commutator between the operator A and a quadratic operator BC to a similar form as a function of the "elementary" (anti)commutators.

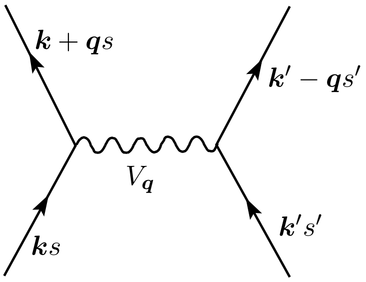

Figure 4.6: Interaction vertex for the Hamiltonian (4.105): The incoming vectors represent the annihilation operators $c_{\boldsymbol{k}s}$, $c_{\boldsymbol{k}'s'}$, the outgoing vectors represent the creation operators $c^\dagger_{\boldsymbol{k}+\boldsymbol{q}s}$, $c^\dagger_{\boldsymbol{k}'-\boldsymbol{q}s'}$. The potential $V_{\boldsymbol{q}}$ is represented by the wavy line.

Of course, we can also work in momentum space. The Hamilton operator has the form

$$H=\sum_{\boldsymbol{k}s}\frac{\hbar^2k^2}{2m}\,c^\dagger_{\boldsymbol{k}s}c_{\boldsymbol{k}s}+\frac{1}{2}\sum_{\boldsymbol{k}\boldsymbol{k}'\boldsymbol{q}s's}V_{\boldsymbol{q}}\,c^\dagger_{\boldsymbol{k}+\boldsymbol{q}s}c^\dagger_{\boldsymbol{k}'-\boldsymbol{q}s'}c_{\boldsymbol{k}'s'}c_{\boldsymbol{k}s}, \tag{4.105}$$

see (4.72) and Figure 4.6. and the equation of motion for the operators $c_{\boldsymbol{k}s}(t)\equiv(c_{\boldsymbol{k}s})_H(t)$ is (with $V_{-\boldsymbol{q}}=V_{\boldsymbol{q}},\varepsilon_{\boldsymbol{k}}=\hbar^2k^2/2m$)

$$\begin{aligned} i\hbar\frac{dc_{\boldsymbol{k}s}(t)}{dt} &= \varepsilon_{\boldsymbol{k}}c_{\boldsymbol{k}s}(t)+\sum_{\boldsymbol{k}'\boldsymbol{q}s'}V_{\boldsymbol{q}}\,c^\dagger_{\boldsymbol{k}'+\boldsymbol{q}s'}(t)\,c_{\boldsymbol{k}'s'}(t)c_{\boldsymbol{k}+\boldsymbol{q}s}(t) \\ &= \varepsilon_{\boldsymbol{k}}c_{\boldsymbol{k}s}(t)+\sum_{\boldsymbol{q}}V_{\boldsymbol{q}}\,\rho(-\boldsymbol{q};t)c_{\boldsymbol{k}+\boldsymbol{q}s}(t), \end{aligned} \tag{4.106}$$

with the density operator [summed over both spin directions, cf. (4.61)]

$$\rho(-\boldsymbol{q})=\sum_{\boldsymbol{k}s}c^\dagger_{\boldsymbol{k}+\boldsymbol{q}s}c_{\boldsymbol{k}s}\,. \tag{4.107}$$

Chapter 5

Interacting Electron Systems

In this chapter, we investigate the influence of interactions on electron systems. We will see how the interaction between electrons in metals affects the ground state energy of the Fermi gas in the Hartree-Fock approximation, and we will also calculate the (dynamic) dielectric constant; this allows us to understand screening and plasmons in metals. Furthermore, we will introduce the effect of superconductivity. The focus is on an application of the second quantization introduced in the last chapter. We consider the states only at $T = 0$, so that only the (many-body) ground state is occupied. However, due to the presence of the intrinsic energy scale E_g ($E_g = \varepsilon_F$ for the metal and $E_g = |\Delta|$ for the superconductor), the results remain valid for $T \ll E_g$.

5.1 Homogeneous Electron Gas

The homogeneous electron gas is the simplest model of a metal. The system is described by the Hamiltonian operator of interacting electrons, cf. (4.71),

$$\begin{aligned} H = \frac{\hbar^2}{2m} \int d^3r \sum_s \boldsymbol{\nabla}\Psi_s^\dagger(\boldsymbol{r}) \cdot \boldsymbol{\nabla}\Psi_s(\boldsymbol{r}) + \int d^3r \sum_s \Psi_s^\dagger(\boldsymbol{r}) V_{\text{ion}}(\boldsymbol{r}) \Psi_s(\boldsymbol{r}) \\ + \frac{1}{2} \int d^3r\, d^3r' \sum_{ss'} \Psi_s^\dagger(\boldsymbol{r}) \Psi_{s'}^\dagger(\boldsymbol{r}') V(\boldsymbol{r} - \boldsymbol{r}') \Psi_{s'}(\boldsymbol{r}') \Psi_s(\boldsymbol{r}). \end{aligned} \tag{5.1}$$

The electrons interact via the Coulomb interaction $V(\boldsymbol{r}) = e^2/r$ and are embedded in a background of positively charged ions, which guarantee the electrical neutrality of the entire system and thus hold the electron system together. In reality, the ions form a crystal lattice, which leads to electron bands. For the homogeneous electron gas, one makes the simplifying assumption that the positive background is homogeneously smeared out. Thus, the electrons have a simple parabolic dispersion instead of a complicated band structure. As already known from solid-state lectures, the effects of the ionic cores can often be approximately taken into account with a material-dependent effective mass. This model is also called the Jellium model.

5.1.1 Ground State Energy

We calculate the ground state energy E_{HF} in the Hartree-Fock approximation: For the (homogeneous) electron gas, the optimal Hartree-Fock single-particle wave functions are plane waves $e^{i\boldsymbol{k}\cdot\boldsymbol{r}}\chi_\sigma(s)$, and the Fermi sea $|\Phi_0\rangle = \prod_{k<k_F,\sigma} c^\dagger_{\boldsymbol{k}\sigma}|0\rangle$ is the optimal Hartree-Fock ansatz with the ground state energy

$$E_{\mathrm{HF}} = \langle\Phi_0|H|\Phi_0\rangle = \langle T\rangle_{\mathrm{HF}} + \langle V_{\mathrm{ion}}\rangle_{\mathrm{HF}} + \langle V\rangle_{\mathrm{HF}}. \tag{5.2}$$

Here, the average kinetic energy, see (4.78),

$$\begin{aligned}\langle T\rangle_{\mathrm{HF}} &= \langle\Phi_0|\sum_{\boldsymbol{k}\sigma}\frac{\hbar^2k^2}{2m}c^\dagger_{\boldsymbol{k}\sigma}c_{\boldsymbol{k}\sigma}|\Phi_0\rangle \\ &= \underbrace{2}_{\text{Spin}}\Omega\int_0^{k_F}\frac{4\pi k^2dk}{(2\pi)^3}\frac{\hbar^2k^2}{2m} \\ &= \frac{\Omega}{\pi^2}\frac{\hbar^2}{2m}\frac{1}{5}k_F^5 = \frac{\Omega}{\pi^2}\varepsilon_F\frac{k_F^3}{5} = \frac{3}{5}\varepsilon_F N,\end{aligned} \tag{5.3}$$

is just the energy of the Fermi gas with $N = n\Omega$ and $k_F^3 = 3\pi^2 n$. For the interaction energy $\langle V\rangle_{\mathrm{HF}}$, we obtain

$$\begin{aligned}\langle V\rangle_{\mathrm{HF}} &= \frac{1}{2}\int d^3r\,d^3r'\sum_{s,s'}V(\boldsymbol{r}-\boldsymbol{r}')\underbrace{\langle\Phi_0|\Psi^\dagger_s(\boldsymbol{r})\Psi^\dagger_{s'}(\boldsymbol{r}')\Psi_{s'}(\boldsymbol{r}')\Psi_s(\boldsymbol{r})|\Phi_0\rangle}_{(n/2)^2 g_{ss'}(\boldsymbol{r}-\boldsymbol{r}')} \\ &= \frac{1}{2}\int d^3r\,d^3r'\;V(\boldsymbol{r}-\boldsymbol{r}')\left[\left(\frac{n}{2}\right)^2\cdot\underbrace{2}_{s\neq s'}+\left(\frac{n}{2}\right)^2(1-g_s^2)\underbrace{2}_{s=s'}\right] \\ &= \frac{n^2}{2}\Omega\int d^3r\,V(\boldsymbol{r}) - \frac{n^2}{4}\Omega\int d^3r\,V(\boldsymbol{r})g_s(\boldsymbol{r})^2,\end{aligned} \tag{5.4}$$

with

$$g_s(\boldsymbol{r}) = \frac{2}{n}G_s(r) = \frac{3}{x^3}(\sin x - x\cos x)\Big|_{x=k_Fr}. \tag{5.5}$$

The first term in (5.4) is the Hartree energy; it accounts for the repulsion of the electrons. The second term originates from the symmetry properties of $|\Phi_0\rangle$ and is called exchange energy. The two terms can be visualized using Feynman diagrams[1], see Figure 5.1.

---

[1] Feynman diagrams arise from a perturbative expansion of a quantity (e.g., the full propagator (including interaction), the energy, etc.) in the interaction term, where expectation values $\langle c^\dagger c^\dagger\cdots c\rangle$ are decomposed into products of free propagators $\langle c^\dagger c\rangle$ using Wick's theorem. Each free propagator corresponds to a line in the Feynman diagram, curly lines describe the interaction V, fermionic loops (as in the Hartree term) carry additional signs, and integration is performed over the $\boldsymbol{k}$ values of the internal lines, etc. Once the rules for constructing diagrams are established (these follow from the problem-specific expansion in a small parameter), an analytical expression can be written for each diagram.

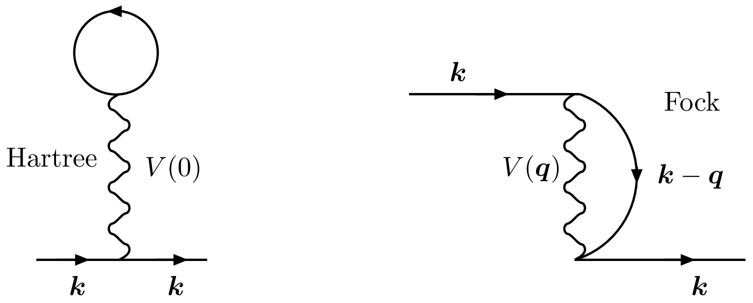

Figure 5.1: Feynman diagrams for the Hartree (left) and Fock (exchange) term (right).

For the Coulomb interaction $V(r) = e^2/r$, the interaction integral $\int d^3r\, V(r) = 4\pi \int dr\, r^2 e^2/r$ is divergent.[2] However, we have not yet taken into account the positively charged background created by the ions, which has the same charge density as the electron gas. This provides additional contributions to the Hartree term. In total, we have the Hartree energy

$$\langle V\rangle_{\mathrm{H}} + \langle V_{\mathrm{ion}}\rangle_{\mathrm{H}} = \frac{Nn}{2}\int d^3r\, \frac{e^2}{r} + \langle V_{\mathrm{ion}}\rangle_{\mathrm{H}} = \frac{Nn}{2}\int d^3r \left(\frac{e^2}{r} + \frac{e^2}{r} - 2\frac{e^2}{r}\right) = 0, \tag{5.6}$$

where the first term accounts for the repulsive electron-electron interaction, the second term accounts for the (also repulsive) ion-ion interaction, and the third term accounts for the interaction between the electrons and the ions. The vanishing of the Hartree potential means that the classical contribution of the Coulomb energy does not lead to metallic binding (energy lowering compared to the vacuum). It is the quantum mechanical exchange effects (Fock term), which are based on the fundamental indistinguishability of electrons, that lead to a finite binding energy.

The Fock term gives the contribution

$$\begin{aligned}\langle V\rangle_{\mathrm{HF}} &= -\frac{9}{4} nN \frac{e^2}{k_F^2} 4\pi \underbrace{\int_0^\infty dx\, \frac{(\sin x - x\cos x)^2}{x^5}}_{1/4} \\ &= -\frac{3}{4\pi} N e^2 k_F \end{aligned} \tag{5.7}$$

to the ground state energy.

To describe an electron gas/an electron liquid, one usually introduces the Seitz radius r_s, which indicates the volume available per electron. If we measure r_s in Bohr radii

---

[2] The divergence is a consequence of the long-range nature of the Coulomb interaction and leads to the fact that the electron system is incompressible; only if the compensating (here ionic) background accommodates the deformation does the entire system become compressible. The finite energy of the plasmons in the limit $\boldsymbol{k} \to 0$ is a consequence of this incompressibility. If the ions oscillate (in a phononic excitation), the energy of the mode disappears for $\boldsymbol{k} \to 0$.

a_B, we obtain

$$\frac{4\pi}{3}(r_s a_B)^3 = \frac{1}{n}, \qquad r_s = \frac{5.44}{\sqrt[3]{n_{22}}}, \tag{5.8}$$

where $n = n_{22} \cdot 10^{22}\,\mathrm{cm}^{-3} = n_{22} \cdot 10\,\mathrm{nm}^{-3}$ indicates the electron density. For typical metals, we have

$$n_{22} \approx \underbrace{0.9}_{\text{Cesium}} - \underbrace{2.5}_{\text{Beryllium}}, \tag{5.9}$$

and thus r_s takes values between $r_s \approx 2 - 6$, i.e., metals are neither at high nor at low density but at intermediate densities, which makes the problem difficult, as one cannot perform perturbation theory.

For the energy (per particle) of the electron gas, we obtain in the Hartree-Fock approximation

$$\frac{E_{\mathrm{HF}}}{N} = \frac{3}{5}\varepsilon_F - \frac{3}{4\pi}e^2 k_F \approx \left(\frac{2.21}{r_s^2} - \frac{0.916}{r_s}\right)\mathrm{Ry}. \tag{5.10}$$

Note that the exact ground state energy $E_0/N < E_{\mathrm{HF}}/N$ since $|\Phi_0\rangle$ is a Rayleigh-Ritz ansatz for the true ground state $|\Phi\rangle$.

The result (5.10) is correct for high densities and correspondingly small radii r_s. Not taken into account in (5.10) are the correlation energies. They are calculated using diagrammatic techniques, and for $r_s < 2.5$ one finds the expansion

$$\frac{E_0}{N\,\mathrm{Ry}} \approx \underbrace{\frac{2.21}{r_s^2} - \frac{0.916}{r_s}}_{E_{\mathrm{HF}}/N\,\mathrm{Ry}} \underbrace{+0.0622\ln r_s - 0.094 + 0.018\,r_s \ln r_s + \cdots}_{E_{\mathrm{korr}}/N\,\mathrm{Ry}<0}. \tag{5.11}$$

Note that the result (5.11) is not analytic as $r_s \to 0$.

For small densities $r_s \to \infty$, one expects the transition to a crystal named after Wigner. For the correlation energy, one obtains for the Wigner crystal

$$\frac{E_{\mathrm{korr}}}{N} \approx -\frac{0.88}{r_s}\mathrm{Ry}; \tag{5.12}$$

an interpolation[3] then yields the expression

$$\frac{E_{\mathrm{korr}}}{N} \approx -\frac{0.88}{r_s + 7.8}\mathrm{Ry} < 0. \tag{5.13}$$

Figure 5.2 finally shows the expected phases in a system with an interaction of the type $e^{-r/\lambda}/r$ that interpolates between long ($\lambda \to \infty$) and short ($\lambda \to 0$) range.

---

[3] The interpolation between two phases – the Fermi gas and the Wigner crystal – should be taken with caution.

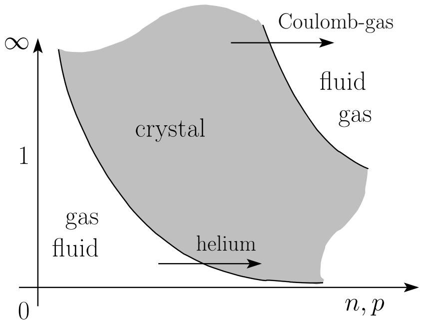

Figure 5.2: Phases in a system with (screened) Coulomb interaction; $\lambda =$ range, $n =$ density, $p =$ pressure, dimensionless parameter $= n\lambda^3$. Such a phase diagram with reentrance into the liquid/gas phase occurs, for example, in helium.

5.1.2 Dielectric Constant $\varepsilon(\boldsymbol{q}; \omega)$

It is not possible to determine the dielectric constant of the homogeneous electron gas exactly. However, there are good approximations that include the essential properties of a metal, screening, and plasmons. One approximation we have already learned in the chapter on atoms as Thomas-Fermi screening. Although the approximation was developed for atoms, at no point in the derivation of the dielectric constant

$$\varepsilon(\boldsymbol{q}) = 1 + \frac{q_{\mathrm{TF}}^2}{q^2} \tag{5.14}$$

with $q_{\mathrm{TF}}^2 = 4k_F/\pi a_B = 6\pi e^2 n/\varepsilon_F$ is reference to the atom. Rather, the result, as already noted in 3.3, is valid for metals and describes their screening effect. However, the Thomas-Fermi method cannot describe dynamic effects. For that, one needs the RPA (random phase approximation), which will be introduced in the following.

We investigate a system of interacting electrons in an external potential $U(\boldsymbol{r}; t)$, which is (partially) screened by the potential $V_s(\boldsymbol{r}; t)$ as in Chapter 3.3. The potential $V_s(\boldsymbol{r}; t)$ is generated internally by the electrons in the metal, so that in the end the total field $V = U + V_s$ is present. The dynamic dielectric constant is then determined by, cf. (3.33),

$$\varepsilon(\boldsymbol{q}; \omega) = \frac{U(\boldsymbol{q}; \omega)}{V(\boldsymbol{q}; \omega)} = 1 - \frac{V_s(\boldsymbol{q}; \omega)}{V(\boldsymbol{q}; \omega)}. \tag{5.15}$$

We want to solve the problem self-consistently and therefore assume that the electrons are exposed to the total field V. The effective (time-dependent) Hamiltonian operator of the electrons is given by

$$\begin{aligned} H_{\text{eff}} &= \int d^3r \sum_s \left[\frac{\hbar^2}{2m} \boldsymbol{\nabla}\Psi_s^\dagger(\boldsymbol{r}) \cdot \boldsymbol{\nabla}\Psi_s(\boldsymbol{r}) + \Psi_s^\dagger(\boldsymbol{r}) V(\boldsymbol{r}; t) \Psi_s(\boldsymbol{r}) \right] \\ &= \sum_{\boldsymbol{k}s} \varepsilon_{\boldsymbol{k}} c_{\boldsymbol{k}s}^\dagger c_{\boldsymbol{k}s} + \frac{1}{\Omega} \sum_{\boldsymbol{q}} V(\boldsymbol{q}; t) \rho(-\boldsymbol{q}) \end{aligned} \tag{5.16}$$

with the volume $\Omega = L^3$ and the (Fourier-transformed) density operator $\rho(-\boldsymbol{q}) = \sum_{\boldsymbol{k}s} c_{\boldsymbol{k}+\boldsymbol{q}s}^\dagger c_{\boldsymbol{k}s}$, cf. (4.107). Note that the electron-electron interaction does not appear directly in the Hamiltonian operator H_{eff}. Its contribution is indirectly included through the screening part V_s to V; i.e., we take screening effects into account but neglect correlation and exchange effects.

We assume that the external potential $U(\boldsymbol{r};t)$ generates a classically oscillating field. We want to find the quantum mechanical response of the electron system to this classical potential. We will assume U to be small and consider the problem only to first order in U; this is referred to as linear response. A potential oscillating with frequency ω $U(\boldsymbol{r};t) = U(\boldsymbol{r};\omega)e^{-i\omega t}$ then leads to a response $\langle\rho(\boldsymbol{r};t)\rangle = \rho(\boldsymbol{r};\omega)e^{-i\omega t}$ at the same frequency. Furthermore, the superposition principle holds, so we only need to calculate the response to a single frequency, and the general result follows by simply adding the contributions at different frequencies.

For the homogeneous electron gas, the expectation value of $\rho(\boldsymbol{q})$ vanishes (except for $\boldsymbol{q} = 0$). Due to the applied potential U, this expectation value becomes finite. The screening charge $-e\langle\rho\rangle$ generates the potential

$$V_s(\boldsymbol{q};\omega) = \frac{4\pi e^2}{q^2}\langle\rho(\boldsymbol{q};\omega)\rangle. \tag{5.17}$$

To obtain an explicit expression for the screening potential V_s, we will approximate the equation of motion for the charge density,

$$\begin{aligned} i\hbar\frac{d}{dt}\rho(-\boldsymbol{q};t) &= [\rho(-\boldsymbol{q};t), H_{\mathrm{eff}}] \\ \Rightarrow \quad \hbar\omega\rho(-\boldsymbol{q};\omega) &= [\rho(-\boldsymbol{q};\omega), H_{\mathrm{eff}}], \end{aligned} \tag{5.18}$$

instead of directly solving the equation of motion for ρ. We first consider the equation of motion for a term

$$\hbar\omega c^\dagger_{\boldsymbol{p}+\boldsymbol{q}\sigma}c_{\boldsymbol{p}\sigma} = [c^\dagger_{\boldsymbol{p}+\boldsymbol{q}\sigma}c_{\boldsymbol{p}\sigma}, H_{\mathrm{eff}}]. \tag{5.19}$$

The result for $\rho(-\boldsymbol{q})$ can then be obtained by summing over $\boldsymbol{p}$ and σ. The commutator on the right side of (5.18) is given by the sum of the two terms

$$\begin{aligned} &\sum_{\boldsymbol{k}s}\varepsilon_{\boldsymbol{k}}[c^\dagger_{\boldsymbol{p}+\boldsymbol{q}\sigma}c_{\boldsymbol{p}\sigma}, c^\dagger_{\boldsymbol{k}s}c_{\boldsymbol{k}s}] = (\varepsilon_{\boldsymbol{p}} - \varepsilon_{\boldsymbol{p}+\boldsymbol{q}})c^\dagger_{\boldsymbol{p}+\boldsymbol{q}\sigma}c_{\boldsymbol{p}\sigma}, \\ &\sum_{\boldsymbol{q}'\boldsymbol{k}s}V(\boldsymbol{q}')[c^\dagger_{\boldsymbol{p}+\boldsymbol{q}\sigma}c_{\boldsymbol{p}\sigma}, c^\dagger_{\boldsymbol{k}+\boldsymbol{q}'s}c_{\boldsymbol{k}s}] = \sum_{\boldsymbol{q}'}V(\boldsymbol{q}')(c^\dagger_{\boldsymbol{p}+\boldsymbol{q}\sigma}c_{\boldsymbol{p}-\boldsymbol{q}'\sigma} - c^\dagger_{\boldsymbol{p}+\boldsymbol{q}+\boldsymbol{q}'\sigma}c_{\boldsymbol{p}\sigma}). \end{aligned} \tag{5.20}$$

In summary, we obtain the equation of motion

$$\begin{aligned} (\varepsilon_{\boldsymbol{p}+\boldsymbol{q}} - \varepsilon_{\boldsymbol{p}} + \hbar\omega)c^\dagger_{\boldsymbol{p}+\boldsymbol{q}\sigma}c_{\boldsymbol{p}\sigma} &= \frac{1}{\Omega}\sum_{\boldsymbol{q}'}V(\boldsymbol{q}';\omega)(c^\dagger_{\boldsymbol{p}+\boldsymbol{q}\sigma}c_{\boldsymbol{p}-\boldsymbol{q}'\sigma} - c^\dagger_{\boldsymbol{p}+\boldsymbol{q}+\boldsymbol{q}'\sigma}c_{\boldsymbol{p}\sigma}) \\ &\overset{\mathrm{RPA}}{\approx} \frac{V(-\boldsymbol{q};\omega)}{\Omega}(c^\dagger_{\boldsymbol{p}+\boldsymbol{q}\sigma}c_{\boldsymbol{p}+\boldsymbol{q}\sigma} - c^\dagger_{\boldsymbol{p}\sigma}c_{\boldsymbol{p}\sigma}), \end{aligned} \tag{5.21}$$

where in the last step we performed the RPA by only taking the term with $\boldsymbol{q}' = -\boldsymbol{q}$ from the sum and neglecting the other terms. This assumption is based on the fact that terms of the form $c^\dagger_{\boldsymbol{k}} c_{\boldsymbol{k}'}$ oscillate with $e^{i(\boldsymbol{k}'-\boldsymbol{k})\cdot\boldsymbol{r}}$, so that their contribution (after integration over a small volume element) cancels out as long as $\boldsymbol{k}' \neq \boldsymbol{k}$.

The approximate equation can now be solved for $c^\dagger_{\boldsymbol{p}+\boldsymbol{q}\sigma} c_{\boldsymbol{p}\sigma}$. Summing the result over $\boldsymbol{p}\sigma$ gives

$$\begin{aligned}\rho(-\boldsymbol{q};\omega) &= \frac{V(-\boldsymbol{q};\omega)}{\Omega} \sum_{\boldsymbol{p}\sigma} \frac{c^\dagger_{\boldsymbol{p}+\boldsymbol{q}\sigma} c_{\boldsymbol{p}+\boldsymbol{q}\sigma} - c^\dagger_{\boldsymbol{p}\sigma} c_{\boldsymbol{p}\sigma}}{\varepsilon_{\boldsymbol{p}+\boldsymbol{q}} - \varepsilon_{\boldsymbol{p}} + \hbar\omega} \\ &\overset{(\boldsymbol{p}\mapsto\boldsymbol{p}-\boldsymbol{q})}{=} \frac{V(-\boldsymbol{q};\omega)}{\Omega} \sum_{\boldsymbol{p}\sigma} \frac{c^\dagger_{\boldsymbol{p}-\boldsymbol{q}\sigma} c_{\boldsymbol{p}-\boldsymbol{q}\sigma} - c^\dagger_{\boldsymbol{p}\sigma} c_{\boldsymbol{p}\sigma}}{\varepsilon_{\boldsymbol{p}-\boldsymbol{q}} - \varepsilon_{\boldsymbol{p}} - \hbar\omega}. \end{aligned} \tag{5.22}$$

From this, we can now calculate the expectation value in the ground state and obtain ($\Theta(x)$ is the step function)

$$\begin{aligned}\langle\rho(\boldsymbol{q};\omega)\rangle &= \frac{V(\boldsymbol{q};\omega)}{\Omega} \sum_{\boldsymbol{p}\sigma} \frac{\langle n_{\boldsymbol{p}+\boldsymbol{q}\sigma}\rangle - \langle n_{\boldsymbol{p}\sigma}\rangle}{\varepsilon_{\boldsymbol{p}+\boldsymbol{q}} - \varepsilon_{\boldsymbol{p}} - \hbar\omega} \\ &= V(\boldsymbol{q};\omega)\, \underbrace{2\int \frac{d^3p}{(2\pi)^3} \frac{\Theta(\varepsilon_F - \varepsilon_{\boldsymbol{p}+\boldsymbol{q}}) - \Theta(\varepsilon_F - \varepsilon_{\boldsymbol{p}})}{\varepsilon_{\boldsymbol{p}+\boldsymbol{q}} - \varepsilon_{\boldsymbol{p}} - \hbar\omega - i0^+}}_{\chi(\boldsymbol{q};\omega)} \end{aligned} \tag{5.23}$$

where the small imaginary part in the denominator guarantees causality. With (5.15) and (5.17), we obtain the relationship

$$\varepsilon_{\mathrm{RPA}}(\boldsymbol{q};\omega) = 1 - \frac{4\pi e^2}{q^2}\chi(\boldsymbol{q};\omega). \tag{5.24}$$

5.1.3 Plasma Resonance

First, we want to examine the dielectric function for small momenta $|\boldsymbol{q}| \ll k_F$. To do this, we expand

$$\Theta(\varepsilon_F - \varepsilon_{\boldsymbol{p}+\boldsymbol{q}}) = \Theta(\varepsilon_F - \varepsilon_{\boldsymbol{p}}) - \delta(\varepsilon_{\boldsymbol{p}} - \varepsilon_F)\boldsymbol{q}\cdot\underbrace{\boldsymbol{\nabla}\varepsilon_{\boldsymbol{p}}}_{\hbar v_F \hat{\boldsymbol{p}}}$$

and obtain

$$\begin{aligned}\chi(\boldsymbol{q};\omega) &= -2\int \frac{d^3p}{(2\pi)^3} \frac{v_F\,\boldsymbol{q}\cdot\hat{\boldsymbol{p}}\,\delta(\varepsilon_{\boldsymbol{p}} - \varepsilon_F)}{v_F\,\boldsymbol{q}\cdot\hat{\boldsymbol{p}} - \omega - i0^+} \\ &\overset{\omega\gg qv_F}{\approx} 2\int \frac{d^3p}{(2\pi)^3} \frac{\boldsymbol{q}\cdot\hat{\boldsymbol{p}}\,\delta(p-k_F)}{\hbar\omega} \left(1 + \frac{v_F\boldsymbol{q}\cdot\hat{\boldsymbol{p}}}{\hbar\omega} + \cdots\right) \\ &= \frac{2}{(2\pi)^2}\int_{-1}^{1} dz \frac{k_F^2 q z}{\hbar\omega}\left(1 + \frac{v_F q z}{\omega}\right) \\ &= \frac{k_F^2 v_F q^2}{3\pi^2\hbar\omega^2} = \frac{nq^2}{m\omega^2} \end{aligned} \tag{5.25}$$

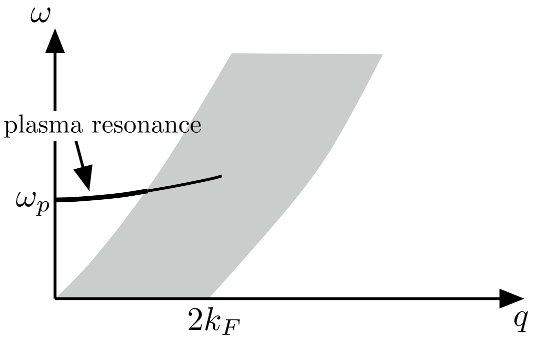

Figure 5.3: Excitation spectrum of the homogeneous electron gas in the ω–q plane. The gray shaded area corresponds to the electron-hole continuum and the solid line outside the continuum corresponds to the plasma resonance with the dispersion determined by $\varepsilon(q;\omega) = 0$, which is damped (Landau damping) as soon as it enters the continuum.

where we have introduced the angle θ between $\boldsymbol{p}$ and $\boldsymbol{q}$ with $z = \cos\theta$. Thus, the dielectric constant $\varepsilon_{\text{RPA}}(0;\omega) = 1 - (\omega_p/\omega)^2$ changes sign at $\omega_p = \sqrt{4\pi e^2 n/m}$. For $\omega < \omega_p$, ε is negative and the metal perfectly reflects all incoming radiation. For $\omega > \omega_p$, the dielectric constant becomes positive as in a normal dielectric and the metal becomes transparent. The frequency ω_p is called the plasma frequency and the corresponding particle is the plasmon, see Figure 5.3.[4] The plasmon frequency is given for typical metals by $\omega_p \simeq 10^{16}\,\text{Hz}$ ($\hbar\omega_p \simeq 10eV$), where we have used $n \simeq 10^{23}\,\text{cm}^{-3}$ and $m \simeq 10^{-27}\,\text{g}$. Thus, metals are opaque to visible light and only become transparent for X-ray radiation.

At $\omega = \omega_p$, $\varepsilon = 0$. This allows for the possibility that the system internally has an excitation with $V, V_s, \rho \neq 0$ without an external field being applied ($U = 0$). This is the plasma oscillation, a collective excitation of the electron gas. However, the plasma oscillation is only a well-defined excitation for small ω, q. When calculating $\chi(\boldsymbol{q},\omega)$ in general, one finds that the plasma oscillation survives as long as $\operatorname{Im}\chi = 0$. The imaginary part of χ leads to damping due to dissipation, see Figure 5.3. In the electron gas, the electron-hole excitations correspond to $\hbar\omega = \varepsilon_{\boldsymbol{p}+\boldsymbol{q}} - \varepsilon_{\boldsymbol{p}}$ with energy ω and momentum $\boldsymbol{q}$, cf. the denominator of 5.23. Since $\boldsymbol{p}$ is free, the electron-hole

---

[4] Note that Planck's constant does not appear in the expression for the plasma frequency, so that this is a purely classical effect with a classical explanation (see, e.g., Feynman Lecture Vol. 2).

excitations form a continuum without sharp energy-momentum relations. In fact, electron-hole excitations fill the range

$$0 \le \hbar\omega \le \hbar v_F q + \varepsilon_{\boldsymbol{q}}, \qquad (q \le 2k_F) \tag{5.26}$$
$$-\hbar v_F q + \varepsilon_{\boldsymbol{q}} \le \hbar\omega \le \hbar v_F q + \varepsilon_{\boldsymbol{q}}, \qquad (q \ge 2k_F)\,. \tag{5.27}$$

5.1.4 Screening

To describe screening effects, we need to evaluate the dielectric function at $\omega \to 0$. Setting $\omega = 0$ in (5.23) allows us to determine the polarization function easily,

$$\begin{aligned}
\operatorname{Re}\chi(\boldsymbol{q}) &= 2\operatorname{Re}\int \frac{d^3p}{(2\pi)^3}\frac{\Theta(\varepsilon_F-\varepsilon_{\boldsymbol{p}+\boldsymbol{q}})-\Theta(\varepsilon_F-\varepsilon_{\boldsymbol{p}})}{\varepsilon_{\boldsymbol{p}+\boldsymbol{q}}-\varepsilon_{\boldsymbol{p}}-i0^+}\\
&= 2\operatorname{Re}\int \frac{d^3p}{(2\pi)^3}\Theta(\varepsilon_F-\varepsilon_{\boldsymbol{p}})\left(\frac{1}{\varepsilon_{\boldsymbol{p}}-\varepsilon_{\boldsymbol{p}-\boldsymbol{q}}-i0^+}-\frac{1}{\varepsilon_{\boldsymbol{p}+\boldsymbol{q}}-\varepsilon_{\boldsymbol{p}}-i0^+}\right)\\
&= -\frac{m}{\pi^2\hbar^2}\int_0^{k_F} dp\, p^2 \operatorname{Re}\int_{-1}^{1} dz\left(\frac{1}{q^2-2qpz+i0^+}+\frac{1}{q^2+2qpz-i0^+}\right)\\
&= -\frac{m}{\pi^2\hbar^2 q}\int_0^{k_F} dp\, p\log\left|\frac{q+2p}{q-2p}\right|\\
&= -\frac{m}{2\pi^2\hbar^2 q}\left(k_F^2\log\left|\frac{2k_F+q}{2k_F-q}\right| + \int_0^{k_F} dp\,\frac{4qp^2}{4p^2-q^2}\right)\\
&= -\frac{m}{2\pi^2\hbar^2 q}\left[k_F q + (k_F^2-\tfrac{1}{4}q^2)\log\left|\frac{2k_F+q}{2k_F-q}\right|\right],
\end{aligned} \tag{5.28}$$

where we have used that $\varepsilon_{\boldsymbol{p}+\boldsymbol{q}}-\varepsilon_{\boldsymbol{p}} = \hbar^2(q^2+2\boldsymbol{q}\cdot\boldsymbol{p})/2m$. Substituting the result into the expression for ε yields the static dielectric function

$$\operatorname{Re}\varepsilon_{\text{RPA}}(\boldsymbol{q}) = 1 + \frac{q_{\text{TF}}^2}{q^2}\left(\frac{1}{2}+\frac{4k_F^2-q^2}{8k_F q}\log\left|\frac{2k_F+q}{2k_F-q}\right|\right). \tag{5.29}$$

For $q \ll k_F$, the dielectric function exactly matches the Thomas-Fermi result (5.14). However, the RPA result has a diverging first derivative at $q = \pm 2k_F$. The reason for this lies in the sharp Fermi surface. Considering a point charge at the origin with $U(q) = 4\pi e^2/q^2$ leads to oscillations in the charge distribution with a wave vector $\simeq 2k_F$ in addition to the exponential screening of the charge;

$$\langle\rho(\boldsymbol{r})\rangle = \int d^3q\,[\varepsilon_{\text{RPA}}^{-1}(\boldsymbol{q})-1]e^{i\boldsymbol{q}\cdot\boldsymbol{r}} \sim \frac{\cos 2k_F r}{r^3} \tag{5.30}$$

These oscillations are called Friedel oscillations. As shown in Figure 5.4, the Friedel oscillations cause the test charge to be alternately over- and under-screened.

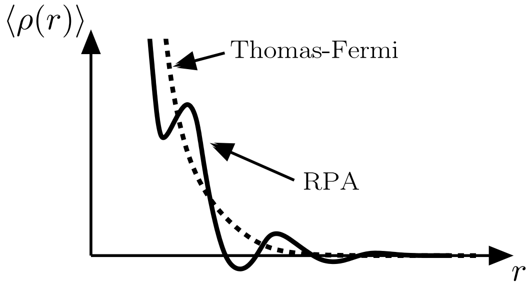

Figure 5.4: Friedel oscillations of the screening charge $\langle\rho\rangle \propto V_s$ as a function of the distance r from a point charge at the origin.

5.2 Superconductivity

Superconductivity was discovered in 1911 by Heike Kamerlingh Onnes. He cooled mercury with helium down to 4 K and found that the resistance of mercury suddenly disappeared at the lowest temperatures. Later experiments have shown that a current in a superconductor can be maintained for long periods ($\gtrsim$ 1 year) without an applied voltage. This confirms that the material is indeed resistance-free. Another property of superconductors is their perfect diamagnetism, called the Meissner-Ochsenfeld effect. We will show in the section on the London equations that the Meissner-Ochsenfeld effect is more characteristic of a superconductor than the disappearance of resistance. The external magnetic field can only penetrate the material near the surface; deeper layers are field-free. This "expulsion" of the magnetic field is independent of whether the sample was already superconducting before the magnetic field was turned on or only became superconducting after the magnetic field was turned on.

5.2.1 London Equations

For some time, superconductivity had no theoretically satisfactory explanation. The brothers Fritz and Heinz London managed to establish at least phenomenological equations in 1935. It took another 20 years for a microscopic theory to emerge. The question that arises is how to describe a material that exhibits infinite conductivity. From the Newtonian equation of motion $m\partial_t \boldsymbol{v} = -e\boldsymbol{E}$ of an electron, one directly finds the first London equation for the current density $\boldsymbol{j} = -ne\boldsymbol{v}$,

$$\partial_t \boldsymbol{j} = \frac{ne^2}{m}\boldsymbol{E}. \tag{5.31}$$

This equation describes a "perfect conductor," as with $\boldsymbol{E} = 0$, it does not necessarily follow that $\boldsymbol{j} = 0$, but it cannot predict the Meissner-Ochsenfeld effect. To show this, we derive the equation of motion for the magnetic field $\boldsymbol{H}$. For this, we need the Maxwell equation $\boldsymbol{\nabla} \times \boldsymbol{H} = 4\pi\boldsymbol{j}/c$ (we consider the stationary case with $\partial_t \boldsymbol{E} = 0$).

Taking the curl of this equation leads to (we use $\boldsymbol{\nabla}\cdot\boldsymbol{H}=0$ and $\boldsymbol{\nabla}\times\boldsymbol{E}=-\partial_t\boldsymbol{H}$)

$$\nabla^2\partial_t\boldsymbol{H} = -\overbrace{\boldsymbol{\nabla}\times\boldsymbol{\nabla}\times}^{\boldsymbol{\nabla}(\boldsymbol{\nabla}\cdot)-\nabla^2}\partial_t\boldsymbol{H} = -\frac{4\pi}{c}\boldsymbol{\nabla}\times\partial_t\boldsymbol{j} \overset{(5.31)}{=} \frac{1}{\lambda_L^2}\partial_t\boldsymbol{H} \tag{5.32}$$

with the London penetration depth

$$\lambda_L = \sqrt{\frac{mc^2}{4\pi ne^2}}. \tag{5.33}$$

The equation (5.32) shows only that a magnetic field in a perfect conductor is time-independent; the magnetic field lines are frozen. However, this is not in accordance with the experiments of Meissner and Ochsenfeld. Therefore, the second London equation

$$\boldsymbol{\nabla}\times\boldsymbol{j} = \frac{ne^2}{mc}\boldsymbol{H} \tag{5.34}$$

requires the vanishing of the integration constant in (5.32). This makes (5.32) become

$$\nabla^2\boldsymbol{H} = \frac{4\pi}{c}\boldsymbol{\nabla}\times\boldsymbol{j} = \frac{1}{\lambda_L^2}\boldsymbol{H} \tag{5.35}$$

and (all) magnetic fields are completely screened on the length scale λ_L; if one looks for a homogeneous solution $\boldsymbol{H}(\boldsymbol{r})=\boldsymbol{H}_0$, one immediately finds $\boldsymbol{H}_0=0$. The ordinary form of the Maxwell equation is obtained with $\lambda_L\to\infty$ $(n\to 0)$. Physically, (5.35) means that the magnetic field (the photon) acquires a "mass" through coupling to the superconducting condensate. This is called the Anderson-Higgs mechanism and is analogous to the effect that in electroweak theory, the W and Z gauge bosons acquire mass through coupling to the Higgs boson.

Using the vector potential $\boldsymbol{A}$ in the London gauge ($\boldsymbol{\nabla}\cdot\boldsymbol{A}=0$) one can combine the two London equations into a single equation,

$$\boldsymbol{j} = -\frac{ne^2}{mc}\boldsymbol{A} = -\frac{c}{4\pi\lambda_L^2}\boldsymbol{A}, \tag{5.36}$$

from which the first and second London equations can be derived by applying ∂_t or $\boldsymbol{\nabla}\times$, respectively. The London gauge ensures that the continuity equation $\boldsymbol{\nabla}\cdot\boldsymbol{j}=0$ holds. Note that the particle density n in the London equations refers only to the density of the superconducting particles n_s, which is generally less than the electron density, and thus $\boldsymbol{j}$ denotes the corresponding current density of the supercurrent $\boldsymbol{j}_s$, which generally differs from the total current density.

5.2.2 BCS Theory

The microscopic theory of superconductors was developed in 1957 by Bardeen, Cooper, and Schrieffer (BCS). It is based on a discovery by Leon Cooper that an arbitrarily weak attractive potential between two electrons at the Fermi surface leads to a bound state of them. The pairing mechanism is important because a superfluid state is typical for bosons, as bosons condense into a macroscopically occupied ground state wave function at low temperatures. Fermions, on the other hand, form a Fermi sea. For fermions to behave superfluid (bosonically), they must first pair up before they can condense.

The problem now is why electrons attract each other at all, as their (Coulomb) interaction is known to be repulsive. Part of the answer was developed in the last section: the repulsion of electrons at high density is not so strong because the interaction is screened on the length scale q_{TF}^{-1}. A hint towards the solution of the problem was provided by the isotope effect: as early as the 1950s, it was found that the transition temperature T_c for superconductivity depends on the isotope ($T_c \propto M_{\text{Ion}}^{-1/2}$). This indicates that superconductivity is not solely an electronic problem but that one must take into account the effect of phonons (lattice vibrations). A (unjustified) simplified calculation leads to an effective electron-electron interaction $V_{\text{eff}} = 4\pi e^2/q^2\varepsilon(q;\omega)$ with

$$\frac{1}{\varepsilon(q;\omega)} \approx \frac{q^2}{q^2+q_{\text{TF}}^2}\left(1+\frac{\omega_q^2}{\omega^2-\omega_q^2}\right), \tag{5.37}$$

where the first term accounts for the polarization of the electrons and the second term accounts for that of the positively charged ions with dispersion $\omega_q = sq$; s is the sound speed in the metal. Note that the time scale of the response of the electrons is given by the short time ω_p^{-1}. We may therefore consider the interaction for the investigated scattering processes of electrons near the Fermi surface as instantaneous, which is why we used the static expression for the electronic part of ε. The response of the (heavy) ions, on the other hand, occurs on the slower time scale ω_D^{-1} (ω_D is the Debye frequency of the phonons) and is much slower, so that the ionic contribution must be taken into account dynamically. The effect of phonon polarization leads to the potential being attractive for $|\omega| < \omega_q \simeq \omega_D$.

Although we only take the effect of phonons into account through an additional term in $\varepsilon(\boldsymbol{q};\omega)$, the problem is still too difficult to solve exactly. Since we want to describe superconductivity, the idea is to only describe the part of the interaction that leads to the pairing of electrons. The effect of the remaining interaction can then, in principle, be taken into account in perturbation theory. We will see that the pairing interaction leads to an energy gap; this suppresses the effects of the remaining interaction. We now consider the reduced (pairing) Hamiltonian operator[5]

$$H_{\text{paar}} = \sum_{\boldsymbol{k}\sigma} \underbrace{(\varepsilon_{\boldsymbol{k}}-\mu)}_{\xi_{\boldsymbol{k}}} c_{\boldsymbol{k}\sigma}^{\dagger} c_{\boldsymbol{k}\sigma} + \sum_{\boldsymbol{k}\boldsymbol{l}} V_{\text{eff}}(\boldsymbol{k}-\boldsymbol{l}) c_{\boldsymbol{k}\uparrow}^{\dagger} c_{-\boldsymbol{k}\downarrow}^{\dagger} c_{-\boldsymbol{l}\downarrow} c_{\boldsymbol{l}\uparrow}; \tag{5.38}$$

---

[5] The chemical potential μ is equal to ε_F at $T = 0$ and is determined by the (average) number of electrons.

the pairing Hamiltonian operator describes only the scattering of Cooper pairs $|\boldsymbol{k}\uparrow, -\boldsymbol{k}\downarrow\rangle = c^\dagger_{\boldsymbol{k}\uparrow} c^\dagger_{-\boldsymbol{k}\downarrow}|0\rangle$, which leads to the pairing of electrons.[6]

We expect that the BCS pairing Hamiltonian operator (5.38) leads to a phase-coherent superposition of Cooper pairs $|\boldsymbol{k}\uparrow, -\boldsymbol{k}\downarrow\rangle$. When the Cooper pairs condense, the operator $c_{-\boldsymbol{k}\downarrow} c_{\boldsymbol{k}\uparrow}$ acquires a finite expectation value $b_{\boldsymbol{k}}$ (coherent state). Due to the macroscopic occupation of the state, we expect that fluctuations are small. This motivates the molecular field ansatz

$$c_{-\boldsymbol{k}\downarrow} c_{\boldsymbol{k}\uparrow} = b_{\boldsymbol{k}} + \underbrace{(c_{-\boldsymbol{k}\downarrow} c_{\boldsymbol{k}\uparrow} - b_{\boldsymbol{k}})}_{\ll b_{\boldsymbol{k}}}; \tag{5.39}$$

by substituting into (5.38) and neglecting terms quadratic in the fluctuations, we obtain the BCS model Hamiltonian operator

$$H_{\mathrm{BCS}} = \sum_{\boldsymbol{k}\sigma} \xi_{\boldsymbol{k}} c^\dagger_{\boldsymbol{k}\sigma} c_{\boldsymbol{k}\sigma} + \sum_{\boldsymbol{k}\boldsymbol{l}} V_{\mathrm{eff}}(\boldsymbol{k}-\boldsymbol{l})(c^\dagger_{\boldsymbol{k}\uparrow} c^\dagger_{-\boldsymbol{k}\downarrow} b_{\boldsymbol{l}} + b^*_{\boldsymbol{k}} c_{-\boldsymbol{l}\downarrow} c_{\boldsymbol{l}\uparrow} - b^*_{\boldsymbol{k}} b_{\boldsymbol{l}}) \tag{5.40}$$

with the self-consistency equation $b_{\boldsymbol{k}} = \langle c_{-\boldsymbol{k}\downarrow} c_{\boldsymbol{k}\uparrow}\rangle$, which can be solved exactly.

Note that due to the molecular field ansatz, the Hamiltonian operator no longer conserves particle number. For large particle numbers, this is not a serious issue. The chemical potential μ simply sets the average particle number, and the relative fluctuations vanish like $N^{-1/2}$, similar to the grand canonical ensemble.[7]

As a first step in solving (5.40), we introduce the energy gap (Gap)

$$\Delta_{\boldsymbol{k}} = -\sum_{\boldsymbol{l}} V_{\mathrm{eff}}(\boldsymbol{k}-\boldsymbol{l}) b_{\boldsymbol{l}} = -\sum_{\boldsymbol{l}} V_{\mathrm{eff}}(\boldsymbol{k}-\boldsymbol{l}) \langle c_{-\boldsymbol{l}\downarrow} c_{\boldsymbol{l}\uparrow}\rangle \tag{5.41}$$

with which the BCS Hamiltonian can be written as

$$H_{\mathrm{BCS}} = \sum_{\boldsymbol{k}\sigma} \xi_{\boldsymbol{k}} c^\dagger_{\boldsymbol{k}\sigma} c_{\boldsymbol{k}\sigma} - \sum_{\boldsymbol{k}} \left(\Delta_{\boldsymbol{k}} c^\dagger_{\boldsymbol{k}\uparrow} c^\dagger_{-\boldsymbol{k}\downarrow} + \Delta^*_{\boldsymbol{k}} c_{-\boldsymbol{k}\downarrow} c_{\boldsymbol{k}\uparrow} - b^*_{\boldsymbol{k}} \Delta_{\boldsymbol{k}} \right). \tag{5.42}$$

Additionally, we want to define new fermionic operators $\beta_{\boldsymbol{k}\sigma}$ that diagonalize the Hamiltonian operator. A transformation to new fermionic operators is achieved through the Bogoliubov-Valatin transformation (see Section 5.2.3)

$$c_{\boldsymbol{k}\uparrow} = u^*_{\boldsymbol{k}} \beta_{\boldsymbol{k}\uparrow} + v_{\boldsymbol{k}} \beta^\dagger_{-\boldsymbol{k}\downarrow}, \qquad c^\dagger_{-\boldsymbol{k}\downarrow} = -v^*_{\boldsymbol{k}} \beta_{\boldsymbol{k}\uparrow} + u_{\boldsymbol{k}} \beta^\dagger_{-\boldsymbol{k}\downarrow}, \tag{5.43}$$

---

[6] In the simplest case we consider here, a Cooper pair is a bound state of two electrons as a singlet with total momentum 0. This is called s-wave pairing. Other pairing states are conceivable. For example, the electrons can pair as a triplet (p-wave) or the electron pair can have a finite total momentum (Larkin-Ovchinnikov-Fulde-Ferrell in a magnetic field). However, for most materials, the s-wave pairing channel with zero total momentum is preferred.

[7] Since one wants to assign a quantum mechanical phase φ to the superconductor, the uncertainty in the particle number N is even essential, as phase and particle number are conjugate variables and thus must satisfy the Heisenberg uncertainty relation $\Delta N\,\Delta\varphi \geq 1$.

with the (unitarity) condition $|u_{\boldsymbol{k}}|^2 + |v_{\boldsymbol{k}}|^2 = 1$. The choice[8]

$$|v_{\boldsymbol{k}}|^2 = 1 - |u_{\boldsymbol{k}}|^2 = \frac{1}{2}\left(1 - \frac{\xi_{\boldsymbol{k}}}{E_{\boldsymbol{k}}}\right),\ 2u^*_{\boldsymbol{k}}v_{\boldsymbol{k}} = \frac{\Delta_{\boldsymbol{k}}}{E_{\boldsymbol{k}}},\ E_{\boldsymbol{k}} = \sqrt{\xi^2_{\boldsymbol{k}} + |\Delta_{\boldsymbol{k}}|^2}, \tag{5.44}$$

leads, after substitution into (5.40) and simple rearrangements, to the diagonalized form (see the following section)

$$H_{\text{BCS}} = \sum_{\boldsymbol{k}}(\xi_{\boldsymbol{k}} - E_{\boldsymbol{k}} + b^*_{\boldsymbol{k}}\Delta_{\boldsymbol{k}}) + \sum_{\boldsymbol{k}\sigma} E_{\boldsymbol{k}}\beta^\dagger_{\boldsymbol{k}\sigma}\beta_{\boldsymbol{k}\sigma}. \tag{5.45}$$

The first term gives the ground state energy and the second term describes the excitations as the creation of Bogoliubov quasiparticles with the excitation energy $E_{\boldsymbol{k}} \geq 0$. For $|\Delta_{\boldsymbol{k}}| > 0$, the quasiparticles exhibit an energy gap, unlike in the metal.

In the following, we will first show that (5.43) and (5.44) indeed lead to the diagonal form (5.45). We will then determine the self-consistent energy gap $\Delta_{\boldsymbol{k}}$.

5.2.3 Excursion: General Quadratic Hamiltonians

Quadratic Hamiltonians, which do not necessarily conserve particle number, generally have the form

$$H = \sum_{i=1}^{n}\sum_{j=1}^{n}(h_{ij}c^\dagger_i c_j + \tfrac{1}{2}\Delta_{ij}c^\dagger_i c^\dagger_j + \tfrac{1}{2}\Delta^*_{ij}c_j c_i) = \boldsymbol{c}^\dagger h\boldsymbol{c} + \tfrac{1}{2}(\boldsymbol{c}^\dagger\Delta\boldsymbol{c}^\dagger + \boldsymbol{c}\Delta^\dagger\boldsymbol{c}) \tag{5.46}$$

with n being the number of fermionic modes, $h = h^\dagger$ and $\Delta = -\Delta^T$.[9] One can diagonalize this Hamiltonian using a Bogoliubov-Valatin transformation. To do this, one writes the Hamiltonian as a quadratic form

$$H = \tfrac{1}{2}\begin{pmatrix}\boldsymbol{c}^\dagger & \boldsymbol{c}\end{pmatrix}\underbrace{\begin{pmatrix} h & \Delta \\ -\Delta^* & -h^T\end{pmatrix}}_{H_{\text{BdG}}}\begin{pmatrix}\boldsymbol{c}\\ \boldsymbol{c}^\dagger\end{pmatrix} + \tfrac{1}{2}\operatorname{tr}h; \tag{5.47}$$

thus, every quadratic second-quantized Hamiltonian H is mapped onto a hermitian $2n \times 2n$ matrix H_{BdG}. The first quantized Hamiltonian (matrix) H_{BdG} is referred to as the "Bogoliubov-de Gennes Hamiltonian."

The Bogoliubov-de Gennes Hamiltonian operator H_{BdG} has twice as many degrees of freedom (namely $2n$) as the original fermionic system. The additional degrees of

---

[8] The phases of $u_{\boldsymbol{k}}$, $v_{\boldsymbol{k}}$, and $\Delta_{\boldsymbol{k}}$ are linked, as $\Delta^*_{\boldsymbol{k}}u_{\boldsymbol{k}}v_{\boldsymbol{k}} > 0$. Without loss of generality, we can choose $u_{\boldsymbol{k}} > 0$ and then find that $v_{\boldsymbol{k}}$ and $\Delta_{\boldsymbol{k}}$ have the same phase.

[9] At first glance, it seems that equation (5.46) does not impose any restriction on Δ. This is correct, but since the symmetric part $\Delta_S = (\Delta+\Delta^T)/2$ does not contribute due to the fermionic commutation relations, $\sum_{ij}(\Delta_S)_{ij}c_ic_j = -\sum_{ij}(\Delta_S)_{ij}c_jc_i = -\sum_{ij}(\Delta_S)_{ij}c_ic_j \Rightarrow \sum_{ij}(\Delta_S)_{ij}c_ic_j = 0$, one may, without loss of generality, choose Δ to be antisymmetric, $\Delta = (\Delta - \Delta^T)/2$.

freedom arise from the fact that $\boldsymbol{c}$ appears both on the right and left of H_{BdG} in the quadratic form (5.47), allowing for the freedom to choose where to place the term $\boldsymbol{c}^\dagger h \boldsymbol{c}$ in the BdG matrix. In (5.47), we have chosen the 'symmetric' variant, and therefore the Bogoliubov-de Gennes Hamiltonian operator has the ('particle-hole') symmetry $\{H_{\mathrm{BdG}}, C\} = 0$ with $C = \tau_x K$; here, K denotes the operator of complex conjugation and τ_x acts on the block form in (5.47). Note that C is not a symmetry in the conventional sense, as it does not commute with the Hamiltonian operator. Moreover, the symmetry in a Bogoliubov-de Gennes Hamiltonian operator is always present by construction (and therefore cannot be broken).

The task is to bring the second-quantized Hamiltonian operator H into the form $H = \sum_j \varepsilon_j \beta_j^\dagger \beta_j$ with fermionic operators β_j; the quadratic Hamiltonian operator is then solved, as all many-body eigenstates correspond to occupation number states with $n_j = \beta_j^\dagger \beta_j$. We will see that one can also require that the single-particle energies $\varepsilon_j \geq 0$, so that the ground state corresponds to the vacuum (with respect to the β operators) and ε_j are precisely the (single-particle) excitation energies. This task can be solved by a so-called Bogoliubov transformation (from $\boldsymbol{c}$ to $\boldsymbol{\beta}$)

$$T \begin{pmatrix} \boldsymbol{\beta} \\ \boldsymbol{\beta}^\dagger \end{pmatrix} = \begin{pmatrix} \boldsymbol{c} \\ \boldsymbol{c}^\dagger \end{pmatrix} \tag{5.48}$$

with $T \in \mathrm{Gl}(2n, \mathbb{C})$. The invariance of the quadratic Hamiltonian operator H under such a transformation requires that

$$H'_{\mathrm{BdG}} = T^\dagger H_{\mathrm{BdG}} T \tag{5.49}$$

where H'_{BdG} is the Bogoliubov-de Gennes Hamiltonian in the β basis. Therefore, we want H'_{BdG} to be a diagonal matrix.

Note that, unlike the 'normal' basis change from Section 4.4, here creators and annihilators are mixed. This is analogous to classical mechanics: in the Lagrangian formalism, general basis transformations are allowed, while in the Hamiltonian formalism, position and momentum coordinates may also be mixed. At first glance, this leads to more degrees of freedom, but only canonical transformations that leave the Poisson bracket invariant are allowed. Here, the canonical commutation relations $\{c_i, c_j^\dagger\} = \delta_{ij}$ and $\{c_i, c_j\} = 0$ take the role of the Poisson bracket. In fact, we want the operators β_i, which diagonalize the Hamiltonian operator, to also be truly fermionic operators so that they generate the usual fermionic Fock space.

We therefore require the invariance of[10]

$$\left\{ \begin{pmatrix} \boldsymbol{c} \\ \boldsymbol{c}^\dagger \end{pmatrix}, \begin{pmatrix} \boldsymbol{c} \\ \boldsymbol{c}^\dagger \end{pmatrix}^\dagger \right\} = I_{2n} \tag{5.50}$$

---

[10] We interpret the anticommutator of two vectors $\boldsymbol{v}$ and $\boldsymbol{w}$ as a matrix with matrix elements $(\{\boldsymbol{v}, \boldsymbol{w}\})_{ij} = \{v_i, w_j\}$. The anticommutator in (5.50) is a quadratic form that plays the role of the metric on the space of creators and annihilators.

under the transformation (5.49). By substituting the transformation (5.49) and using the bilinearity of the anticommutator, and requiring that the anticommutator remains invariant, we obtain the constraint

$$I_{2n} = \left\{ T \begin{pmatrix} \boldsymbol{\beta} \\ \boldsymbol{\beta}^\dagger \end{pmatrix}, \begin{pmatrix} \boldsymbol{\beta} \\ \boldsymbol{\beta}^\dagger \end{pmatrix}^\dagger T^\dagger \right\} = T \underbrace{\left\{ \begin{pmatrix} \boldsymbol{\beta} \\ \boldsymbol{\beta}^\dagger \end{pmatrix}, \begin{pmatrix} \boldsymbol{\beta} \\ \boldsymbol{\beta}^\dagger \end{pmatrix}^\dagger \right\}}_{I_{2n}} T^\dagger = TT^\dagger; \tag{5.51}$$

i.e., T is unitary.

Diagonalization of a Hermitian matrix H_{BdG} with a unitary transformation T is solved by the ordinary eigenvalue problem

$$H_{\mathrm{BdG}} \boldsymbol{t}_j = \varepsilon_j \boldsymbol{t}_j \tag{5.52}$$

where $\boldsymbol{t}_j$ are the columns of T. The particle-hole symmetry C guarantees that for every eigenvector $\boldsymbol{t}_+$ with eigenvalue $\varepsilon \geq 0$, there is an additional eigenvector $\boldsymbol{t}_- = C\boldsymbol{t}_+$ with eigenvalue $-\varepsilon \leq 0$; for

$$\underbrace{H_{\mathrm{BdG}}}_{-C^{-1} H_{\mathrm{BdG}} C} \boldsymbol{t}_+ = \varepsilon \boldsymbol{t}_+ \qquad \Rightarrow \qquad H_{\mathrm{BdG}} \boldsymbol{t}_- = -\varepsilon \boldsymbol{t}_- . \tag{5.53}$$

Now, if we order the eigenvalues such that the positive eigenvalues appear first and then the negative eigenvalues on the diagonal of H'_{BdG}, the particle-hole symmetry guarantees that $\boldsymbol{\beta}^\dagger$ in the transformation (5.49) are precisely the adjoint operators to $\boldsymbol{\beta}$. In summary, we obtain

$$\begin{aligned} H &= \tfrac{1}{2} \begin{pmatrix} \boldsymbol{\beta}^\dagger & \boldsymbol{\beta} \end{pmatrix} \begin{pmatrix} \varepsilon_1 & & & & & \\ & \ddots & & & & \\ & & \varepsilon_n & & & \\ & & & -\varepsilon_1 & & \\ & & & & \ddots & \\ & & & & & -\varepsilon_n \end{pmatrix} \begin{pmatrix} \boldsymbol{\beta} \\ \boldsymbol{\beta}^\dagger \end{pmatrix} + \tfrac{1}{2} \operatorname{tr} h \\ &= \sum_{j=1}^{n} \varepsilon_j \beta_j^\dagger \beta_j + \tfrac{1}{2} \Big(\operatorname{tr} h - \sum_{j=1}^{n} \varepsilon_j \Big). \end{aligned} \tag{5.54}$$

As an example, consider the model Hamiltonian (5.42), which can be written in the Bogoliubov-de Gennes form

$$H = \sum_{\boldsymbol{k}} \left[\begin{pmatrix} c^\dagger_{\boldsymbol{k}\uparrow} & c_{-\boldsymbol{k}\downarrow} \end{pmatrix} H_{\boldsymbol{k}} \begin{pmatrix} c_{\boldsymbol{k}\uparrow} \\ c^\dagger_{-\boldsymbol{k}\downarrow} \end{pmatrix} + \xi_{\boldsymbol{k}} + b^*_{\boldsymbol{k}} \Delta_{\boldsymbol{k}} \right] \tag{5.55}$$

with

$$H_{\boldsymbol{k}} = \begin{pmatrix} \xi_{\boldsymbol{k}} & -\Delta_{\boldsymbol{k}} \\ -\Delta^*_{\boldsymbol{k}} & -\xi_{\boldsymbol{k}} \end{pmatrix}. \tag{5.56}$$

We see that due to translational symmetry, the problem reduces to the diagonalization of the 2×2 Bogoliubov-de Gennes Hamiltonian $H_{\boldsymbol{k}}$. The two eigenstates of the Hamiltonian are given by

$$H_{\boldsymbol{k}} \begin{pmatrix} u^*_{\boldsymbol{k}} \\ -v^*_{\boldsymbol{k}} \end{pmatrix} = E_{\boldsymbol{k}} \begin{pmatrix} u^*_{\boldsymbol{k}} \\ -v^*_{\boldsymbol{k}} \end{pmatrix}, \qquad H_{\boldsymbol{k}} \begin{pmatrix} v_{\boldsymbol{k}} \\ u_{\boldsymbol{k}} \end{pmatrix} = -E_{\boldsymbol{k}} \begin{pmatrix} v_{\boldsymbol{k}} \\ u_{\boldsymbol{k}} \end{pmatrix} \tag{5.57}$$

with $u_{\boldsymbol{k}}$ and $v_{\boldsymbol{k}}$ as in (5.44).[11] The transformation to the basis $\beta_{\boldsymbol{k}\uparrow}, \beta^\dagger_{-\boldsymbol{k}\downarrow}$ yields the result (5.45),

$$\begin{aligned} H &= \sum_{\boldsymbol{k}} [E_{\boldsymbol{k}}(\beta^\dagger_{\boldsymbol{k}\uparrow}\beta_{\boldsymbol{k}\uparrow} - \beta_{-\boldsymbol{k}\downarrow}\beta^\dagger_{-\boldsymbol{k}\downarrow}) + \xi_{\boldsymbol{k}} + b^*_{\boldsymbol{k}}\Delta_{\boldsymbol{k}}] \\ &= \underbrace{\sum_{\boldsymbol{k}} (\xi_{\boldsymbol{k}} - E_{\boldsymbol{k}} + b^*_{\boldsymbol{k}}\Delta_{\boldsymbol{k}})}_{E_g} + \sum_{\boldsymbol{k}\sigma} E_{\boldsymbol{k}} \beta^\dagger_{\boldsymbol{k}\sigma}\beta_{\boldsymbol{k}\sigma}, \end{aligned} \tag{5.58}$$

with the ground state energy E_g and the excitation energies $E_{\boldsymbol{k}}$.

5.2.4 Self-consistency equation

In the next step, we need to solve the self-consistency equation (5.41) to see if for a superconductor $|\Delta_{\boldsymbol{k}}| > 0$ will indeed hold. The trivial solution of the self-consistency equation with $\Delta_{\boldsymbol{k}} = 0$, so that $v_{\boldsymbol{k}} = 1$ for $\xi_{\boldsymbol{k}} < 0$ and $v_{\boldsymbol{k}} = 0$ for $\xi_{\boldsymbol{k}} > 0$, describes the Fermi sea in the normal conducting state. The self-consistency equation is given by

$$\begin{aligned} \Delta_{\boldsymbol{k}} &= -\sum_{\boldsymbol{l}} V_{\text{eff}}(\boldsymbol{k} - \boldsymbol{l}) \langle c_{-\boldsymbol{l}\downarrow} c_{\boldsymbol{l}\uparrow} \rangle \overset{(5.43)}{=} -\sum_{\boldsymbol{l}} V_{\text{eff}}(\boldsymbol{k} - \boldsymbol{l}) u^*_{\boldsymbol{l}} v_{\boldsymbol{l}} \\ &\overset{(5.44)}{=} -\frac{1}{2} \sum_{\boldsymbol{l}} V_{\text{eff}}(\boldsymbol{k} - \boldsymbol{l}) \frac{\Delta_{\boldsymbol{l}}}{E_{\boldsymbol{l}}}, \end{aligned} \tag{5.59}$$

where we have used the expectation value of the pairing term in the ground state $\langle c_{-\boldsymbol{l}\downarrow} c_{\boldsymbol{l}\uparrow} \rangle$, noting that the ground state $|0\rangle$ represents the vacuum for the operators $\beta_{\boldsymbol{k}}$ with $\beta_{\boldsymbol{k}}|0\rangle = 0$.

To describe superconductivity, we need an attractive interaction. As we have seen before, the effective electron-electron potential V_{eff} is attractive for energy transfers with $|\xi_{\boldsymbol{k}} - \xi_{\boldsymbol{l}}| < \hbar\omega_D$. To solve the self-consistency equation, we make the stronger assumption that V_{eff} is attractive if both $|\xi_{\boldsymbol{k}}|$ and $|\xi_{\boldsymbol{l}}|$ are less than $\hbar\omega_D$. Furthermore, we replace the interaction in this region with a constant, i.e., $V_{\text{eff}}(\boldsymbol{k} - \boldsymbol{l}) = -g\,\Theta(\hbar\omega_D - |\xi_{\boldsymbol{k}}|)\,\Theta(\hbar\omega_D - |\xi_{\boldsymbol{l}}|)/\Omega$, $g > 0$.[12] It is easy to see that for this model, the self-consistency

---

[11] We have thus $T_{\boldsymbol{k}} = \begin{pmatrix} u^*_{\boldsymbol{k}} & v_{\boldsymbol{k}} \\ -v^*_{\boldsymbol{k}} & u_{\boldsymbol{k}} \end{pmatrix}$. The unitarity of T is guaranteed by (5.44).

[12] These assumptions are based on the work of BCS: we expect that the solution of the self-consistency equation does not depend on the specific form of the potential, but only on the typical strength $-g$ and the cutoff energy $\hbar\omega_D$.

equation is solved by $\Delta_{\boldsymbol{k}} = \Delta\,\Theta(\hbar\omega_D - |\xi_{\boldsymbol{k}}|)$. Substituting the ansätze for $\Delta_{\boldsymbol{k}}$ and V_{eff} into the self-consistency equation and canceling the common factor $\Delta \neq 0$, we obtain[13]

$$\begin{aligned} 1 &= \frac{g}{2\Omega} \sum_{\substack{\boldsymbol{k} \\ |\xi_{\boldsymbol{k}}|<\hbar\omega_D}} \frac{1}{E_{\boldsymbol{k}}} = \frac{g}{2} \overbrace{\int_{|\xi|<\hbar\omega_D} d\xi \frac{\rho(\xi)}{\sqrt{|\Delta|^2+\xi^2}}}^{\approx \rho_0 \int_{|\xi|<\hbar\omega_D} d\xi (\xi^2+|\Delta|^2)^{-1/2}} \\ &\approx g\rho_0 \,\operatorname{arsinh}(\hbar\omega_D/|\Delta|); \end{aligned} \tag{5.60}$$

here, $\rho_0 = \rho(0)$ denotes the density of states at the Fermi edge, which we have assumed to be constant over the small integration range $\simeq \omega_D \ll \varepsilon_F$. Solving for $|\Delta|$ yields the final result

$$|\Delta| = \frac{\hbar\omega_D}{\sinh(1/\rho_0 g)} \approx 2\hbar\omega_D e^{-1/\rho_0 g} \tag{5.61}$$

where we have used in the last step that the system is typically weakly coupled with $\rho_0 g \simeq 0.3$. Equation (5.61) confirms Cooper's result that any arbitrarily weak attractive potential pairs electrons and thus creates a finite energy gap.

5.2.5 Condensation energy

The transition into the superconducting phase is accompanied by a lowering of the ground state energy, which is referred to as condensation energy in analogy to the gas-liquid transition. Using the expression for E_g from (5.58) and $\sum_{\boldsymbol{k}} b_{\boldsymbol{k}} = |\Delta|\Omega/g$, one obtains the condensation energy density

$$\begin{aligned} u_{\text{kond}} &= \frac{1}{\Omega}[E_g(\Delta) - E_g(\Delta = 0)] \\ &= \frac{1}{\Omega} \sum_{|\boldsymbol{k}|\geq k_F} (\xi_{\boldsymbol{k}} - E_{\boldsymbol{k}}) + \frac{1}{\Omega} \sum_{|\boldsymbol{k}|\leq k_F} (\overbrace{-\xi_{\boldsymbol{k}}}^{|\xi_{\boldsymbol{k}}|} - E_{\boldsymbol{k}}) + \overbrace{\frac{|\Delta|^2}{g}}^{\rho_0 \int_0^{\hbar\omega_D} d\xi \frac{|\Delta|^2}{\sqrt{|\Delta|^2+\xi^2}}} \\ &\approx 2\rho_0 \int_0^{\hbar\omega_D} d\xi \left(\xi - \sqrt{|\Delta|^2+\xi^2} + \frac{|\Delta|^2}{2\sqrt{|\Delta|^2+\xi^2}} \right) \\ &= \rho_0 \int_0^{\hbar\omega_D} d\xi \, \frac{2\xi\sqrt{|\Delta|^2+\xi^2} - 2\xi^2 - 1}{\sqrt{|\Delta|^2+\xi^2}} \\ &= \rho_0 \xi \left(\xi - \sqrt{|\Delta|^2+\xi^2} \right) \Big|_{\xi=0}^{\hbar\omega_D} \\ &\overset{\hbar\omega_D \gg |\Delta|}{\approx} -\tfrac{1}{2}\rho_0 |\Delta|^2. \end{aligned} \tag{5.62}$$

---

[13] The density of states is defined as $\rho(\xi) = \sum_{\boldsymbol{k}} \delta(\xi - \xi_{\boldsymbol{k}})$. Thus, for a general function $f(x)$, we have $\sum_{\boldsymbol{k}} f(\xi_{\boldsymbol{k}}) = \int d\xi \, \rho(\xi) f(\xi)$.

5.2.6 Density of states

We have seen that the fermionic quasiparticles $\beta^\dagger_{\boldsymbol{k}}$, which describe the excitations above the superconducting ground state, are in a one-to-one correspondence with the electron excitations $c^\dagger_{\boldsymbol{k}}$ in the metal. This insight allows us to relate the density of states of the Bogoliubov quasiparticles $\rho_s(E)$ to the density of states ρ_0 in the normal state, $\rho_s(E) = \sum_{\boldsymbol{k}} \delta(E - E_{\boldsymbol{k}}) = (d\xi/dE) \sum_{\boldsymbol{k}} \delta(\xi - \xi_{\boldsymbol{k}}) = (d\xi/dE)\rho_0$. This leads to the simple result (the quasiparticle excitations satisfy the spectrum $E = \sqrt{|\Delta|^2 + \xi^2}$)

$$\frac{\rho_s(E)}{\rho_0} = \frac{d\xi}{dE} = \begin{cases} \frac{E}{\sqrt{E^2 - |\Delta|^2}} & E > |\Delta|, \\ 0 & E < |\Delta|, \end{cases} \tag{5.63}$$

with a diverging density of states above the energy gap. Note that due to the aforementioned relationship between the excitations in the superconducting and normal conducting states, the integrated density of states is the same. Upon entering the superconducting state, the states with energy below the energy gap are simply transferred over the energy gap, leading to the divergence.

5.2.7 Derivation of the London equations

With the BCS equation and its solution, we have seen that an attractive electron-electron potential leads to an energy gap, thereby lowering the total energy of the system by the condensation energy. However, it is not yet clear that the new state with $|\Delta| > 0$ is indeed a superconducting state. We have already seen that the London equations provide a phenomenological description (Meissner-Ochsenfeld effect, perfect conductivity) of a superconductor. We will now show that the response of the quasiparticles in BCS to an external magnetic field leads exactly to the London equation, confirming that the state is indeed a superconductor.

We describe the constant magnetic field $\boldsymbol{H}$ by a vector potential $\boldsymbol{A}$ with $\boldsymbol{H} = \boldsymbol{\nabla} \times \boldsymbol{A}$. We choose the London gauge $\boldsymbol{\nabla} \cdot \boldsymbol{A} = 0$. The magnetic field shifts the canonical momentum, so that the kinetic term takes the form $(\boldsymbol{p} + e\boldsymbol{A}/c)^2/2m$, neglecting effects due to the Zeeman term. To first order in $\boldsymbol{A}$, this leads to the perturbation term[14]

$$\begin{aligned} H_A &= \frac{e}{mc} \int d^3r \sum_\sigma \Psi^\dagger_\sigma(\boldsymbol{r}) \boldsymbol{A} \cdot \boldsymbol{p} \Psi_\sigma(\boldsymbol{r}) = \frac{e\hbar}{mc} \sum_{\boldsymbol{k}\sigma} \boldsymbol{A} \cdot \boldsymbol{k}\, c^\dagger_{\boldsymbol{k}\sigma} c_{\boldsymbol{k}\sigma} \\ &= \frac{e\hbar}{mc} \sum_{\boldsymbol{k}\sigma} \boldsymbol{A} \cdot \boldsymbol{k}\, \beta^\dagger_{\boldsymbol{k}\sigma} \beta_{\boldsymbol{k}\sigma}. \end{aligned} \tag{5.64}$$

In the next step, we want to calculate the current density $\boldsymbol{j} = -ne\boldsymbol{v} = \langle \boldsymbol{j}_p \rangle + \langle \boldsymbol{j}_A \rangle$. The two terms $\boldsymbol{j}_p$ and $\boldsymbol{j}_A$ denote the paramagnetic and diamagnetic current density

---

[14] We use that $c^\dagger_{\boldsymbol{k}\uparrow} c_{\boldsymbol{k}\uparrow} - c^\dagger_{-\boldsymbol{k}\downarrow} c_{-\boldsymbol{k}\downarrow} = (u_{\boldsymbol{k}} \beta^\dagger_{\boldsymbol{k}\uparrow} + v^*_{\boldsymbol{k}} \beta_{-\boldsymbol{k}\downarrow})(u^*_{\boldsymbol{k}} \beta_{\boldsymbol{k}\uparrow} + v_{\boldsymbol{k}} \beta^\dagger_{-\boldsymbol{k}\downarrow}) - (-v^*_{\boldsymbol{k}} \beta_{\boldsymbol{k}\uparrow} + u_{\boldsymbol{k}} \beta^\dagger_{-\boldsymbol{k}\downarrow})(-v_{\boldsymbol{k}} \beta^\dagger_{\boldsymbol{k}\uparrow} + u^*_{\boldsymbol{k}} \beta_{-\boldsymbol{k}\downarrow}) = \beta^\dagger_{\boldsymbol{k}\uparrow} \beta_{\boldsymbol{k}\uparrow} - \beta^\dagger_{-\boldsymbol{k}\downarrow} \beta_{-\boldsymbol{k}\downarrow}$.

operators, respectively, according to the expression $\boldsymbol{v} = \boldsymbol{p}/m + e\boldsymbol{A}/mc$ for the velocity of the particles. The diamagnetic current gives the simple result

$$\langle \boldsymbol{j}_A \rangle = -\frac{e^2\boldsymbol{A}}{mc}\frac{1}{\Omega}\underbrace{\left\langle \sum_{\boldsymbol{k}\sigma} c^\dagger_{\boldsymbol{k}\sigma} c_{\boldsymbol{k}\sigma} \right\rangle}_{N} = -\frac{ne^2}{mc}\boldsymbol{A}, \tag{5.65}$$

which corresponds exactly to the London equation as long as we interpret n as the superconducting particle density n_s. However, in equation (5.65), n is always the total particle density.

To obtain the total current $\boldsymbol{j}$, we still need to determine the paramagnetic contribution to the current density $\langle \boldsymbol{j}_p \rangle$ with the current operator

$$\boldsymbol{j}_p = -\frac{e\hbar}{m}\frac{1}{\Omega}\sum_{\boldsymbol{k}\sigma} \boldsymbol{k} c^\dagger_{\boldsymbol{k}\sigma} c_{\boldsymbol{k}\sigma} = -\frac{e\hbar}{m}\frac{1}{\Omega}\sum_{\boldsymbol{k}\sigma} \boldsymbol{k}\, \beta^\dagger_{\boldsymbol{k}\sigma} \beta_{\boldsymbol{k}\sigma}. \tag{5.66}$$

The perturbation term H_A shifts the energy of the particles with momentum $\boldsymbol{k}$ by $e\hbar\boldsymbol{A}\cdot\boldsymbol{k}/mc$. At $T = 0$, all states with negative energy are occupied, and we obtain

$$\begin{aligned}\langle \beta^\dagger_{\boldsymbol{k}\uparrow}\beta_{\boldsymbol{k}\uparrow}\rangle - \langle \beta^\dagger_{-\boldsymbol{k}\downarrow}\beta_{-\boldsymbol{k}\downarrow}\rangle &= \Theta(-E_{\boldsymbol{k}} - e\hbar\boldsymbol{A}\cdot\boldsymbol{k}/mc) - \Theta(-E_{\boldsymbol{k}} + e\hbar\boldsymbol{A}\cdot\boldsymbol{k}/mc)\\ &= -\frac{2e\hbar\boldsymbol{A}\cdot\boldsymbol{k}}{mc}\delta(E_{\boldsymbol{k}}) \end{aligned} \tag{5.67}$$

to first order in $\boldsymbol{A}$. Substituting this result into equation (5.64) yields

$$\begin{aligned}\langle \boldsymbol{j}_p \rangle &= \frac{2e^2\hbar^2}{m^2c}\overbrace{\int \frac{d^3k}{(2\pi)^3}\delta(E_{\boldsymbol{k}})}^{\rho_s(0)\langle\cdot\rangle_{S^2}}\overbrace{(\boldsymbol{A}\cdot\boldsymbol{k})}^{\propto\cos\theta}\overbrace{\boldsymbol{k}}^{\propto\cos\theta}\\ &= \frac{2e^2\hbar^2}{m^2c}\rho_s(0)k_F^2\underbrace{\langle\cos^2\theta\rangle_{S^2}}_{1/3}\boldsymbol{A} = \frac{ne^2}{mc}\underbrace{\frac{4\varepsilon_F\rho_s(0)}{3n}}_{\rho_s(0)/\rho_0}\boldsymbol{A}\end{aligned} \tag{5.68}$$

where θ is the angle between $\boldsymbol{k}$ and $\boldsymbol{A}$ and $\langle\cdot\rangle_{S^2}$ denotes the average over the unit sphere. The sum of the paramagnetic and diamagnetic terms yields the final result

$$\boldsymbol{j} = -\frac{n_s e^2}{mc}\boldsymbol{A} \tag{5.69}$$

with the superfluid density

$$n_s = n[1 - \rho_s(0)/\rho_0] = \begin{cases} n & |\Delta| > 0, \\ 0 & \Delta = 0. \end{cases} \tag{5.70}$$

For finite temperatures, the tail of the Fermi-Dirac distribution leads to $n_s = n(1 - e^{-|\Delta|/k_BT})$ as long as $|\Delta| \gg k_BT$. The phase transition occurs precisely at the point where $n_s = 0$.

Note that in the normal state, there is no Meissner-Ochsenfeld effect at all, as the paramagnetic and diamagnetic currents exactly cancel each other. The origin of the paramagnetic response in the normal conductor lies in the fact that a vector potential $\boldsymbol{A}$ causes the Fermi sphere in momentum space to shift, leading to a non-vanishing $\langle \boldsymbol{p} \rangle$. For the superconductor, the particles are condensed in the state with $\langle \boldsymbol{p} \rangle = 0$. At the Fermi surface, there are also no quasiparticles present that could respond to an applied magnetic field, so that the pure diamagnetic response, which is always present, remains.

Chapter 6

Relativistic Particles: Dirac Equation

The quantum mechanics we have dealt with so far is based on non-relativistic mechanics and can be motivated using the correspondence principle. With this, we were able to successfully explain an important part of quantum physics. Interesting and fundamentally new perspectives arise when we incorporate special relativity into our formulation of quantum mechanics. The relativistic extension of quantum mechanics is the foundation of high-energy physics.

6.1 Klein-Gordon Equation

Non-relativistic mechanics and quantum mechanics are invariant under Galilean transformations between inertial systems,

$$\boldsymbol{x} \mapsto \boldsymbol{x}' = \boldsymbol{x} - \boldsymbol{v}t \qquad \text{and} \qquad t \mapsto t' = t, \tag{6.1}$$

where $\boldsymbol{v}$ is the relative velocity. Energy and momentum are related by the equation $E = p^2/2m$, so that the Galilean transformation leads to

$$\boldsymbol{p} \mapsto \boldsymbol{p}' = \boldsymbol{p} - m\boldsymbol{v} \qquad \text{and} \qquad E \mapsto E' = E - \boldsymbol{p}\cdot\boldsymbol{v} + \tfrac{1}{2}mv^2 = \frac{p'^2}{2m} \tag{6.2}$$

i.e., the energy is form-invariant under Galilean transformations. The correspondence principle states that

$$E \mapsto i\hbar\partial_t \qquad \text{and} \qquad \boldsymbol{p} = -i\hbar\boldsymbol{\nabla}. \tag{6.3}$$

The Galilean-invariant relationship between momentum and energy yields the Schrödinger equation

$$i\hbar\partial_t\psi = -\frac{\hbar^2}{2m}\nabla^2\psi, \tag{6.4}$$

which has been our fundamental equation so far.

Relativistic mechanics is no longer Galilean but Lorentz-invariant. A Lorentz transformation from $(t, \boldsymbol{x})$ to $(t', \boldsymbol{x}')$ leaves the length[1] $x_\mu x^\mu = c^2t^2 - x^2 = x'_\mu x'^\mu$ of the four-vector $x^\mu = (ct, \boldsymbol{x})$ invariant. The covariant vector x_μ is obtained from the covariant vector x^μ and the Lorentz metric

$$(g_{\mu\nu}) = (g^{\mu\nu}) = \begin{pmatrix} 1 & & & \\ & -1 & & \\ & & -1 & \\ & & & -1 \end{pmatrix}. \tag{6.5}$$

Energy and momentum are also combined into a four-vector in special relativity $p^\mu = (E/c, \boldsymbol{p})$, with the invariant length

$$p_\mu p^\mu = p'_\mu p'^\mu = m^2c^2. \tag{6.6}$$

This is the invariant energy-momentum relationship, which we can use to derive relativistic quantum mechanics with the correspondence principle. First, we replace p^μ with a differential operator

$$p_\mu = i\hbar\partial_\mu. \tag{6.7}$$

The first attempt yields the Hamilton operator $H = \sqrt{m^2c^4 + p^2c^2}$, with the wave equation

$$i\hbar\partial_t\psi = mc^2(1 - \lambda_C^2\nabla)^{1/2}\psi \tag{6.8}$$

with the Compton wavelength $\lambda_C = \hbar/mc = \alpha a_B \approx 3.8 \times 10^{-11}$ cm. However, this approach raises serious problems. First, space and time are treated differently, and both do not appear obviously as a covariant four-vector. Another problem is the square root, as we must develop the derivative $\boldsymbol{\nabla}$ to infinite order. This means that the equation describes a non-local theory. This violates causality, as the right side of the equation links the point $\boldsymbol{x}$ through the derivative with points (instantaneously) that lie outside the causal light cone. For these reasons, the above approach must be discarded. The problem of covariance and non-locality is solved at once when we start from the square of the energy, i.e., $H^2 = m^2c^4 + p^2c^2$ with the Klein-Gordon equation

$$-\hbar\partial_t^2\psi = (-\hbar^2c^2\nabla^2 + m^2c^4)\psi \quad \mapsto \quad (\partial_\mu\partial^\mu + \lambda_C^{-2})\psi = 0. \tag{6.9}$$

A further analysis of the Klein-Gordon equation shows that although causality is guaranteed, the equation still has ‘problems’ since the Hamilton operator is not positive definite and there is also no positive definite conserved quantity (particle density). However, this is not really a problem, as one can interpret this fact such that the density corresponds to a charge density $e\rho$, and therefore particles of positive and

---

[1] In this chapter, we used Einstein’s summation convention, which states that summation is performed over repeated indices.

negative energy have different charges. Thus, the continuity equation holds for charge density but not for particle density. The Klein-Gordon equation introduces a new aspect into quantum mechanics, which first manifests itself through the breakdown of single-particle theory. In quantum mechanical processes, the number of particles can change while the total charge remains conserved. This announces the concept that for every particle, there exists a corresponding antiparticle that has the charge and energy with the opposite sign. In fact, the Klein-Gordon equation is suitable for describing bosonic particles, such as the π mesons, where particles and antiparticles are equivalent.

6.2 Dirac Equation

The simplest relativistic equation we have constructed so far, the Klein-Gordon equation, has the following properties: it is

- scalar,
- covariant,
- of 2^{nd} order in time,
- and has a non-positive definite norm, which means that the Hamiltonian H is not Hermitian.

Next, we raise our ambitions and try to construct a theory based on a Hamilton operator with the following properties: the Hamilton operator

- may be tensorial,[2]
- should be covariant,
- should be of 1^{st} order in time,
- should lead to a positive definite norm so that we obtain a Hermitian Hamilton operator H.

The most general Ansatz for a Hamilton operator with these properties (linear in ∂_t and covariant implies linearity in space, i.e., in $\boldsymbol{\nabla}$) has the form

$$i\hbar\partial_t\Psi \;=\; H\Psi = \left(c\boldsymbol{\alpha}\cdot\boldsymbol{p} + \beta mc^2\right)\Psi, \tag{6.10}$$

with Ψ a (Dirac) spinor with n components, $\boldsymbol{\alpha}$, β are $n\times n$ matrices, Hermitian and dimensionless; the momentum is defined as usual, $\boldsymbol{p} = -i\hbar\boldsymbol{\nabla}/\hbar$. Our task is to find n, $\boldsymbol{\alpha}$ and β such that (6.10) reproduces the usual relativistic dispersion

$$E^2 = p^2c^2 + m^2c^4. \tag{6.11}$$

---

[2] The restriction to a scalar theory produces no result.

To do this, we square the equation according to

$$\begin{aligned}
E^2\Psi \mapsto -\hbar^2\partial_t^2\Psi &= i\hbar\partial_t\left(c\boldsymbol{\alpha}\cdot\boldsymbol{p}+\beta mc^2\right)\Psi \\
&= \left(c\boldsymbol{\alpha}\cdot\boldsymbol{p}+\beta mc^2\right)i\hbar\partial_t\Psi \\
&= \left(c\boldsymbol{\alpha}\cdot\boldsymbol{p}+\beta mc^2\right)^2\Psi \\
&\overset{!}{=} \left(p^2c^2+m^2c^4\right)\Psi. \qquad (6.12)
\end{aligned}$$

Thus, it must hold

$$\left(c\alpha_i p^i+\beta mc^2\right)\left(c\alpha_j p^j+\beta mc^2\right) = \underbrace{c^2\alpha_i^2(p^i)^2}_{c^2p^2} \qquad (6.13)$$

$$+\underbrace{\beta^2m^2c^4}_{m^2c^4}+\underbrace{\left(\alpha_i\beta+\beta\alpha_i\right)p^imc^3}_{0}+\underbrace{\frac{1}{2}\left(\alpha_i\alpha_j+\alpha_j\alpha_i\right)_{i\neq j}p^ip^jc^2}_{0}$$

Thus, we obtain the conditions

$$\alpha_i^2 = I_n, \qquad \beta^2 = I_n, \qquad (6.14)$$

$$\{\alpha_i,\beta\} = 0, \qquad \{\alpha_i,\alpha_j\}_{i\neq j} = 0, \qquad (6.15)$$

where $\{\cdot,\cdot\}$ denotes the anticommutator as usual. We thus need four Hermitian, anticommuting matrices whose squares yield I_n. It turns out that these conditions can only be satisfied if $n \geq 4$. To prove this, one notes that

1. The anticommutator $\{\alpha_i,\beta\}=0$ implies that $\beta\alpha_i\beta=-\alpha_i$ and thus $\operatorname{tr}\alpha_i = -\operatorname{tr}[\beta\alpha_i\beta] = -\operatorname{tr}[\beta^2\alpha_i] = -\operatorname{tr}\alpha_i$ and thus $\operatorname{tr}\alpha_i = 0$. Similarly, from $\alpha_i\beta\alpha_i = -\beta$, it follows that $\operatorname{tr}\beta = 0$, so all four matrices α_i, β are traceless.
2. The four matrices α_i and β have eigenvalues ±1, since α_i,β are supposed to be Hermitian, thus also diagonalizable; since $\alpha_i^2=\beta^2=I_n$, the squares of the eigenvalues must equal 1.
3. n must be even, $n = 2m$, with $m \in \mathbb{N}$, since with $\operatorname{tr}\alpha_i = 0, \operatorname{tr}\beta = 0$, the eigenvalues 1 and -1 must occur in pairs.
4. Finally, $n > 2$ must hold, since a Hermitian matrix has a real main diagonal and complex conjugate elements symmetrically placed with respect to the main diagonal, thus we find the following number of degrees of freedom

$$\underbrace{n}_{\text{real HD}}+\underbrace{2}_{\text{complex}}\cdot\underbrace{(n^2-n)}_{\text{offdiag.}}\underbrace{/\ 2}_{\text{symm.}} = n^2; \qquad (6.16)$$

additionally, tr $= 0$ and n^2-1 degrees of freedom remain. For $n = 2$, we can find three independent Hermitian matrices like the Pauli matrices σ_i,

$$\left[\begin{pmatrix}0&1\\1&0\end{pmatrix},\begin{pmatrix}0&-i\\i&0\end{pmatrix},\begin{pmatrix}1&0\\0&-1\end{pmatrix}\right] = [\sigma_1,\sigma_2,\sigma_3] \ = \ \boldsymbol{\sigma}. \qquad (6.17)$$

with $\sigma_i^2 = I_2$ and the commutation relations $\sigma_i\sigma_j + \sigma_j\sigma_i = 0$.

For $n = 4$, we find 15 independent matrices with trace 0; from these, we choose the matrices,

$$\begin{aligned}
\beta &= \begin{pmatrix} 1 & 0 & 0 & 0 \\ 0 & 1 & 0 & 0 \\ 0 & 0 & -1 & 0 \\ 0 & 0 & 0 & -1 \end{pmatrix} = \begin{pmatrix} I_2 & 0 \\ 0 & -I_2 \end{pmatrix}; \\
\alpha_1 &= \begin{pmatrix} 0 & 0 & 0 & 1 \\ 0 & 0 & 1 & 0 \\ 0 & 1 & 0 & 0 \\ 1 & 0 & 0 & 0 \end{pmatrix} = \begin{pmatrix} 0 & \sigma_1 \\ \sigma_1 & 0 \end{pmatrix}; \\
\alpha_2 &= \begin{pmatrix} 0 & 0 & 0 & -i \\ 0 & 0 & i & 0 \\ 0 & -i & 0 & 0 \\ i & 0 & 0 & 0 \end{pmatrix} = \begin{pmatrix} 0 & \sigma_2 \\ \sigma_2 & 0 \end{pmatrix}; \\
\alpha_3 &= \begin{pmatrix} 0 & 0 & 1 & 0 \\ 0 & 0 & 0 & -1 \\ 1 & 0 & 0 & 0 \\ 0 & -1 & 0 & 0 \end{pmatrix} = \begin{pmatrix} 0 & \sigma_3 \\ \sigma_3 & 0 \end{pmatrix};
\end{aligned} \tag{6.18}$$

with the required properties $\beta^2 = \alpha_i^2 = I_4$ and $\{\alpha_i, \alpha_j\} = 0$, $\{\alpha_i, \beta\} = 0$.

Thus, we obtain the Dirac equation in the form

$$i\hbar\partial_t\Psi = \left(-i\hbar c\alpha_i\partial_{x_i} + \beta mc^2\right)\Psi, \tag{6.19}$$

with the Dirac 4th spinor

$$\Psi = \begin{pmatrix} \Psi_i \\ \vdots \\ \Psi_4 \end{pmatrix} = \begin{pmatrix} \chi \\ \eta \end{pmatrix}, \tag{6.20}$$

and the 2nd spinors χ and η.

The covariant form of the Dirac equation is obtained by multiplying (6.19) by β and defining the Dirac matrices

$$\begin{aligned}
\gamma^\mu &= \left(\beta, \beta\alpha^i\right), \\
\gamma^0 &= \begin{pmatrix} I_2 & 0 \\ 0 & -I_2 \end{pmatrix}, \\
\gamma^i &= \begin{pmatrix} 0 & \sigma_i \\ -\sigma_i & 0 \end{pmatrix},
\end{aligned} \tag{6.21}$$

the Dirac matrices are characterized by the following anticommutators [3],

$$\{\gamma^\mu, \gamma^\nu\} = 2g^{\mu\nu} I_n, \tag{6.22}$$

with $g^{\mu\nu}$ being the metric tensor. From (6.19) we then obtain (we again set $\hbar = c = 1$ for covariant formulas; it is $\partial_\mu = \partial_{x^\mu}$)

$$\left(i\gamma^\mu \partial_\mu - m\right) \Psi(x) = 0. \tag{6.23}$$

We use Einstein's summation convention and introduce the notation of the 'slash' operator, $\not{a} \; = \; \gamma^\mu a_\mu$; thus (6.23) simplifies to

$$\left(i\not{\partial}_x - m\right) \Psi(x) = 0. \tag{6.24}$$

(6.24) is covariant if Ψ transforms under Lorentz transformations such that the identical equation holds in the new system. This condition defines the behavior of $\Psi \in \mathcal{H}$ (the Hilbert space of states) under Lorentz transformations and thus defines a 4-dimensional representation of the Lorentz group in $\mathcal{H}$: For $\Lambda \in \mathcal{L}$ a Lorentz transformation, there exists a representation matrix $S(\Lambda)$ such that

$$\begin{aligned} \Psi'(x') &= S(\Lambda)\Psi(x), \\ x' &= \Lambda x, \end{aligned} \tag{6.25}$$

the wave function in the new (primed) coordinate system. Covariance then requires that

$$\left(i\gamma^\mu \partial'_\mu - m\right) \Psi'(x') = 0 \tag{6.26}$$

is satisfied. (6.26) establishes the representation $S(\Lambda)$ of the Lorentz group: With

$$\begin{aligned} x'^\mu &= \Lambda^\mu{}_\nu \, x^\nu \\ \partial'_\mu &= \left(\Lambda^{-1}\right)^\nu{}_\mu \, \partial_\nu \end{aligned} \tag{6.27}$$

and

$$S^{-1}\left(\Lambda\right) \big(i\gamma^\mu \left(\Lambda^{-1}\right)^\nu{}_\mu \partial_\nu - m\big\} \, S\left(\Lambda\right) \Psi(x) \overset{!}{=} \left(i\gamma^\mu \partial_\mu - m\right) \Psi = 0.$$

$S(\Lambda)$ must satisfy the following conditions,

$$\begin{aligned} \left(\Lambda^{-1}\right)^\nu{}_\mu S^{-1}\left(\Lambda\right) \gamma^\mu S\left(\Lambda\right) &= \gamma^\nu, \\ \Rightarrow \quad S^{-1}\left(\Lambda\right) \gamma^\mu S\left(\Lambda\right) &= \Lambda^\mu{}_\nu \gamma^\nu. \end{aligned} \tag{6.28}$$

Using (6.28), we can determine the representation $S(\Lambda)$. We present the final result here without proof. An infinitesimal Lorentz transformation is characterized by $\epsilon^\mu{}_\nu$ with $\Lambda^\mu{}_\nu = \delta^\mu{}_\nu + \epsilon^\mu{}_\nu$. Multiplying this relation by $g^{\mu\lambda}$ gives us

$$\Lambda^{\mu\lambda} = g^{\mu\lambda} + \epsilon^{\mu\lambda}. \tag{6.29}$$

---

[3] A set γ^ν of Dirac matrices is consistent if (6.19) is satisfied.

A Lorentz transformation is characterized by leaving the metric invariant, i.e., $g_{\mu\nu} = \Lambda^{\sigma}{}_{\mu} g_{\sigma\tau} \Lambda^{\tau}{}_{\nu}$ or in matrix notation $g = \Lambda^T g \Lambda$. This leads to the following condition for the infinitesimal transformation,

$$g_{\mu\nu} = g_{\mu\nu} + \epsilon^{\sigma}{}_{\mu} g_{\sigma\nu} + g_{\mu\tau}\epsilon^{\tau}{}_{\nu} + O(\epsilon^2) \quad \Rightarrow \quad 0 = \epsilon^{\sigma}{}_{\mu} g_{\sigma\nu} + g_{\mu\tau}\epsilon^{\tau}{}_{\nu}. \tag{6.30}$$

Raising the indices μ and ν leads to the relation $0 = \epsilon^{\nu\mu} + \epsilon^{\mu\nu}$, i.e., ϵ is an antisymmetric tensor in μ and ν. The Lorentz transformation corresponding to Λ is given by

$$S(\epsilon^{\mu\nu}) = I_n - \frac{i}{4}\sigma_{\mu\nu}\epsilon^{\mu\nu} \tag{6.31}$$

with

$$\sigma_{\mu\nu} = \frac{i}{2}(\gamma_\mu\gamma_\nu - \gamma_\nu\gamma_\mu) = \frac{i}{2}[\gamma_\mu, \gamma_\nu]. \tag{6.32}$$

Substituting into (6.28) yields[4]

$$S^{-1}(\epsilon^{\nu\lambda})\gamma^\mu S(\epsilon^{\nu\lambda}) = \gamma^\mu + \frac{i}{4}[\sigma_{\nu\lambda}, \gamma^\mu]\epsilon^{\nu\lambda} + O(\epsilon^2). \tag{6.33}$$

To show the covariance of the Dirac equation, we need

$$\begin{aligned}\frac{2}{i}[\sigma^{\nu\lambda}, \gamma^\mu] &= [\overbrace{[\gamma^\nu, \gamma^\lambda]}^{-2g^{\nu\lambda} + 2\gamma^\nu\gamma^\lambda}, \gamma^\mu] = 2[\gamma^\nu\gamma^\lambda, \gamma^\mu] = 2\gamma^\nu\{\gamma^\lambda, \gamma^\mu\} - 2\{\gamma^\nu, \gamma^\mu\}\gamma^\lambda \\ &= 4g^{\lambda\mu}\gamma^\nu - 4g^{\nu\mu}\gamma^\lambda. \end{aligned}\tag{6.34}$$

We use this result in (6.33) and obtain

$$\begin{aligned}S^{-1}(\epsilon^{\nu\lambda})\gamma^\mu S(\epsilon^{\nu\lambda}) &= \gamma^\mu + \frac{i}{4}[\sigma_{\nu\lambda}, \gamma^\mu]\epsilon^{\nu\lambda} = \gamma^\mu - \frac{1}{2}(\gamma_\nu\epsilon^{\nu\mu} - \gamma_\lambda\epsilon^{\mu\lambda}) \\ &= (\delta^\mu{}_\nu + \epsilon^\mu{}_\nu)\gamma^\nu = \Lambda^\mu{}_\nu\gamma^\nu. \end{aligned}\tag{6.35}$$

Thus, it is shown that the S in (6.31) satisfies the condition (6.28) and the Dirac equation is Lorentz-invariant with this choice.

It is important to recognize that the transformation matrix $S(\epsilon^{\mu\nu})$ is not unitary. From the fact that γ^μ is Hermitian for $\mu = 0$ and anti-Hermitian otherwise, it follows that $\gamma^0(\gamma^\mu)^\dagger\gamma^0 = \gamma^\mu$ and thus

$$\gamma^0(\sigma^{\mu\nu})^\dagger\gamma^0 = -\frac{i}{2}\gamma^0[(\gamma^\nu)^\dagger, (\gamma^\mu)^\dagger]\gamma^0 = \frac{i}{2}[\gamma^0(\gamma^\mu)^\dagger\gamma^0, \gamma^0(\gamma^\nu)^\dagger\gamma^0] = \sigma^{\mu\nu}.$$

With this relation, we obtain the generalized unitarity relation (up to first order in ϵ)

$$\begin{aligned}S^\dagger(\epsilon^{\mu\nu})\gamma^0 S(\epsilon^{\mu\nu}) &= (I_n + \frac{i}{4}\sigma^\dagger_{\mu\nu}\epsilon^{\mu\nu})\gamma^0(I_n - \frac{i}{4}\sigma_{\mu\nu}\epsilon^{\mu\nu}) \\ &= \gamma^0 + \frac{i}{4}\underbrace{\sigma^\dagger_{\mu\nu}\gamma^0}_{\gamma^0\sigma^{\mu\nu}}\epsilon^{\mu\nu} - \frac{i}{4}\gamma^0\sigma_{\mu\nu}\epsilon^{\mu\nu} = \gamma^0 \end{aligned}\tag{6.36}$$

---

[4] Note that for an infinitesimal transformation $S^{-1}(\epsilon^{\mu\nu}) = S(-\epsilon^{\mu\nu})$, since $S^{-1}(\epsilon^{\mu\nu})S(\epsilon^{\mu\nu}) = (I_n + \frac{i}{4}\sigma_{\mu\nu}\epsilon^{\mu\nu})(I_n - \frac{i}{4}\sigma_{\mu\nu}\epsilon^{\mu\nu}) = I_n + O(\epsilon^2)$.

or, alternatively written, $\gamma^0 S^\dagger \gamma^0 = S^{-1}$.

Finally, we want to consider the electromagnetic interaction, which we achieve through the substitution

$$-i\hbar\,\partial^\mu = p^\mu \to p^\mu - eA^\mu \tag{6.37}$$

leading to

$$i\hbar\partial_t\Psi \;=\; H\Psi = \left[c\alpha_i\left(-i\hbar\partial_{x_i} - eA_i/c\right) + e\phi + \beta mc^2\right]\Psi, \tag{6.38}$$

or in covariant notation with $\hbar = c = 1$,

$$\left[\gamma^\mu\left(i\partial_\mu - eA_\mu\right) - m\right]\Psi(x) = 0. \tag{6.39}$$

6.3 Conserved Norm

Let Ψ_a and Ψ_b be solutions of the Dirac equation, which we multiply with the corresponding spinor as follows,

$$\begin{aligned} \Psi_a^\dagger \cdot \left(i\hbar\partial_t\Psi_b = H\Psi_b\right), \\ \left(-i\hbar\partial_t\Psi_a^\dagger = (H\Psi_a)^\dagger\right)\cdot\Psi_b. \end{aligned} \tag{6.40}$$

Subtracting the two equations yields

$$\begin{aligned} i\hbar\partial_t(\Psi_a^\dagger\Psi_b) &= \Psi_a^\dagger H\Psi_b - (H\Psi_a)^\dagger\Psi_b \\ &= \frac{\hbar}{i}\,\alpha_i\Psi_a^\dagger(\overrightarrow{\partial}_{x_i} + \overleftarrow{\partial}_{x_i})\Psi_b \\ &= \frac{\hbar}{i}\,\partial_{x_i}(\Psi_a^\dagger\,\alpha_i\Psi_b) \end{aligned} \tag{6.41}$$

and we obtain

$$\partial_t(\Psi_a^\dagger\Psi_b) + \partial_{x_i}(\Psi_a^\dagger\,\alpha_i\Psi_b) = 0, \tag{6.42}$$

or, after inserting ones considering $I_n = \beta^2 = \left(\gamma^0\right)^2$ and $\alpha_i = \beta\,\beta\alpha_i = \gamma^0\gamma^i$,

$$\partial_\mu\left(\overline{\Psi_a}\gamma^\mu\Psi_b\right) = 0; \tag{6.43}$$

here we have defined the Dirac adjoint

$$\overline{\Psi_a} \equiv \Psi_a^\dagger\gamma^0 \tag{6.44}$$

The integration over the spatial coordinates considering the boundary conditions ($\int d^3r\,\boldsymbol{\nabla}\cdot\boldsymbol{j} = \int d\sigma\,\boldsymbol{j}\cdot\boldsymbol{n} = 0$) gives us the conserved quantity

$$\begin{aligned} \text{const.} &= \int d^3r\;\overline{\Psi_a}\gamma^0\Psi_b \\ &= \int d^3r\;\Psi_a^\dagger\Psi_b \;=\; \langle\Psi_a,\Psi_b\rangle. \end{aligned} \tag{6.45}$$

(6.45) defines a norm, $\|\Psi\| = \langle\Psi,\Psi\rangle \geq 0$.

Note: The quantity $\Psi^\dagger\Psi = \overline{\Psi}\gamma^0\Psi$ is not a scalar under Lorentz transformations, but the 0th component of the 4th vector

$$\rho^\mu = \overline{\Psi}\gamma^\mu\Psi. \tag{6.46}$$

The density ρ^μ transforms like a 4th vector:

$$\begin{aligned}\rho'^\mu(x') &= \overline{\Psi'}(x')\gamma^\mu\Psi'(x')\\ &= \overline{\Psi}(x)\,\underbrace{S^{-1}(\Lambda)\gamma^\mu S(\Lambda)}_{(6.28)\to\Lambda^\mu_\nu\gamma^\nu}\,\Psi(x)\\ &= \Lambda^\mu_\nu\rho^\nu(x),\end{aligned} \tag{6.47}$$

where we have used that

$$\begin{aligned}\overline{\Psi'}(x') &= \Psi^{\dagger'}(x')\gamma^0 = \Psi^\dagger(x)S^\dagger\gamma^0\\ &= \underbrace{\Psi^\dagger(x)\gamma^0}\,\underbrace{\gamma^0 S^\dagger\gamma^0}\\ &= \quad\overline{\Psi}(x)\quad\;\; S^{-1}.\end{aligned} \tag{6.48}$$

6.4 Free Particles

We make the (block) Ansatz[5],

$$\Psi^{(\pm)}_{\boldsymbol{p}}(\boldsymbol{r};t) = N_p\, e^{i(\boldsymbol{p}\cdot\boldsymbol{r}\mp E_p t)/\hbar}\begin{pmatrix}\chi\\ \eta\end{pmatrix}, \tag{6.49}$$

with χ, η two 2nd spinors, the momentum $\boldsymbol{p} = \hbar\boldsymbol{k}$, $\boldsymbol{k} = 2\pi\boldsymbol{n}/L$ and $E_p > 0$. Substituting into the Dirac equation (6.19) yields

$$\pm E_p\begin{pmatrix}\chi\\ \eta\end{pmatrix} = \begin{pmatrix}mc^2 & c\boldsymbol{\sigma}\cdot\boldsymbol{p}\\ c\boldsymbol{\sigma}\cdot\boldsymbol{p} & -mc^2\end{pmatrix}\begin{pmatrix}\chi\\ \eta\end{pmatrix}. \tag{6.50}$$

The secular determinant is

$$(mc^2 \mp E_p)(-mc^2 \mp E_p) - c^2(\boldsymbol{\sigma}\cdot\boldsymbol{p})^2, \tag{6.51}$$

and we obtain solutions if the dispersion

$$E_p^2 = c^2p^2 + m^2c^4 \tag{6.52}$$

is satisfied, where we have used that $(\boldsymbol{\sigma}\cdot\boldsymbol{p})^2 = \sigma_i^2 p_i^2 + \{\sigma_i,\sigma_j\}p_ip_j/2 = \sigma_i^2\,p_i^2 = I_2\,p_i^2 = p^2$. For the eigenvectors, we obtain

$$\begin{aligned} + : \eta &= \left(\frac{c\boldsymbol{\sigma}\cdot\boldsymbol{p}}{E_p + mc^2}\right)\chi,\\ - : \chi &= -\left(\frac{c\boldsymbol{\sigma}\cdot\boldsymbol{p}}{E_p + mc^2}\right)\eta,\end{aligned} \tag{6.53}$$

---

[5] Despite the positive semi-definite norm $\|\cdot\| \geq 0$, we will find solutions with negative energies.

and with $\chi^\dagger\chi \equiv 1$, as well as $\eta^\dagger\eta \equiv 1$ we obtain for the normalization[6]

$$\begin{aligned}
\langle \Psi_{\boldsymbol{p}}^{(+)} \Psi_{\boldsymbol{p}}^{(+)} \rangle &= 1 = N_p^2 \Omega \chi^\dagger \left(1, \frac{c\boldsymbol{\sigma}\cdot\boldsymbol{p}}{E_p + mc^2}\right) \begin{pmatrix} 1 \\ \frac{c\boldsymbol{\sigma}\cdot\boldsymbol{p}}{E_p+mc^2} \end{pmatrix} \chi \\
&= N_p^2 \Omega \left(1 + \frac{c^2 p^2}{(E_p + mc^2)^2}\right) \\
&= N_p^2 \Omega \left(1 + \frac{E_p^2 - m^2 c^4}{(E_p + mc^2)^2}\right) \\
&= N_p^2 \Omega \frac{2E_p}{E_p + mc^2}
\end{aligned} \tag{6.54}$$

and the same result holds for $\Psi_{\boldsymbol{p}}^{(-)}$.

To simplify this cumbersome notation, we switch to the Dirac spinors.

6.4.1 Dirac Spinors

The free solutions of the Dirac theory can be expressed with the definition of the Dirac spinors

$$\begin{aligned}
u(\boldsymbol{p}, s) &\equiv \sqrt{E_p + mc^2} \begin{pmatrix} 1 \\ \dfrac{c\boldsymbol{\sigma}\cdot\boldsymbol{p}}{E_p + mc^2} \end{pmatrix} \chi^{(s)}, \\
v(\boldsymbol{p}, s) &\equiv \sqrt{E_p + mc^2} \begin{pmatrix} \dfrac{c\boldsymbol{\sigma}\cdot\boldsymbol{p}}{E_p + mc^2} \\ 1 \end{pmatrix} (-i\sigma_2 \chi^{(s)}),
\end{aligned} \tag{6.55}$$

simply expressed by

$$\begin{aligned}
\Psi_{\boldsymbol{p},s}^{(+)}(\boldsymbol{r}; t) &= \frac{1}{\sqrt{2E_p \Omega}}\, u(\boldsymbol{p}, s)\, e^{i(\boldsymbol{p}\cdot\boldsymbol{r} - E_p t)/\hbar}, \\
\Psi_{-\boldsymbol{p},-s}^{(-)}(\boldsymbol{r}; t) &= \frac{1}{\sqrt{2E_p \Omega}}\, v(\boldsymbol{p}, s)\, e^{-i(\boldsymbol{p}\cdot\boldsymbol{r} - E_p t)/\hbar}.
\end{aligned} \tag{6.56}$$

The 2nd spinor $\chi^{(s)}$ describes the spin of a spin-1/2 particle,

$$\begin{aligned}
\chi^{1/2} &= \begin{pmatrix} 1 \\ 0 \end{pmatrix}, \\
\chi^{-1/2} &= \begin{pmatrix} 0 \\ 1 \end{pmatrix};
\end{aligned} \tag{6.57}$$

---

[6] The result is not Lorentz-covariant, as $\|\cdot\|$ is not a scalar but the 0-component of a 4-vector.

similarly, $-i\sigma_2\chi^{(s)}$ describes a spin, but

$$\begin{aligned}
-i\sigma_2\chi^{(1/2)} = \eta^{(1/2)} &= \begin{pmatrix} 0 & -1 \\ 1 & 0 \end{pmatrix}\begin{pmatrix} 1 \\ 0 \end{pmatrix} = \begin{pmatrix} 0 \\ 1 \end{pmatrix}, \\
-i\sigma_2\chi^{(-1/2)} = \eta^{(-1/2)} &= \begin{pmatrix} -1 \\ 0 \end{pmatrix}, \qquad (6.58)
\end{aligned}$$

and $\eta^{(s)}$ describes a down (up)-spin for $s = 1/2$ $(= -1/2)$, just the opposite of $\chi^{(s)}$,

$$\chi^{(s)} \propto \eta^{(-s)}. \qquad (6.59)$$

6.5 Interpretation

The Dirac equation again has solutions with negative energy, see $\Psi^{(-)}_{-\boldsymbol{p},-s}$ in (6.56). In addition to the component structure $\binom{\chi}{\eta}$, which we also found for the Klein-Gordon equation and interpreted as a particle-antiparticle pair, the Dirac equation has a 2nd spinor structure in χ and η. We interpret this spinor structure as the spin state of a spin-1/2 particle. Thus, $\Psi^{(+)}_{\boldsymbol{p},s}$ describes a particle with momentum $\boldsymbol{p}$ and spin s, while the state $\Psi^{(-)}_{-\boldsymbol{p},-s}$ with momentum $-\boldsymbol{p}$ and spin $-s$ describes an antiparticle with momentum $\boldsymbol{p}$ and spin s. The states $\Psi^{(+)}$ and $\Psi^{(-)}$ are orthogonal, since

$$v^\dagger(-\boldsymbol{p}, s') \cdot u(\boldsymbol{p}, s) = u^\dagger(\boldsymbol{p}, s) \cdot v(-\boldsymbol{p}, s') = 0 \qquad (6.60)$$

and thus

$$\begin{aligned}
&\int d^3r\ \Psi^{(-)\dagger}_{\boldsymbol{p},-s'}\Psi^{(+)}_{\boldsymbol{p},s'} = \int \frac{d^3r}{2E_p\Omega}\, e^{-i(\boldsymbol{p}\cdot\boldsymbol{r}+E_pt)/\hbar} v^\dagger(-\boldsymbol{p}, s') \cdot u(\boldsymbol{p}, s)\, e^{i(\boldsymbol{p}\cdot\boldsymbol{r}-E_pt)/\hbar} \\
&= \frac{1}{2E_p}\, e^{-2iE_pt/\hbar}\, v^\dagger(-\boldsymbol{p}, s') \cdot u(\boldsymbol{p}, s) \\
&= \frac{E_p + mc^2}{2E_p}\, e^{-2iE_pt/\hbar}\, \eta^{(s')\dagger} \underbrace{\left(\frac{-c\boldsymbol{\sigma}\cdot\boldsymbol{p}}{E_p + mc^2}, 1\right)\begin{pmatrix} 1 \\ \dfrac{c\boldsymbol{\sigma}\cdot\boldsymbol{p}}{E_p + mc^2} \end{pmatrix}}_{0} \chi^{(s)}. \\
&= 0. \qquad (6.61)
\end{aligned}$$

Note that other combinations with $\boldsymbol{p} \neq \boldsymbol{p}'$ vanish due to $\int d^3r \cdots = 0$, but for $\Psi^{(-)\dagger}\Psi^{(+)}$ we find $\int d^3r \cdots = \Omega$.

Finally, the free solutions form a complete system,

$$\sum_{\boldsymbol{p},s} \left(\Psi^{(+)}_{\boldsymbol{p},s}(\boldsymbol{r})\Psi^{(+)\dagger}_{\boldsymbol{p},s}(\boldsymbol{r}') + \Psi^{(-)}_{\boldsymbol{p},s}(\boldsymbol{r})\Psi^{(-)\dagger}_{\boldsymbol{p},s}(\boldsymbol{r}')\right) = \begin{pmatrix} -I_2 & 0 \\ 0 & -I_2 \end{pmatrix} \delta^{(3)}(\boldsymbol{r} - \boldsymbol{r}'). \qquad (6.62)$$

The antiparticles are again obtained through charge conjugation.

6.5.1 Charge Conjugation C

The charge conjugation

$$C:\ \Psi \to \Psi^C \;=\; C\beta\Psi^* \tag{6.63}$$

with

$$C = -i\alpha_2 \;=\; \begin{pmatrix} 0 & -i\sigma_2 \\ -i\sigma_2 & 0 \end{pmatrix} \tag{6.64}$$

transforms states with negative energy into those with positive energy, which obey a dynamics with reversed charge: With

$$i\hbar\Psi = \left[c\,\alpha_i\left(-i\hbar\partial_{x_i} - eA_i/c\right) + e\phi + \beta mc^2\right]\Psi \tag{6.65}$$

it holds through complex conjugation and multiplication with $C\,\beta$:

$$\begin{aligned}
-i\hbar\partial_t\Psi^C &= C\beta\left[c\,\alpha_i^*\left(i\hbar\partial_{x_i} - eA_i/c\right) + e\phi + \beta mc^2\right]\Psi^* \\
\downarrow C\beta\alpha_i^*\Psi^* \;&=\; \underbrace{C\beta C^{-1}}_{-\beta}\underbrace{C\alpha_i^* C^{-1}}_{-\alpha_i}\underbrace{C\beta C^{-1}}_{-\beta}\underbrace{C\beta\Psi^*}_{\Psi^C} \\
&=\; -\beta\alpha_i\beta\Psi^C \;=\; \alpha_i\Psi^C, \\
\\
\downarrow C\beta^2\Psi^* \;&=\; \underbrace{C\beta C^{-1}}_{-\beta}\underbrace{C\beta\Psi}_{\Psi^C} = -\beta\Psi^C, \\
&= \left[c\,\alpha_i\left(i\hbar\partial_{x_i} - eA_i/c\right) + e\phi - \beta mc^2\right]\Psi^C,
\end{aligned} \tag{6.66}$$

and thus Ψ^C follows the dynamics

$$\begin{aligned}
i\hbar\partial_t\Psi^C &= \left[c\,\alpha_i\left(-i\hbar\partial_{x_i} + eA_i/c\right) - e\phi + \beta mc^2\right]\Psi^C, \\
&= H(-e)\Psi^C.
\end{aligned} \tag{6.67}$$

Charge conjugation C also maps the states $\Psi^{(-)}_{-\boldsymbol{p},-s}$ to $\Psi^{(+)}_{\boldsymbol{p},s}$, since

$$\begin{aligned}
C\beta v^*(\boldsymbol{p},s) &= \sqrt{E_p + mc^2}\begin{pmatrix} 0 & -i\sigma_2 \\ -i\sigma_2 & 0 \end{pmatrix}\begin{pmatrix} \dfrac{c\boldsymbol{\sigma}^*\cdot\boldsymbol{p}}{E_p + mc^2} \\ -1 \end{pmatrix}\left(-i\sigma_2\chi^{(s)}\right) \\
&= \sqrt{E_p + mc^2}\begin{pmatrix} 1 \\ \dfrac{c\boldsymbol{\sigma}\cdot\boldsymbol{p}}{E_p + mc^2} \end{pmatrix}\chi^{(s)} = u(\boldsymbol{p},s).
\end{aligned} \tag{6.68}$$

Here we have used that $\sigma_2\boldsymbol{\sigma}^*\sigma_2 = -\boldsymbol{\sigma}$. Analogously to (6.68), we have

$$C\beta u^*(\boldsymbol{p},s) = v(\boldsymbol{p},s). \tag{6.69}$$

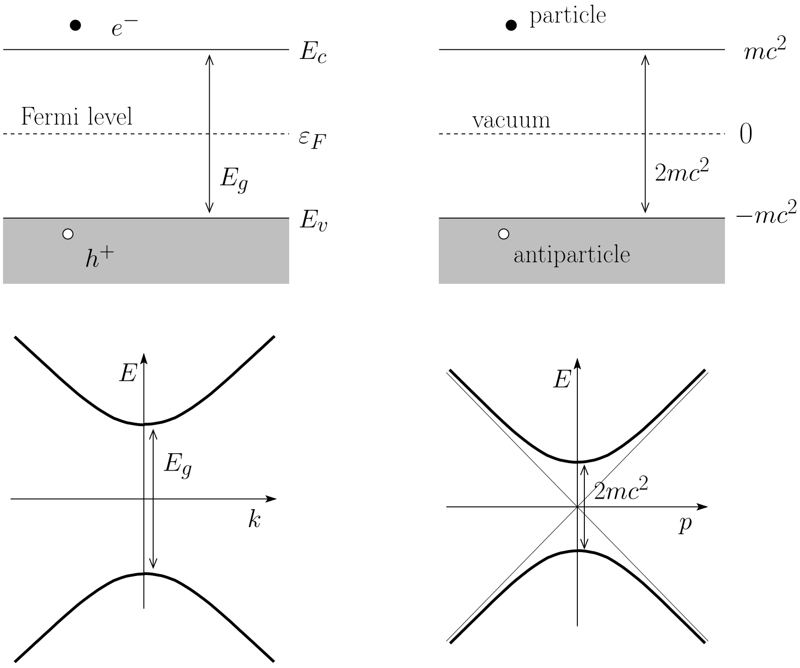

Figure 6.1: Left: Conduction and valence band (top) and dispersion (bottom) of electrons in a semiconductor with a direct energy gap (e.g., GaAs, ZnO, ...). The excitations (missing electrons) in the valence band are interpreted as holes. Right: Hole theory of the Dirac equation. The states with negative energy are filled and block the decay of states with positive energy. The excitations with negative energy are interpreted as antiparticles.

Accordingly, we find that

$$\Psi^{(-)C}_{-\boldsymbol{p},-s} = C\beta\Psi^{(-)*}_{-\boldsymbol{p},-s} \ = \ \Psi^{(+)}_{\boldsymbol{p},s}\,, \tag{6.70}$$

and we identify the (+) energy state $\Psi^{(-)C}_{-\boldsymbol{p},-s}$, which obeys the $-e$ dynamics as an antiparticle with identical mass and spin and with momentum $\boldsymbol{p}$ and spin component s:

$\Psi^{(+)}_{\boldsymbol{p},s}$ = particle with $E_p > 0$, momentum $\boldsymbol{p}$ and spin s,

$\Psi^{(-)}_{-\boldsymbol{p},-s}$ = state with $E_p < 0$, momentum $-\boldsymbol{p}$ and spin $-s$, interpreted as an antiparticle with $E_p > 0$, momentum $\boldsymbol{p}$ and spin s.

Since these particles are fermions, the Pauli exclusion principle applies, and we can provide an interesting interpretation, which was not possible for the bosonic Klein-Gordon particles:

If we interpret the physical vacuum as filled with negative energy states, then the $E_p > 0$ states are stable due to Pauli blocking. Thus, the lowest state has energy

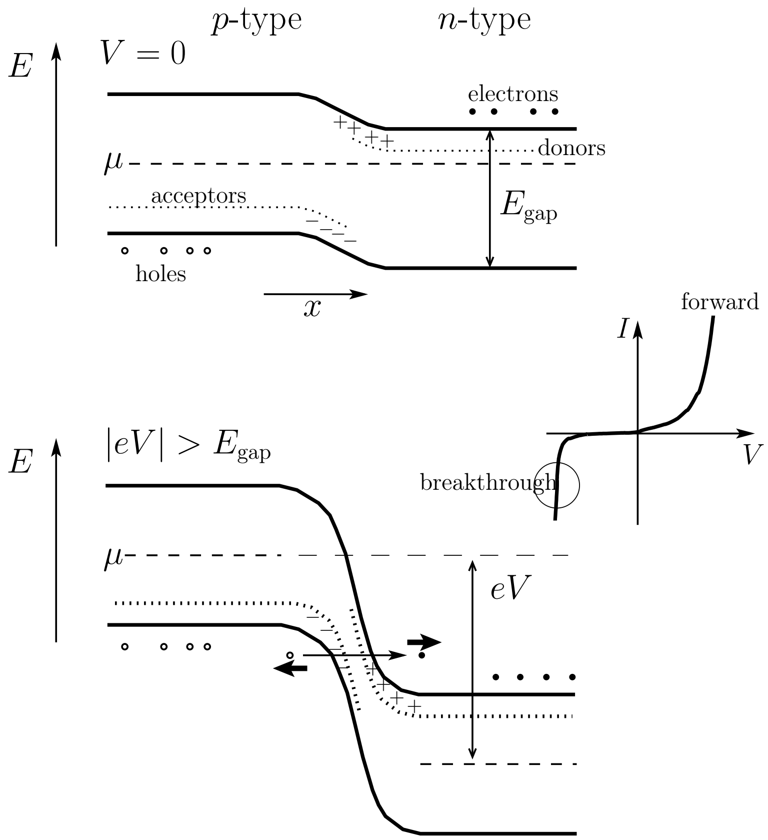

Figure 6.2: Electron-hole pair production in the electric field of a p–n semiconductor junction. Top: Situation in equilibrium without applied voltage, $V = 0$. Bottom: Situation in the reverse biased p–n junction in the breakdown regime where particle-hole pairs are produced via tunneling process. Compare the current-voltage characteristic of the p–n diode.

mc^2 and not $-\infty$. The state $\Psi^{(-)}_{-\boldsymbol{p},-s}$ describes the absence of the particle with the same mass and the same spin, but, since it is a hole, of opposite charge. Its energy is

$$0 - (-E) \;=\; \underbrace{0}_{\text{Vacuum Energy}} \overbrace{-}^{\text{Particle missing}} \underbrace{(-E)}_{\text{en. of the particle}} = E > 0, \tag{6.71}$$

its momentum $0 - (-\boldsymbol{p}) = \boldsymbol{p}$ and its spin $0 - (-s) = s$. This hole theory of the Dirac equation is the relativistic generalization of the hole theory in semiconductors, as shown in Figure 6.1.

Furthermore, it is interesting to discuss Klein's paradox (scattering at a potential step) for fermions (although pair production only really makes sense in a many-body physics context). One finds the following results: 1) for $eV > 2mc^2$, both bosons and fermions are totally reflected. 2) For fermions, due to the Pauli principle, no pair can accompany the reflected particle. 3) Reflected bosons can be accompanied by further boson pairs (stimulated emission in the channel of the reflected boson). 4) For fermions, particle-antiparticle pairs can be produced spontaneously. As a counterpart to the spontaneous electron-positron (e^-–e^+) pair production in a strong electric field, we mention the particle-hole pair production via tunneling effect at a semiconductor p–n junction in the breakdown region, see Figure 6.2.

6.6 Non-relativistic Limit

We want to derive the non-relativistic limit up to the order p^4/m^3, that is $p^2/2m \cdot (v/c)^2$, thus including first relativistic corrections. It is $p^2/2m \simeq e\phi \ll mc^2$. Unfortunately, the simplest way does not work: first, we consider a solution

$$\Psi = \begin{pmatrix} \chi \\ \eta \end{pmatrix} e^{-iEt/\hbar} \tag{6.72}$$

with $E > 0$, $\chi = \chi(\boldsymbol{r})$ and $\eta = \eta(\boldsymbol{r})$. With $E = T + mc^2$ we can write

$$\begin{aligned} T\chi &= e\phi\chi + c\boldsymbol{\sigma} \cdot (\boldsymbol{p} - e\boldsymbol{A}/e)\,\eta, \\ (2mc^2 + T)\eta &= e\phi\eta + c\boldsymbol{\sigma} \cdot (\boldsymbol{p} - e\boldsymbol{A}/c)\,\chi. \end{aligned} \tag{6.73}$$

The second equation gives

$$\eta = \frac{1}{2mc^2 + T - e\phi} c\boldsymbol{\sigma} \cdot (\boldsymbol{p} - e\boldsymbol{A}/c)\chi \tag{6.74}$$

and substituting into (6.73) leads to

$$T\chi = \Big[e\phi + c\boldsymbol{\sigma} \cdot (\boldsymbol{p} - e\boldsymbol{A}/e)\frac{1}{2mc^2 + T - e\phi}c\boldsymbol{\sigma} \cdot \big(\boldsymbol{p} - e\boldsymbol{A}/e\big)\Big]\chi. \tag{6.75}$$

If we want to go up to order p^4/m^3, we must develop the denominator accordingly and obtain

$$\begin{aligned} T\chi = &\Big[(e\phi + \frac{1}{2m}\Big[\boldsymbol{\sigma} \cdot \big(\boldsymbol{p} - e\boldsymbol{A}/c\big)\Big]^2 - \frac{1}{4m^2c^2}\boldsymbol{\sigma} \cdot \big(\boldsymbol{p} - e\boldsymbol{A}/c\big) \\ &\times \big(T - e\phi\big)\boldsymbol{\sigma} \cdot \big(\boldsymbol{p} - e\boldsymbol{A}/c\big)\Big]\chi = H(\text{Energy})\chi. \end{aligned} \tag{6.76}$$

The dependence on T on the right side is not pleasing to us as it imposes an energy-dependent Hamilton operator. Therefore, we replace T with the lowest approximation

$$T \approx e\phi + \frac{1}{2m}\left[\boldsymbol{\sigma} \cdot \big(\boldsymbol{p} - e\boldsymbol{A}/c\big)\right]^2. \tag{6.77}$$

However, this step is not unambiguous; since the order $(\boldsymbol{p}-e\boldsymbol{A}/c)(T-e\phi)$ generates a term $\boldsymbol{p}\,e\phi \propto e\boldsymbol{E}$, while the expression $T-e\phi \approx \left[\boldsymbol{\sigma}\cdot(\boldsymbol{p}-e\boldsymbol{A}/c)\right]^2/2m$ commutes with $\boldsymbol{\sigma}\cdot\big(\boldsymbol{p}-e\boldsymbol{A}/c\big)$. Alternatively, one can first commute the factor $\boldsymbol{\sigma}\cdot\big(\boldsymbol{p}-e\boldsymbol{A}/c\big)$ with $(T-e\phi)$ and only then use (6.77), but this approach is also not unambiguous and additionally generates non-Hermitian terms.

A unique non-relativistic limit can be constructed using the Foldy-Wouthuysen transformation, a unitary transformation that makes the off-diagonal terms small. In the transformed system, we can then solve the coupled system of equations. We start from the Dirac equation in the form

$$\begin{aligned} T\begin{pmatrix}\chi\\ \eta\end{pmatrix} &= \left[-mc^2+e\phi+c\boldsymbol{\alpha}\cdot(\boldsymbol{p}-e\boldsymbol{A}/c)+mc^2\beta\right]\begin{pmatrix}\chi\\ \eta\end{pmatrix}\\ &= H\begin{pmatrix}\chi\\ \eta\end{pmatrix} \qquad (6.78)\\ &\widehat{=} mc^2\left[-1+\left(\frac{v}{c}\right)^2+\left(\frac{v}{c}-\left(\frac{v}{c}\right)^2\right)+1\right]\begin{pmatrix}\chi\\ \eta\end{pmatrix}; \qquad (6.79)\end{aligned}$$

the last equation lists the order of the terms in the relativistic parameter v/c, where the term $c\boldsymbol{\alpha}\cdot\boldsymbol{p}\propto v/c$ is large. In contrast, only terms $\propto 1,\ (v/c)^2$ appeared in the Klein-Gordon equation, which is why its non-relativistic limit was unproblematic. It is precisely the term $c\boldsymbol{\alpha}\boldsymbol{p}\propto(v/c)mc^2$ that gives us trouble, and we will transform it away. To do this, we set a unitary transformation of the form

$$U=U^\dagger=\underbrace{\sqrt{1-\frac{\lambda^2p^2}{m^2c^2}}}_{\Lambda}\,\beta+\frac{\lambda}{mc}\boldsymbol{\alpha}\cdot\boldsymbol{p}, \qquad (6.80)$$

with the suitably chosen parameter λ; we will choose λ such that in the transformed system the term $c\boldsymbol{\alpha}\cdot\boldsymbol{p}$ vanishes[7]. We define the transformed spinor

$$\begin{pmatrix}\chi'\\ \eta'\end{pmatrix}=U\begin{pmatrix}\chi\\ \eta\end{pmatrix}, \qquad (6.81)$$

transform (6.78) with U,

$$UT\begin{pmatrix}\chi\\ \eta\end{pmatrix}=T\begin{pmatrix}\chi'\\ \eta'\end{pmatrix}\ =\ UHU^{-1}\begin{pmatrix}\chi'\\ \eta'\end{pmatrix}, \qquad (6.82)$$

---

[7] The Ansatz (6.80) actually defines a unitary transformation,

$$\begin{aligned} UU^\dagger &= \left(\Lambda\beta+\frac{\lambda}{mc}\boldsymbol{\alpha}\cdot\boldsymbol{p}\right)^2\\ &= \Lambda^2\beta^2+\frac{\lambda}{mc}\Lambda\{\beta,\alpha_i\}p_i+\frac{\lambda^2}{m^2c^2}[\{\alpha_i,\alpha_j\}\ p_ip_j/2+p^2]\\ &= \Lambda^2+\frac{\lambda^2}{m^2c^2}p^2=1.\end{aligned}$$

and obtain the transformed Hamiltonian operator

$$H' = UHU^{-1}. \tag{6.83}$$

We transform the terms mc^2, $e\phi$, $c\boldsymbol{\alpha}\cdot(\boldsymbol{p}-e\boldsymbol{A}/c)$, and $mc^2\beta$ and obtain

$$\begin{aligned}
U\,[mc^2]\,U^{-1} &= mc^2, && \text{(a)}\\
U\,[e\phi]\,U^{-1} &= \Lambda\, e\phi\,\Lambda + \beta\frac{\lambda}{mc}\,(\Lambda\, e\phi\,\boldsymbol{\alpha}\cdot\boldsymbol{p} - \boldsymbol{\alpha}\cdot\boldsymbol{p}\, e\phi\,\Lambda) && \text{(b)}\\
&\quad + \frac{\lambda^2}{m^2c^2}\boldsymbol{\alpha}\cdot\boldsymbol{p}\, e\phi\,\boldsymbol{\alpha}\cdot\boldsymbol{p},\\
U\left[c\boldsymbol{\alpha}\cdot\left(\boldsymbol{p}-e\boldsymbol{A}/c\right)\right]U^{-1} &= \underline{-\Lambda c\,\boldsymbol{\alpha}\cdot(\boldsymbol{p}-e\boldsymbol{A}/c)\,\Lambda} && \text{(c)}\\
&\quad + \beta\frac{\lambda}{m}[\Lambda\,\boldsymbol{\alpha}\cdot(\boldsymbol{p}-e\boldsymbol{A}/c)\ \boldsymbol{\alpha}\cdot\boldsymbol{p} + \boldsymbol{\alpha}\cdot\boldsymbol{p}\ \boldsymbol{\alpha}\cdot(\boldsymbol{p}-e\boldsymbol{A}/c)\,\Lambda] && \text{(6.84)}\\
&\quad + \frac{\lambda^2}{m^2c}\boldsymbol{\alpha}\cdot\boldsymbol{p}\ \boldsymbol{\alpha}\cdot(\boldsymbol{p}-e\boldsymbol{A}/c)\,\boldsymbol{\alpha}\cdot\boldsymbol{p},\\
U\,[mc^2\beta]\,U^{-1} &= mc^2\beta\Lambda^2 + \underline{2\lambda\Lambda c\boldsymbol{\alpha}\cdot\boldsymbol{p}} - \beta\lambda^2p^2/m. && \text{(d)}
\end{aligned}$$

The critical terms are the (underlined) off-diagonal terms of odd order in $\boldsymbol{\alpha}$ and of relative order v/c. With

$$\Lambda \approx 1 - \frac{\lambda^2p^2}{2m^2c^2} = 1 - \mathcal{O}[(v/c)^2], \tag{6.85}$$

we obtain (the index nd stands for 'non-diagonal')

$$\begin{aligned}
H'_{\text{nd},v/c} &= -c\boldsymbol{\alpha}\cdot\left(\boldsymbol{p}-e\boldsymbol{A}/c\right) + 2\lambda c\boldsymbol{\alpha}\cdot\boldsymbol{p} + \mathcal{O}[(v/c)^3]\\
&\overset{\lambda\,=\,1/2}{=}\ e\boldsymbol{\alpha}\cdot\boldsymbol{A} \simeq\ \mathcal{O}[(v/c)^2].
\end{aligned}\tag{6.86}$$

The equation (6.82) then takes the form

$$T\begin{pmatrix}\chi'\\ \eta'\end{pmatrix} = \begin{pmatrix}H'_{11} & e\boldsymbol{\alpha}\cdot\boldsymbol{A}\\ e\boldsymbol{\alpha}\cdot\boldsymbol{A} & -2mc^2\end{pmatrix}\begin{pmatrix}\chi'\\ \eta'\end{pmatrix}, \tag{6.87}$$

with (we refer to (6.84); the terms $\propto mc^2$ in (a) and (d) combine to $(-I_4+\beta)mc^2$ and do not contribute to H'_{11} but contribute $-2mc^2$ to H'_{22})

$$\begin{aligned}
H'_{11} \approx\ & \underbrace{e\phi - \frac{p^2}{8m^2c^2}\,e\phi - e\phi\,\frac{p^2}{8m^2c^2}}_{\text{(b): }\Lambda\, e\phi\,\Lambda} + \underbrace{\frac{\boldsymbol{\sigma}\cdot\boldsymbol{p}\, e\phi\,\boldsymbol{\sigma}\cdot\boldsymbol{p}}{4m^2c^2}}_{\text{(b)}}\\
&+ \underbrace{\frac{1}{2m}\left[\boldsymbol{\sigma}\cdot\left(\boldsymbol{p}-e\boldsymbol{A}/c\right)\ \boldsymbol{\sigma}\cdot\boldsymbol{p} + \boldsymbol{\sigma}\cdot\boldsymbol{p}\ \boldsymbol{\sigma}\cdot\left(\boldsymbol{p}-e\boldsymbol{A}/c\right)\right] - \frac{p^4}{8m^3c^2}}_{\text{(c)}} - \underbrace{\frac{p^2}{2m}}_{\text{(d)}}.
\end{aligned}\tag{6.88}$$

The rest are rearrangements; with $\sigma_i\sigma_j = \delta_{ij} + i\varepsilon_{ijk}\sigma_k$ one obtains for the (c)-term

$$\begin{aligned}
&\boldsymbol{\sigma}\cdot\big(\boldsymbol{p} - e\boldsymbol{A}/c\big)\boldsymbol{\sigma}\cdot\boldsymbol{p} + \boldsymbol{\sigma}\cdot\boldsymbol{p}\;\boldsymbol{\sigma}\cdot\big(\boldsymbol{p} - e\boldsymbol{A}/c\big) \\
&\quad = 2p^2 - \boldsymbol{\sigma}\cdot\boldsymbol{p}\;\boldsymbol{\sigma}\cdot(e\boldsymbol{A}/c) - \boldsymbol{\sigma}\cdot(e\boldsymbol{A}/c)\;\boldsymbol{\sigma}\cdot\boldsymbol{p} \\
&\quad = 2p^2 - (e/c)\big(\boldsymbol{p}\cdot\boldsymbol{A} + \boldsymbol{A}\cdot\boldsymbol{p}\big) - i(e/c)\boldsymbol{\sigma}\cdot\big[\big(\boldsymbol{p}\wedge\boldsymbol{A}\big) - \big(\boldsymbol{A}\wedge\boldsymbol{p}\big)\big] \\
&\quad = \big(\boldsymbol{p} - e\boldsymbol{A}/c\big)^2 + p^2 - \big(e\boldsymbol{A}/c\big)^2 - (e\hbar/c)\boldsymbol{\sigma}\cdot\big(\boldsymbol{\nabla}\wedge\boldsymbol{A}\big) \\
&\quad = \big(\boldsymbol{p} - e\boldsymbol{A}/c\big)^2 + p^2 - (e/c)^2A^2 - (e\hbar/c)\boldsymbol{\sigma}\cdot\boldsymbol{B}.
\end{aligned} \tag{6.89}$$

The (b)-terms can also be simplified according to

$$\begin{aligned}
p^2\phi + \phi p^2 &= (p^2\phi) + 2(\boldsymbol{p}\phi)\cdot\boldsymbol{p} + 2\phi p^2, \\
\boldsymbol{\sigma}\cdot\boldsymbol{p}\;\phi\;\boldsymbol{\sigma}\cdot\boldsymbol{p} &= \boldsymbol{\sigma}\cdot(\boldsymbol{p}\phi)\;\boldsymbol{\sigma}\cdot\boldsymbol{p} + \phi p^2 \\
&= (\boldsymbol{p}\phi)\cdot\boldsymbol{p} + i\boldsymbol{\sigma}\cdot[(\boldsymbol{p}\phi)\wedge\boldsymbol{p}] + \phi p^2
\end{aligned}$$

and we obtain

$$\begin{aligned}
&-(e/8m^2c^2)\{p^2\phi + \phi p^2 - 2\boldsymbol{\sigma}\cdot\boldsymbol{p}\;\phi\;\boldsymbol{\sigma}\cdot\boldsymbol{p}\} \\
&\qquad = -(e/8m^2c^2)\{(p^2\phi) - 2i\boldsymbol{\sigma}\cdot[(\boldsymbol{p}\phi)\wedge\boldsymbol{p}]\}.
\end{aligned}$$

Substituting into (6.88) yields the Hamiltonian operator (the diamagnetic term $\propto A^2$ is obtained from $\eta' = (e/2mc^2)\boldsymbol{\alpha}\cdot\boldsymbol{A}\;\chi' + \mathcal{O}(v^4/c^4)$)

$$\begin{aligned}
H'_{11} + \frac{e^2}{2mc^2}A^2 = \frac{1}{2m}\left(\boldsymbol{p} - \frac{e}{c}\boldsymbol{A}\right)^2 + e\phi - \frac{e\hbar}{2mc}\boldsymbol{\sigma}\cdot\boldsymbol{B} - \frac{p^4}{8m^3c^2} \\
+ \frac{e\hbar^2(\nabla^2\phi)}{8m^2c^2} + \frac{e\hbar}{4m^2c^2}\boldsymbol{\sigma}\cdot\big[(\boldsymbol{\nabla}\phi)\wedge\boldsymbol{p}\big].
\end{aligned} \tag{6.90}$$

The dynamics of a spin-1/2 particle in the electromagnetic field $\phi, \boldsymbol{A}$ with relativistic corrections up to order $(v/c)^2$ is given by (with $\phi(\boldsymbol{r}) = \phi(r)$ we can replace $\boldsymbol{\nabla}\phi\wedge\boldsymbol{p}$ by $[r^{-1}(\partial_r\phi)\boldsymbol{L}]$

$$\begin{aligned}
H = \underbrace{\frac{1}{2m}\left(\boldsymbol{p} - \frac{e}{c}\boldsymbol{A}\right)^2 + e\phi}_{H_0} \underbrace{- \frac{1}{2mc^2}\left(\frac{p^2}{2m}\right)^2 + \frac{e\hbar}{4m^2c^2}\frac{(\partial_r\phi)}{r}\boldsymbol{\sigma}\cdot\boldsymbol{L} + \frac{e\hbar^2\,(\nabla^2\phi)}{8m^2c^2}}_{\text{fine structure}} \\
\underbrace{- \frac{e\hbar}{2mc}\boldsymbol{\sigma}\cdot\boldsymbol{B}}_{\text{Zeeman}}.
\end{aligned} \tag{6.91}$$

Combining the orbital and spin Zeeman terms yields

$$H_{\text{Zeeman}} = -\frac{e}{2mc}\boldsymbol{B}\cdot(\boldsymbol{L} + 2\boldsymbol{S}), \tag{6.92}$$

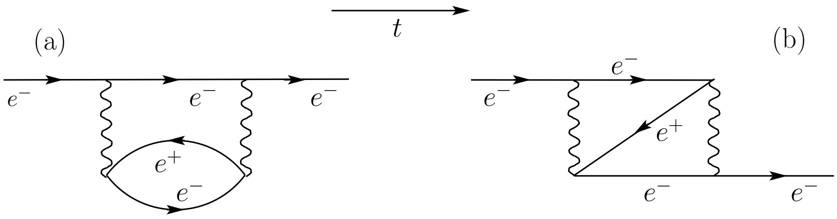

Figure 6.3: Feynman diagrams for virtual electron-hole pair creation: (a) Vacuum polarization (direct term) and (b) Zitterbewegung (exchange term for vacuum polarization). The electron disappears (via pair annihilation) only to reappear at another location (via pair creation).

and from this the gyromagnetic factor of the electron spin, $g = 2$. One can argue that the Darwin term $\propto \nabla^2\phi$ arises from the smearing of the electron over the Compton scale[8] $\hbar/mc$: The averaging of the potential

$$\begin{aligned}\langle e\phi(\boldsymbol{r}+\delta\boldsymbol{r})\rangle &\approx \langle e\phi(\boldsymbol{r}) + e\delta\boldsymbol{r}\cdot\boldsymbol{\nabla}\phi(\boldsymbol{r}) + \frac{e}{2}(\delta\boldsymbol{r}\cdot\boldsymbol{\nabla})^2\phi(\boldsymbol{r})\rangle \\ &\approx e\phi(\boldsymbol{r}) + \frac{e}{6}\frac{\hbar^2}{m^2c^2}(\nabla^2\phi),\end{aligned} \tag{6.93}$$

yields a term of the corresponding structure and order. The corresponding quantum fluctuations in the position of the electron are referred to as ‘zitterbewegung’. It is unfortunate that this argument does not involve spin, as the Klein-Gordon equation does not show a corresponding term.

A deeper analysis shows that the zitterbewegung arises from the interference of positive and negative energy states: a state with purely positive (negative) energy shows no zitterbewegung. Scattering off a potential always mixes a state with $E > 0$ with states with $E < 0$. Within the hole theory, the zitterbewegung is interpreted as follows: The potential mixes components with $E < 0$ into a state with $E > 0$. The interference effects that lead to zitterbewegung correspond to virtual e^+–e^- pairs. The scattering e^- annihilates the e^+ and the e^- of the e^+–e^- pair takes its place. This means that the electron jumps. The process as outlined in Figure 6.3 is an exchange process.

The extent of the zitterbewegung can be estimated as follows: The lifetime Δt of the virtual e^+–e^- pair is given by the uncertainty relation[9]: $\Delta t \simeq \hbar/2mc^2$, from which the distance $\Delta r \simeq c\Delta t \simeq \hbar/mc$ follows.

Applying this to the hydrogen atom $\phi(r) = e/r$ yields a fine structure that only involves the quantum numbers n and j, although the Darwin term contributes only to orbital angular momentum $l = 0$ and the spin-orbit term to $l \neq 0$. The compensation

---

[8] The Compton scale $\hbar/mc$ is the length scale of the relativistic differential equation.

[9] According to the Heisenberg uncertainty principle, $\Delta E\,\Delta t \geq \hbar$, where ΔE is given by the rest energy mc^2 of the electron.

of these contributions then gives the energy

$$T = E_{nj} = -mc^2 \left[\frac{(Z\alpha)^2}{2n^2} + \frac{(Z\alpha)^4}{2n^4} \left(\frac{n}{j+1/2} - \frac{3}{4} \right) \right] . \qquad (6.94)$$

Appendix A

Spherical Bessel Functions

A.1 Definition

The Bessel functions J_n are the solutions of the differential equation

$$\left[\partial_x^2 + \frac{1}{x}\partial_x + \left(1 - \frac{n^2}{x^2}\right)\right] J_n(x) = 0. \tag{A.1}$$

For half-integer $n = l + \frac{1}{2}$, one usually considers the equivalent differential equation

$$\left[\partial_x^2 + \frac{2}{x}\partial_x + \left(1 - \frac{l(l+1)}{x^2}\right)\right] z_l(x) = 0. \tag{A.2}$$

with the spherical Bessel and Neumann functions,

$$\text{Bessel} \to j_l(x) = \sqrt{\frac{\pi}{2x}}\, J_{l+\frac{1}{2}}(x), \tag{A.3}$$

$$\text{Neumann} \to n_l(x) = (-1)^{l+1}\sqrt{\frac{\pi}{2x}}\, J_{-l-\frac{1}{2}}(x). \tag{A.4}$$

as a solution. Note that (A.2) is symmetric under $l + \frac{1}{2} \mapsto -l - \frac{1}{2}$, and thus the Neumann solutions transition into the Bessel solutions. Examples of the spherical Bessel and Neumann functions are (see also Figures A.1 and A.2)

$$\begin{aligned} j_0 &= \frac{\sin x}{x}, & n_0 &= -\frac{\cos x}{x}, \\ j_1 &= \frac{\sin x}{x^2} - \frac{\cos x}{x}, & n_1 &= -\frac{\cos x}{x^2} - \frac{\sin x}{x}, \\ j_2 &= \left(\frac{3}{x^3} - \frac{1}{x}\right)\sin x - \frac{3}{x^2}\cos x, & n_2 &= -\left(\frac{3}{x^3} - \frac{1}{x}\right)\cos x - \frac{3}{x^2}\sin x. \end{aligned} \tag{A.5}$$

The spherical Bessel functions exhibit the following behavior for small (series

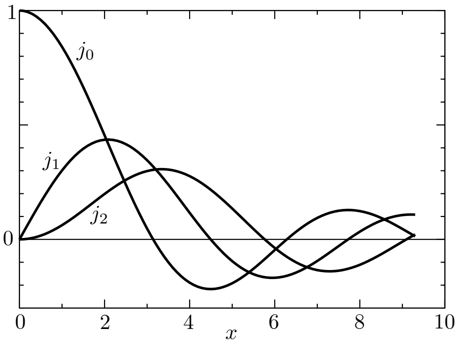

Figure A.1: Bessel functions $j_0(x)$, $j_1(x)$, $j_2(x)$.

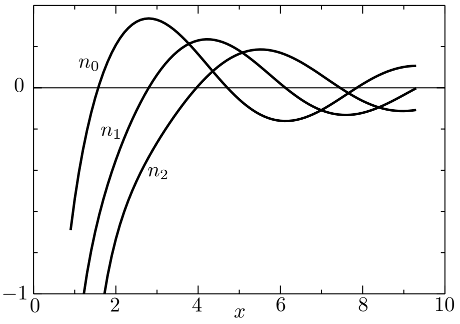

Figure A.2: Neumann functions $n_0(x)$, $n_1(x)$, $n_2(x)$.

expansion for $x \to 0$) and large (asymptotic for $x \to \infty$) arguments:

$$\begin{aligned} & x \to 0: && x \to \infty: \\ & j_l \sim \frac{x^l}{(2l+1)!!}, && j_l \sim \frac{1}{x}\cos[x-(l+1)\pi/2], \\ & n_l \sim -\frac{(2l-1)!!}{x^{l+1}}, && n_l \sim \frac{1}{x}\sin[x-(l+1)\pi/2]. \end{aligned} \tag{A.6}$$

where $(2l-1)!! = 1\cdot 3\cdot \ldots \cdot (2l-3)\cdot(2l-1) = \frac{(2l)!}{2^l l!}$ denotes the double factorial. For the spherical Bessel functions $z_l = j_l, n_l$, the recursion formulas ($l > 0$) also hold

$$\begin{aligned} z_{l-1} + z_{l+1} &= \frac{2l+1}{x}\, z_l, \\ \partial_x z_l &= z_{l-1} - \frac{l+1}{x}\, z_l. \end{aligned} \tag{A.7}$$

Note that n_l is always singular for $x \to 0$. Additionally, we define the spherical Hankel functions as linear combinations

$$\begin{aligned} h_l^{(1)}(x) &= j_l(x) + i\, n_l(x), \\ h_l^{(2)}(x) &= j_l(x) - i\, n_l(x), \end{aligned} \tag{A.8}$$

with the asymptotic behavior

$$h_l^{(1,2)} \sim \frac{1}{x}\, e^{\pm i[x-(l+1)\pi/2]}. \tag{A.9}$$

A.2 Expansion of the Plane Wave

The plane wave $e^{ikr\cos\theta}$ is a solution of (**??**) and thus of (1.33) with $V \equiv 0$. As discussed in the last chapter, $j_l(x = kr)$ solves the differential equation (1.33), so we can choose the ansatz

$$e^{ikr\cos\theta} = \sum_l A_l\, j_l(kr)\, \underbrace{P_l(\cos\theta)}_{\propto Y_{l0}} \tag{A.10}$$

which separates the radial and angular dependence. Finally, we need to determine the coefficients A_l. Using (1.29), i.e. $P_l \perp P_{l'}$, we obtain through integration by utilizing the normalization $\int dz\, P_l(z)^2 = 2/(2l+1)$

$$\frac{2}{2l+1} A_l\, j_l(kr) = \int_{-1}^{1} dz\, P_l(z) e^{ikrz}. \tag{A.11}$$

We consider $r \to 0$, expand $\exp(ikrz)$ on the right side and $j_l(kr)$ on the left side in $x = kr$ with subsequent coefficient comparison. First, the right side: We expand $\exp(ikrz)$ and obtain

$$\int_{-1}^{1} dz\, P_l(z) \sum_{s=0}^{\infty} \frac{(ikrz)^s}{s!} \approx \int_{-1}^{1} dz\, P_l(z) \frac{(ikrz)^l}{l!}, \tag{A.12}$$

where we have used the fact that in the limit of small x, only the term $s = l$ provides a significant contribution [Terms with $s < l$ give no contribution since $P_l \perp z^s = \sum_{i\leq s} c_i P_i$; Terms with $s > l$ give a small correction of the order $O(x^{l+2})$]. Next, we replace z^l with Legendre polynomials $P_{l'}(z)$ with $l' \leq l$. Under the integral, terms with $l' < l$ vanish (orthogonality of the Legendre polynomials). We have

$$P_l(z) = \frac{(2l-1)!!}{l!} z^l + O(z^{l-2}). \tag{A.13}$$

for the term with $l' = l$, so we can replace z^l under the integral with $l! P_l(z)/(2l-1)!!$. Finally, we use the normalization of $P_l(z)$ to perform the integral over z and obtain

$$\int_{-1}^{1} dz\, P_l(z) \sum_{s=0}^{\infty} \frac{(ikrz)^s}{s!} \approx \frac{2(ikr)^l}{(2l+1)!!} \tag{A.14}$$

For the left side: The expansion of $j_l(x)$ for small x yields [see (A.6)]

$$\frac{2}{2l+1} A_l\, j_l(kr) \approx A_l \frac{2(kr)^l}{(2l+1)(2l+1)!!} \tag{A.15}$$

and the coefficient comparison gives us the desired result

$$A_l = i^l (2l+1). \tag{A.16}$$

For the general case with $\boldsymbol{k}$ and $\boldsymbol{r}$ arbitrary, we can use the addition theorem for Y_{lm} and express $P_l(\cos\vartheta)$ in terms of the spherical functions

$$\sum_{m=-l}^{l} Y_{lm}(\theta,\varphi) Y^*_{lm}(\theta',\varphi') = \frac{2l+1}{4\pi} P_l(\cos\vartheta); \tag{A.17}$$

thus we obtain for the plane wave the expression

$$e^{i\boldsymbol{k}\cdot\boldsymbol{r}} = 4\pi \sum_{l=0}^{\infty} \sum_{m=-l}^{l} i^l \, j_l(kr) Y_{lm}^*(\Omega_{\boldsymbol{k}}) Y_{lm}(\Omega_{\boldsymbol{r}}). \tag{A.18}$$

Appendix B

Spin and Orbital Symmetry

The analysis of the N spin-$1/2$ fermion problem is important for the discussion of atoms and is very instructive in terms of understanding the role of permutation symmetry. The topic is also a nice application of group theory. Here is an attempt to present the problem as simply as possible. First, we will briefly discuss the representation theory of S_N. Then we will explain the connection between spin and symmetry in the reduction of $\mathcal{H}_{1/2}^{\otimes N}$.

This chapter introduces all necessary tools and shows examples of how to use them. The results are made plausible. Proofs of the statements can be found, for example, in the books by Morton Hamermesh 'Group theory and its application to physics problems' or Hermann Weyl 'The classical groups: their invariants and representations'.

B.1 Symmetric Group S_N

The elements π of the group S_N are the permutations of N objects,

$$\begin{aligned}\pi &= \begin{pmatrix} 1 & 2 & \cdots & N \\ \pi(1) & \pi(2) & \cdots & \pi(N) \end{pmatrix} \\ &= \begin{pmatrix} 2 & 4 & 3 & \cdots \\ \pi(2) & \pi(4) & \pi(3) & \cdots \end{pmatrix}; \end{aligned} \tag{B.1}$$

here, π is a mapping from $\mathbb{Z}_N$ to $\mathbb{Z}_N$, which maps the upper row to the lower one, that is, k to $\pi(k)$. The inverse of the permutation π is

$$\pi^{-1} = \begin{pmatrix} \pi(1) & \pi(2) & \cdots & \pi(N) \\ 1 & 2 & \cdots & N \end{pmatrix}. \tag{B.2}$$

The group S_N has $N!$ elements, and the order g of S_N is $N!$.

An important class of permutations is the k-cycles

$$\pi_{(\alpha_1\cdots\alpha_k)} = \begin{pmatrix} \alpha_1 & \alpha_2 & \alpha_3 & \cdots & \alpha_k & \beta_1 & \cdots\beta_{n-k} \\ \alpha_2 & \alpha_3 & \alpha_4 & \cdots & \alpha_1 & \beta_1 & \cdots\beta_{n-k} \end{pmatrix}; \tag{B.3}$$

$\pi_{(\alpha_1\cdots\alpha_k)}$ is also briefly denoted by $(\alpha_1\alpha_2\ldots\alpha_k)$; the cycle maps α_1 to α_2, α_2 to α_3, $\ldots$, α_k to α_1 and leaves the elements β_k, which are not involved in the cycle, invariant. The simplest cycle is the two-cycle or the transposition $\pi_{(\alpha_1\alpha_2)} = (\alpha_1\alpha_2)$, e.g.

$$\pi_{(35)} = (35) = \begin{pmatrix} 3 & 5 & \beta_1 & \cdots & \beta_{n-2} \\ 5 & 3 & \beta_1 & \cdots & \beta_{n-2} \end{pmatrix}. \tag{B.4}$$

Every permutation can be built from transpositions. A permutation is called even (odd) if it can be constructed from an even (odd) number of transpositions. We denote

$$(-1)^\pi \text{ the signature of } \pi, \text{ with} \begin{cases} (-1)^\pi = 1, & \pi \text{ even}, \\ (-1)^\pi = -1, & \pi \text{ odd}. \end{cases} \tag{B.5}$$

The decomposition of π into independent cycles[1] determines the equivalence class of the permutation[2] For example, S_3 has a total of three equivalence classes: the identity e forms (as always) an equivalence class, the three two-cycles $(\alpha_1\alpha_2)$ with $1 \le \alpha_1 < \alpha_2 \le 3$ form the second equivalence class, and the two three-cycles $(\alpha_1\alpha_2\alpha_3)$ with $1 \le \alpha_1 < \alpha_2 < \alpha_3 \le 3$ also form their own equivalence class.

In general, one can show that π and π' are equivalent if and only if they have the same cycle structure; consider a permutation with the cycle structure $3+2$,

$$\pi = \begin{pmatrix} 1 & 2 & 3 & 4 & 5 \\ 5 & 3 & 2 & 1 & 4 \end{pmatrix} = \left(\begin{array}{ccc|cc} 1 & 5 & 4 & 2 & 3 \\ 5 & 4 & 1 & 3 & 2 \end{array}\right) = (1\,5\,4)(2\,3). \tag{B.6}$$

In fact, the transformation $\nu\pi\nu^{-1}$ with $\nu \in S_N$ leaves the cycle structure invariant; we illustrate this with the above example using a specific ν,

$$\begin{aligned} \nu &= \begin{pmatrix} 1 & 2 & 3 & 4 & 5 \\ 2 & 4 & 1 & 3 & 5 \end{pmatrix} = \begin{pmatrix} 5 & 4 & 1 & 3 & 2 \\ 5 & 3 & 2 & 1 & 4 \end{pmatrix} \\ \nu^{-1} &= \begin{pmatrix} 2 & 4 & 1 & 3 & 5 \\ 1 & 2 & 3 & 4 & 5 \end{pmatrix} = \begin{pmatrix} 2 & 5 & 3 & 4 & 1 \\ 1 & 5 & 4 & 2 & 3 \end{pmatrix}. \end{aligned} \tag{B.7}$$

Then, $\nu\pi\nu^{-1}$ can be easily constructed,

$$\begin{aligned} \nu\pi\nu^{-1} &= \begin{pmatrix} 2 & 5 & 3 & 4 & 1 \\ 1 & 5 & 4 & 2 & 3 \\ 5 & 4 & 1 & 3 & 2 \\ 5 & 3 & 2 & 1 & 4 \end{pmatrix} \begin{matrix} \\ \leftarrow \quad \nu^{-1} \\ \leftarrow \quad \pi \\ \leftarrow \quad \nu \end{matrix} \\ &= \begin{pmatrix} 2 & 5 & 3 & 4 & 1 \\ 5 & 3 & 2 & 1 & 4 \end{pmatrix} = (2\,5\,3)(4\,1), \end{aligned} \tag{B.8}$$

---

[1] that is, each number appears only once.

[2] Two permutations π and π' are equivalent if there exists a $\nu \in S_N$ such that $\nu\pi\nu^{-1} = \pi'$.

and the cycle structure remains preserved. This fact can be proven in general, and thus the cycle structure defines an equivalence criterion.

To find the number of equivalence classes of S_N, we need all partitions of N. We denote $[\lambda_1, \lambda_2, \ldots, \lambda_k] \equiv \lambda$ a partition of N if $\lambda_i \geq 1$ are integers sorted according to $\lambda_1 \leq \lambda_2 \leq \cdots \leq \lambda_k$ and

$$\lambda_1 + \lambda_2 + \cdots + \lambda_k = N. \tag{B.9}$$

The partitions of N yield the equivalence classes of S_N. For the example with $N = 5$, one finds by simple counting 7 equivalence classes,

$$S_5\colon \quad 5 \left.\begin{aligned} &= 5 \\ &= 4+1 \\ &= 3+2 \\ &= 3+1+1 \\ &= 2+2+1 \\ &= 2+1+1+1 \\ &= 1+1+1+1+1 \end{aligned}\right\} \to 7 \text{ classes.}$$

The number of irreducible representations of S_N is equal to the number K of classes. Let d_i be the dimension of the i-th irreducible representation. Then the group order $g = N!$ is given by[3]

$$g = \sum_{i=1}^{K} d_i^2. \tag{B.10}$$

In concrete examples, one finds by trial and error

$$\begin{aligned}
&S_2\colon && K = 2, && 2! = 1+1, \\
&S_3\colon && K = 3, && 3! = 1+1+2^2, \\
&S_4\colon && K = 5, && 4! = 24 = 1+1+2^2+3^2+3^2, \\
&S_5\colon && K = 7, && 5! = 120 = 1+1+4^2+4^2+5^2+5^2+6^2.
\end{aligned}$$

The two one-dimensional representations always occur. These are the antisymmetric (A) and the symmetric (S) representations. They are generated by the (anti-)symmetrization operators

$$\mathcal{A} = \frac{1}{N!} \sum_{\pi \in S_N} (-1)^{\pi} \pi, \tag{B.11}$$

$$\mathcal{S} = \frac{1}{N!} \sum_{\pi \in S_N} \pi, \tag{B.12}$$

---

[3] This relationship between the group order and the sum of the squares of the dimensions of all irreducible representations holds in general for any finite group.

respectively their representations in the Hilbert space. We have already seen in Chapter 2.3 that the representation of the (anti-)symmetrization operator projects onto a one-dimensional subspace of the total Hilbert space. The application of any permutation π then only results in multiplication by $(\pm 1)^\pi$. These properties can be easily derived from the multiplication rules

$$\pi\mathcal{S} = \mathcal{S}\pi = \mathcal{S} \quad \text{and} \quad \pi\mathcal{A} = \mathcal{A}\pi = (-1)^\pi\mathcal{A} \tag{B.13}$$

.

B.2 Example: 2 Spin-1/2 Fermions

In the study of N spin-1/2 fermions, the central question is how spin, spin symmetry, and orbital symmetry are related. To introduce the topic, we analyze the problem of two spin-1/2 fermions. We separate the total wave function into spin and orbital parts, $\Psi(x_1, x_2) = \varphi(\boldsymbol{r}_1, \boldsymbol{r}_2)\,\chi(s_1, s_2)$. The (total) spin determines the spin symmetry,

$$\begin{aligned} S = 1: &\qquad \chi_t = \begin{cases} |\uparrow\uparrow\rangle \\ \big(|\uparrow\downarrow\rangle + |\downarrow\uparrow\rangle\big)/\sqrt{2}, \\ |\downarrow\downarrow\rangle \end{cases} \quad \text{symmetric under } S_2, \\ S = 0: &\qquad \chi_s = \big(|\uparrow\downarrow\rangle - |\downarrow\uparrow\rangle\big)/\sqrt{2}, \quad \text{antisymmetric under } S_2. \end{aligned} \tag{B.14}$$

The fermionic antisymmetry determines the orbital symmetry

$$S = 1 \qquad \rightarrow \chi_t \text{ symmetric} \qquad \rightarrow \varphi_{\mathcal{A}} \text{ antisymmetric,} \tag{B.15}$$

$$S = 0 \qquad \rightarrow \chi_s \text{ antisymmetric} \qquad \rightarrow \varphi_{\mathcal{S}} \text{ symmetric.} \tag{B.16}$$

The connection between spin and orbital symmetry, which follows from Weyl's theorem and the Pauli exclusion principle, generalizes this fact for a system of N fermions. In general, the other irreducible representations of S_N will also appear, which are different from the one-dimensional representations S and A. The total spin determines the spin symmetry (under permutation with S_N) and via the Pauli principle the orbital symmetry (under S_N). Here, the terms spin and orbital symmetry refer to the 'quantum numbers' associated with the irreducible representation of the permutation symmetry (just as L is the angular momentum quantum number associated with the irreducible representation of rotational symmetry). The spin and orbital symmetries thus determine how the spin and orbital functions transform according to which irreducible representation of S_N they belong to. We anticipate the result of the decomposition of the Hilbert space of N spin-1/2 particles.

B.3 N Spin-1/2 Particles

For the decomposition of the spin Hilbert space of N particles into irreducible representations, we have

$$\begin{aligned}\left(\mathcal{H}_{1/2}\right)^{\otimes N} &= \oplus_S \, \mu_S(N)\, \mathcal{H}_S, \qquad S = \text{ spin quantum number,} \\ &= \oplus_S \, (2S+1)\, \mathcal{H}_{\mu_S}.\end{aligned} \tag{B.17}$$

Here, $\mathcal{H}_{1/2}$ is the two-dimensional Hilbert space of a spin-1/2 particle, $\mathcal{H}_{\mu_S}$ is the $\mu_S(N)$-dimensional representation space for the $\mu_S(N)$-dimensional irreducible representation of the permutations S_N, and $\mathcal{H}_S$ is the $(2S+1)$-dimensional representation space for the $(2S+1)$-dimensional irreducible representation of the rotation group $SU(2)$. The spin S determines the spin symmetry μ_S, thus specifying how the spin wave function transforms according to which irreducible representation of S_N it belongs to. If the spin S appears $\mu_S(N)$ times in the decomposition of $\left(\mathcal{H}_{1/2}\right)^{\otimes N}$, we obtain a $\mu_S(N)$-dimensional irreducible representation of S_N $(2S+1)$ times, i.e., the irreducible representation of S_N with symmetry μ_S appears exactly $(2S+1)$ times. Furthermore, the spin symmetry μ_S, via the condition of total antisymmetry for the total wave function Ψ, uniquely determines the orbital symmetry μ_B. We will explain and illustrate this result in the following. For this, we need the irreducible representations of S_N.

B.4 Irreducible Representations of S_N

We consider the decomposition of permutations into cycles, for example

$$\begin{aligned}\begin{pmatrix}1 & 2 & 3 & 4\\ 2 & 3 & 1 & 4\end{pmatrix} &= (1\,2\,3)(4) \\ \begin{pmatrix}1 & 2 & 3 & 4\\ 4 & 3 & 2 & 1\end{pmatrix} &= (1\,4)(2\,3) \\ \begin{pmatrix}1 & 2 & 3 & 4\\ 4 & 3 & 1 & 2\end{pmatrix} &= (1\,4\,2\,3)\end{aligned} \tag{B.18}$$

Each partition of N defines an equivalence class of S_N. For example, for $N=5$, we find 7 classes with the partitions $5=5,\ 4+1,\ 3+2,\ 3+1+1,\ 2+2+1,\ 2+1+1+1,\ 1+1+1+1+1$. To each of these partitions, we define a Young diagram with

h rows and k columns,

$S_5\colon 5 = 5$ 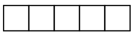 $[5]$

$= 4 + 1$ 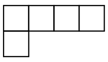 $[4, 1]$

$= 3 + 2$ 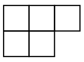 $[3, 2]$

$= 3 + 1 + 1$ 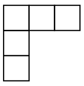 $[3, 1^2]$

$= 2 + 2 + 1$ 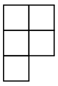 $[2^2, 1]$

$= 2 + 1 + 1 + 1$ 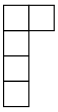 $[2, 1^3]$

$= 1 + 1 + 1 + 1 + 1$ 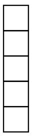 $[1^5]$

Each class or partition generates an irreducible representation of S_N. To each partition, there is an associated partition,

$$\text{Partition } \lambda \to \text{associated partition } \tilde{\lambda} \tag{B.19}$$

and an associated Young diagram,

$$\text{Young diagram } Y \to \text{ associated Young diagram } \tilde{Y} \tag{B.20}$$

which arises from swapping rows and columns, compare the following example with the corresponding mirror axis,

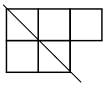

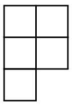

$Y_\lambda \qquad \to \qquad \tilde{Y}_\lambda = Y_{\tilde{\lambda}}$

$$\lambda = [3, 2] \qquad\qquad \tilde{\lambda} = [2^2, 1] \tag{B.21}$$

In addition to the Young diagrams, we define the Young tableaux by filling the Young diagrams Y with the numbers $1, 2, \dots N$:

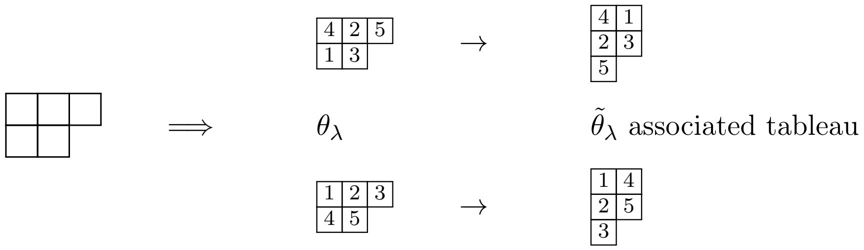

To each Young tableau, we define the row symmetrizer

$$\mathcal{S}_\lambda = \frac{1}{\lambda_1! \cdots \lambda_h!} \sum_{\pi_\lambda} \pi_\lambda \tag{B.22}$$

and the antisymmetrizer

$$\mathcal{A}_\lambda = \frac{1}{\lambda_1! \cdots \lambda_h!} \sum_{\pi_\lambda} (-1)^{\pi_\lambda} \pi_\lambda . \tag{B.23}$$

Here, π_λ permutes only elements within but not between the rows, i.e., each cycle in π_λ contains elements from only one row. As an example, consider the $\lambda = [3, 2]$ tableau[4]

$$\begin{array}{|c|c|c|}\hline 1 & 2 & 3 \\ \hline 4 & 5 \\ \cline{1-2}\end{array} . \tag{B.24}$$

$\mathcal{S}_\lambda$ is given by

$$\begin{aligned}\mathcal{S}_\lambda = \frac{1}{3!\,2!}\big[&(1)(2)(3)(4)(5) + (12)(3)(4)(5) + (1)(23)(4)(5) \\ &+ (13)(2)(4)(5) + (23)(1)(4)(5) \\ &+ (123)(4)(5) + \text{ all with } (45)\big]\end{aligned} \tag{B.25}$$

It holds that $\mathcal{S}_{\lambda=[N]} = \mathcal{S}$, $\mathcal{A}_{\lambda=[N]} = \mathcal{A}$. The associated symmetrizers permute elements in the columns,

$$\begin{aligned}\tilde{\mathcal{S}}_\lambda &= \frac{1}{\tilde{\lambda}_1! \cdots \tilde{\lambda}_k!} \sum_{\tau_\lambda} \tau_\lambda , \\ \tilde{\mathcal{A}}_\lambda &= \frac{1}{\tilde{\lambda}_1! \cdots \tilde{\lambda}_k!} \sum_{\tau_\lambda} (-1)^{\tau_\lambda} \tau_\lambda ;\end{aligned} \tag{B.26}$$

---

[4] For the $\lambda = [3, 2]$ tableau, $\lambda_1 = 3$ and $\lambda_2 = 2$.

the permutations τ_λ leave the columns of the Young tableau θ_λ invariant, i.e., τ_λ permutes only elements within the columns. In the above example, from $\lambda = [3, 2]$ we obtain $\tilde{\lambda} = [2^2, 1]$ and

$$\tilde{\mathcal{S}}_\lambda = \frac{1}{2!\,2!\,1!}\big[(1)(2)(3)(4)(5) + (14)(2)(3)(5) + (14)(25)(3) + (1)(4)(25)(3)\big].$$

It holds that $\tilde{\mathcal{S}}_{\lambda=[1^N]} = \mathcal{S}$, $\tilde{\mathcal{A}}_{\lambda=[1^N]} = \mathcal{A}$.

The irreducible symmetrizers

$$\begin{aligned} i_\lambda &= \mathcal{S}_\lambda \tilde{\mathcal{A}}_\lambda \quad \text{(irreducible symmetrizer)} \\ j_\lambda &= \tilde{\mathcal{A}}_\lambda \mathcal{S}_\lambda \quad \text{(irreducible antisymmetrizer)} \end{aligned} \tag{B.27}$$

define the irreducible representations of S_N (i_λ and j_λ define equivalent representations). The operators i_λ and j_λ are generalizations of $\mathcal{S}$ and $\mathcal{A}$, which define the one-dimensional representations S and A respectively. It holds[5]

$$\begin{aligned} i_{\lambda=[N]} &= \mathcal{S}_{[N]}\tilde{\mathcal{A}}_{[N]} = \mathcal{S}e = \mathcal{S}, \\ j_{\lambda=[N]} &= \tilde{\mathcal{A}}_{[N]}\mathcal{S}_{[N]} = e\mathcal{S} = \mathcal{S}, \\ i_{\lambda=[1^N]} &= \mathcal{S}_{[1^N]}\tilde{\mathcal{A}}_{[1^N]} = e\mathcal{A} = \mathcal{A}, \\ j_{\lambda=[1^N]} &= \tilde{\mathcal{A}}_{[1^N]}\mathcal{S}_{[1^N]} = \mathcal{A}e = \mathcal{A}. \end{aligned} \tag{B.28}$$

To find the dimension of the irreducible representation associated with Y, we write down all standard tableaux associated with Y. A standard tableau Y is a tableau in which the numbering of the cells is done such that the numbers increase from top to bottom in each column and from left to right in each row; again, we consider S_5 as an example,

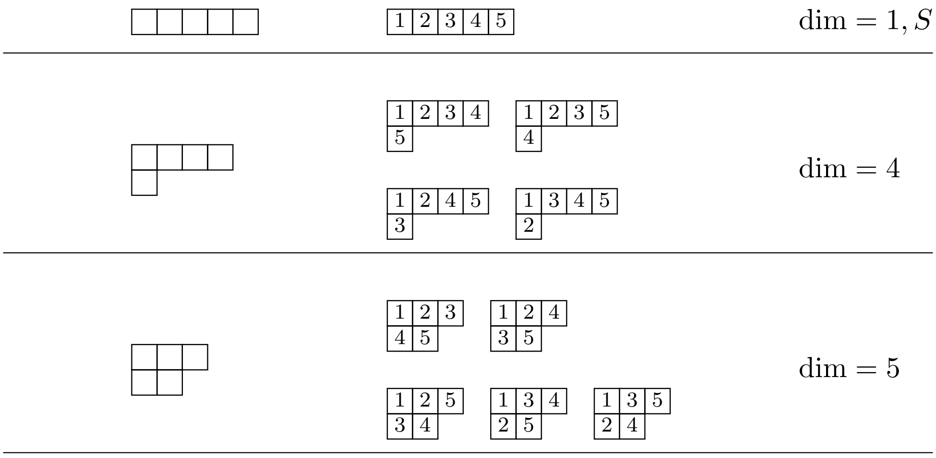

---

[5] e is the identity.

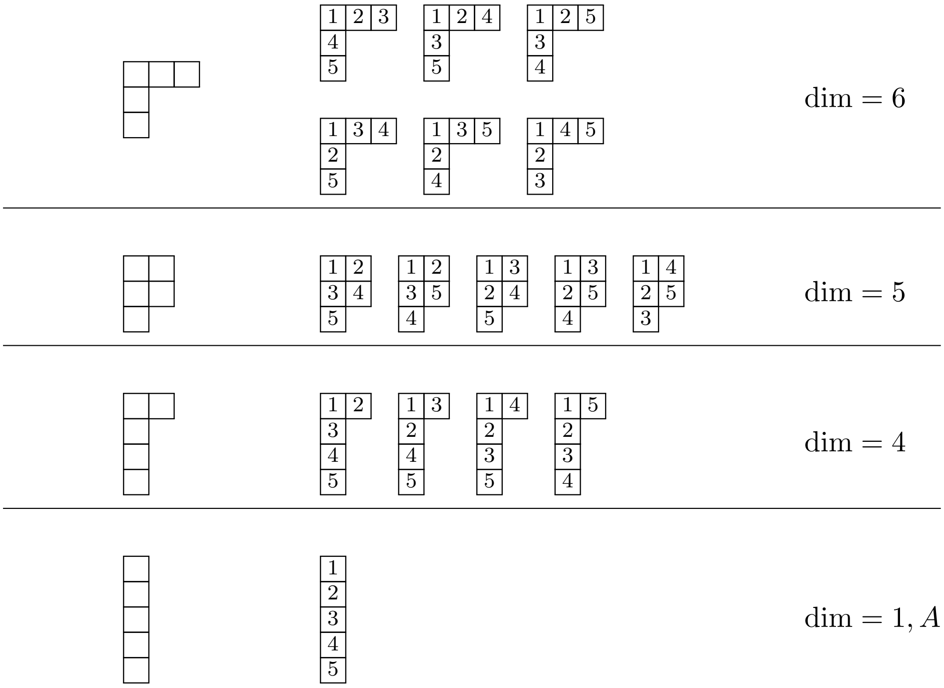

Here, the first representation is the so-called 'normal ordered tableau'. As expected, we obtain the usual relationship between the order of the group $N!$, the number of classes K, and the dimensions d_i of the irreducible representations, see (B.10),

$$N! = \sum_{i=1}^{K} d_i^2: \qquad 5! = 120 = 1 + 4^2 + 5^2 + 6^2 + 4^2 + 5^2 + 1. \tag{B.29}$$

Next, we use the above structures to define orbital and spin wave functions with well-defined symmetry under permutations.

B.5 Orbital Functions with Defined Symmetry

Let $u(x)$, $v(x)$, $w(x), \ldots$ be single-particle wave functions. We seek multi-particle functions of the type[6]

$$\Psi(1, \cdots, N) = \sum \cdots u(\cdot)v(\cdot)w(\cdot)\cdots \tag{B.30}$$

with well-defined symmetry, that is, defined symmetry under permutation. We assume that the functions $u(x)$, $v(x)$, $w(x), \ldots$ are orthonormal. In the following, we consider the cases $N = 2$ and $N = 3$.

---

[6] For the general case $u \neq v$, $v \neq w$, $u \neq w$, ….

***N* = 2:** Y is either $Y = \begin{array}{|c|c|}\hline \ & \ \\ \hline\end{array}$ thus S or $Y = \begin{array}{|c|}\hline \ \\ \hline \ \\ \hline\end{array}$ and thus A. The basis vectors of the irreducible representation are obtained by applying the (anti-)symmetrizers to the product state $\varphi(1,2) = u(1)\,v(2) = uv$[7] We suppress the arguments of the functions in the following and understand that the first function receives argument 1, the second argument 2, etc. Thus, we have

$$\begin{aligned}
S\colon \begin{array}{|c|c|}\hline 1 & 2 \\ \hline\end{array} \qquad & i_{[2]} = \mathcal{S}_{[2]} = [e + (12)]/2, \qquad e = (1)(2) \\
& i_{[2]}\varphi = (uv + vu)/2 \equiv \varphi_{\mathcal{S}}/\sqrt{2} \\
A\colon \begin{array}{|c|}\hline 1 \\ \hline 2 \\ \hline\end{array} \qquad & i_{[1^2]} = \tilde{\mathcal{A}}_{[1^2]} = [e - (12)]/2 \\
& i_{[1^2]}\varphi = (uv - vu)/2 \equiv \varphi_{\mathcal{A}}/\sqrt{2}.
\end{aligned} \tag{B.31}$$

***N* = 3:** There are three possible arrangements of tableaux Y: $Y = \begin{array}{|c|c|c|}\hline \ & \ & \ \\ \hline\end{array}$ (S), $Y = \begin{array}{|c|}\hline \ \\ \hline \ \\ \hline \ \\ \hline\end{array}$ (A), and the third variant $Y = \begin{array}{|c|c|}\hline \ & \ \\ \hline \ \\ \cline{1-1}\end{array}$ which we denote by Z.

$$\begin{aligned}
S\colon \begin{array}{|c|c|c|}\hline 1 & 2 & 3 \\ \hline\end{array} \qquad & i_{[3]} = [e + (12) + (23) + (13) + (123) + (132)]/6 \\
& i_{[3]}\varphi = (uvw + vuw + uwv + wvu + wuv + vwu)/6 \\
& \phantom{i_{[3]}\varphi} \equiv \varphi_{\mathcal{S}}/\sqrt{6}, \\
A\colon \begin{array}{|c|}\hline 1 \\ \hline 2 \\ \hline 3 \\ \hline\end{array} \qquad & i_{[1^3]} = [e - (12) - (23) - (13) + (123) + (132)]/6 \\
& i_{[1^3]}\varphi = (uvw - vuw - uwv - wvu + wuv + vwu)/6 \\
& \phantom{i_{[1^3]}\varphi} \equiv \varphi_{\mathcal{A}}/\sqrt{6}, \\
Z\colon \begin{array}{|c|c|}\hline 1 & 2 \\ \hline 3 \\ \cline{1-1}\end{array} \qquad & i_{[21]} = \mathcal{S}_{[21]}\tilde{\mathcal{A}}_{[21]} \\
& \phantom{i_{[21]}} = \frac{1}{2!\,1!}[e + (12)]\frac{1}{2!\,1!}[e - (13)] \\
& \phantom{i_{[21]}} = [e + (12) - (13) - (132)]/4 = e_{\mathcal{Z}}/4 \\
& i_{[21]}\varphi = (uvw + vuw - wvu - vwu)/4 \\
& \phantom{i_{[21]}\varphi} \equiv \varphi_{\mathcal{Z}}/2, \\
\begin{array}{|c|c|}\hline 1 & 3 \\ \hline 2 \\ \cline{1-1}\end{array} \qquad & i'_{[21]} = [e + (13) - (12) - (123)]/4 = e'_{\mathcal{Z}}/4 \\
& i'_{[21]}\varphi = (uvw + wvu - vuw - wuv)/4 \\
& \phantom{i'_{[21]}\varphi} \equiv \varphi'_{\mathcal{Z}}/2.
\end{aligned}$$

---

[7] In this chapter, we let the operator act on the product function. It permutes the factors $u, v, \ldots$ with π.

The application of all group elements to $\varphi_{\mathcal{Z}}$ generates a two-dimensional representation of S_3; we write $4\, i_{[21]} = e_{\mathcal{Z}}$, then it holds

$$\begin{aligned} e\, e_{\mathcal{Z}} &= e_{\mathcal{Z}}, \\ (12)e_{\mathcal{Z}} &= e_{\mathcal{Z}}, \\ (23)e_{\mathcal{Z}} &= (23) + (132) - (123) - (12) \equiv \bar{e}_{\mathcal{Z}}, \\ (31)e_{\mathcal{Z}} &= -e_{\mathcal{Z}} - \bar{e}_{\mathcal{Z}}, \\ (123)e_{\mathcal{Z}} &= -e_{\mathcal{Z}} - \bar{e}_{\mathcal{Z}}, \\ (132)e_{\mathcal{Z}} &= \bar{e}_{\mathcal{Z}}. \end{aligned} \tag{B.32}$$

Thus, $e_{\mathcal{Z}} = e + (12) - (13) - (132)$ and $\bar{e}_{\mathcal{Z}} = (23) + (132) - (123) - (12)$ respectively $\varphi_{\mathcal{Z}} = e_{\mathcal{Z}}\varphi/2$ and $\bar{\varphi}_{\mathcal{Z}} = \bar{e}_{\mathcal{Z}}\varphi/2$ span a two-dimensional irreducible representation (we call it Z) of S_3. Similarly,

$$\begin{aligned} e'_{\mathcal{Z}} &= e + (13) - (12) - (123), \\ \bar{e}'_{\mathcal{Z}} &= (23) + (123) - (132) - (23), \end{aligned} \tag{B.33}$$

span a second two-dimensional irreducible representation Z' of S_3; with $(e'_{\mathcal{Z}} e_{\mathcal{Z}}) = 0$, this representation is different from Z. The reduction of the 6-dimensional representation space spanned by the product wave functions $u(\pi_1)v(\pi_2)w(\pi_3)$, $\pi \in S_3$ thus yields

$$S \oplus A \oplus Z \oplus Z'. \tag{B.34}$$

The standard tableaux define a generating vector in each of these irreducible representations.

B.6 Spin Functions with Defined Symmetry

We consider the spin problem for N spin-1/2 fermions. The states $\chi_\uparrow$ and $\chi_\downarrow$ span the Hilbert space $\mathcal{H}_{1/2}$ and the product functions

$$\chi_{\sigma_1} \otimes \chi_{\sigma_2} \otimes \cdots \chi_{\sigma_N} \tag{B.35}$$

define a basis in the 2^N-dimensional product space $(\mathcal{H}_{1/2})^{\otimes N}$. The operators S^2, S_z, $\pi \in S_N$, with $\boldsymbol{S} = \sum_{i=1}^N \boldsymbol{s}_i$ being the total spin, commute pairwise and can thus be simultaneously 'diagonalized'; that is, we can simultaneously reduce the representations of $SU(2)$ (with quantum numbers S for $\boldsymbol{S}^2$ and M_S for S_z) and of S_N (with quantum numbers given by the standard tableaux).

$SU(2)$: $\mathcal{H}_{1/2}^{\otimes N} = \oplus_S\, \mu_S(N)\mathcal{H}_S$ according to the rules of spin addition. As examples, we again consider the cases $N = 2, \ldots, 5$:

$$
\begin{aligned}
N = 2\colon \qquad & \mathcal{H}_{1/2}^{\otimes 2} = \mathcal{H}_0 \oplus \mathcal{H}_1, \\
& \qquad \mu_0(2) = \mu_1(2) = 1. \\
N = 3\colon \qquad & \mathcal{H}_{1/2}^{\otimes 3} = \Big(\mathcal{H}_0 \oplus \mathcal{H}_1\Big) \otimes \mathcal{H}_{1/2}, \\
& \qquad = 2\mathcal{H}_{1/2} \oplus \mathcal{H}_{3/2}, \\
& \qquad \mu_{1/2}(3) = 2, \quad \mu_{3/2}(3) = 1. \\
N = 4\colon \qquad & \mathcal{H}_{1/2}^{\otimes 4} = \Big(\mathcal{H}_{1/2} \oplus \mathcal{H}_{1/2} \oplus \mathcal{H}_{3/2}\Big) \otimes \mathcal{H}_{1/2}, \\
& \qquad = 2\mathcal{H}_0 \oplus 3\mathcal{H}_1 \oplus \mathcal{H}_2, \\
& \qquad \mu_0(4) = 2, \quad \mu_1(4) = 3, \quad \mu_2(4) = 1. \\
N = 5\colon \qquad & \mathcal{H}_{1/2}^{\otimes 5} : \mu_{1/2}(5) = 5 \quad \mu_{3/2}(5) = 4, \quad \mu_{5/2}(5) = 1.
\end{aligned}
\tag{B.36}
$$

In general, it holds

$$
\mu_S(N) = \frac{(2S+1)N!}{(N/2 - S)!(N/2 + S + 1)!}
\tag{B.37}
$$

And thus

$$
\sum_S \mu_S(N) \cdot (2S+1) = 2^N, \qquad \mu_{\frac{N}{2}}(N) = 1.
\tag{B.38}
$$

S_N: In the spin problem, there are only two basis vectors $\chi_\uparrow$ and $\chi_\downarrow$. Thus, the Young tableaux can have at most 2 rows; otherwise, the corresponding projector onto the product basis vanishes. For example, if we had three rows,

$$
\begin{array}{|c|}\hline \uparrow \\ \hline \downarrow \\ \hline \downarrow \\ \hline \end{array} = i_{[1^3]}\, \chi_\uparrow \chi_\downarrow \chi_\downarrow = \mathcal{A}\, \chi_\uparrow \chi_\downarrow \chi_\downarrow
$$

the antisymmetrization of the two spin-↓ states would yield 0. Furthermore, in each column, the state ↑ must be paired with a state ↓, as the wave function also vanishes in this case. For example, the operation i_Z with $Z = \begin{array}{|c|c|}\hline 1 & 2 \\ \hline 3 \\ \cline{1-1} \end{array}$ applied to $\chi_\uparrow \chi_\downarrow \chi_\uparrow$ with 1 and 3 both in the state ↑ yields

$$
\begin{aligned}
i_{[2,1]}\, \chi_\uparrow \chi_\downarrow \chi_\uparrow &= \frac{1}{4}[e + (12)][e - (13)]\chi_\uparrow \chi_\downarrow \chi_\uparrow \\
&= \frac{1}{4}[e + (12)](\chi_\uparrow \chi_\downarrow \chi_\uparrow - \chi_\uparrow \chi_\downarrow \chi_\uparrow) = 0.
\end{aligned}
\tag{B.39}
$$

We parameterize a general Young diagram with two rows

$$\mu_S = \tag{B.40}$$

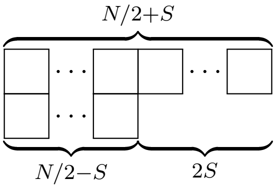

by the number

$$S = \begin{cases} 0, 1, \ldots \frac{N}{2}, & \text{N even,} \\ \frac{1}{2}, \frac{3}{2}, \ldots \frac{N}{2}, & \text{N odd,} \end{cases} \tag{B.41}$$

which later turns out to be the spin quantum number S. Through elementary combinatorics, one obtains the result that there are exactly $\mu_S(N)$ normal ordered Young tableaux with symmetry μ_S. In the following, we will prove that the representation space $\mathcal{H}_{1/2}^{\otimes N}$ contains the representation associated with the Young diagram μ_S exactly $(2S+1)$ times.

The space for the fixed magnetic quantum number (eigenvalue of S_z)

$$M_S = \nu \cdot \frac{1}{2} - (N-\nu) \cdot \frac{1}{2} = \nu - \frac{N}{2} \in \left\{ -\frac{N}{2}, -\frac{N}{2}+1, \ldots, \frac{N}{2} \right\}. \tag{B.42}$$

is spanned by the product states with ν times spin-$\uparrow$ and $(N-\nu)$ times spin-$\downarrow$ states, $\nu \in \{0, \ldots, N\}$. The vector space for fixed S_z is $N!/\nu!\,(N-\nu)!$-dimensional, as it is determined by specifying the particles with spin-$\uparrow$ (without regard to order). Within this space, we can seek orthogonal subspaces for fixed $\boldsymbol{S}^2$. The allowed values of S are

$$S = \frac{N}{2}, \frac{N}{2} - 1, |M_S| + 1, |M_S|; \tag{B.43}$$

there are $N/2 - |M_S| + 1$ different possibilities.[8]

As we have seen in the reduction to $SU(2)$, the subspace for fixed S, M_S appears exactly $\mu_S(N)$ times. It thus defines a $\mu_S(N)$-dimensional representation of S_N, since a permutation $\pi \in S_N$ does not change S or M_S. The subspace in $\mathcal{H}_{1/2}^{\otimes N}$ for fixed S, M_S therefore generates a representation space of S_N. We have seen that $\mu_S(N)$ also precisely indicates the number of normal ordered Young tableaux of symmetry μ_S. It is therefore a (correct) conjecture that the representation is irreducible, which we would like to prove in the following.

First, let us consider the case $S = M_S$. We need a wave function with maximum spin projection. For a fixed Young diagram of the form $\mu_S = [N/2+S, N/2-S]$, this is

---

[8] It holds $\sum_{S=|M_S|}^{N/2} \mu_S(N) = N!/\nu!(N-\nu)!$

achieved by the following wave function

$$\chi_{S,M_S} \propto \begin{array}{|c|c|c|c|c|c|}\hline \uparrow & \cdots & \uparrow & \uparrow & \cdots & \uparrow \\ \hline \downarrow & \cdots & \downarrow & \multicolumn{3}{c}{} \\ \cline{1-3} \multicolumn{3}{c}{} & \multicolumn{3}{c}{\underbrace{\hspace{4em}}_{2M_S}} \end{array} \tag{B.44}$$

The application of permutations π from S_N to the wave function yields the $\mu_S(N)$-dimensional subspace for fixed S and M_S, which transforms according to the irreducible representation μ_S of S_N. By applying the operator S_-, which commutes with all $\pi \in S_N$, we obtain equivalent representations, namely exactly $2S+1$ for $M_S = -S, \dots, S$. Thus, $\mathcal{H}_{1/2}^{\otimes N}$ decomposes as

$$\mathcal{H}_{1/2}^{\otimes N} = \bigoplus_S (2S+1)\mathcal{H}_{\mu_S}, \tag{B.45}$$

with $\mathcal{H}_{\mu_S}$ being the irreducible representation associated with μ_S.

We verify the result with the usual examples $N = 2, \dots, 5$,

$$N=2 \qquad \begin{array}{|c|c|}\hline \ & \ \\ \hline\end{array} \qquad \dim = 1, \qquad S = 1,\ \text{triplet} \begin{cases} \mathcal{S}|\uparrow\uparrow\rangle, \\ \mathcal{S}|\uparrow\downarrow\rangle, \\ \mathcal{S}|\downarrow\downarrow\rangle, \end{cases}$$

$$\begin{array}{|c|}\hline \ \\ \hline \ \\ \hline\end{array} \qquad \dim = 1, \qquad S = 0,\ \text{singlet} \ \left\{\mathcal{A}|\uparrow\downarrow\rangle\right. .$$

$$N=3 \qquad \begin{array}{|c|c|c|}\hline \ & \ & \ \\ \hline\end{array} \qquad \dim = 1, \qquad S = \tfrac{3}{2},$$

$$\begin{array}{|c|c|}\hline \ & \ \\ \hline \multicolumn{1}{|c|}{\ } & \multicolumn{1}{c}{} \\ \cline{1-1}\end{array} \qquad \dim = 2 = \mu_{\frac{1}{2}}(3), \qquad S = \tfrac{1}{2}.$$

$$N=4 \qquad \begin{array}{|c|c|c|c|}\hline \ & \ & \ & \ \\ \hline\end{array} \qquad \dim = 1 = \mu_2(4), \qquad S = 2,$$

$$\begin{array}{|c|c|c|}\hline \ & \ & \ \\ \hline \multicolumn{1}{|c|}{\ } & \multicolumn{2}{c}{} \\ \cline{1-1}\end{array} \qquad \begin{array}{|c|c|c|}\hline 1 & 2 & 3 \\ \hline \multicolumn{1}{|c|}{4} & \multicolumn{2}{c}{} \\ \cline{1-1}\end{array} \quad \begin{array}{|c|c|c|}\hline 1 & 3 & 4 \\ \hline \multicolumn{1}{|c|}{2} & \multicolumn{2}{c}{} \\ \cline{1-1}\end{array} \quad \begin{array}{|c|c|c|}\hline 1 & 2 & 4 \\ \hline \multicolumn{1}{|c|}{3} & \multicolumn{2}{c}{} \\ \cline{1-1}\end{array}$$

$$\dim = 3 = \mu_1(4), \qquad S = 1,$$

$$\begin{array}{|c|c|}\hline \ & \ \\ \hline \ & \ \\ \hline\end{array} \qquad \begin{array}{|c|c|}\hline 1 & 2 \\ \hline 3 & 4 \\ \hline\end{array} \quad \begin{array}{|c|c|}\hline 1 & 3 \\ \hline 2 & 4 \\ \hline\end{array}$$

$$\dim = 2 = \mu_0(4), \qquad S = 0.$$

$$N=5 \qquad \begin{array}{|c|c|c|c|c|}\hline \ & \ & \ & \ & \ \\ \hline\end{array} \qquad \mu_{\frac{5}{2}}(5) = 1, \qquad S = \tfrac{5}{2},$$

$$\begin{array}{|c|c|c|c|}\hline \ & \ & \ & \ \\ \hline \multicolumn{1}{|c|}{\ } & \multicolumn{3}{c}{} \\ \cline{1-1}\end{array} \qquad \mu_{\frac{3}{2}}(5) = 4, \qquad S = \tfrac{3}{2},$$

$$\begin{array}{|c|c|c|}\hline \ & \ & \ \\ \hline \ & \ & \multicolumn{1}{c}{} \\ \cline{1-2}\end{array} \qquad \mu_{\frac{1}{2}}(5) = 5, \qquad S = \tfrac{1}{2}.$$

Thus, we have the decompositions (Weyl's theorem, Schur-Weyl duality)

$$\mathcal{H}_{1/2}^{\otimes N} = \bigoplus_S \mu_S(N)\mathcal{H}_S = \bigoplus_S (2S+1)\mathcal{H}_{\mu_S}; \tag{B.46}$$

the spin S determines the Young diagram μ_S and thus the spin symmetry. The representation space $\mathcal{H}_{\mu_S}$ is spanned by the $|S, M_S\rangle$ for fixed S and M_S.

As a conclusion, here is the example for 4 particles with spin 1/2,

$$\begin{aligned}\mathcal{H}_{1/2}^{\otimes 4} &\overset{SU(2)}{=} 2\mathcal{H}_0 \oplus 3\mathcal{H}_1 \oplus \mathcal{H}_2 \\ &\overset{S_4}{=} \mathcal{H}_{\mu_0} \oplus 3\mathcal{H}_{\mu_1} \oplus 5\mathcal{H}_{\mu_2}\end{aligned}$$

$=$

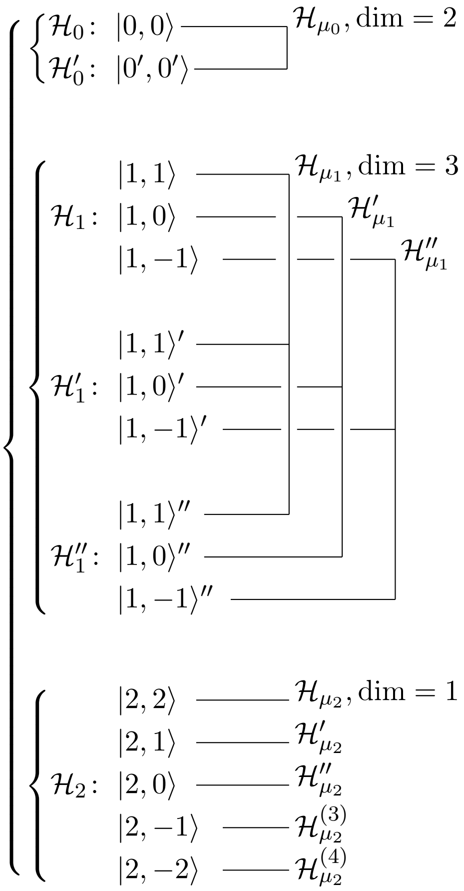

with

$$\mu_0 = \ydiagram{2,2}, \qquad \mu_1 = \ydiagram{3,1}, \qquad \mu_2 = \ydiagram{4},$$
$$\mu_0(4) = 2, \qquad \mu_1(4) = 3, \qquad \mu_2(4) = 1.$$

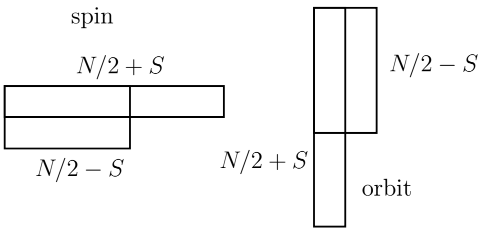

Figure B.1: Young tableaux associated with the spin and orbital wave functions for N spin-$1/2$ fermions with total spin S.

B.7 Spin and Orbital

We consider an N-particle system with total spin S. The spin wave function has the symmetry μ_S. Let the symmetry of the orbital function be given by the diagram μ_B. It holds: The tensor product $\mu_B \otimes \mu_S$ of the two representations contains the representation

$$\begin{aligned} &(\text{Bosons}) \quad S \Leftrightarrow \mu_B = \mu_S \\ &(\text{Fermions}) \quad A \Leftrightarrow \mu_B = \tilde{\mu}_S . \end{aligned} \tag{B.47}$$

It follows that the spin symmetry, given by μ_S, determines the orbital symmetry μ_B: For bosons, the orbital symmetry corresponds to the spin symmetry, $\mu_B = \mu_S$, while for fermions, the orbital and spin symmetries are associated with each other, $\mu_B = \tilde{\mu}_S$, see Figure B.1.

As an example, we consider $N = 3$ electrons in the p-shell for which we want to explicitly find a wave function with $S = 1/2$. As we know, the spin determines the spin representation

$$\mu_S = [21] = \begin{array}{|c|c|}\hline & \\ \hline & \multicolumn{1}{c}{} \\ \cline{1-1}\end{array} \tag{B.48}$$

We also know that the state with $M_S = 1/2$ corresponds to the Young tableau $\begin{array}{|c|c|}\hline \uparrow & \uparrow \\ \hline \downarrow & \multicolumn{1}{c}{} \\ \cline{1-1}\end{array}$. Thus, we obtain a wave function for $S = 1/2$, $M_S = 1/2$

$$\begin{aligned} \chi_{1/2,1/2}(s_1,s_2,s_3)/\sqrt{2} &= i_{[21]}\, \chi_\uparrow(s_1)\chi_\uparrow(s_2)\chi_\downarrow(s_3) = \mathcal{S}_{\mu_S}\tilde{\mathcal{A}}_{\mu_S}\chi_\uparrow(s_1)\chi_\uparrow(s_2)\chi_\downarrow(s_3) \\ &= \frac{1}{2}\mathcal{S}_{\mu_S}[\chi_\uparrow(s_1)\chi_\uparrow(s_2)\chi_\downarrow(s_3) - \chi_\uparrow(s_3)\chi_\uparrow(s_2)\chi_\downarrow(s_1)] \\ &= \frac{1}{4}[\chi_\uparrow(s_1)\chi_\uparrow(s_2)\chi_\downarrow(s_3) + \chi_\uparrow(s_2)\chi_\uparrow(s_1)\chi_\downarrow(s_3) \\ &\quad - \chi_\uparrow(s_3)\chi_\uparrow(s_2)\chi_\downarrow(s_1) - \chi_\uparrow(s_2)\chi_\uparrow(s_3)\chi_\downarrow(s_1)] \\ &= \frac{1}{2}[\chi_\uparrow(s_1)\chi_\uparrow(s_2)\chi_\downarrow(s_3) - \chi_\downarrow(s_1)\chi_\uparrow(s_2)\chi_\uparrow(s_3)] \end{aligned}$$

We know that the space for fixed S is exactly $[\mu_S(N) = 2]$-fold degenerate. We obtain a second basis state by applying the transposition $(s_2 \leftrightarrow s_3)$ to $\chi_{1/2,1/2}$ with the result

$$\chi'_{1/2,1/2}(s_1,s_2,s_3) = \frac{1}{\sqrt{2}}[\chi_\uparrow(s_1)\chi_\downarrow(s_2)\chi_\uparrow(s_3) - \chi_\downarrow(s_1)\chi_\uparrow(s_2)\chi_\uparrow(s_3)]; \tag{B.49}$$

The two states χ and χ' are linearly independent and therefore lie in the different representations Z and Z' of (B.34). The application of other elements of S_3 to χ will always yield linear combinations of χ and χ'. Of course, the spin wave functions for a given S and M_S can also be found using a Clebsch-Gordan table.

Next, we want to determine the possible orbital wave functions. We know that the orbital representation μ_B must correspond to the associated diagram $\tilde{\mu}_S$. In our case, we have

$$\mu_B = \tilde{\mu}_S = \mu_S = \ydiagram{2,1}\,. \tag{B.50}$$

In the p-shell, there are wave functions with $M_L = -1, 0, 1$. We denote the wave functions by φ_{M_L}. Since in a column of the Young tableau each quantum number can only occur once (see the discussion on spin), the following states are allowed

$$\underbrace{\begin{array}{ccccccccc} & \begin{ytableau} 1 & 1 \\ 0 \end{ytableau} & \begin{ytableau} 1 & 1 \\ -1 \end{ytableau} & \begin{ytableau} 1 & 0 \\ 0 \end{ytableau} & \begin{ytableau} 1 & 0 \\ -1 \end{ytableau} & \begin{ytableau} 1 & -1 \\ 0 \end{ytableau} & \begin{ytableau} 1 & -1 \\ -1 \end{ytableau} & \begin{ytableau} 0 & 0 \\ -1 \end{ytableau} & \begin{ytableau} 0 & -1 \\ -1 \end{ytableau} \\ M_L = & 2 & 1 & 1 & 0 & 0 & -1 & -1 & -2 \end{array}}_{\text{8 possibilities (corresponding to } L=1 \text{ and } L=2\text{).}} \tag{B.51}$$

We only consider the case with $M_L = 2$.[9] For this, we must symmetrize the orbital wave function $\varphi_1(\boldsymbol{r}_1)\varphi_0(\boldsymbol{r}_2)\varphi_1(\boldsymbol{r}_3)$ with the associated Young tableau $\begin{ytableau} 1 & 3 \\ 2 \end{ytableau}$ and obtain

$$\begin{aligned} \varphi_{2,2}(\boldsymbol{r}_1, \boldsymbol{r}_2, \boldsymbol{r}_3) &= \frac{1}{\sqrt{2}} i'_{[2,1]} \varphi_1(\boldsymbol{r}_1)\varphi_0(\boldsymbol{r}_2)\varphi_1(\boldsymbol{r}_3) \\ &= \frac{1}{\sqrt{2}} [\varphi_1(\boldsymbol{r}_1)\varphi_0(\boldsymbol{r}_2)\varphi_1(\boldsymbol{r}_3) - \varphi_0(\boldsymbol{r}_1)\varphi_1(\boldsymbol{r}_2)\varphi_1(\boldsymbol{r}_3)]. \end{aligned} \tag{B.52}$$

We know that the product $\Psi = \varphi_{2,2}\chi_{1/2,1/2}$ must contain the antisymmetric representation. To obtain an antisymmetric wave function, we therefore only need to antisymmetrize the wave function

$$\begin{aligned} \Psi^{\mathcal{A}} &\propto \mathcal{A}\varphi_{2,2}(\boldsymbol{r}_1, \boldsymbol{r}_2, \boldsymbol{r}_3)\chi_{1/2,1/2}(s_1, s_2, s_3) \\ &= \mathcal{A}\varphi_{1\uparrow}(x_1)\varphi_{0\uparrow}(x_2)\varphi_{1\downarrow}(x_3) - \mathcal{A}\varphi_{1\downarrow}(x_1)\varphi_{0\uparrow}(x_2)\varphi_{1\uparrow}(x_3) \\ &\quad - \mathcal{A}\varphi_{0\uparrow}(x_1)\varphi_{1\uparrow}(x_2)\varphi_{1\downarrow}(x_3) + \underbrace{\mathcal{A}\varphi_{0\downarrow}(x_1)\varphi_{1\uparrow}(x_2)\varphi_{1\uparrow}(x_3)}_{=0} \\ &= 3\mathcal{A}\varphi_{1\uparrow}(x_1)\varphi_{0\uparrow}(x_2)\varphi_{1\downarrow}(x_3) \end{aligned} \tag{B.53}$$

where $\varphi_{M_L M_S}(\boldsymbol{r}, s) = \varphi_{M_L}(\boldsymbol{r})\chi_{M_S}(s)$. The wave function $\Psi^{\mathcal{A}}$ is now the fermionic three-particle wave function for $M_S = S = 1/2$ and $M_L = L = 2$.

---

[9] Since M_L is maximal, we also know that this is a state with $L = 2$.

Appendix C

$SU(n)$ with Young Diagrams

In Appendix B, we saw that the representations of $SU(2)$ can be characterized using Young diagrams. For this, we used N copies of $SU(2)$, so that in addition to the action of $SU(2)$ (on all copies simultaneously), the action of the symmetric group S_N is also defined. The representations of $SU(2)$ then follow from those of S_N (described by the Young diagrams with Weyl's theorem). This approach can be generalized to $SU(n)$. In this chapter, we will understand aspects of the representation theory of $SU(n)$ and in particular $SU(3)$ using Young diagrams. As a physical application, we will derive the multiplet structure of the quark model (the "Eightfold Way") at the end. We begin this chapter by formulating the results of the last section in a somewhat more general way for the case of $SU(n)$.

C.1 $SU(n)$ tensors and the Schur-Weyl duality

To describe the action of the group $SU(n)$, we need an n-dimensional Hilbert space $\mathcal{H}$ with the basis $|1\rangle, \ldots, |n\rangle$. Thus, we have

$$U|j\rangle = \sum_{i=1}^{n} U_{ij}|i\rangle, \qquad U \in SU(n), \quad j = 1, \ldots, n\,. \tag{C.1}$$

This representation is referred to as the defining (or fundamental) representation of $SU(n)$. In the case of $SU(2)$, the above representation is the spin-1/2 representation with basis vectors $|1\rangle = |{\uparrow}\rangle$ and $|2\rangle = |{\downarrow}\rangle$.

For systems of N identical particles, one considers the product space $\mathcal{H}^{\otimes N} = \mathcal{H} \otimes \cdots \otimes \mathcal{H}$. This transforms under the so-called product representation $U^{\otimes N}$ of $SU(n)$, i.e., each basis vector transforms with the defining representation, and thus we have

$$U^{\otimes N} = \underbrace{U \otimes \cdots \otimes U}_{N \text{ times}}\,. \tag{C.2}$$

This product representation is generally reducible, and an important task in physics is to determine which irreducible representations are contained in $\mathcal{H}^{\otimes N}$. In relation to $SU(2)$, this question means which spins can occur in an N-particle system. More generally, one can use this approach to obtain (all) irreducible representations of the Lie group $SU(n)$ with the help of the (known) representation theory of S_N.

To do this, we define the action of the symmetric group S_N on the product space $\mathcal{H}^{\otimes N}$ by[1]

$$\pi|j_1,\dots,j_N\rangle = |\pi(j_1),\dots,\pi(j_N)\rangle. \tag{C.3}$$

For what follows, it is crucial that the actions of S_N and $SU(n)$ commute. In fact, we obtain

$$\begin{aligned}
\pi U^{\otimes N}\,|j_1,\dots,j_N\rangle &= \sum_{i_1,\dots,i_N} \pi\,|i_1,\dots,i_N\rangle U_{i_1 j_1}\cdots U_{i_N j_N} \\
&= \sum_{i_1,\dots,i_N} |\pi(i_1),\dots,\pi(i_N)\rangle U_{i_1 j_1}\cdots U_{i_N j_N} \\
&= \sum_{i_1,\dots,i_N} |\pi(i_1),\dots,\pi(i_N)\rangle U_{\pi(i_1)\pi(j_1)}\cdots U_{\pi(i_N)\pi(j_N)} \\
&= U^{\otimes N}|\pi(j_1),\dots,\pi(j_N)\rangle = U^{\otimes N}\pi\,|j_1,\dots,j_N\rangle\,.
\end{aligned}$$

The crucial step occurs from the second to the third line, where the U matrices are rearranged by utilizing the fact that π is a bijection. Thus, the representations of S_N can be reduced simultaneously with those of $SU(n)$ on the product space $\mathcal{H}^{\otimes N}$.

From the last chapter, we know that the irreducible representations of S_N are determined by Young diagrams λ. The corresponding basis vectors in $\mathcal{H}^{\otimes N}$ are generated by the irreducible symmetrizers i_λ. The number of standard tableaux determines the dimension $\lambda(N)$ of the irreducible subspace. When projecting the vector space $\mathcal{H}^{\otimes N}$ onto a specific standard tableau, one generally obtains a d_λ-dimensional subspace with $d_\lambda = 0, 1, \dots$. Each basis vector in this subspace now generates its own irreducible representation of the type λ under S_N, see Chapter B.5. Thus, d_λ does not depend on the chosen tableau, and we obtain the reduction

$$\mathcal{H}^{\otimes N} = \bigoplus_\lambda d_\lambda \mathcal{H}_\lambda \tag{C.4}$$

into irreducible representations $\mathcal{H}_\lambda$ of S_N. It holds that $\sum_\lambda d_\lambda \lambda(N) = \dim(\mathcal{H}^{\otimes N}) = n^N$. It is even possible to determine d_λ in closed form. One obtains after a longer derivation[2]

$$d_\lambda = \frac{D(l_1, l_2, \dots l_N)}{D(n-1, n-2, \dots, 0)} \quad . \quad D(l_1, l_2, \dots, l_N) = \prod_{i<j}(l_i - l_j) \tag{C.5}$$

---

[1] On the right-hand side, we denote the result after swapping the factors, i.e., $(123)|u, v, w\rangle = |w, u, v\rangle$; in other words, $\pi|j_1,\dots,j_N\rangle = |j_{\pi^{-1}(1)},\dots j_{\pi^{-1}(N)}\rangle$.

[2] See T. Inui, Y. Tanabe, Y. Onodera 'Group Theory and Its Applications in Physics', Chapter 15.5.

with $l_j = \lambda_j + n - j$ and λ_j being the length of the j-th row in λ.

Since π and $U^{\otimes N}$ commute, π cannot change the quantum numbers that characterize the irreducible representations of $SU(n)$. Thus, the irreducible representations of S_N also have fixed quantum numbers under $SU(n)$. Exactly this was seen for $SU(2)$: The irreducible representations of S_N, described by μ_S, have a fixed S. Furthermore, $U^{\otimes N}$ does not change the type of a state, so the representations of $SU(n)$ have a fixed type. For $SU(2)$, this even means that the spin S uniquely determines the type $\lambda = \mu_S$ of the state. Thus, the dimension $(2S+1)$ of the representation $\mathcal{H}_S$ under $SU(2)$ is exactly the multiplicity d_λ with which the type μ_S appears. This unique relationship between the irreducible representations continues for the groups $SU(n)$.

From (C.4), we know that the $\lambda(N)$-dimensional irreducible representation $\mathcal{H}_\lambda$ of S_N with type λ appears d_λ times. Under the action of $SU(n)$, the irreducible representation $\mathcal{H}^\lambda$ is assigned to the type λ.[3] Since the action of S_N commutes with that of $SU(n)$, the irreducible representation $\mathcal{H}^\lambda$ appears $\lambda(N)$ times. Thus, we obtain the decomposition (Schur-Weyl duality)

$$\mathcal{H}^{\otimes N} = \underbrace{\bigoplus_\lambda \lambda(N)\, \mathcal{H}^\lambda}_{SU(n)} = \underbrace{\bigoplus_\lambda d_\lambda\, \mathcal{H}_\lambda}_{S_N} . \tag{C.6}$$

From the dimension, it follows that $\lambda(N)\dim(\mathcal{H}^\lambda) = d_\lambda \dim(\mathcal{H}_\lambda) = d_\lambda \lambda(N)$. Thus, the dimension $\dim(\mathcal{H}^\lambda) = d_\lambda$ of the irreducible representations of $SU(n)$ is determined by (C.5). The representation theory of $SU(n)$ thus follows from that of S_N.

The connection between Young diagrams and the irreducible representations of $SU(n)$ is called Schur-Weyl duality. The remarkable thing about this is that one can determine the irreducible representations of $SU(n)$ without studying continuous Lie groups. Everything follows from the representation theory of the finite-dimensional symmetric group S_N. In the next sections, we will discuss this in more detail using $SU(2)$ and $SU(3)$ as examples.

C.2 $SU(2)$ with Young Diagrams

We will first examine $SU(2)$ using the methods developed in the last section to prepare for the analysis of $SU(3)$. The defining representation of $SU(2)$ is spin-1/2, so there are only two basis vectors $|\uparrow\rangle, |\downarrow\rangle$. Thus, the Young diagrams can have a maximum of 2 rows, otherwise the antisymmetrizer always produces a 0. Therefore, for a fixed N, each Young diagram can be completely described by specifying a single

---

[3] It can be shown that this assignment is unique.

constant S (the spin). As already shown in (B.40), we use the convention [4]

$$\mu_S = \overbrace{\begin{matrix} \square \cdots \square & \square \cdots \square \\ \underbrace{\square \cdots \square}_{N/2-S} & \underbrace{}_{2S} \end{matrix}}^{N/2+S} . \tag{C.7}$$

For fixed N, $2S$ thus describes the "overhang" of the Young diagram. The spin $S = 0, \frac{1}{2}, 1, \frac{3}{2}, 2, \ldots$ is directly related to the Casimir operator $\boldsymbol{S}^2$ of $SU(2)$, which determines the irreducible representations of $SU(2)$. A Casimir operator is an operator that commutes with all generators of the Lie group, here with S_x, S_y, S_z. To label the states in the representations of $SU(2)$, one chooses, in addition to $\boldsymbol{S}^2$, another operator, conventionally S_z, which uniquely determines the various basis states in the representation. Here, the basis states $|S, M_S\rangle$ in $\mathcal{H}^{\mu_S} \equiv \mathcal{H}_S$ have the additional quantum number $M_S = -S, \ldots, S$. The dimension of the representation associated with S is immediately obtained using equation (C.5)

$$\begin{aligned} d_{\mu_S} &= \frac{D(l_1, l_2)}{D(1,0)} = l_1 - l_2 = (\mu_1 + 2 - 1) - (\mu_2 + 2 - 2) \\ &= (\mu_1 - \mu_2) + 1 = 2S + 1. \end{aligned}$$

Through elementary combinatorics (just like in B), one can now also determine $\mu_S(N) = \dim(\mathcal{H}_\lambda)$. In summary, we find the already known decomposition:

$$\mathcal{H}^{\otimes N} = \bigoplus_S \mu_S(N)\, \mathcal{H}_S = \bigoplus_S (2S+1)\, \mathcal{H}_{\mu_S} \tag{C.8}$$

As seen in the last chapter, one can also determine basis vectors for the spin-S representation using Schur-Weyl duality.

C.3 $SU(3)$ with Young Diagrams

For the group $SU(3)$, the procedure is completely analogous. Physically, this group describes, for example, the flavor symmetry of quarks. The fundamental representation of $SU(3)$ is 3-dimensional, and the basis vectors are denoted by $|u\rangle$ (up quark), $|d\rangle$ (down quark), and $|s\rangle$ (strange quark).

Since there are only 3 different basis vectors, the Young diagrams can have a maximum of 3 rows. In this case, for fixed N, two numbers p and q are needed to uniquely specify a Young diagram. In the literature on Lie group theory, the tuple (p, q) is

---

[4] The constant must be chosen such that the result for d_λ is independent of N.

referred to as Dynkin indices. We define the type as

$$\lambda_{(p,q)} = (q,p) =$$

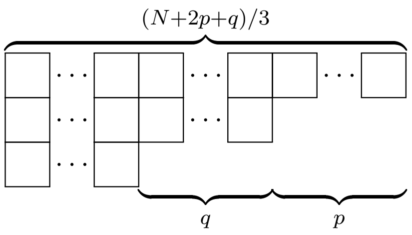

$$, \tag{C.9}$$

where $p, q = 0, 1, 2, \dots$ describes the lengths of the overhangs.

Just like for $SU(2)$, the numbers (p,q) are directly related to the Casimir operators of the group. Thus, the irreducible representations of $SU(3)$ are determined by two Casimir operators, one for p and one for q. We denote this irreducible representation by $\mathcal{H}^{\lambda} = \mathcal{H}^{(p,q)}$. To specify the states within a representation $\mathcal{H}^{(p,q)}$, another arbitrary element of the Lie algebra is chosen, yielding a complete set of quantum numbers.[5]

The dimension of the representation $\mathcal{H}^{(p,q)}$ is again determined using equation (C.5) as (again, $d_{(p,q)}$ does not depend on N)

$$\begin{aligned} d_{(p,q)} &= \frac{D(l_1,l_2,l_3)}{D(2,1,0)} = \frac{(l_1-l_2)\cdot(l_1-l_3)\cdot(l_2-l_3)}{(2-1)\cdot(2-0)\cdot(1-0)} \\ &= \frac{1}{2}(p+1)(q+1)(p+q+2). \end{aligned} \tag{C.10}$$

This central result of Lie group theory is again obtained directly from the representation theory of S_N.

As a simple example, consider the fundamental representation of $SU(3)$, described by the diagram $\square$. This diagram corresponds to $N = 1, (p,q) = (1,0)$, so that the dimension with equation (C.10) yields $d_{(1,0)} = 3$ as expected.

For $N = 2$, there are now two possible diagrams: On the one hand, $\square\square$ with $(p,q) = (2,0)$ and $d_{(2,0)} = 6$, and on the other hand, $\begin{smallmatrix}\square\\\square\end{smallmatrix}$ with $(p,q) = (0,2)$ and $d_{(0,2)} = 6$. Just like for $SU(2)$, one can now determine basis vectors with Young symmetrizers that transform under an irreducible representation of $SU(3)$.

The extension of the procedure to $SU(n)$ is relatively clear. The Young diagrams of $SU(n)$ can have a maximum of n rows, as the fundamental representation has exactly n basis vectors. For fixed N, exactly $n-1$ constants are needed to completely describe a Young diagram of $SU(n)$. Thus, $SU(n)$ has a total of $(n-1)$ Casimir operators. A Young diagram receives an index $(p_1, p_2, \dots, p_{n-1})$, by which it is uniquely described. The constants $(p_1, p_2, \dots, p_{n-1})$ must again be defined such that the dimension d_λ becomes independent of N, which concretely means that the constants describe the overhang in the diagram. Then, the dimensions of the representations, as well as basis vectors, can be easily determined using the Young diagrams.

---

[5] This is also referred to in the literature as the Cartan subalgebra.

C.4 Conjugate Representation

In addition to the normal irreducible representations, conjugate irreducible representations $\overline{U} = U^*$ are also important in physics.[6] Here, U^* denotes the complex conjugate matrix. Starting from an irreducible representation $\mathcal{H}_\lambda$, it is clear that $\overline{\mathcal{H}_\lambda}$ is also irreducible. Therefore, the question immediately arises as to whether $\mathcal{H}_\lambda$ and $\mathcal{H}_{\overline{\lambda}} \equiv \overline{\mathcal{H}_\lambda}$ are the same irreducible representation.[7]

The conjugate representation $\overline{\lambda}$ can also be easily described with Young diagrams. In $SU(n)$, for fixed N, a Young diagram λ is described by a tuple $\boldsymbol{p} = (p_1, \dots, p_{n-1})$ of the "overhangs". The conjugate representation corresponds simply to the conjugate Young diagram $\overline{\lambda}$, which is given by $\overline{\boldsymbol{p}} = (p_{n-1}, p_{n-2}, \dots, p_1)$, where a different N may be needed to obtain a valid Young diagram. Note that conjugation is an involution, i.e., $\overline{\overline{\lambda}} = \lambda$.

In the example of $SU(2)$, there is only one overhang. Thus, the conjugate representation is equivalent to the normal representation. In fact, for the fundamental representation[8] of $SU(2)$, we have

$$U^* = \sigma_2 U \sigma_2, \qquad U \in SU(2)\,. \tag{C.11}$$

This nontrivial relationship is also written as $\mathcal{H}_{1/2} \simeq \overline{\mathcal{H}_{1/2}}$. To show it, one can use the parameterization $U = \exp(i\boldsymbol{n}\cdot\boldsymbol{\sigma})$, $\boldsymbol{n} \in \mathbb{R}^3$, along with the property $\sigma_j^* = -\sigma_2\sigma_j\sigma_2$ of the Pauli matrices.

However, for $SU(3)$, the conjugate representation differs from the normal representation. As an example, consider the (1,0) and (1,1) representations of $SU(3)$. We obtain

$$\overline{(1,0)} = \overline{\ydiagram{1}} = \ydiagram{1,1} = (0,1) \tag{C.12}$$

$$\overline{(1,1)} = \overline{\ydiagram{2,1,1}} = \ydiagram{2,1,1} = (1,1) \tag{C.13}$$

In general, it holds that $\overline{(p,q)} = (q,p)$. The indices p and q are thus conjugate to each other.

While in $SU(2)$ the different representations can be identified solely by their dimension, this is not possible for $SU(3)$. In fact, different combinations of (p,q) lead to the same dimension. With the concept of conjugate representations, however, it is possible to describe the physically relevant "small" representations (p,q) with $pq \leq 3$ solely by

---

[6] If $|j\rangle$ transforms with U, then $\langle j|$ transforms with U^*.

[7] Formally, this means that there exists a unitary transformation T such that $TUT^\dagger = U^*$ for all U.

[8] This suffices, as the "higher" representations are generated by forming tensor products of the fundamental representation.

their dimension $d_{(p,q)} = \dim \mathcal{H}^{(p,q)}$. In particle physics, one often uses the convention

$$\mathcal{H}^{(p,q)} \equiv \begin{cases} \boldsymbol{d}_{(p,q)}, & p \geq q \\ \overline{\boldsymbol{d}_{(p,q)}}, & p < q\,. \end{cases} \tag{C.14}$$

That is, one writes $\mathcal{H}^{(1,0)} = \mathbf{3}$ and $\mathcal{H}^{(0,1)} = \overline{\mathbf{3}}$, instead of specifying the tuple (p, q). This notation is particularly useful when discussing the transformation of particles and antiparticles in product representations. In fact, the up, down, and strange quarks (by definition) transform with the fundamental representation **3**. Thus, the corresponding antiparticles transform with $\overline{\mathbf{3}}$.

C.5 Product Representations and the Quark Model

Young diagrams allow for the graphical reduction of product representations. We want to explain this in this chapter using the example of $SU(3)$ to better understand the quark model. So far, we have always reduced tensor products of the fundamental representation of $SU(3)$. Graphically represented, this means that we have decomposed tensor products of $\square$ into direct sums. For example, for $SU(3)$, we have

$$3 \otimes 3 = \square \otimes \square = \square\!\square \oplus \begin{array}{c}\square\\[-4pt]\square\end{array}. \tag{C.15}$$

This result is obtained directly from the following rule for the graphical tensor product of an irreducible representation with the fundamental representation (a single box):

> The additional box $\square$ is added in all positions, with the condition that a valid Young diagram is formed. The result is the direct sum of all these diagrams.

A nice application of the methods introduced in the last sections can be found in the (static) quark model of particle physics. In the static quark model, two types of particles are distinguished: baryons (consisting of 3 quarks) and mesons (consisting of a quark and an antiquark). As already mentioned above, a quark transforms with the fundamental representation **3**, while an anti-quark transforms with the conjugate representation $\overline{\mathbf{3}}$. This transformation behavior is understood in modern particle physics as a consequence of the flavor symmetry of quarks. The strong interaction depends only on the color charge of the quarks and not on the flavor. Therefore, if one replaces a quark with another while keeping the color the same, the mass of the hadron does not change significantly, as long as the respective quark masses are much smaller than the interaction scale of the strong interaction. This is satisfied for the light quarks (u, s, d), so that they can be exchanged without significantly changing the mass of the hadron. This exchange is described by the representation **3**, and $\overline{\mathbf{3}}$. Historically, this symmetry was derived from experimental data.

The question now arises as to why stable states consist only of 3 quarks ($\mathbf{3}\otimes\mathbf{3}\otimes\mathbf{3}$) or a quark-antiquark pair ($\mathbf{3}\otimes\overline{\mathbf{3}}$) and not, for example, just two quarks ($\mathbf{3}\otimes\mathbf{3}$). The reason lies in the strong interaction. Due to "color confinement", all matter must be colorless. This means that the wave function must be invariant (a singlet) under a transformation in color space (r, g, b). Since the color charge is also described by the symmetry group $SU(3)$, the representations can also be described by Young diagrams. The only one-dimensional representation is obtained with $p = q = 0$, which corresponds to the Young tableau $\begin{ytableau} r \\ g \\ b \end{ytableau}$. Thus, 3 quarks are needed for a color singlet, which corresponds to baryons. The only other way to create a colorless wave function is the combination of color with anti-color, as $\square\otimes\overline{\square}$ contains a singlet. In fact, the state $|r\overline{r}\rangle + |g\overline{g}\rangle + |b\overline{b}\rangle$ forms a color singlet, which corresponds to mesons.

The stable particles are now represented by basis vectors of irreducible representations in the tensor product spaces $\mathbf{3}\otimes\mathbf{3}\otimes\mathbf{3}$ (baryons) and $\mathbf{3}\otimes\overline{\mathbf{3}}$ (mesons). Thus, we need to decompose the product representations into irreducible representations to find the corresponding particles. We will use the graphical method for this.

We start with the baryons:

$$\begin{aligned}\mathbf{3}\otimes\mathbf{3}\otimes\mathbf{3} = \square\otimes\square\otimes\square &= \left(\ydiagram{1,1}\oplus\ydiagram{2}\right)\otimes\square \\ &= \left(\ydiagram{1,1}\otimes\square\right)\oplus\left(\ydiagram{2}\otimes\square\right) \\ &= \ydiagram{1,1,1}\oplus\ydiagram{2,1}\oplus\ydiagram{2,1}\oplus\ydiagram{3}\end{aligned}\tag{C.16}$$

In conventional notation, this result is written as

$$\mathbf{3}\otimes\mathbf{3}\otimes\mathbf{3} = \mathbf{1}\oplus\mathbf{8}\oplus\mathbf{8}\oplus\mathbf{10}.\tag{C.17}$$

Here, only **8** and **10** correspond to physical particles. The singlet state **1** is forbidden due to the Pauli principle.

The Pauli principle requires that the total wave function (spin, flavor, and color) is antisymmetric. As we have already seen, the color degree of freedom is a singlet due to color confinement and thus antisymmetric. Therefore, the spin-flavor wave function must be symmetric. Each quark has spin-1/2, so the 3 quarks can combine to a total spin $S = \frac{1}{2}$ (with the type $\ydiagram{2,1}$) or to a total spin $S = \frac{3}{2}$ (with the type $\ydiagram{3}$). With (B.47), we know that the corresponding flavor wave functions must have the same type so that the spin-flavor wave function has an overall symmetric representation. Thus, we obtain only the particles **8** for spin-1/2 and **10** for spin-3/2.

The decomposition is graphically represented in Figure C.1. Due to the symmetry, we expect that the particles in **8** (the light baryons) and in 10 (the heavy baryons) have the same mass (up to the small mass differences of the quarks). This statement holds except for effects of the electroweak interaction. The flavor wave functions

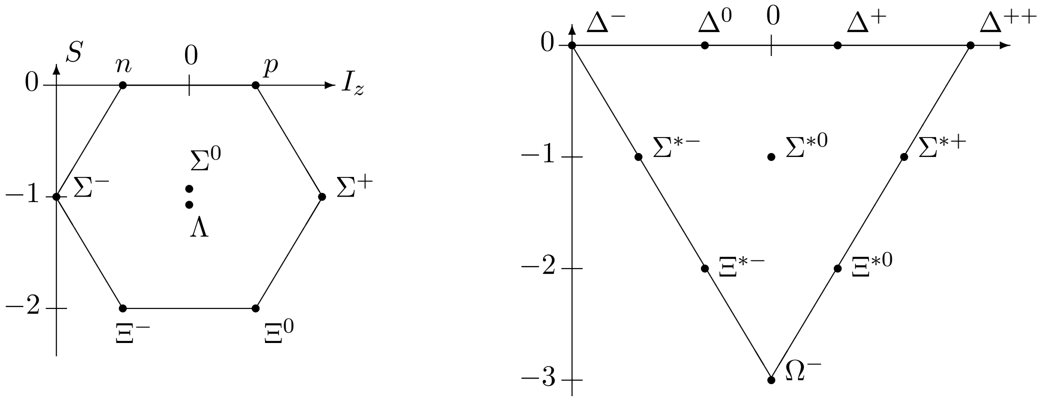

Figure C.1: Baryon octet **8** for spin-1/2 (left) and baryon decuplet **10** for spin-3/2 (right). The x-axis in this graph describes the isospin quantum number I_z (proportional to the number of up quarks minus the number of down quarks), while the y-axis describes the strangeness S (respectively the hypercharge Y). We will not go into this characterization further here (for more information, see S. Coleman 'Aspects of Symmetry').

corresponding to the individual particles can now be determined using Young tableaux. As an example, consider the Δ^+ particle with spin-3/2 consisting of the quarks uud (strangeness 0, isospin 1/2). The wave function is given by $\begin{array}{|c|c|c|}\hline u & u & d \\ \hline\end{array}$. In comparison, the proton (p) with spin-1/2 (with the same quark content) has its flavor wave function determined by $\begin{array}{|c|c|}\hline u & u \\ \hline d & \multicolumn{1}{c}{} \\ \cline{1-1}\end{array}$.

The procedure for the mesons is analogous. Here, the decomposition holds

$$3 \otimes \overline{3} = \square \otimes \overline{\square} = \square \otimes \begin{array}{|c|}\hline \ \\ \hline \ \\ \hline\end{array} = \begin{array}{|c|}\hline \ \\ \hline \ \\ \hline \ \\ \hline\end{array} \oplus \begin{array}{|c|c|}\hline \ & \ \\ \hline \ & \multicolumn{1}{c}{} \\ \cline{1-1}\end{array}. \tag{C.18}$$

In conventional notation, this result is written as

$$\mathbf{3} \otimes \overline{\mathbf{3}} = \mathbf{1} \oplus \mathbf{8}. \tag{C.19}$$

In contrast to the baryons, here the singlet **1** is allowed. It describes an η' meson. The reason is that mesons are composed of distinguishable particles (quark and antiquark), so that the Pauli principle does not apply. We have summarized the meson octet in Figure C.2. Again, the mesons in the octet have similar masses. Thus, we want to conclude our excursion into the world of representation theory. The representation theory is a field of great relevance for physics, of which we could only show a small excerpt here. A good starting point for further study of this topic is the book 'Group theory and its application to physical problems' by Morton Hamermesh, where you can also find proofs of the methods that we have only motivated here.

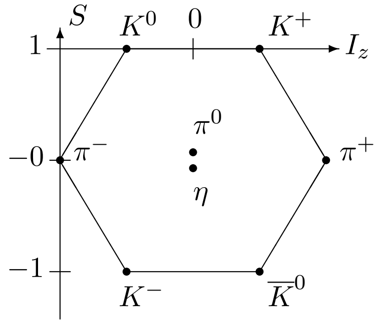

Figure C.2: Meson octet **8**